University of Kent

Kent Academic Repository

Miller, Christopher (2017) *Establishing Cryptosporidium parvum as a model organism.* Doctor of Philosophy (PhD) thesis, University of Kent,.

Downloaded from

https://kar.kent.ac.uk/66710/ The University of Kent's Academic Repository KAR

The version of record is available from

This document version

UNSPECIFIED

DOI for this version

Licence for this version

UNSPECIFIED

Additional information

Versions of research works

Versions of Record

If this version is the version of record, it is the same as the published version available on the publisher's web site. Cite as the published version.

Author Accepted Manuscripts

If this document is identified as the Author Accepted Manuscript it is the version after peer review but before type setting, copy editing or publisher branding. Cite as Surname, Initial. (Year) 'Title of article'. To be published in *Title of Journal* , Volume and issue numbers [peer-reviewed accepted version]. Available at: DOI or URL (Accessed: date).

Enquiries

If you have questions about this document contact ResearchSupport@kent.ac.uk. Please include the URL of the record in KAR. If you believe that your, or a third party's rights have been compromised through this document please see our Take Down policy (available from https://www.kent.ac.uk/guides/kar-the-kent-academic-repository#policies).

UNIVERSITY OF KENT

Establishing Cryptosporidium parvum as a model organism

School of Biosciences PhD Thesis for the title of Doctorate of Philosophy in Microbiology

Author: Christopher. N. Miller. Supervisor: Dr Anastasios Tsaousis

September 2017

Word Count: 48,373

Declaration

I have read and understood the School's definition of plagiarism and cheating given in the Research Degrees Handbook. I declare that this thesis is my own work, and that I have acknowledged all results and quotations from the published or unpublished work of other people.

I have read and understood the School's definition and policy on the use of third parties (either paid or unpaid) who have contributed to the preparation of this thesis by providing copy editing and, or, proof reading services. I declare that no changes to the intellectual content or substance of this thesis were made as a result of this advice, and, that I have fully acknowledged all such contributions.

Signed: 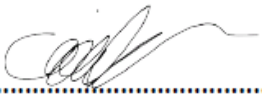 Date:02-09-17

Full name:Christopher Neil Miller (please print clearly)

Abstract

Cryptosporidium parvum is among the most common parasites in the known world and represents one of the leading causes of death among the immunocompromised. As an apicomplexan, *C. parvum* has many similarities to other globally important parasites such as *Plasmodium falciparum* and *Toxoplasma gondii*. Among these similarities are a complex life cycle and the ability to invade host cells. However, unlike most other apicomplexans, the cryptosporidia appear to have lost their namesake organelle, the apicoplast, and drastically reduced the size of their genome. For decades this caused issues in classifying the cryptosporidia. This has been potentially resolved, however, by recent phylogenetic studies that revealed a strong relationship between the cryptosporidia and the gregarines. The gregarines were parasites exclusively of invertebrates, until the reclassification to include the cryptosporidia. Though research into apicomplexan evolution and biology is still a nascent field, even less is known about the invertebrate portion. This is largely due to the lack of molecular tools and culturing techniques that are required to explore any organism beyond basic phylogenetics, in addition to their medical irrelevance prior to the inclusion of *Cryptosporidium*.

Therefore, *C. parvum* represents a potential model organism for the gregarines and the evolutionary adaptations of apicomplexans from invertebrate to vertebrate hosts. It was the purpose of this thesis, therefore, to establish the tools and methodologies that would be required to begin developing *C. parvum* as such. To achieve this, first I successfully developed the world's first long-term culturing system of *C. parvum*, capable of maintain a live parasite culture for 60 days. Additionally, I developed novel methods of detecting and characterising the infection, including NMR based characterisation of infection metabolomes which also revealed a potentially more involved role for Taurine in the pathology of the infection. Furthermore, to demonstrate the power and applicability of this new system I produced the first experimental evidence for a functional ISC system within *C. parvum*. This also adds to a now growing list of non-canonical mitochondria containing organisms that still maintain an active mitochondrial Fe/S cluster biosynthetic pathway.

In conclusion, this thesis represents a large step forward for both the *C. parvum* and gregarine fields and establishes many of the necessary techniques required for a new push in understanding these apicomplexans and their organelles.

Acknowledgements

I would first like to offer my heartfelt thanks to my family for supporting me these last 4 years. Especially to my wife, Rosie, you were my sanity when I needed it most and my reason for trying. This thesis is a testament to the man you've helped me grow up to be.

I'd like to thank my parents, Mum and Dad, for always providing a warm bed and warmer company whenever I or Rosie needed it and for having the confidence in me that I could only pretend to have.

I'd also like to thank my little brother, Edward, for reminding me of the passion I had for science when things began to overwhelm me and for being my best friend and loudest supporter. I'd like to thank my other brother Ben, for grounding me but also for showing me how I can find enjoyment in things even if I don't find them interesting.

I'd like to thank my supervisor, Dr. A. Tsaousis, as much for his academic tutelage as for his tireless patience with his first PhD student. I like to think that after me things can only be easier. I'd also like to thank him for his friendship, which made my PhD immeasurably more enjoyable.

Lyne, Lyto and Tracey, we certainly had plenty of laughs and conversations, but you were also a calming presence and helped me become a more responsible and mature researcher that I certainly could not have finished my PhD without.

Ian, you helped foster my now fervent passion for microscopy. A passion which I think will define my career.

Julian, Lisa, Robert and Linda: I will truly miss our conversations and rants. Without you I wouldn't have had a clue what I was doing in the teaching labs and probably more so in my actual lab.

I'd like to offer my special thanks to the Space Wars and Cool Kid groups: Alex, Ben, Rokas, Linas, Emi, Ruk, Joe and Tim. They say you should never be the smartest person in the room, being a part of this group guaranteed that I never was. I sincerely hope this is not goodbye and I look forward to many adventures yet to come.

Table of Contents

Chapter 1 An Introduction to *Cryptosporidium parvum* and the Cryptosporidia

1.1 The Cryptosporidia

The first species of *Cryptosporidium* to be described was the mouse parasite *C. muris*, in 1907 by E. Tyzzer, who formed the name from the Greek for "hidden seed". The "hidden seed" referred to the appearance of the oocyst and the almost imperceptible sporozoites that were characteristically visible in other spore forming protozoa (Tyzzer, 1910). Tyzzer also noted that, unlike the majority of sporalating protozoa, members of cryptosporidia appeared to sporolate whilst still associated with the host cell, as opposed to once passed into the environment like the majority of sporalates (Tyzzer, 1910, Morrison, 2009).

As Apicomplexans, Cryptosporidia are closely related to many other parasites of medical and veterinary importance such as *Toxoplasma, Babesia* and, perhaps most infamously, the malarial parasites *Plasmodium* (Kuo et al., 2008, Morrison, 2009, Abrahamsen et al., 2004). *Plasmodium* and *Toxoplasma* are especially important parasites, as the causative agents of Malaria and Toxoplasmosis, respectively. Both of these diseases are notable for, among other things, a significant lack of preventative or curative treatment options, a common theme amongst the Apicomplexa (Flegr et al., 2014, Torgerson and Macpherson, 2011, Liu et al., 2012).

Among its similarities to the other Apicomplexans are the multitudes of life cycle stages that *Cryptosporidium* experiences. In order to complete a full cycle, from the excystation of sporozoites from an oocyst, back to the sporulation of an oocyst and its eventual release from the host, members of the Cryptosporidia undergo both asexual and sexual life cycle stages (Borowski et al., 2010, Hijjawi et al., 2010, Leitch and He, 2012). Paradoxically, several aspects of the life cycle mark it as significantly different from the rest of its apicomplexan relatives, for example members of *Cryptosporidium* sporulate prior to release from the host, whereas close relative *Toxoplasma gondii* only undergoes sporulation *after* release into the environment (Tyzzer, 1910, Dubey, 1998, Wilhelm and Yarovinsky, 2014). Similarly, unlike members of *Eimeria, Toxoplasma* or *Plasmodium,*

members of *Cryptosporidium* are uniquely capable of autoinfection; the ability to complete an entire life cycle, sexual stages included, within one host and infect again without passing into the environment (Kuo et al., 2008, Muller and Hemphill, 2013). Also, unlike all coccidia, many *Cryptosporidium* species are capable of infecting and completing entire life cycles within a broad range of hosts, as opposed to being host species specific. This is a trend seen throughout the biology of the parasite, including the absence of an otherwise essential organelle, the apicoplast, found unilaterally throughout all members of the Apicomplexa, with the exception of the gregarines, confounding the difficulty found in placing the parasite phylogenetically (Carreno et al., 1999, Borowski et al., 2010, Fichera and Roos, 1997, Lim and McFadden, 2010, Lemgruber and Lupetti, 2012, Abrahamsen et al., 2004, Omoto et al., 2004). This observation has led many to begin proposing that the *Cryptosporidium spp.* may, therefore, be better suited within the gregarines as opposed to their own separate class. Recent attempts using 18S rDNA sequencing techniques have shown compelling evidence for the official classification of *Cryptosporidium* as a gregarine (Figure 1-1)(Cavalier-Smith, 2014).

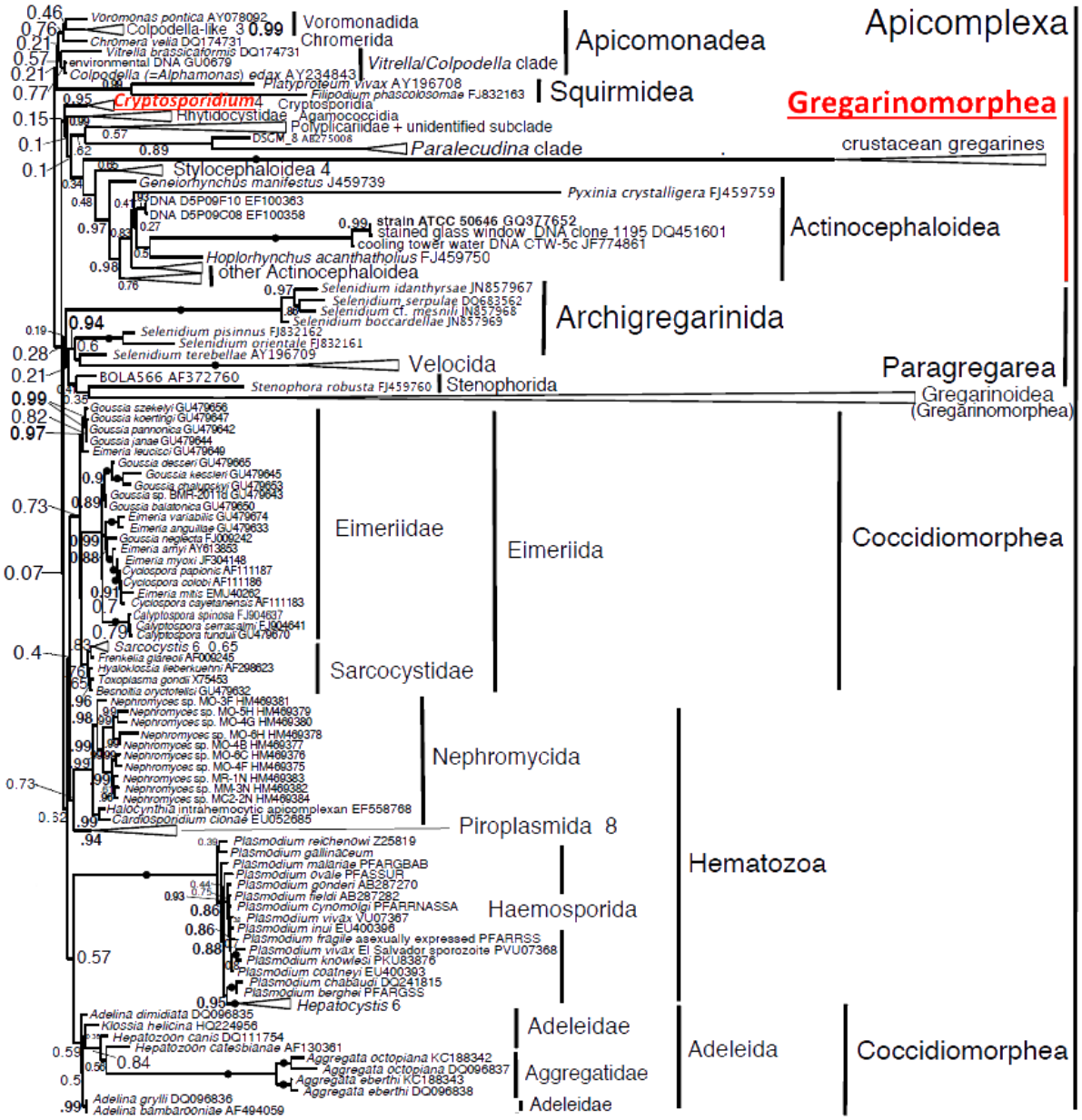

Figure 1-1: Phylogeny of the Apicomplexa. A recent phylogenetic placement of *Cryptosporidium spp.* (highlighted in red) removed them from the coccidia and placed them with the gregarines (also in red). This new placement was informed via "18S rDNA alignments and a PhyloBayes CAT-GTR-GAMMA tree and 1577 well-aligned nucleotide positions" as demonstrated in Cavalier-Smith (2014, Figure 4). Although not a universally accepted model, it nonetheless highlights the interesting nature of *Cryptosporidium's* genetic heraldry.

Recent publications have also presented a strong case for the re-location via observations in cell biology, including the discovery of extra-cellular gamete stages and the purported ability to culture several species of *Cryptosporidium in-vitro* without host cells (Arrowood, 2002, Hijjawi et al., 2010, Karanis and Aldeyarbi, 2011, Carreno et al., 1999, Ryan et al., 2016).

This lack of organelles, which will be described in greater details in subsequent chapters, indicates that what remains within *Cryptosporidium* represents the core, essential components of any apicomplexan, *Gregarina*, *Coccidia* or *Haematozoa*. It is theoretically possible, therefore, that *Cryptosporidium* could be established as a model around which aspects of a conceptual Last Apicomplexan Common Ancestor (LACA) may be built and thus a model for the evolution of Apicomplexa. In addition to its reduced organellar complement, the members of *Cryptosporidium*, especially the human pathogen *Cryptosporidium parvum.* possesses a radically reduced genome compared to its closest genetic relatives. Compared to the 22.9 Mb genome of *P. falciparum*, *C. parvum* holds only 9 Mb (Widmer and Sullivan, 2012, Gardner et al., 2002). This sharp reduction in genome size and phylogenetic placing suggest that *C. parvum* lost approximately half its genome since diverging from the rest of the apicomplexan.

1.2 Cryptosporidiosis

Cryptosporidiosis is a disease of global significance, constituting a significant burden on developing economies in addition to being the cause of a considerable number of infantile deaths (<5 years old) and is among the leading causes of fatalities in HIV patients (Shirley et al., 2012, Striepen, 2013, Checkley et al., 2014, Torgerson and Macpherson, 2011, Wanyiri et al., 2014). As our knowledge of this disease has progressed, it has become apparent that it needs an urgent response. Advances in epidemiological research, including wider and more reliable networks of communication, have identified cryptosporidiosis among the top four causes of pathogen-induced diarrhoea (Briggs et al., 2014, Checkley et al., 2014, Deshpande et al., 2014, Wanyiri et al., 2014).

Whilst the disease is termed from the collective group of *Cryptosporidium*, their medical relevance varies from species to species. Amongst them, many species of *Cryptosporidium* have shown an ability to infect and cause symptoms in humans, including those commonly found in house hold pets such as *C. muris*, *C. felis*, and *C. canis* (Table 1-1). Cattle also appear to be a source of human infectious *Cryptosporidium*, both *C. andersoni* and *C. bovis* are common parasites of cattle that can also infect humans (Table 1-1). However, the causes of human cryptosporidiosis are overwhelmingly populated by *C. parvum* and to a lesser extent *C. hominis*. This is in large part due to the

highly zoonotic nature of *C. parvum*, showing a much broader range of suitable hosts than many of the other Cryptosporidia, enhancing its coverage.

Table 1-1: Host specificity of Cryptosporidium. Although members of the Cryptosporidia display relatively specific host specificity, several them can infect humans in addition to their typical hosts. In this table, the column entitled; Major hosts, lists the animal in which the species of *Cryptosporidium* is most commonly found. The authors listed are typically the preliminary publishers of human infection. *Additionally, though originally described as a parasite of many ruminants, *C. parvum* is increasingly detected within Humans and in some studies had comparable or even higher incidences in human populations than *C. hominis*, which is considered to have the highest preference for humans of the Cryptosporidia (Xiao, 2010)

Species name	Author(s)	Major host(s)
C. erinacei	Kváč et al., 2014b	Hedgehogs, horses
C. scrofarum	Kváč et al., 2013	Pigs
C. viatorum	Elwin et al., 2012	Humans
C. tyzzeri	Tyzzer, 1912; Ren et al., 2012	Rodents
C. cuniculus	Robinson et al., 2010	Rabbits
C. ubiquitum	Fayer et al., 2010	Ruminants, rodents, primates
C. xiaoi	Fayer et al., 2010	Sheep and goats
C. fayeri	Ryan et al., 2008	Marsupials
C. bovis	Fayer et al., 2005	Cattle
C. suis	Ryan et al., 2004	Pigs
C. hominis	Morgan Ryan et al., 2002	Humans
C. canis	Fayer et al., 2001	Dogs
C. andersoni	Lindsay et al., 2000	Cattle
C. parvum	Tyzzer, 1912	Ruminants and humans*
C. meleagridis	Slavin, 1955	Birds and humans
C. felis	Iseki, 1979	Cats
C. muris	Tyzzer, 1907; and 1910	Rodents

It is also of interest to note that different species will typically infect different regions of the gastro-intestinal tract, a trait that appears to be relatively conserved within phylogenetic groupings (Fayer and Ungar, 1986, Widmer et al., 2007). For example, *C. parvum* and the closely related *C. hominis* are frequently found to infect regions of the

intestinal tract, typically the ileum, whereas *C. muris* is most commonly found within the stomach of the host (Widmer et al., 2007, Gertler et al., 2015, Slapeta, 2017).

As a waterborne and zoonotic disease, the parasite is particularly prevalent in developing countries, particularly rural areas and especially those which lack sufficient water treatment networks (Caccio, 2005, Striepen, 2013, Checkley et al., 2014, Wanyiri et al., 2014, Ungar et al., 1989). It is therefore unsurprising that human cryptosporidiosis outbreaks most often occur in the equatorial climates, in regions such as Sub-Saharan Africa and Central America. In one study, it was estimated that 6 % of travellers returning from Mexico had contracted cryptosporidiosis during their visit (Nair et al., 2008). However, outbreaks still occur in modern countries, with typical water treatment infrastructure still largely incapable of filtering out the parasites, resulting in almost yearly outbreaks (Dreelin et al., Cantey et al., 2012, Widmer and Sullivan, 2012, Deshpande et al., 2014, Gertler et al., 2015, McKerr et al., 2015, Thivierge et al., 2016, Utsi et al., 2016). Several mass outbreaks have been recorded in the US in recent decades (Yoder et al., 2008, Yoder et al., 2010, Brunkard et al., 2011, Hlavsa et al., 2011, Hlavsa et al., 2014, Cope et al., 2015, Hlavsa et al., 2015, Mac Kenzie et al., 1994). The most notable, being that of Milwaukee, Wisconsin in 1993 which saw over 400,000 homes affected and a record 104 deaths from a single outbreak (Mac Kenzie et al., 1994).

A significant factor which contributes to the seeming world-wide distribution of cryptosporidiosis is the extremely resistant environmental stage of the parasite, the oocyst. Responsible for protecting the infectious forms of the parasite until ingestion by a potential host, the oocyst has been shown to resist most forms of water purification; such as heating, bleaching and biological filtering (Kar et al., 2011, Chauret et al., 1998, Widmer et al., 2007, Hayes et al., 2013). Whilst heat inactivation of the parasite is possible, it requires a sustained temperature of 60°C for greater than 15 minutes, a largely inefficient and unachievable methodology for large scale water purification plants. UV irradiation is an effective, yet uncommon technique employed by water companies, killing a significant number of oocysts in a relatively short period of time (Hayes et al., 2013). Unfortunately, this is difficult to implement in the construction of water services and even more so retroactively. This leaves much of the world, regardless of economic prosperity, woefully ill-prepared to prevent or control an outbreak of cryptosporidiosis.

Cryptosporidiosis symptoms can vary from asymptomatic to severe, with abdominal pain and diarrhoea being most common. For those with compromised immune systems, particularly HIV sufferers, death from dehydration is the most imminent threat; particularly in those areas identified above that lack sufficient water infrastructure (DuPont et al., 1995, Meisel et al., 1976, Egger et al., 1990, Flanigan and Graham, 1990, Gatei et al., 2006). In immunocompromised individuals the parasite can also be found in other epithelial tissues, including most of the upper stages of the digestive tract and the respiratory tract (Wanyiri et al., 2014, Sponseller et al., 2014). However, emerging evidence has shown that immunocompetent individuals may also be at risk of respiratory infections (Sponseller et al., 2014).

Unfortunately, current methods of treatment are limited to basic symptomatic relief and a handful of promising yet ultimately insufficiently effective drugs (Checkley et al., 2014, Domjahn et al., 2014, Sparks et al., 2015, Manjunatha et al., 2016). With no universally accepted treatment regimen, patients can expect treatment with any combination of therapies including anti-parasitics such as paromomycin or azithromycin and diarrheal treatments such as loperamide.

For otherwise immunocompetent individuals, the only established treatment, although not approved within the EU for treating cryptosporidiosis, is the broad-spectrum anti-parasitic nitazoxanide (Sparks et al., 2015, Manjunatha et al., 2016). Nitazoxanide is a thiazolide, which acts by interfering with the respiratory system of the parasite, effectively preventing it from proliferating within the host until effective clearance by the immune system (Rossignol, 1994, Rossignol, 1999). Trials and subsequent widespread use of the drug throughout the US have shown moderate efficacy in reducing symptoms and disease patent period. However, nitazoxanide appears to be largely ineffective in treating the disease in the most at risk groups; the young, the old and medically immunocompromised due to a reliance on a healthy immune system for effective drug action (Rossignol et al., 1998, Hussien et al., 2013, Sparks et al., 2015, Manjunatha et al., 2016). Additionally, nitazoxanide has been associated with an array of unpleasant side effects including diarrhoea, headache, nausea and stomach pain (Stockis et al., 2002) .

Alternative treatments rely on other broad-spectrum drugs with varying degrees of efficacy. Paromomycin, an anti-parasitic, has been shown to significantly reduce diarrheal episodes in patients, although complete eradication of the parasite is seen in less

than half of cases (Hussien et al., 2013). Azithromycin, an antibiotic typically used in treating bacterial infections, has shown promising potential to reduce parasite load, clearing the patient of the symptoms of cryptosporidiosis, however studies have shown that the drug failed to eradicate the infection entirely, with the parasite's ability to autoinfect rendering the treatment ultimately symptomatic only (Fichera and Roos, 1997, Wang and Zhang, 2013). In each case a functioning immune system is required for the effective patient responses, for immunocompromised individuals, available treatments are restricted to bed rest, hydration and symptomatic treatments (Checkley et al., 2014, Mead, 2014, Sparks et al., 2015, Goodgame et al., 1995, Wanyiri et al., 2014). Although anti-cryptosporidial drug development investment is similar to neglected tropical diseases and is therefore largely lacking in novel compounds, a few potential therapeutics have been discovered recently. Combination treatment with garlicin and acetylspiramycin had an average success rate of 76.2% in clearing the parasite in a study in China, in addition to the identification of the compounds: broxyquinoline, cloxyquin, cloxacillin sodium and sodium dehdrocholate, which showed effective reduction of *Cryptosporidium* activity *in-vitro* (Huang et al., 2015, Fritzler and Zhu, 2012)

1.3 Life cycle of the cryptosporidia

A defining feature of almost all apicomplexans, especially the species of *Cryptosporidium,* is a complex life cycle. Though the exact nature of the life-cycles can vary between groups, most apicomplexans incorporate elements of sexual and asexual reproduction (Morrison, 2009). Species of *Cryptosporidium* are no different, displaying characteristic apicomplexan stages such as merogony (asexual) and gametogony (sexual) (Figure 1-2) (Current et al., 1986, Borowski et al., 2010, Hijjawi et al., 2010, Leitch and He, 2012, Ryan et al., 2016). In most cases, the host within which the parasite completes its sexual stages is determined as the definitive (as opposed to reservoir or secondary) host. For *Plasmodium* species the definitive hosts are the female members of the *Anopheles* group of mosquito (Florens et al., 2002). For *Toxoplasma gondii* the definitive hosts are members of the *Felidae*, or domestic cats (Dubey, 1998). Unlike *Plasmodium* or *Toxoplasma*, which are parasites with indirect life cycles (more than one host is required for a complete life cycle); members of the cryptosporidia are direct life cycle

parasites; requiring only one host to begin and finish both sexual and asexual life cycles stages. Because they only require one host to complete the life cycle, the parasite is capable of propagating in almost any environment, regardless of zoological diversity. Additionally, unlike many apicomplexans, the cryptosporidia are capable of autoinfection, *i.e.* infecting the same host from a new infectious cycle without entering the environment first (Dubey, 1998, Florens et al., 2002, Leitch and He, 2012, Morrison, 2009).

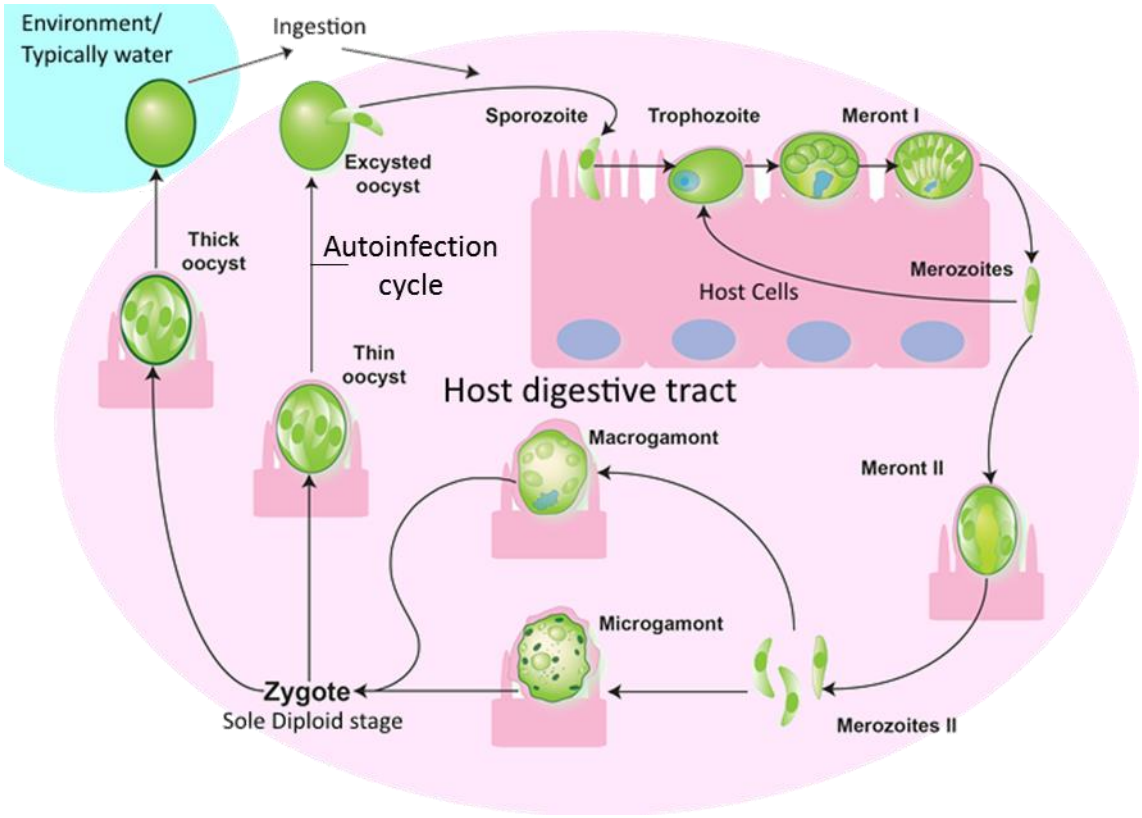

Figure 1-2: The general life cycle of *Cryptosporidium* species. Upon consumption of the oocyst by the host, typically through drinking water, the parasite passes into the gut and undergoes the process of excystation. At this point 4 sporozoites, each haploid, emerge from the approximately 5-6µm diameter oocyst and proceed via a gliding motility to interact with and invade host epithelial cells, developing into trophozoites and soon merozoites. This represents the asexual stages of replication within the life cycle. (Adapted from Bouzid et al., 2013)

The progression of the life cycle stages for *Cryptosporidium* is one of the few extensively covered areas of research into this group of parasites (Current et al., 1986, Arrowood, 2002, Girouard et al., 2006, Borowski et al., 2010, Hijjawi et al., 2010, Hijjawi, 2010, Karanis and Aldeyarbi, 2011, King et al., 2011, Leitch and He, 2012, Muller and Hemphill, 2013, Ryan et al., 2016). Typically, the infection begins with the consumption

of an oocyst by the potential host, usually by drinking contaminated water, although infection through contaminated food stuffs is possible (Torgerson et al., 2014, McKerr et al., 2015). Upon entering the host digestive tract, a yet unknown series of chemical and/or physiological triggers cause the four sporozoites contained within the oocyst to make their way out during a process termed "excystation". Once free in the host gut, typically the ileum, these sporozoites will proceed to move along the epithelial surface in what has been described as "gliding" motility. Eventually settling on the surface of a potential host cell and invading. At this point, unlike many intracellular apicomplexans (excluding the gregarines), the parasite develops its parasitophorous vacuole (PV) separate from the host cytoplasm, usually along the brush boarder of the epithelial cilia. This aspect of the life cycle of *Cryptosporidium* is like the gregarines, which also appear to form a parasitophorous vacuole at the point of contact with the host cell. However, gregarines are typically too large to be fully engulfed by host membranous intrusions. It is the exact nature of the location of the PV that has become a topic of much contention within the research community, with much debate over the definition of the terms *intra*- and *epi*-cellular (Fritzler and Zhu, 2012, Guo et al., 2016, Leitch and He, 2012, Wilhelm and Yarovinsky, 2014, Ryan et al., 2016).

Once fully enclosed by the PV the sporozoite then undergoes a transformation from its rod like form to a genetically dispersed roughly spherical stage termed the trophozoite. Like both *Plasmodium* and *Toxoplasma* trophozoites in form, it has not yet been determined whether the *Cryptosporidium* trophozoite is the main feeding stage as it is for the other apicomplexans or an adaptation step where the parasite prepares for the following infectious stages.

From the disseminated genetic mass begins to form individual rod like bodies, approximately two micrometres in length. Eventually a division becomes apparent, between a central genetic mass and surrounding individual bodies, from six to eight in total, signalling the formation of a type I meront from the trophozoite. These smaller bodies eventually mature into individual merozoites and emerge from the PV back into the host ileum.

The merozoites, morphologically similar to smaller sporozoites, migrate across the gut epithelia before invading new cells in a similar manner to the sporozoites, establishing another PV within the membrane of an epithelial cell at the cilia brush border. Once

encapsulated by the PV, the merozoites undergo merogony where either a type I meront is formed again or the next step, a type II meront, is produced. The pathways and signals responsible for the determination of type I or type II are yet unknown.

Merozoites that emerge from a type II meront are typically fewer in number but larger in size when compared to their type I analogues. After emerging from the host cell, like each time before, the type II merozoite will find a new host cell, invade and form a PV. This marks the end of the asexual section of the life cycle and the beginning of the sexual stage. After the establishment of the PV, instead of forming into another meront stage, the encapsulated merozoite instead transforms into either of the main sexual forms of *Cryptosporidium*: the macrogamont or the microgamont. Despite the naming scheme, microgamonts are only slightly smaller than the macrogamonts on average. Rather, microgamonts are named for the less than one micrometre long microgametes, analogous to sperm, that they produce. Each microgamete is theoretically capable of fertilising a single microgamont, in turn producing a zygote. It is not known how many microgametes can be produced by a microgamont.

At this point the zygote which forms is the only diploid stage of *C. parvum*. During the process of maturing from a zygote to a sporolated oocyst, the organism becomes haploid again through the production of four sporozoites after one round of mitosis and another of meiosis.

Unlike most apicomplexans, the matured oocyst that forms from the zygote leaves the host cell fully sporulated and infectious. Many cyst forming apicomplexans, such as *Toxoplasma gondii* do not fully sporulate until after release from the host cell and often not until being passed back into the environment (Dubey, 1998). *C. parvum* oocysts come in two varieties: the typical form, produced in roughly 80% of cases from a zygote, is the "thick walled" oocyst. This particularly resilient form of the parasite is often found in contaminated water supplies and is incredibly resistant to a plethora of environmental hardships, including UV exposure, heat, dehydration, salt and pH levels. Alternatively, in theoretically 20% of cases, a "thin walled" oocyst can form (Current et al., 1986). As the name implies, the normally environmentally resistant shell surrounding the four sporozoites is substantially thinner and less resilient than the "thick walled" edition. "Thin walled" oocysts excyst rapidly upon emergence from the host cell, repeating the entire life cycle asexual to sexual, within the original host. This makes *Cryptosporidium* the

only apicomplexans capable of true autoinfection. These assumptions, however, are mainly based on *in-vitro* studies and due to the nature of thin walled oocysts, observations via *in-vivo* studies are lacking.

1.4 Cell biology of cryptosporidia

1.4.1 Similarities between cryptosporidia and other apicomplexans

The organelle complement of the sporozoite stage of *Cryptosporidium* species shares many similarities to the sporozoites of other apicomplexans, including the presence of the apical complex and its complement of micronemes and a single rhoptry (although other apicomplexans typically have four). In the Apicomplexa, the apical complex is a region found on the apical (hence the name) end of motile life-cycle stages. It is typically electron dense and houses a variety of enzymes, depending on the organisms, that interact with the potential host cell to initiate and/or facilitate invasion. *C. parvum* is no different and a number of proteins have been expressed, localised and functionally characterised from its apical complex, including a potentially protective antigen involved in invasion (Elongation factor-1α) and a glycoprotein that acts as a ligand (CSL), facilitating binding between the sporozoite stage and a host epithelial cell (Langer and Riggs, 1999, Matsubayashi et al., 2013).

Additionally, upon invading a host cell *C. parvum* demonstrates the generation of a parasitophorous vacuole (PV), a common feature among intracellular stages of the apicomplexans (Morrison, 2009). The PV forms upon successful invasion of the host cell and serves to separate the host cytoplasm from that of the parasite, providing a number of advantages such as limiting the effectiveness of the host MHC class I based immune response and other defences such as phagolysosomes (Lingelbach and Joiner, 1998). In *Cryptosporidium* this structure is derived primarily from host cytoskeleton and membrane, with high concentrations of actin at the site of invasion preceding the creation of the PV (Leitch and He, 2012, Elliott and Clark, 2000). Host membrane proteins, however, are excluded to a significant degree by all known apicomplexans in the formation of their respective PVs (Lingelbach and Joiner, 1998).

Species of *Cryptosporidium* also display a cryptic organelle currently termed the "Crystalloid Body" (CB), found in only a select few other apicomplexans such as *Plasmodium*. The CB of *Cryptosporidium* is an electron dense, honeycomb like structure like that of the other apicomplexans. Though little is known about this diminutive organelle, one study demonstrated localisation of the *C. parvum* pyruvate:$NADP^+$ oxidoreductase fusion protein (*Cp*PNO) to the CB, suggesting an active membrane potential (Ctrnacta et al., 2006). However, doubt has been raised as to whether they are the same organelle and the structure remains largely unexplored and unexplained (Lemgruber and Lupetti, 2012)

1.4.2 Differences between the cell biology of cryptosporidia and other apicomplexans

Perhaps most immediately noticeable is the lack of the phylum namesake organelle: the apicoplast (Rider and Zhu, 2010). Thought to be a remnant plastid obtained via secondary endosymbiosis by an ancestor of LACA. This is proposed due to the presence of 4 membranes, suggesting multiple endosymbiotic events and genes with close homology to plant/algal plastids and ultimately a bacterial origin (Lim and McFadden, 2010, Seeber and Soldati-Favre, 2010, Lemgruber and Lupetti, 2012, van Dooren and Striepen, 2013). Although the apicoplast no longer performs any photosynthetic role, it is typically involved in biosynthetic pathways of important biological compounds such as iron sulphur clusters, heme groups and Fatty Acid Synthesis. As such the organelle is typically essential for the survival of the parasite (Seeber and Soldati-Favre, 2010, Kumar et al., 2011, van Dooren and Striepen, 2013, Fichera and Roos, 1997, Lemgruber and Lupetti, 2012).

These characteristics make a compelling case for the apicoplast as an essential aspect of apicomplexan biology and yet it is completely absent from *Cryptosporidium* and potentially many gregarines. The only evidence of the prior existence of anything resembling the organelle is the presence of several plant derived proteins encoded within the genome of *Cryptosporidium* which may have been exported from an Apicoplast containing ancestor before it was lost, though this remains unexplored (Abrahamsen et al., 2004).

Another defining feature of the *Cryptosporidium* is the success to which they survive in the environment due to an effective protective shell, termed an oocyst. The components of this resilient structure largely comprise of fatty acids and carbohydrates although the majority (>90%) is composed of proteins (Reduker et al., 1985, Kar et al., 2011, Widmer et al., 2007, Mitschler et al., 1994, Nanduri et al., 1999).

1.5 Cell biology of *C. parvum*

Whilst basic microscopic observation of *C. parvum* provides little evidence for the singling out of this particular species of *Cryptosporidium*, it is nevertheless an observational truth that *C. parvum* is distinct from many other members of *Cryptosporidium*. Epidemiologically *C. parvum* is capable of a far greater range of hosts than most, biologically *C. parvum* displays both structural and enzymatic diversions.

1.5.1 The mitosome

The primary differences of *C. parvum* can be linked to the organism's mitochondria, or rather lack thereof. Unlike the majority of the Apicomplexa and indeed several Cryptosporidia (such as the physically and genetically larger *C. muris*), *C. parvum* lacks typical or 'canonical' mitochondria. Instead, the motile stages of *C. parvum* appear to maintain a single mitosome, a morphologically and metabolically distinct organelle from mitochondria (Mogi and Kita, 2010). The mitosome is a member of a recently described group of potential mitochondrial adaptations or descendants; the other member so far has been labelled the hydrogenosome and is also both morphologically and metabolically distinct from the canonical mitochondrion, collectively the organelles in this group are referred to as Mitochondrial Related Organelles or MROs (Dyall and Johnson, 2000, Makiuchi and Nozaki, 2014, Regoes et al., 2005). The distribution of MROs across the tree of life covers most known organisms, with only members of Plantae and Rhizaria lacking examples of either mitosomes or hydrogenosomes. However recent publications have used genomic data to predict the absence of a canonical mitochondrion in the rhizarian *Mikrocytos mackini* (Dyall and Johnson, 2000, Mogi and Kita, 2010, Burki et

al., 2013, Makiuchi and Nozaki, 2014, Regoes et al., 2005). Additionally, study of the *Monocercomonoides* species has revealed evidence for the first amitochondriate to have evolved through secondary loss of the organelle (Karnkowska et al., 2016). This discovery lends further credence to the idea that all Eukaryotes descended from an organism with an organelle that developed into the modern mitochondrion/MROs, as opposed to previous proposals that some eukaryotes may have diverged before the endosymbiotic event.

The current hypothesis regarding the evolution of the mitosome suggests it is a descendant of original canonical mitochondria from the Last Eukaryotic Common Ancestor (LECA) (Dyall and Johnson, 2000, Makiuchi and Nozaki, 2014). As such, understanding the roles and functions of these MROs may hold the key to understanding the evolution of modern eukaryotes, by deciphering which aspects of the original symbiont were significant in the development of the endosymbiotic event.

The mitosome displays a host of modifications, usually losses, compared to the canonical organelle, for example: genome sequences of organisms containing mitosomes appear to show an almost complete loss of ATP generation via oxidative phosphorylation, lack of organellar genome, with little to no components of the TCA cycle or electron transport chain remaining (Mogi and Kita, 2010, Makiuchi and Nozaki, 2014).

This loss of function also correlates with the organelle's structural changes, whilst mitosomes have retained the dual membrane aspect of the mitochondrion, electron microscopy has revealed that the mitosome has nonetheless lost all traces of the characteristic cristae (Figure 1-3) (Regoes et al., 2005). It is possible, that with the absence of the TCA cycle and majority of the electron transport chain, that the surface area provided by the cristae no longer provided any benefit to the organelle and therefore was not conserved. In its stead, *C. parvum* appears to rely entirely on ATP production from a plant type glycolytic pathway, although ATP scavenging from the host is theorised there ultimately remains no evidence to support this (Entrala and Mascaro, 1997, Mogi and Kita, 2010, Cook et al., 2012, Abrahamsen et al., 2004). Mitosomes also show a significant reduction in locally stored genetic content, with some examples (such as those within *C. parvum*) showing a complete translocation of mitochondrial sequences to the organism's nucleus (Regoes et al., 2005, Mogi and Kita, 2010, Makiuchi and Nozaki, 2014, Tovar et al., 1999).

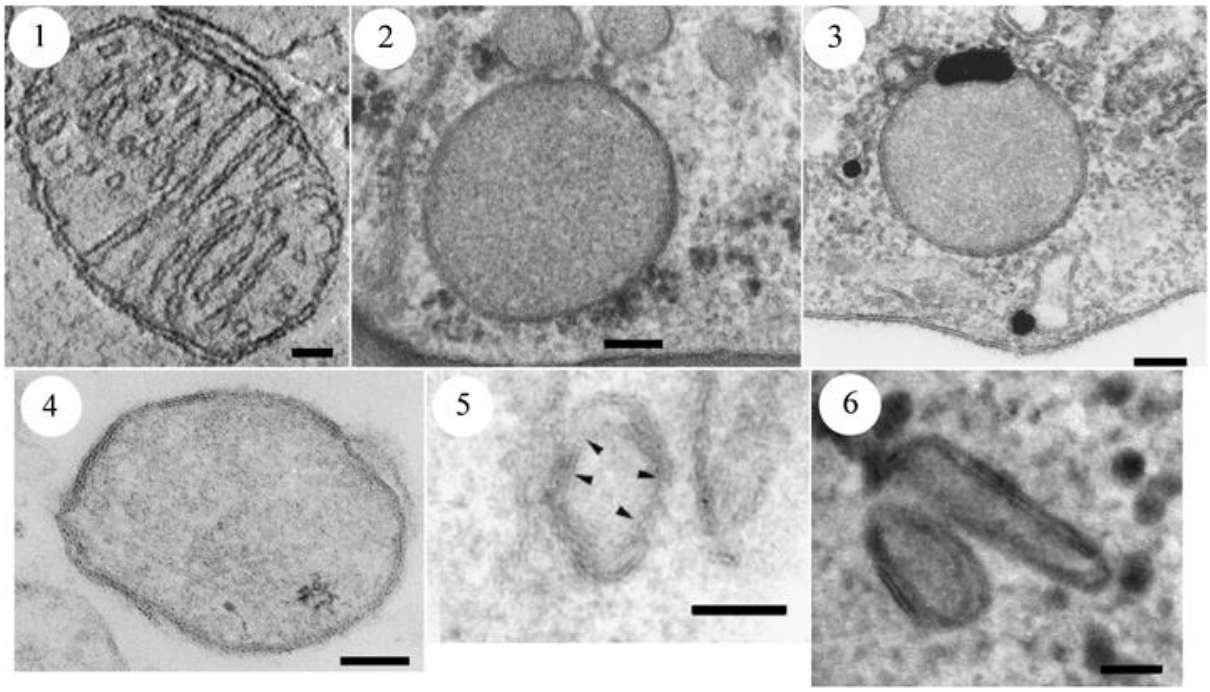

Figure 1-3: The spectrum of Mitochondrial Related Organelles (MROs). The distribution of structural changes between canonical mitochondria (1, from chicken cerebellum), hydrogenosomes (2 and 3 from *Neocallimastic patricarium* and *Tritrichomonas foetus*) and mitosomes (4-6 from *Entamoeba histolytica, Trachipleitophora hominis* and *Giardia intestinalis*). The size of the mitosome can vary greatly between species, with some reaching several µm in size such as those seen in *Entamoeba histolytica* (4) to others of less than 500nm such as those found in *Trachipleistophora hominis* and *Giardia intestinalis* (5 and 6). The scale bars represent 100nm from 1-4 and 50nm for 5-6. (Reproduced from van der Giezen and Tovar, 2005)

Many other traditionally conserved aspects of mitochondrial metabolism have also been lost. In the apicomplexans, porphyrin biosynthesis is highly reported to be performed within the apicoplast organelle, which interestingly neither the gregarines nor Cryptosporidia have retained. It has been confirmed that Cryptosporidia lack the ability to synthesise porphyrin groups and by extension haem or cytochrome compounds (Lim and McFadden, 2010, Seeber and Soldati-Favre, 2010, van Dooren and Striepen, 2013).

In contrast, iron-sulphur cluster biosynthesis has been conserved within organisms with MROs, and *C. parvum* is no exception. Iron-sulphur clusters are amongst the most ubiquitous compounds in life, conserved almost unilaterally across all domains of life (Xu and Moller, 2011, Lill et al., 2012, Ali and Nozaki, 2013). The methods of biosynthesis of these compounds is therefore unsurprisingly also highly conserved.

Current understanding of these pathways identifies three predominant types: The Sulphur mobilisation (SUF), Iron-Sulphur Cluster formation (ISC) and Cytosolic Iron-sulphur protein Assembly (CIA) pathways. ISC and CIA pathways are the most common pathways found in eukaryotic cells, typically within the mitochondrion and cytosol respectively (Ali and Nozaki, 2013). The SUF pathway appears to have been a bacterial innovation and appears throughout those eukaryotes typically containing plastids and all apicomplexans with an apicoplast (Kumar et al., 2011, Xu and Moller, 2011, Ali and Nozaki, 2013). Of these pathways, it has been observed that even organisms with an MRO have maintained the mitochondrial ISC pathway, often in addition to CIA or SUF (Kumar et al., 2011, Xu and Moller, 2011, Tsaousis et al., 2012, Ali and Nozaki, 2013).

The mitosome of *C. parvum* appears as circle or oval, five-hundred nanometres in diameter, encased in a dual membrane. The only mitochondrial proteins that have thus far been localised to this organelle are the heat shock proteins 60 (hsp60) and hsp70 (Mogi and Kita, 2010, Ali and Nozaki, 2013, Makiuchi and Nozaki, 2014, Alcock et al., 2012, Putignani et al., 2004). The *C. parvum* mitosome also appears to be completely absent of the typical mitochondrial proteins such as cytochromes, with only the Alternative Oxidase (AOX) remaining of any complex Electron Transport Chain (ETC) biosynthetic pathway (Roberts et al., 2004, Suzuki et al., 2004). *In-silico* predictions and preliminary functional studies also describe the presence of a complete ISC pathway, as is also typical of mitosomes (Ali and Nozaki, 2013, LaGier et al., 2003). Whilst genome sequencing has also identified the presence of the CIA machinery, it appears to have lost (or never inherited) the SUF pathway that other Apicomplexa maintain within the apicoplast (Kumar et al., 2011, Abrahamsen et al., 2004). Current understanding of the mitosome within *C. parvum* is limited and based primarily on *in-silico* predictions, with the only experimental evidence being the localisation of recombinant *C. parvum* ISC components to yeast mitochondria, though no such experiments have been performed in *C. parvum* itself (Figure 1-4) (LaGier et al., 2003).

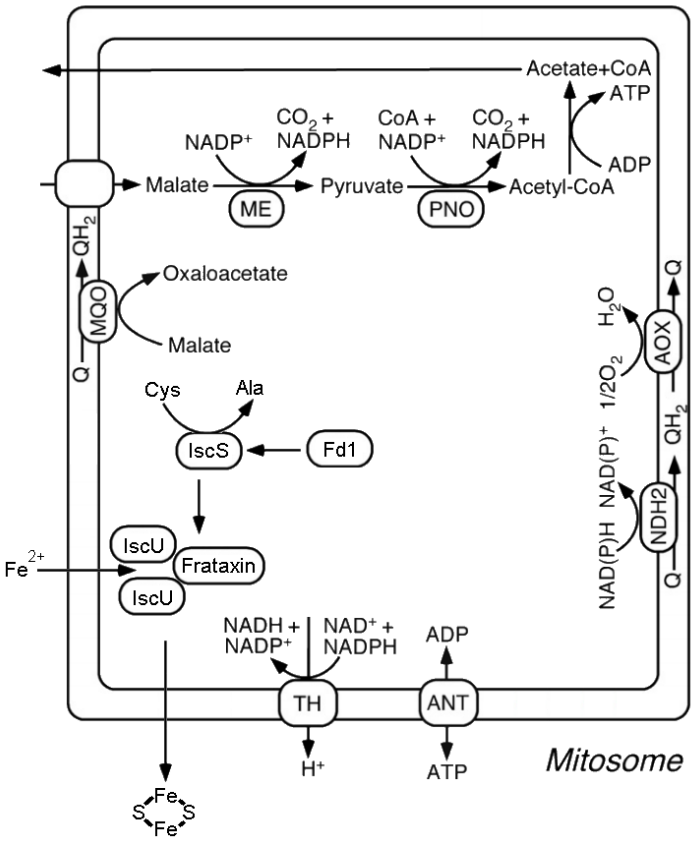

Figure 1-4: Metabolic pathways of the 'typical' mitosome. The metabolic content of the mitosome within *C. parvum* as predicted so far via the published genome has both a basic glycolytic and ISC iron-sulphur cluster biosynthesis pathways, with putative mitochondrial/mitosomal targeting sequences. Mitochondrial targeting of recombinant Isu1/2 (IscU), Ferrodoxin (Fd1) and Nfs1 (IscS) has been confirmed within yeast expression systems although no experimental evidence exists replicating this in a mitosome. (Adapted from Mogi and Kita, 2010)

As can be expected from a group so lacking in apparently essential organelles, members of the Cryptosporidia are obligate parasites, entirely reliant on scavenging components from a host to survive.

1.5.2 Metabolism of *C. parvum*

Most of that which is currently understood of the metabolic pathways of *C. parvum* is based on *in-silico* predictions, from genome sequences that have been published over the last decade (Abrahamsen et al., 2004). The data has produced numerous interesting observations regarding the metabolism of *C. parvum*, a significantly reduced ability to produce essential biological compounds *de novo* (Rider and Zhu, 2010).

Perhaps foremost amongst this is that *C. parvum* is incapable of synthesising fatty acids, with the absence of an apicoplast resulting in the loss of the type II Fatty Acid Synthases (FAS) typically found in the Apicomplexa. *C. parvum* does, however, maintain a cytosolic, type 1 fatty acid synthase (CpFAS1), although it appears to be incapable of *de novo* fatty acid synthesis (Zhu et al., 2000). Functional analysis of CpFAS1 revealed that it instead acted as an elongase, showing a preference for 16 carbon chains, to which CpFAS1 has been shown to add an additional six carbons (Zhu, 2004, Zhu et al., 2004, Zhu et al., 2010). The lack of *de novo* fatty acid synthesis is unusual, considering the high fatty acid content of the parasite's environmentally resistant oocyst stage (Jenkins et al., 2010). This suggests that the parasite is capable of scavenging fatty acids from either the host cell or extracellular matrix surrounding it, which is not unusual for a parasite (Mazumdar and Striepen, 2007). This hypothesis is further supported by the nature of the individual fatty acid compounds found within the parasite; whilst both 12 and 14 carbon long chains (dodecanoic acid and tetradecanoic acid) have been identified the oocyst wall consists exclusively those fatty acids CpFAS1 is capable of 'producing'.

Additionally, *C. parvum* appears to be completely incapable of synthesising core biological compounds such as the amino acids Valine and Leucine, with limited ability to produce others such as Glycine and Tryptophan

Table 1-2) (Rider and Zhu, 2010, Abrahamsen et al., 2004).

Table 1-2: Essential and non-essential amino acids of *Cryptosporidium parvum*. Although *C. parvum* lacks the metabolic functions to produce most of amino acids *de novo*, it retains some limited capacity to produce most of the uncharged and a single hydrophobic amino acid through 1 or 2 step processes. This list is split into two major columns: essential and non-essential amino acids. It is important to note, that except for proline, *C. parvum* cannot produce any amino acid without obtaining already complex molecules from an external source (Zhu and Guo, 2014, Rider and Zhu, 2010).

C. parvum's Ability to synthesise AA *de-novo*

Metabolically Capable	Limited capability (2 upstream steps or less)	No capability	
Proline	Asparagine	Histidine	Isoleucine
	Glutamine	Lysine	Leucine
	Serine	Arginine	Valine
	Tryptophan	Glutamate	Tyrosine
Colour Key:	Glycine	Aspartate	Phenylalanine
Charged		Threonine	Methionine
Uncharged		Cysteine	Alanine
Hydrophobic		Selenocysteine	

The trend continues into folate biosynthesis. Traditionally targeted during drug design against Apicomplexa, as a means of interrupting pyrimidine synthesis, it appears that the *C. parvum* maintains only two enzymes within the pathway (Abrahamsen et al., 2004). Of the two folate enzymes that are maintained by *C. parvum*, a putative phosphodiesterase/alkaline phosphatase D appears to be either plant or bacterial in origin, a common theme amongst the Apicomplexa in general, which appear to have benefited from numerous horizontal gene transfer events. Similar blast searches also reveal that

several components of the glycolytic pathway within *C. parvum* are also more likely to be bacterial or plant in origin.

C. parvum also displays several interesting adaptations within its ATP biosynthetic pathways. A mitochondrial-type AOX, which is not found in any other apicomplexans, has been expressed and characterised from the *C. parvum* (Putignani et al., 2004, Mogi and Kita, 2010, Roberts et al., 2004, Suzuki et al., 2004). In *C. parvum* as well as much of *Cryptosporidium* species AOX is acting as the terminal enzyme in the electron transport chain, donating an electron to the final oxygen in the pathway.

Traditionally, AOX is often found as a part of damage mitigation pathways in a variety of organisms, particularly obligate anaerobes, as it coveys resistance to oxygen free radical formation by curtailing the electron transport chain at complex II (Mogi and Kita, 2010, Williams et al., 2010, Saha et al., 2016, Dahal and Vanlerberghe, 2017). Similarly, *C. parvum* also maintains a pyruvate-$NADP^+$ oxidoreductase (PNO), though most apicomplexans do not (Rotte et al., 2001, Mogi and Kita, 2010). Interestingly, outside of the Apicomplexa, *C. parvum* becomes less unique as the parasitic early dinoflagellate *Perkinsus marinus* and the photosynthetic chromerid *Vitrella brassicaformis* both share homology with CpAOX and the genome of *V. brassicaformis* also contains a significantly similar (E value of $2e^{-92}$) sequence to the putative phosphodiesterase/alkaline phosphatase D.

From this it is clear that *C. parvum* is greatly lacking several key biological pathways, often completely incapable of producing essential biochemical components. This makes it clear as to why *C. parvum* cannot survive as a facultative parasite; however, it does not explain how *C. parvum* compensates for these deficiencies. To understand this, it is important to consider the interactions between host and parasite on a molecular level.

1.5.3 Host-parasite interactions

During host cell invasion by a sporozoite, *C. parvum* has been observed inducing an array of physiological effects upon the host cell, this preliminary aspect of the infection is so far, the most studied and well understood of the host-parasite interactions in *C. parvum* infections. Among the reactions determined to be necessary for successful host-cell

invasion are host-cell tyrosine phosphorylation, which allows the recruitment of host-cell actin to the site of invasion (Elliott and Clark, 2000, Chen et al., 2003). *C. parvum* has also been shown activating host-cell Cdc42, a component of membrane import via endocytosis, through the recruitment of phosphatidylinositol 3-kinase to the host-parasite interface during invasion, the inhibition of which was shown to significantly reduce the parasite's ability to invade the host cell (Chen et al., 2004a, Chen et al., 2004b). Inhibition of host-cell Galactose-N-acetylgalactosamine (Gal/GalNAc) has also been shown to prevent parasite invasion of host-cells and a putative Gal/GalNAc binding lectin has recently been localised to the apical region of the *C. parvum* sporozoite (Joe et al., 1994, Bhat et al., 2007, Edwinson et al., 2016). There have been numerous additional proteins/molecules identified which appear to be involved in some manner with host-cell invasion, including multiple Calvin Cycle proteins, Lectins and several glycoproteins such as GP900 and GP40/15, although many of their exact roles and/or importance remain largely unexplored (Petersen et al., 1997, Barnes et al., 1998, Bonnin et al., 2001, Bhat et al., 2007, Sturbaum et al., 2008, Chatterjee et al., 2010).

Once established within the host cell, plaques consisting of host f-actin and α-actinin were described within the host membrane, localised to the interface with the PV, although other typical components of actin utilisation were unusually absent (Elliott and Clark, 2000). This accumulation of actin at the host-parasite interface is not observed in similar PV forming parasite *Toxoplasma gondii*.

Once established within a host-cell, *C. parvum* undergoes merogony and the remainder of its life cycle, alternating through various extra and intracellular stages (Figure 1-2) (Leitch and He, 2012). Although, as previously mentioned *C. parvum* cannot produce many essential metabolic compounds *de novo*, which suggests that they are instead scavenged from the host during the intracellular stages. Keeping with the theme of *C. parvum*, however, experimental evidence of metabolite scavenging remains largely at the *in-silico* or even purely hypothetical level.

Whilst the exact nature of which compounds are scavenged remains largely unexplored, investigations into how the intracellular stages interact with the host have provided some insight into the host-parasite interactions at this stage. Ultra-structural analysis of the parasites routinely reveal that *C. parvum* never makes direct contact with the host cytoplasm, instead residing within the PV, and as such may possess some means of

'channelling' scavenged nutrients through it, into the parasite cytoplasm (Current et al., 1986, Arrowood, 2002, Borowski et al., 2010, Karanis and Aldeyarbi, 2011, King et al., 2011, Leitch and He, 2012, Muller and Hemphill, 2013). Observation via electron microscopy has revealed a potential candidate for this role, termed the 'feeder organelle' due to its proposed function, consisting of an unusual highly folded membrane that forms between the host membrane and PV (Leitch and He, 2012). However, unlike other Apicomplexa, the PV of *C. parvum* has not been observed penetrating the host cytoplasm, remaining ultimately extra-cytoplasmic.

Attempts to characterise the metabolic activity of the feeder organelle have revealed an ATP-binding cassette (ABC) protein CpABC1, with sequence and structural homologies suggesting a role in ion and possibly organic anion transport (Zapata et al., 2002, Sauvage et al., 2009, Perkins et al., 1999).

Preliminary investigations into the effects *C. parvum* infections have on patient metabolomes have also provided some insight into the nature of the host-parasite interaction. Of the observations made, one of note is the change in Hexadecanoic acid content of host faecal samples (Ng Hublin et al., 2012, Ng Hublin et al., 2013). Hexadecanoic acid is the shortest chained fatty acid *C. parvum* is capable of metabolising, as the preferred substrate of CpFAS1, routinely metabolised into the 22 chained Docosanoic acid (Zhu et al., 2010, Zhu et al., 2000).

Despite this, knowledge regarding *C. parvum* remains scattered. Investigations into its cellular biology are marred by ineffective culturing systems and this in turn makes it difficult to properly interpret the results of experiments such as the metabolomics just discussed.

1.5.4 Culturing *C. parvum*

The limits in our knowledge regarding this particular parasite, as well as the restrictive pool of available medications are in large part due to the state of available culturing techniques (Striepen, 2013). *C. muris* and *C. hominis* have shown some progress in *in-vitro* culture systems, especially those of a host-cell-free nature and over the last 40 years a multitude of tissue based cultures have been developed to allow the growth of *C. parvum*

in-vitro also (Hijjawi et al., 2010, Upton et al., 1994, Meloni and Thompson, 1996, Arrowood, 2002, Hijjawi, 2010, Yin et al., 2010, Karanis and Aldeyarbi, 2011, King et al., 2011, Muller and Hemphill, 2013, Miller et al., 2017, Morada et al., 2016). To date *C. parvum* culture relies primarily on infected HCT-8 cell lines or variations of the previously identified CACO-2 or MDCK cells. Unfortunately, these solutions bring with them numerous crippling flaws, such as short culture life-spans and aberrant life-cycles. Recent advances in the field have seen the introduction of more advanced culturing systems, such as simulated micro-gravity and hollow fibre/organoid approaches, in attempts to overcome the inherent issues of these cell lines with promising results (Morada et al., 2016, Alcantara Warren et al., 2008).

Despite these advances, however, the culturing systems are still insufficient for most research purposes and the most reliable systems that exist at this time for *C. parvum* production require the continued infection of immune-suppressed or naive animals, typically the young of livestock such as cows or sheep, or laboratory animals such as mice (Girouard et al., 2006, Striepen, 2013).

This has resulted in a seasonal, expensive and labour-intensive supply method, with heavy reliance on animals in an age of rapidly declining tolerance for animal experimentation.

1.6 The hypothesis

As covered in the preceding introduction, *C. parvum* is among one of the more unique members of the eukaryotes and especially the apicomplexans, eschewing traditional levels of genetic and organellar conservation for a highly streamlined and presumably efficient cellular biology. These traits, combined with the presence of a largely unexplored organelle, a potentially basal phylogenetic routing among the apicomplexans, in addition to *C. parvum's* rising global medical importance, show there has never been a more important time to study this parasite.

Therefore, it is the purpose of this thesis to provide the building blocks and preliminary experimental evidence required to establish *C. parvum* as a model organism for the Cryptosporidia and potentially the Gregarina and Apicomplexa. This will be achieved through the exploration of three key hypothesis or objectives, as listed below:

1. *C. parvum* can be successfully cultured on a scale, both volume and time-wise, conducive to broad experimentation. Because of the production levels, the developed culturing technique will allow unprecedented exploration of the parasites' genetic, metabolic and cellular biology as well as opening new routes into exploring the genetic tractability of the currently difficult to modify organism.

Once established, the culture will allow the exploration of *C. parvum's* adaptations to parasitism and the role played by the mitosome. These concepts will be explored via the following hypotheses:

2. The parasitic adaptations of *C. parvum* have led to the development of specific host-parasite interactions, which directly affect the host's metabolic machinery, including host mitochondria. The identification and cataloguing of these effects will allow for metabolomics-based diagnosis of the disease. Furthermore, this work will shed light on the role of host-specificity and the adaptations *C. parvum* maintains that provide it with a significantly larger repertoire of potential hosts compared with almost any other apicomplexan.
3. The ISC pathway is present and active within the mitosome of *C. parvum*. Specifically, the components: IscS, IscU and Frataxin. This would show for the first time a metabolic function for the relict mitochondrion of *C. parvum*.

The results of these theories and how they were tested is described in the following chapters of this thesis, in addition to suggestions how they may be further improved upon and explored in subsequent investigations.

Chapter 2 Materials and Methods

2.1 Cell culture

During the initial experiments in *3.3* the following cell lines were used: COLO-680N (Human oesophageal squamous-cell carcinoma), obtained from Cell Line Services, Eppelheim, Germany; DLD-1 (Human colon adenocarcinoma), KYSE-30 (Human oesophageal squamous-cell carcinoma) and HCT-15 (human colorectal adenocarcinoma), obtained from DSMZ, Braunschweig, Germany; SJSA-1 (osteosarcoma) and HCT-8 (ileocecal colorectal adenocarcinoma), obtained from ATCC, Manassas, VA, US, Cat No. CRL-2098 and CCL-244, respectively; MKN-1 (gastric carcinoma), obtained from JCRB Cell Bank, Osaka, Japan.

Cells were cultivated in RPMI-1640 medium (Sigma-Aldrich, Cat No R8758) supplemented with 10 % foetal bovine serum (Sigma-Aldrich, Cat No F8084), 100 U/mL penicillin, 100 µg/mL streptomycin and 250 ng/mL amphotericin B (Antibiotic Antimycotic solution, Sigma-Aldrich, Cat No A5955) at 37 °C and 5 % CO_2. All experiments used the COLO-680N cell line unless otherwise stated. Experiments using the standard RPMI-1640 + FBS +Antibiotic mixture are referred to as using "complete" RPMI-1640 in the rest of this thesis.

2.2 Sources of *Cryptosporidium* oocysts

Several species and strains of *Cryptosporidium* were used for the experiments described hence. Their origins are as follows:

Initial studies were performed on *Cryptosporidium parvum* oocysts provided by the Creative Science Company pre-purified and identified as the 'Moredun' strain, which was originally acquired from the gastrointestinal contents of a dead red deer calf (*Cervus elaphus*), sourced from the Glen Saugh experimental deer farm (Scotland, UK) in 1987 (*Moredun strains of Cryptosporidium parvum* 2015).

C. parvum Iowa II was obtained from Bunch Grass Farm in the United States, isolated from infected calves and is a commercially available species/strain that is frequently used in *C. parvum* experimentation (Girouard et al., 2006, Sturbaum et al., 2008)

C. parvum, Weru strain was supplied courtesy of Dr. Martin Kváč of the Institute of Parasitology Biology Centre CAS, Czech Republic. The Weru strain was originally isolated from an infected human patient and subsequently maintained by passing through SCID mice.

C. hominis was supplied courtesy of Prof. Rachel Chalmers from the *Cryptosporidium* Reference Unit, Singleton Hospital of NHS Wales. The *C. hominis* used in this experiment was from an original stock purified from a patient's stool sample.

2.3 Cell line infections

Infections of cell cultures were performed at 1 x 10^5 oocysts per 10ml of cultured cells in a 25 cm^2 cell culture flask, once the cell culture density had reached 70% coverage of the flask surface (70% confluent) unless otherwise stated.

Excystation was achieved by adding 100 µl of 0.01% Trypsin and 400 µl of 0.5 % Sodium Hypochlorite to a pellet containing the desired number of oocysts, as had been established by prior publications (Upton et al., 1994, Gold et al., 2001). The oocyst suspension was incubated in a 37°C water bath for one hour, with intermittent vortexing. The excystation procedure was monitored by phase contrast microscopy, using a haemocytometer and stopped when visible sporozoites exceeded 80 % of the theoretical maximum (4x the original number of oocysts present per sample). Samples were pelleted at 2,200 *g* for eight minutes, and suspended in cell culture medium, prior to cell infection. 24-26 h post-infection, T25 flasks were washed twice with 10 ml of 1x PBS, to remove un-excysted oocysts and remaining sporozoites. Fresh media was then added. To ensure that extracellular parasites (included non-excysted oocysts) had been efficiently removed following the wash procedure and that no traces of *Cryptosporidium parvum* could be found, washes and final media were subjected to PCR analysis.

2.4 Purification of Cryptosporidium from infected cultures

Growth media from infected cultures and a subsequent 5 mL wash (with 1x PBS) were collected. The suspensions were centrifuged at 500 *g* for 5 minutes to remove host cells and debris. The supernatant, which contain the oocysts, was then transferred to fresh tubes, and the oocysts were pelleted by centrifugation at 2,100 *g* for 8 minutes. The pellets were re-suspended in 1 mL of 1x PBS and carefully laid on top of 9 mL of saturated (37%) sodium chloride solution, in a 15 mL Falcon tube. These two layers were then topped up with 1 mL of sterile water before being centrifuged at 2,100 *g* for 8 minutes. This centrifugation steps resulted in the formation of a milky white phase between the PBS and salt layers, which contained the live oocysts. Using this methodology, empty and non-viable oocysts fall to the bottom of the tube during centrifugation. The oocysts were carefully pipetted from the interface. Because, the isolated oocysts may contain a carryover from the sodium chloride solution, 9 mL of 1x PBS were added to dilute the mixture and the oocysts were pelleted again at 2,100 *g* for 8 minutes. The pipetting/ dilution steps were repeated twice.

2.5 Cryopreservation and resuscitation of infected cells

Medium was discarded from infected cell cultures and the cell monolayer was washed once with 1x PBS. Cells were then trypsinised and suspended in 9 mL of cell culture medium prior to centrifugation at 500 x g for 5 minutes at 4°C. The supernatant was discarded, and the pellet suspended in 10 mL of cryo-media (RPMI-1640, 20% FBS, 10% DMSO). The cell suspension was then aliquoted into 2 mL samples in cryo-tubes and stored at -80°C inside a Mr. Frosty TM freezing container (ThermoFisher Scientific, Cat No 5100-0001). The cells were left for a minimum of two weeks before resuscitation. To resuscitate cells, cryo-tubes were removed from the freezer and immediately thawed at 37°C in a water bath for 5 minutes. The cell suspension was then added to 8 mL of cell culture medium, mixed gently, and then centrifuged at 500 x g for 5 minutes at 4°C. The

supernatant was discarded, and the cell pellet suspended in 10 mL of pre-warmed cell culture medium.

2.6 DNA extraction from oocysts and infected cultures

COLO-680N cells infected using the protocol above, were washed twice with 1x PBS, prior to DNA extraction. Samples were taken six hours post infection and subsequently on days 1, 2, 3, 4, 5, 6, 9 and 12.

For COLO-680N cells and epicellular *Cryptosporidium* stages, DNA extraction was performed using the Qiagen DNeasy Blood and Tissue kit (Qiagen, Cat. No 69504) following the manufacturer's instruction. For *C. parvum* oocysts, samples were collected from cell culture supernatants as described above. Then, DNA extraction was performed using the Omega E.Z.N.A. fungal extraction kit (Cat. No. D3390-1) following the manufacturer's instructions. Extracted DNA was quantified using a NanoDrop 1000 Spectrophotometer, by placing 2 µl drops of the sample on the detector and observing the readout obtained, samples were restricted to those that gave relatively high purities for wavelengths between 260/280 (~1.7-1.8) to reduce the possibility of unreliable results from RNA/Protein contamination.

2.7 PCR amplification

PCR reactions were performed with the following general parameters:

For a reaction total volume of 50µl: 10 µL PCR 5x Flexibuffer (Promega M8291), 2 µL MgCl2 (1µM), 1 µL dNTPs (10 µM), 2 µL of forward primer and 2µL of reverse primer (10 µM)(See Table 2-1 for combinations used), 31.75 µL H_2O, 0.25 µL of GoTaq G2 Hot Start Polymerase (Promega, Cat. No. M740A) and 1 µL of DNA (concentration varied dependant on sample source, final total DNA content did not exceed 1 µg).

PCR set up conditions were as follows: 1 cycle of 95 °C of initial denaturation for 5 minutes, followed by 36 cycles of 35 seconds denaturation steps at 95 °C, 30 second

annealing steps (see Table 2-1 for temperature) and an elongation step at 72 °C (see Table 2-1 for time). Then a final 10 minutes elongation step at 72 °C.

Table 2-1: PCR Primers. Custom Nucleotide sequences of the PCR primers used in Chapter 5 to produce recombinant ISC structures in a selection of plasmids. Sequences are colour coded to highlight GC clamp (blue) and restriction site (red). Each was designed based on sequences obtained from using Blasting yeast ISC sequences against published *C. parvum* genomes.

Label	Sequence	Species	Target Gene	Restriction site	Intended plasmid	Target organism
CpFrat_Nde1F	CCGGGCATATGAATTCAATAAAATTATTAAAC	*C. parvum*	FXN	Nde1	Pet14b	*Escherichia coli*
CpFrat_BamH1R	GCGCGGATCCTTATAAATTGACATGTATTCCAGTAGC	*C. parvum*	FXN	BamH1	Pet14b	*Escherichia coli*
CpIscS_Nde1F	CGGCATATGATCGTTCACAGATATTGCAGGC	*C. parvum*	ISCS	Nde1	Pet14b	*Escherichia coli*
CpIscS_BamH1R	GCGGATCCTCACGTCCATTTGAGTGAATCCTC	*C. parvum*	ISCS	BamH1	Pet14b	*Escherichia coli*
CpIscU_Nde1F	CGGCATATGTTGCAATTAAGACAGCTTATCG	*C. parvum*	ISCU	Nde1	Pet14b	*Escherichia coli*
CpIscU_BamH1R	CCGGATCCTCATGATTTGAGCTGTTTGTCTTG	*C. parvum*	ISCU	BamH1	Pet14b	*Escherichia coli*
Cp_IscSN_Xma1_F	GCATCCCGGGATGATCGTTCACAGATATTG	*C. parvum*	ISCS	Xma1	pBEVY-1	*Saccharomyces cerevisiae*
Cp_IscSN_Sac1_R	GCATGAGCTCTCACGTCCATTTGAGTGAATC	*C. parvum*	ISCS	Sac1	pBEVY-1	*Saccharomyces cerevisiae*

The resulting amplified DNA was visualised on a 1.8 % agarose-TAE gel and stained with ethidium bromide.

2.8 Electron Microscopy (EM)

0.5 cm diameter, 200 µm thick aclar film discs (Honeywell international Inc. 5042525) were sterilised by UV light/Ozone exposure for 30-60 minutes in a sterilised tissue culture cabinet. The disks were then deposited into 24-well plates. For each well, 1 mL of COLO-680N cells at a concentration of 2.4 x 10^4 cells/ml was added. Once the cells had reached 50 to 60 % confluency, the cultures were infected with 50,000 *C. parvum* oocysts, giving an approximate MOI of 0.4. On days 6, 7, 8, 9, 12, the supernatant was removed, and cells were washed with 200 mM cacodylate buffer (pH 7.4). The buffer was aspirated and 1 mL of fixative, containing 2.5% Glutaraldehyde in 100 mM cacodylate buffer (pH 7.4), was then added and left at 4oC overnight. Next, each well was washed twice (10 minutes) with cacodylate buffer prior to staining with 1 mL of 1% osmium for 30 minutes at room temperature. The samples were washed and dehydrated through an ethanol series (30 %, 50%, 70 %, 90% and twice 100%) before being embedded in Agar (Agar Scientific) low viscosity resin.

Sections were cut initially with a glass knife and ultrathin sections of 65 nm were cut with a DiATOME™ diamond knife on a RMC-MTXL ultramicrotome. The sections were

placed onto 400 mesh uncoated copper grids. The grids were then stained for 45 minutes in 4.5 % aqueous Uranyl Acetate, washed again, and subsequently stained for 7 minutes with Reynold's lead citrate. Stained grids were then dried for 10 minutes before being visualised with a Jeol 1230 Transmission Electron Microscope at 80kV equipped with a Gatan Multiscan digital camera.

2.9 Fluorescence microscopy

50-60% confluent cultures were infected with *Cryptosporidium* oocysts in 2-well permanox base chamber slides (Sigma-Aldrich, Cat No C6682), with varying oocyst numbers dependant on the nature of the experiment. Detection was achieved through extensive use of Indirect Immuno-fluorescence assays (IFA) and a variety of fluorophores (Table 2-2)

Table 2-2: Fluorophore Emission and Excitation peaks. A variety of fluorescent antibodies and stains were used in the experiments to detect and visualise the infection and a variety of organelles. This list encompasses the various wavelengths utilised by these fluorophores and the colour used to represent them in the relevant figures.

Stain/Anti-body	Target/s	Excitation peak	Emission peak	Colour in Figures
DAPI	Nuclear material	350	470	Blue
Crypt-a-glo	Cryptosporidium oocyst wall protein	490	525	Green
SporoGlo	Apicomplexan sporozoites	490	525	Green
Propidium Iodide	Nuclear Material	535	617	Red
CMXRos	Mitochondria	580	600	Red
VVL	Various parasite proteins	490	525	Green
Anti-rabbit	rabbit derived antibodies	557	576	Red
Anti-rat	rat derived antibodies	557	576	Red

2.9.1 Infection quantification

At harvesting points, cultures were washed with 1x PBS and then fixed in methanol for 10 minutes at room temperature. Next, the methanol was removed, and the cells were permeabilised with 0.002 % Triton-X100 in 1x PBS at room temperature for 30 minutes. Cells were then washed three times prior to incubation for 1 hour with FITC conjugated *Cryptosporidium*-specific antibodies (Crypt-a-glo, WaterborneTM, dilution 1:10; SporoGlo, WaterborneTM, dilution 1:10), non-conjugated anti-CpClec (dilution 1:60), propidium iodide (500 nM), or FITC conjugated Vicia Villosa lectin (VVL, 0.5µg/ml).

Cells were washed a further three times with 1x PBS and then mounted with an aqueous mounting medium. This was done using either Fluromount (Sigma-Aldrich, Cat No F4680, with no DAPI) or Fluoroshield (Sigma-Aldrich, Cat No F6057, with DAPI). Slides were visualised by fluorescence microscopy using an Olympus 1X82 or Zeiss Elyra P1 confocal microscope.

On ten days post-infection, the supernatant of infected cells (containing oocysts and COLO-680N cells and debris) was filtered through 40 µm nylon Corning cell strainers. The flow through was spun down at 2,000 x g for 8 min. The supernatant was then discarded, the oocysts and debris were resuspended in 100 µl 1x PBS and added on poly-L lysine coated slides. The slides were rinsed once in 1x PBS, then the oocysts were fixed with 4% paraformaldehyde for 30 min. The slides were rinsed one more time in 1x PBS and blocked overnight in 3% filtered BSA. The slides were washed once in 1x PBS and 1 drop of FITC conjugated Crypt-a-glo (Waterborne inc.) was added for 1 hour. The slide was quickly rinsed and mounting media containing DAPI (Sigma-Aldrich, Cat No F6057) was then added prior to covering with coverslip and sealing with nail polish.

2.9.2 Cellular biology and localisation

COLO-680N cells were used exclusively and infected with $1x10^6$ *Cryptosporidium* oocysts. For comparison, control non-infected cells were seeded on the same day. Following 48 hours post-infection the supernatant was replaced by fresh media for all samples.

At seven and ten days post infection the media was aspirated from the cultures and washed twice with 1 x PBS. The media was removed and replaced with further pre-warmed

complete RPMI-1640 (1% Antibiotic/Antimycotic), containing 3.5% formaldehyde, for 15 minutes at 37°C as per the manufacturer's protocol.

For mitochondrial observation fresh, pre-warmed, serum free RPMI-1640 (Sigma Aldrich, Cat. No R8758) (1% Antibiotic/Antimycotic) containing 200 nM ThermoFisher Mitotracker Red CMXRos (Molecular probes; Cat. No M7512), was added to the wells and incubated in the dark at 37°C for 45 minutes prior to fixation.

The cells were then briefly permeabilised with 0.2% Triton-x100 in 1x PBS for 10 minutes, washed twice with 1x PBS and four drops of FITC conjugated SporoGlo™ (WATERBORNE, INC) or Crypt-a-glo (WATERBORNE, INC) added, with incubation at 37°C for a further 45 minutes. The final sample was then washed three times with PBS, dried and Fluoroshield™ with DAPI (Sigma Aldrich, Cat. No F6057) or ProLong Gold Antifade mount (Sigma Aldrich, Cat. No P10144) was added before applying a glass coverslip and sealing. Slides were visualised by fluorescence microscopy using an Olympus IX82 or Zeiss Elyra P1 confocal microscope.

2.10 Atomic Force Microscopy (AFM)

1 x 10^5 oocysts were suspended in 25 µL 1x PBS, pipetted onto a freshly cleaved mica sheet pre-mounted on a magnetic specimen disc (Agar scientific) and left to sediment for an hour at 4oC in a humidified chamber. Oocysts were then fixed for 1h with 25 µL of 5% Glutaraldehyde in 1x PBS. Samples were then washed twice with 1x PBS, once with deionised water and air-dried at room temperature in a dust free area for 2 hours. Samples were then washed twice more with deionised water, left to air-dry again followed by a final drying step using a gentle stream of nitrogen.

Samples were analysed by Atomic force microscopy (AFM) using a Bruker multimode 8 (Bruker Corporation, Massachusetts) scanning probe microscope with a Nanoscope V controller. The samples were imaged using the ScanAsyst peak force tapping mode, with RTESPA silicon cantilever probes (Bruker Corporation, Massachusetts), which have a nominal spring constant of 40 N/m and a nominal tip radius of 8 nm. Data collection and processing was performed using the Nanoscope software (version 1.40, Bruker Corporation, Massachusetts). Images were scanned over a surface area of at least 10 x

10 μm at a resolution of 2048 x 2048 pixels. The scan rate was 0.2 Hz. Images were processed using the Nanoscope Analysis software (version 1.40, Bruker Corporation, Massachusetts) and custom scripts written in MATLAB to remove the sample surface tilt and scanner bow. 3-D representations of the data in height and peak-force error channels were subsequently rendered in Nanoscope Analysis.

2.11 MALDI-ToF Mass Spectrometry – Lipid analysis of oocysts

Aliquots of 1.25 x 10^5 or 2.5 x 10^5 cattle-produced or COLO-680N-produced oocysts suspended in 1x PBS were pelleted at 2,100 x g for 8 minutes. A matrix buffer was prepared by dissolving 20 mg/mL (saturated) alpha-cyano-4-hydroxycinnamic acid matrix into a 40% acetonitrile 0.15% trifluoroacetic acid, which was then placed in a sonicating water bath for 15 minutes. Undissolved matrix was subsequently removed by centrifugation at 16,000 x g for 10 minutes. The oocysts were re-suspended in 50 μL of matrix buffer. Samples were left to incubate in suspension for 30 minutes. The samples were then re-suspended by gently tapping the tubes before 1μL samples were added to 384 MTP ground steel MALDI-ToF plate wells (Bruker) in triplicate. Samples were allowed to air dry before the plate was placed into the MALDI-ToF mass spectrometry instrument (Bruker UltrafleXtreme).

For negative polarity compounds the following set-up was used; Laser frequency: 2000 Hz;

Ion sources: (1) 19.94 kV, (2) 17.79 kV; Lens 6.09 kV; Reflector 1: 21.22 kV, 2: 10.74 kV; Suppress at 500 Da; Pulsed ion extraction 80 nS; Matrix Suppression mode-Deflection; Range 600-2000 Da; Sample rate 1 Gs/s; For each sample 7500 shots were summed and saved.

For positive polarity compounds the following set up was used; Laser frequency: 2000 Hz;

Ion sources: (1) 24.92 kV, (2) 22.27 kV; Lens 7.47 kV; Reflector 1: 26.53 kV 2: 13.39kV;

Suppress at 500 Da; Pulsed ion extraction 80 nS; Matrix Suppression mode- Deflection; Range 600-2000 Da; Sample rate 1 Gs/s; For each sample 7500 shots were summed and saved.

The mass spectrometry data files were exported from the Bruker Flex Analysis software in ASCII format for pre-processing in MATLAB prior to the application of PCA 41.

2.12 MALDI-ToF Mass Spectrometry of infected cultures

Cell cultures were trypsinised and cell numbers adjusted to 3 x 10^4 cells/mL. 1 mL of each sample was then transferred into a fresh tube and pelleted at 500 x g for 5 minutes at 4°C. The samples were then mixed in the alpha-cyano matrix as per the lipidomics protocol.

To analyse the cell pellets, the MALDI-ToF Mass Spectrometry instrument (Bruker UltrafleXtreme) was calibrated before use with the commercially available Bruker Calibration Standard 1 protein mixture (Bruker, part number 206355). The spectra of the intact cell pellets were then collected using the MALDI-ToF Mass Spectrometry instrument settings described below and the inbuilt calibration program for this calibration mixture provided with the instrument.

The spectra were collected using the following settings on the mass spectrometer: Linear mode; Laser frequency: 500 Hz.

A positive polarity was implemented with the following set up was used; Ion sources: (1)

24.93 kV, (2) 23.08 kV; Lens 7.49 kV; Suppress at 5000 Da; Pulsed ion extraction: 400 nS;

Range 5000–60,000 Da; Sample rate 0.13 Gs/s; Resolution enhanced 100 mV electronic gain; Smooth high. For each sample 3600 shots were summed and saved.

The mass spectrometry data files were exported from the Bruker Flex Analysis software in ASCII format for pre-processing in MATLAB prior to the application of PCA1.

2.13 Scanning electron microscopy (SEM)

Samples were prepared using the same method as with the specimens for AFM with the exception that instead of the mica the sample was deposited on a 15 mm SEM carbon tape disc. The samples were visualised in a Hitachi s3400 variable pressure SEM at 50 pa and 5 kV.

2.14 Real-time cell viability analysis

Cell viability and proliferation was determined by electrical impedance monitoring using the xCELLigence system (Acea Biosciences, San Diego, CA, US). 16 well xCELLigence plates, containing 100 µl of complete RPMI 1640 were incubated at 37°C on the xCELLigence system for 30 minutes prior to initial calibration. Non-negative-control wells were then seeded with $3x10^4$ COLO-680N cells in 100 µl of prepared, complete RPMI-1640 negative controls had 100µl of additional empty media). Recesses present between the wells were topped up to approximately 75% full with pre-warmed PBS at 37°C. The plates were again incubated for a further 30 minutes before executing the xCELLigence programme. The programmes used were monitored and altered during experimentation to either elongate or prematurely end the observation of the 'cell index' depending on whether a continued growth trend or early complete senescence was observed. The results were exported to an excel spreadsheet and the data analysed.

2.15 Animals and infection

For this study, seven-day old BALB/c mice (n=9) were infected at the Czech Institute of Parasitology, Biology Centre using pre-established protocols detailed in Meloni and Thompson, totalling three mice per condition (Meloni and Thompson 1996). Three separate groups were used, one infected with 100,000 oocysts of *C. parvum* Iowa II, another group was infected with 100,000 oocysts of the *C. parvum* Weru isolate and the

final group were given a PBS control. The groups were kept physically spate and never allowed to interact. Infection was monitored from Day-1 post-infection by aniline-carbol-methyl violet staining of faecal smears staining of faecal smears (Figure 2-1), in addition to an antigen based strip test "RIDA®QUICK Cryptosporidium", supplied by R-Biopharm (Milacek and Vitovec 1985). At ten days post-infection, the mice were euthanized by cervical dislocation and decapitation. This study was carried out in accordance with Act No 246/1992 Coll. of the Czech Republic. The protocol was approved by the 'Committee for Animal Welfare of Biology Centre Czech Academy of Science and the veterinary administration authorities with regards to the animal experiments.

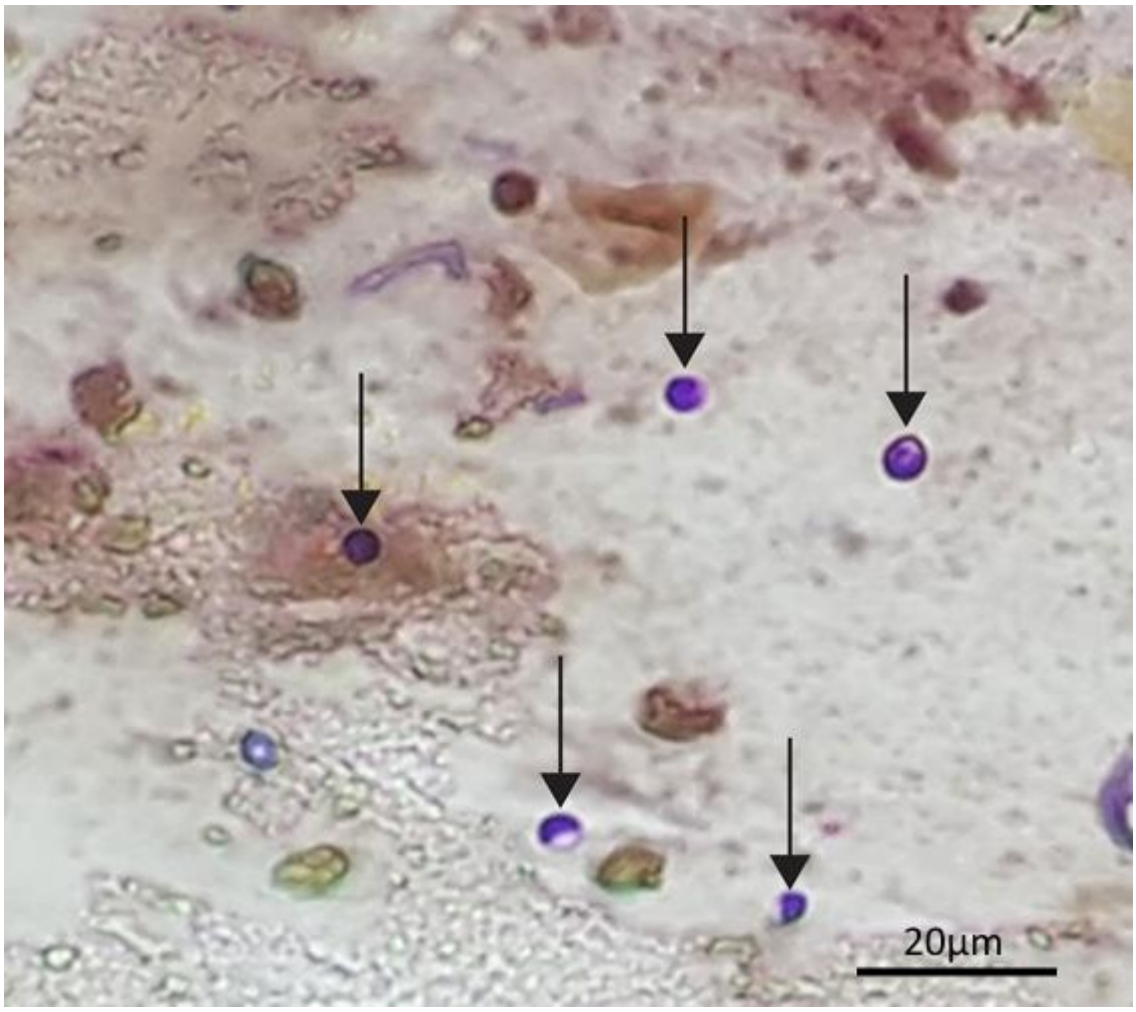

Figure 2-1: Confirmation of a mouse infection via modified aniline-carbol-methyl stain. Following a similar rationale as acid fast staining, the purple methyl-violet stain cannot be decoloured by ethanol when taken up by the oocyst. This leaves *Cryptosporidium* oocysts as bright purple objects, as indicated by the arrows. Estimates regarding parasite-load of the animal can be made from the

enumeration of average oocysts per oil field (shown is an image representative of a 1000x magnification oil field from a mouse of typical infection).

2.16 Sample preparation for NMR

Sample preparation was largely based upon an original methodology published by Gonzalez *et al* in 1997 (Gonzalez et al., 1997).

2.16.1 Animal samples

Animal samples were retrieved from the contents of the ileum and surrounding intestinal structure by dissecting out the area of interest and washing through with three ml 100% ethanol at room temperature via syringe inserted into the opening, collecting the wash through.

2.16.2 Tissue culture samples

COLO-680N models of infection (n=18) were established as noted in *2.3*, in 30ml cultures within 75 cm^2 flasks and maintained for 10 days. The infected monolayers were then washed three times with PBS and removed from the surface of the flask via cell scraper. Cells were collected from the flask via 5 ml of PBS.

2.16.3 Metabolite extraction and NMR analysis

Collected samples were then centrifuged for three minutes at 10,000 x *g*, the supernatant discarded and the pellet weights recorded. The samples were then suspended by vortex in two ml of 75% ethanol then transferred to a new tube and an additional five ml of 75% ethanol added.

Two ml of two mm diameter glass beads were added to the samples and agitated by vortex for 30 seconds before incubating the samples for three minutes at 80°C. The samples were vortexed for a further 30 seconds or until the sample was completely homogenised. Tissue culture samples were collected by draining the media, adding six ml of ethanol at 80°C to the culture flask and scraping the cells off the surface by cell scraper, decanting the mixture of lysed cells into 15 ml polyethylene tubes.

The samples were then decanted into two ml tubes, retaining the glass beads in the falcon tubes. The beads were washed with an additional two ml of 80°C, 75% ethanol and again the liquid was decanted into sterile two ml tubes, retaining the glass beads in the tube.

Cell debris and general detritus were removed from the samples by centrifugation at 16,000 x *g* for 10 minutes and the supernatant transferred to new, sterile two ml microcentrifuge tubes. The samples were then dried via Rotorvac overnight at 40°C, suspended in 330 µl double distilled water and centrifuged at 2,500 *g* for 10 minutes. The supernatant for the samples were recombined into a single 1.5 ml microcentrifuge tube per original samples and frozen at -20 °C until the day before NMR analysis. Twenty-four hours prior to analysis, the sample tubes were placed into a freeze drier until completely desiccated. For NMR analysis, the samples were suspended in one ml of deuterated water and spiked with the sodium salt of the calibration control compound 3-(Trimethylsilyl)-1-propanesulfonic acid (DSS) to a final concentration of 20 mM and a tested pH of 7.5.

2.17 NMR protocol and analysis

Samples were analysed using a 4-channel Bruker Avance III 14.1 T NMR spectrometer (600 MHz 1H) equipped with a 5 mm QCI-F cryoprobe. For controls: six separate, uninfected 25 cm2 COLO-680N 100% confluent monolayer cultures were analysed in addition to three uninfected BALB/c mice. Infected samples consisted of six 25 cm2 COLO-680N 100% confluent monolayers in addition to three Iowa infected BALB/c and three Weru infected BALB/c mice. One-dimension NMR datasets were acquired with a pulse repetition rate of 5 s over 128 scans, preceded by eight equilibrating dummy scans and suppression of the residual Deuterium Oxide solvent (D_2O) resonance using

presaturation. Processed NMR spectrographic datasets were produced by Topspin 3.2 and analysed using Chenomx NMR Suite version 8.2. Partial Least Squares Discriminant Analysis (PLS-DA) of the Chenomx data were generated with the freely available Microsoft Excel Add-in "multi-base 2015" by Numerical Dynamics, Japan (Mutlibase for Microsoft Excel 2015). Pathway predictions were produced by the MetaboAnalyst 3.0 web tool, using a hypergeometric test and relative-betweenness centrality against Homo sapiens and *Mus musculus* databases for the tissue culture and mouse models respectively (Xia et al. 2015).

2.18 ISC antibodies

2.18.1 Identification of target gene sequences

Frataxin, IscS and IscU sequences were successfully identified within the genome of *C. parvum* utilising blast searches against the NCBI database, using the published sequences of the protein homologues of *S. cerevisiae* as the search template (Table 2-3).

Table 2-3: Accession numbers of the putative *C. parvum* ISC genes identified via a blastn search and the corresponding *S. cerevisiae* homologues. These sequences were used to identify potential mitochondrial targeting sequences in addition to the design of suitable primers for gene amplification via PCR.

	Accession number	
C. parvum Protein (yeast homologue)	*C. parvum*	*S. cerevisiae*
IscS (Nfs1p)	AY029212	NP_009912
IscU (Isu1p)	XM_627477	KZV07380
Frataxin (YFH1p)	XM_625594	AJV18575

Complementary primers were then designed for each sequence, to allow for the amplification of the target gene, with the intentional addition of a 3' or 5' restriction endonuclease site that would facilitate insertion into the vector (Table 2-1).

2.18.2 pET14b recombinant protein construct cloning

To produce the desired antibodies, it was first necessary to construct plasmids containing the recombinant proteins, suitable for expression in an *E. coli* line. pET14b (Figure 2-2) was chosen due to its high expression rate, n-terminal poly-histamine tail addition, T7 promoter and Ampicillin resistance selection marker. This would allow quick and efficient identification of successful transformants as well as easy purification of the desired protein via affinity chromatography.

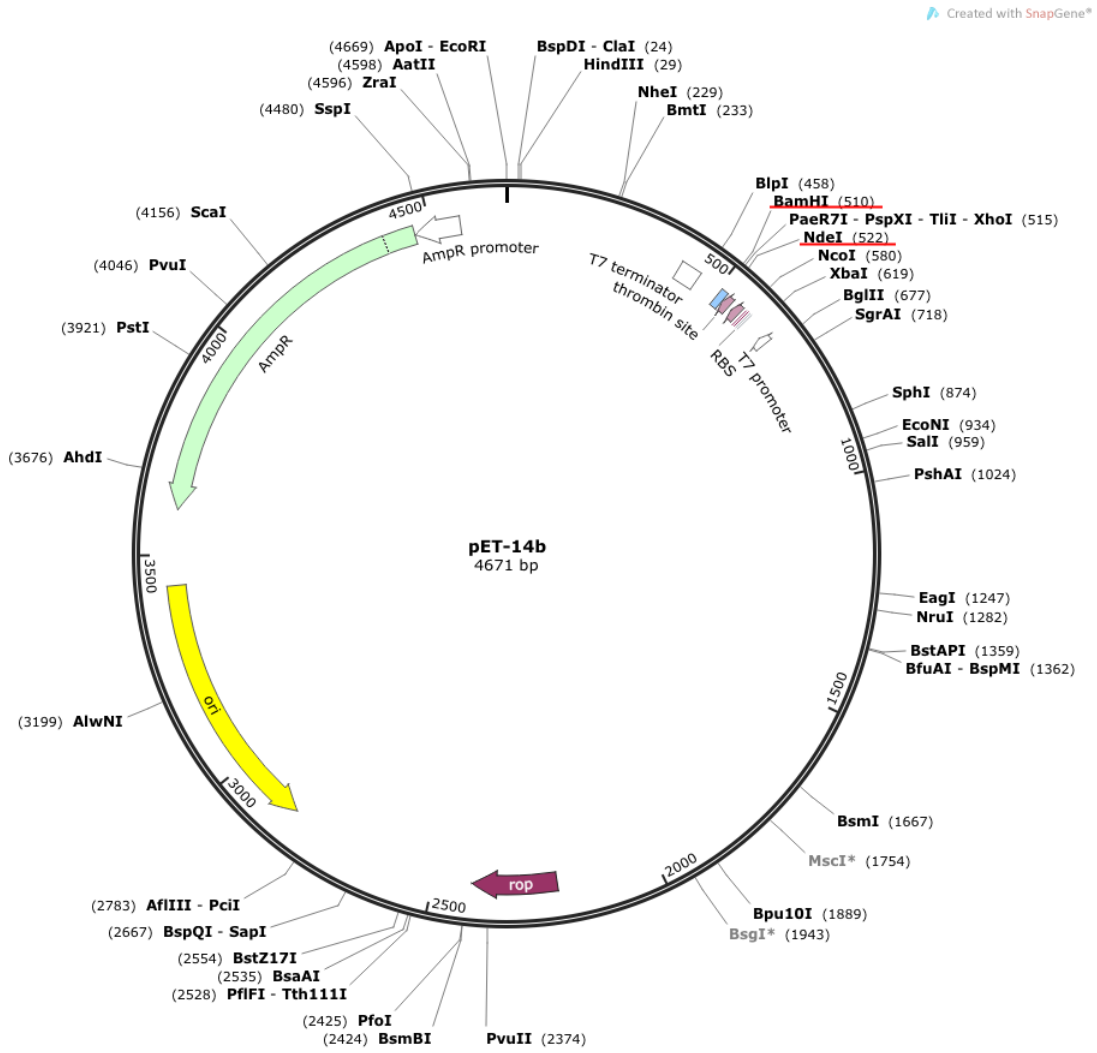

Figure 2-2 Site map of pET14b. Map obtained from addgene 2017, restriction sites utilised in these experiments have been underlined with red (BamHI and NdeI). pET14b was utilised for its combination of restriction sites that would allow universal insertion of any of the 3 target recombinant sequences without conflicting restriction sites.

Initial plasmid cloning and production was achieved via transformation of competent DH5α *E. coli*, due to their rapid replication rate and lack of T7 expression. The recombinant protein was expressed via the transformation of the plasmid into BL21(DE3)pLysS competent *E. coli* cells. This strain was chosen due to their inducible expression of T7, via a *lac* UV5 promoter, decreased protease activity and low background expression levels.

Transformations were performed with pre-prepared, chemically competent E. coli cells otherwise stored at -80°C. All further steps are performed under flamed sterile conditions. Once removed from the -80°C freezer, the cells were allowed to thaw on ice for no more than five minutes before aliquoting 50 µl of cells into sterile 1.5 ml eppendorf tubes. 5 µl of plasmid mixture would then be added to the thawed cells and mixed by gently tapping the edge of the eppendorf. The cell/plasmid mixture would be left to incubate, on ice, for fifteen minutes. During this time freshly prepared LB agar plates, with appropriate selective antibiotic, would be removed from cold storage and placed into a 37°C incubator to pre-warm. A heat block or water-bath would also be set to warm to 42°C. After the cells had completed their incubation, the containing eppendorfs would be added to the 42°C heat block/water-bath and left for 45 seconds then immediately placed back on ice. The tubes would be left on ice for a minimum of one minute and a maximum of two before adding 250 µl of SOC medium. Two aliquots, one of 50 µl and another of 250 µl would then be taken from each eppendorf by pipette and used to seed a pre-warmed agar growth plate. The seeded plates would be left, agar side up, for two minutes before placing them back into the 37°C incubator and incubating for 16 hours. Once colonies had formed they were picked via sterile pipette tip and used to inoculate 5 ml of sterile LB broth with selective anti-biotic in a sterile test-tube and incubated for a further 16 hours at 37°C, shaking. Plasmids could then be purified from the culture utilising the reagents and protocol of the QIAGEN, QIAprep Spin Miniprep Kit (QIAGEN: Cat No./ID: 27104), typically yielding 50 µl of plasmid. Successful plasmid extraction and gene insertion were then tested for by digesting 1 µl of the purified plasmid with complementary restriction endo-nucleases and visualising the results on an ethidium bromide agarose gel. Any plasmid that appeared to contain the desired insert was then mailed to Eurogentec for sanger sequencing. Only those plasmids that displayed the insert without mutation were used in the transformation of the expressing E. coli lines.2.18.3 Expression and purification of recombinant ISC proteins

Cultures of successfully transformed BL21(DE3)pLysS *E. coli* were incubated at 37°C for 16 hours in a shaking incubator and used to inoculate 2 litres of sterile LB media,

which was incubated and shaken until an OD_{600} of 0.5 was achieved at which point IPTG was added to a final concentration of 0.5 mM. The cultures were then left to incubate for 4 hours before centrifuging at 3,000 x g for 30 minutes. The supernatant was then discarded, and the pellet washed twice in PBS. The pellet was then weighed before resuspending in Novagen BugBuster reagent at 5ml/g of pellet and 1µl/ml of Benzonase was added to the mixture to inhibit proteolysis. The mixture was left to shake at a low setting for 20 minutes at room temperature and subsequently centrifuged at 16,000 x g for 20 minutes at 4°C.

The supernatant was then added to an equilibrated NiCl affinity column and the flow-through and elution fractions collected.

Aliquots of the fractions were then mixed 3:1 with 4x SDS-PAGE loading buffer and boiled at 95°C for 10 minutes to denature the enzymes and any remaining DNA. The mixture was then passed through a 20-gauge needle to ensure any remaining cells were completely shredded before being loaded on a suitable SDS-PAGE gel. The identity of potential bands was corroborated by subsequent poly-his antibody detection based western blot. Once fractions containing the protein of interest were identified, the remaining volume of the correct fractions were combined and added to large scale SDS-PAGE gels. The bands corresponding to the proteins of interest were then excised from the gels and used to inoculate Rabbits (for IscS) or Rats (for IscU or Frataxin) which subsequently produced polyclonal antibodies to the target proteins.

2.18.4 Target verification

Antibody target verification was performed via a two-step process:

1. Western blot of recombinant expressed target peptide and a negative control
2. Mass spec identification of the labelled peptide, via analysis of the appropriately sectioned acrylamide gel slice

Additional confirmation was performed using lysates from purified oocysts to test for the presence of the native protein.

2.18.5 Localisation in *in-vitro* cultures

The main methodologies followed are as written in Chapter 2.9. The dilutions used for antibody staining of the cultures was originally inferred from the optimum Western blot dilutions, but later optimised based on the results of the IFA (Table 2-3). Anti-rat (CpIscU and CpFrataxin) and anti-rabbit (anti-IscS) secondaries, conjugated to TRITC (Excitation 557, Emission 576), were used in the IFA to visualise the locations of protein-antibody binding.

Table 2-4: Antibody dilutions. Optimum dilutions for the use of custom antibodies for *C. parvum* ISC detection, as inferred through a trial and error process.

	Optimum dilution of antibody	
Antibody Target	Western blot	IFA
CpIscS	1 in 300	1 in 100
CpFrataxin	1 in 1000	1 in 200
CpIscU	1 in 200	1 in 50

2.19 IscS Complementation in yeast

To demonstrate CpIscS was truly a functional homologue NFS1, it was necessary to utilise a transgenic method, recovering Nfs1p function with the *C. parvum* protein. I elected to use plasmid transformation of an NFS1 knockout strain. Plasmid transformation would provide a quick, efficient and easy method of introducing recombinant CpIscS to the yeast, using tools already at hand from the production of the recombinant proteins for antibody generation.

2.19.1 pBEVY-L recombinant protein construct cloning

pBEVY-L (Figure 2-3) was selected as the most suitable vector for CpIscS due to the following key aspects:

- High copy number in DH5α *E. coli*
- Ampicillin resistance marker

- LEU2 selection
- Compatible restriction sites for target gene insertion that did not conflict with the sequence of CpIscS
- simple expression profile (constitutive)

These traits would provide for a simple but effective process to confidently assess the complementation of CpIscS in yeast.

The CpIscS construct was assembled in a manner similar to that noted in Chapter 2.18.1, with appropriate use of restriction endo-nucleases as listed in Table 2-1. In place of *C. parvum* genomic DNA, the CpIscS pET14b plasmid was used as the template in PCR. Similarly, successful PCR/transformants were tested for using a complementary restriction endo-nuclease digest and visualising the results on an agarose gel.

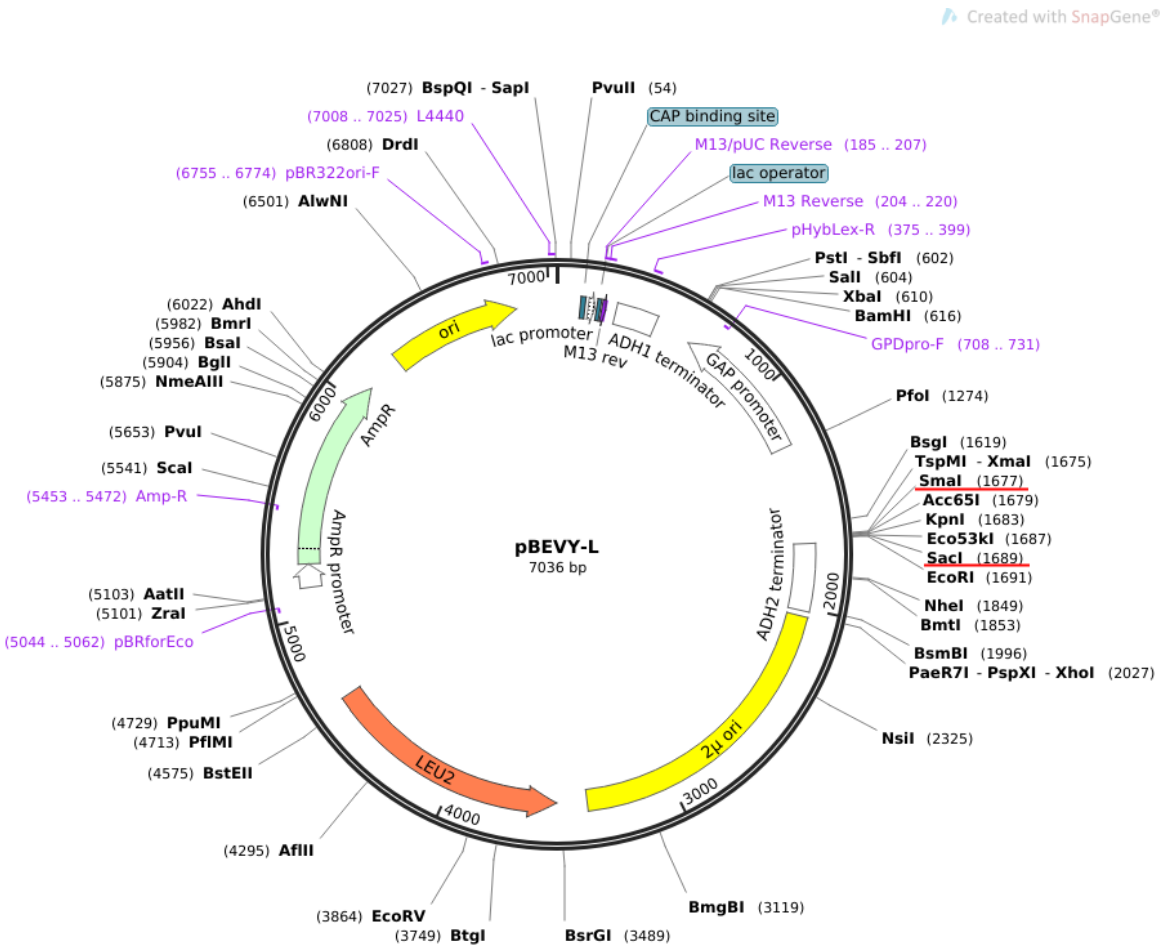

Figure 2-3: Site map for pBEVY-L. Obtained from addgene in 2017, restriction sites utilised in these experiments have been underlined in red (SmaI and SacI). Selection of this plasmid was based on optimum insertion site restriction sequences, absent from the target recombinant sequence and a high expression ratio.

2.19.2 Transformation of IscS heterozygous knockouts

Transformation of the IscS heterozygous knockout strains of yeast were performed via the following protocol:

A frozen aliquot of the yeast HetDip NFS1 Knock Out Strain, YCL017C (CloneId:23424), was removed from a -80°C freezer and scraped, under flamed sterile conditions (as are all further steps), with a sterile pipette tip which was then used to inoculate a pre-warmed (to 30°C) YPD agar plate containing the G418 selective antibiotic. Once inoculated, the plate was placed agar side up in a 30°C incubator and left for 30 hours. A sterile pipette tip was then used to pick approximately 20 µl of cells from a single colony on the plate and added to 1 ml of sterile, de-ionised water in a 1.5 ml eppendorf. The tube was then spun at 17,000 x g for 20 seconds and the supernatant carefully removed then replaced with 1 ml of 0.1 M LiAc. The tube was spun again at 17,000 x g for a further 20 seconds and the supernatant again carefully discarded. The following was then added in the order of listing:

1. 240µl of 50% PEG
2. 36µl of 1M LiAc
3. 10µ Salmon sperm ssDNA
4. 5µl of CpIscS/pBEVY-L plasmid
5. 69µl of water

The tube, now containing all the above in addition to the yeast cells, was vortexed for 1 minute before placing into a 30°C incubator for 25 minutes. During this team a heat block was warmed to 42°C. The tube was then placed in the 42°C, pre-warmed heat block for another 25 minutes. The tube was then removed from the heat block and spun at 800 x g for 2 minutes and once more the supernatant was carefully discarded. The cells within the tube were then re-suspended in 200 µl of sterile, de-ionised water. Aliquots of 200 µl and then the remaining mixture were used to inoculate pre-warmed G418/LEU- minimal media agar plates.

2.19.3 Sporulation of transformants

Successful colonies from the G418/LEU- selective plates were picked and grown for 8 hours in 5% Glucose YPD. They were then spun down at 17,000 x g for 20 seconds, the supernatant discarded, washed with water and finally re-suspended in a glass test-tube at an OD_{600} of approximately 0.25 in 1 ml of 1%KAc, at 25°C for 4 days, shaking. Aliquots were taken from the culture and analysed for signs of sporulation. If less than 60% of the culture was sporolated at this point, the mixture was incubated for a further 24 hours.

Spheroblasting of the spores was performed by taking 500µl of sporolated culture and adding 500 µl of sterile, de-ionised water and 150 µl of 10,000 units/ml lyticase and incubating at room temperature for 30 minutes. The mixture was then observed under the microscope to confirm the formation of spheroblasts. If spheroblasting was insufficient, the mixture was left to incubate for a further 30 minutes.

Complete disruption of the spheroblasted ascii was achieved by the addition of 100 µl sterile mineral oil and vortexing for two minutes. The mixture was then spun down at 17,000 x g for 20 seconds.

The hydrophobic spores, now liberated from the ascii, would remain in the mineral oil layer, on the surface of the mixture. 90 µl of the top, mineral oil, layer was removed by careful pipetting and diluted 1 in 20 YPD. Serial dilutions of this mixture were then added to YPD plates in 10 µl aliquots and incubated at 30°C, upside down, for 48 hours.

2.19.4 Identification of functional complementation

20 randomly selected colonies from the sporolated YPD plate were analysed for mating type via PCR using primers specific to either mating type α or a Table 2-5).

Table 2-5: Yeast mating type primers. Oligonucleotide sequences of specific primers for the detection of yeast mating types via PCR, used in the complementation experiment to detect alpha, A or heterozygous mating types.

Label	Nucleotide sequence
Yst_3'_MAT	AGTCACATCAAGATCGTTTATGG
Yst_Alpha_Mat_HML	GCACGGAATATGGGACTACTTCG
Yst_a_Mat_HML	ACTCCACTTCAAGTAAGAGTTTG

The successful sporulation of *Saccharomyces cerevisiae* would result in haploid cells, identified by a single mating type, a or α (Figure 2-4). Haploid cells would contain either native NFS1 or the G418 resistance gene selective marker, in addition to the plasmid.

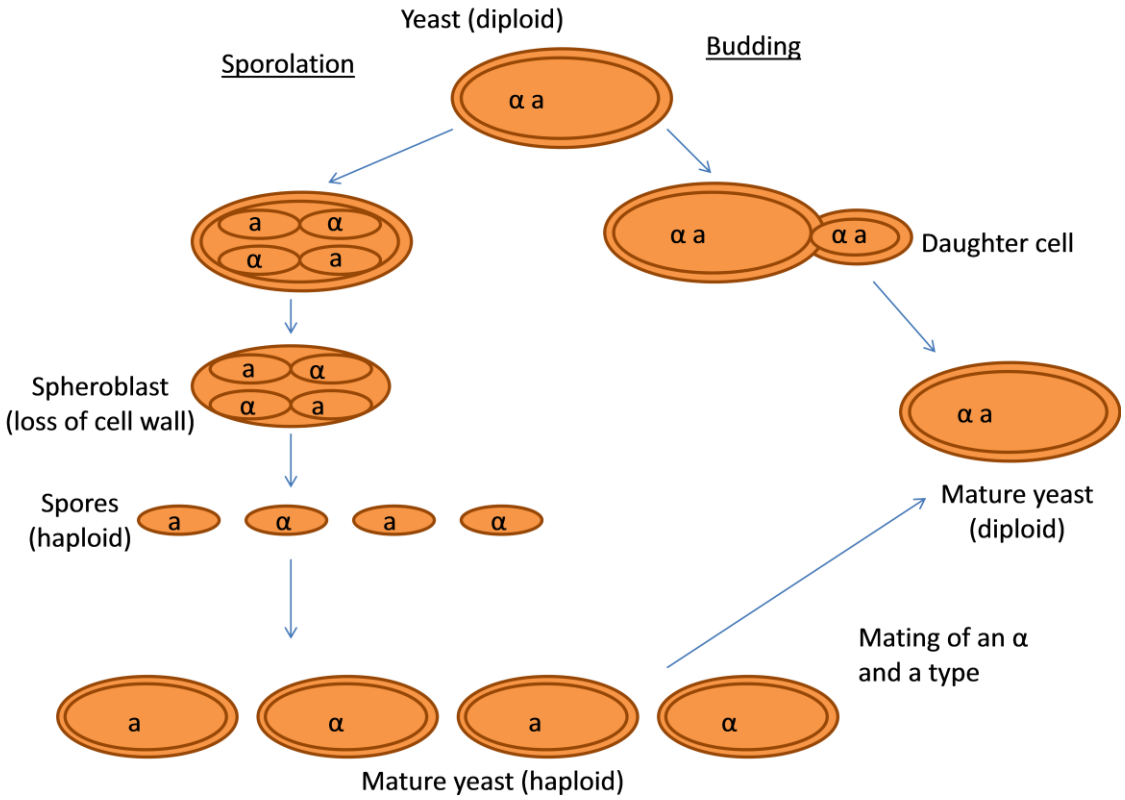

Figure 2-4: The mating cycle of the yeast *Saccharomyces cerevisiae*. Under normal conditions, the yeast replicates asexually, via budding and the creation of a daughter cell (Budding). Under stressful conditions, such as insufficient environmental nutrients, the yeast replicates sexually via the production of haploid spores through meiosis (Sporolation). The use of KAc as a growth media, immediately after growth in glucose rich YPD instigates the sexual reproduction cycle.

Chapter 3 Developing a robust and easy to use *Cryptosporidium parvum* culturing system

3.1 An introduction to *C. parvum* culture

C. parvum culture is an inherently complicated matter. During the natural life cycle of the parasite, *C. parvum* has both intra-cellular and extra-cellular life cycle stages, invading a multitude of host cells during this time (Leitch and He, 2012). Though different species of *Cryptosporidium* can infect a variety of regions along the digestive tract, *C. parvum* typically infects epithelial tissues of the upper intestinal region, typically the ileum (Current Wl Fau - Reese and Reese, 1986).

Typical pathophysiology of a *C. parvum* infection includes localised deterioration of microvilli, leading to dehydration and a variety of nutrient based deficiencies as the gut lining loses its capacity to absorb passing foodstuffs (Leitch and He, 2012). In immunocompromised individuals, *C. parvum* can also be found in most other epithelial tissues, including most of the upper stages of the digestive and respiratory tracts as well as other unrelated organ systems such as the liver and heart (Flanigan and Graham, 1990, DuPont et al., 1995, Sponseller et al., 2014). In each case, *C. parvum* undergoes the same complex life cycle, consisting of multiple intracellular and extracellular stages, many of which share morphological similarities with other apicomplexans (Morrison, 2009). As such, developing a means of studying these life cycle stages in detail would provide an insight not just into *C. parvum* or *Cryptosporidium* genus but possibly the gregarines or even Apicomplexa. The new understandings that could arise from this work range from determining the contributions of host versus parasite during the invasion processes, to mapping the chronological generation of various organelles in each life cycle stage.

Though animal models of *C. parvum* infection are well established, they contain a large number of disadvantages with regards to studying the parasite (Striepen, 2013). *In-vivo* studies are inherently impractical for any live cell experimentation and whilst there are times the inclusion of a whole organism can help understand the pathology of a parasite, a more limited model can provide a better resolution of cause and effect. As is often the

case in molecular pathology, a simpler, *in-vitro* monoculture can be used to equal effect, often opening up avenues of research previously unexplored (Striepen, 2013).

Unfortunately, whilst many attempts have been made and partial success witnessed over the last 30 years, a sufficiently effective long term *in-vitro* culture of *C. parvum* still does not exist (Striepen, 2013). Human Colo-rectal carcinoma (HCT-8) and Madin Darby Caninine Kidney (MDCK) cells have both shown promise during the previous decades of *C. parvum* experiments, yet often fall short either due to rapid culture senescence or an inability to properly cultivate the range of endogenous phases of *C. parvum* noted in the medical literature (Upton et al., 1994, Hijjawi et al., 2001, Girouard et al., 2006, Arrowood, 2002). However, with the advent of increasing advanced mono-culture systems, advances have been made whilst maintaining the use of HCT-8 and MDCK cells (Alcantara Warren et al., 2008, Karanis and Aldeyarbi, 2011, Muller and Hemphill, 2013, Morada et al., 2016). A recent publication tackled the challenge of cell culture-based oocyst production using a hollow fiber technology that mimics the dynamic oxygen gradient of a blood vessel system within the gut (Morada et al., 2016). However, specialised equipment is needed, and the required cell culture media supplements are expensive. In addition, the complex nature of the system precludes the studying of the *C. parvum* life cycle or cell biology in real time, relying instead on destructive sample acquisition for static time point observations.

As a direct result of this lack in suitable culture systems, *C. parvum* research is also lacking an effective genetic manipulation tool. CRISPR (Clustered Regularly Interspaced Short Palindromic Repeats) is a technique that has rapidly gained popularity across the various fields of biology as both an effective and easy to use system. Whilst some headway has been made showing the viability of *C. parvum* as a target of CRISPR mediated genetic exploration; the current HCT-8 and MDCK models are incapable of sustaining the transgenic results (Vinayak et al., 2015). This has left the field relying on *in-vivo* models, again, which are highly inappropriate solutions due to cost, laboriousness and ethical issues.

3.2 Goals

It is clear from the advances made, that whilst HCT-8 and MDCK cells provide useful platforms for *C. parvum* study, they nevertheless continue to fall short of providing a comprehensive model of infection. It is of significant importance that new methodologies and systems for culturing this parasite are found, especially those that allow live observation of the infection and parasite biology (Striepen, 2013). Therefore, I decided to approach the issue by attempting to develop a *C. parvum* culture from a different cell culture than those already studied, continuing in the footsteps of previous attempts whilst applying modern techniques and knowledge of the parasite. To achieve this would involve a preliminary screening of semi-randomly selected tissue cultures, with the only selection based on the shared usage of a single media type. This would allow for both a simpler execution of a large-scale experiment, as well as minimising the possibility of disassociating media-based effects with the host cells.

I also intend to validate these results using a multitude of established and novel methodologies, not only to ensure the best reliability but also to develop and present new methods of exploring and validating future culturing techniques.

3.3 Results

3.3.1 Screening for new host-cell cultures

A panel of seven human cancer cell lines were tested for their capacity to support *C. parvum* propagation including COLO-680N (oesophageal squamous-cell carcinoma), DLD-1 (colon adenocarcinoma), KYSE-30 (oesophageal squamous-cell carcinoma), HCT-15 (colorectal adenocarcinoma), SJSA-1 (osteosarcoma), MKN-1 (gastric carcinoma), and the colon adenoma carcinoma cell line HCT-8, which has most commonly been used for the investigation of *C. parvum* in cell culture. The cell lines were infected with the *C. parvum* strain Moredun using an input of 50,000 of excysted oocysts per ml, as described in *2.3*. After an incubation period of two weeks, COLO-680N cultures were the only ones that had produced a noteworthy number of *C. parvum*

oocysts, with an approximate increase of 75-fold over the number of input oocysts (Figure 3-1a). Additionally, while the HCT-8 cultures had succumbed to senescence after 14 days of infection, COLO-680N cultures remained viable and produced oocysts for almost eight weeks in total without sub-culturing, requiring only weekly media replacement (Figure 3-1b). As a result, total *C. parvum* oocyst production in the COLO-680N cell line exceeded the HCT-8-mediated oocyst production (2.5 x 10^5 oocysts/ mL) by 20 times (5 x 10^6) after ten days of incubation (Figure 3-1c). At day 60, COLO-680N cells had produced a total of 1.2 x 10^7 oocysts/ ml.

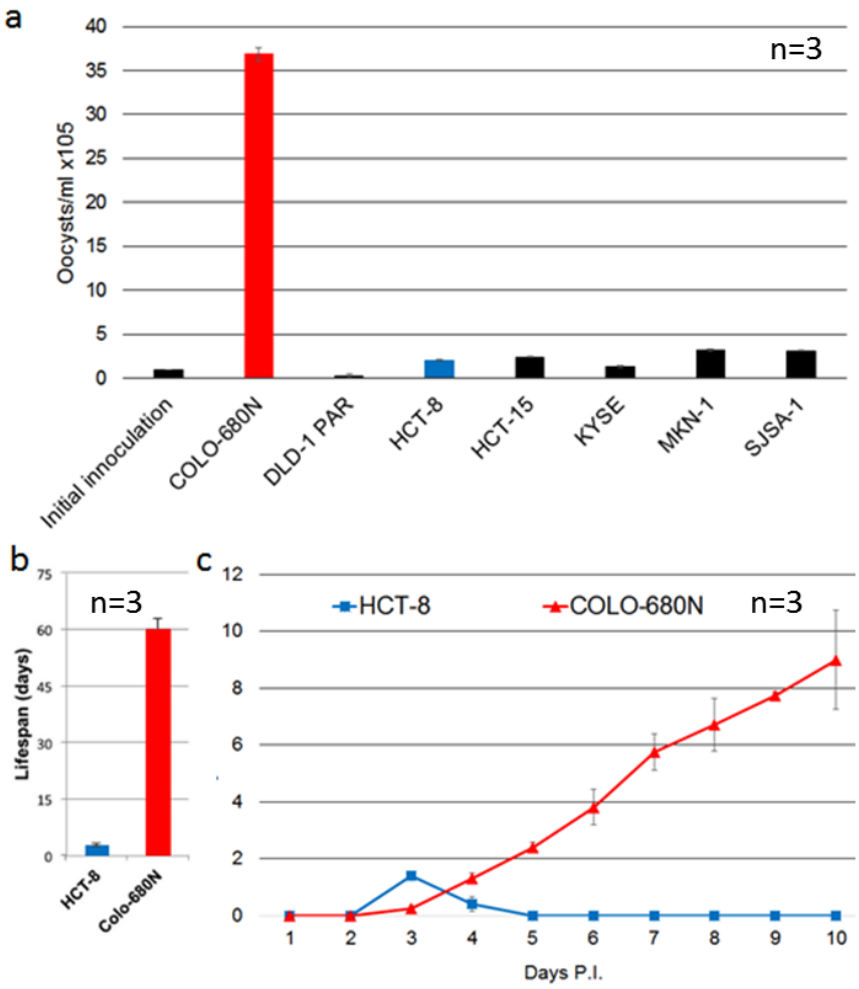

Figure 3-1: *C. parvum* culture screen results. (a) Oocysts recovered from culture after an initial inoculum of 1x10^5 and a 2-week incubation period. Initial tests showed a clear disparity between a single cell type, COLO-680N, and the other cultures. COLO-680N appeared to demonstrate a much higher capacity for producing *C. parvum* oocysts than the previous gold-standard HCT-8 (b) culture lifespans of infected COLO-680N and HCT-8, when compared, showed that COLO-680N was capable of maintain a viable and productive culture for a longer period than HCT-8. Although

uninfected cultures showed similar disparities and therefore this result should be interpreted as an innate advantage of COLO-680N, independent from either cell type's specific response to infection(c) oocyst production of HCT-8 and COLO680N cultures over the course of a culture lifespan.

3.3.2 Verification

3.3.2.1 by PCR

C. parvum infection of COLO-680N cells was further confirmed using PCR to detect *C. parvum* DNA. The primers were designed around *C. parvum* specific sequences and optimised by testing on DNA obtained from purified commercial oocysts (Figure 3-2). *C. parvum*-specific primers did not produce bands in non-infected COLO-680N cells. Examination of culture media taken during a standard 12-day infection revealed successful detection by day six by the HSP70 primers and day nine by the 18sRNA primers Figure 3-3. The amplified DNA regions were sequenced to confirm their identity.

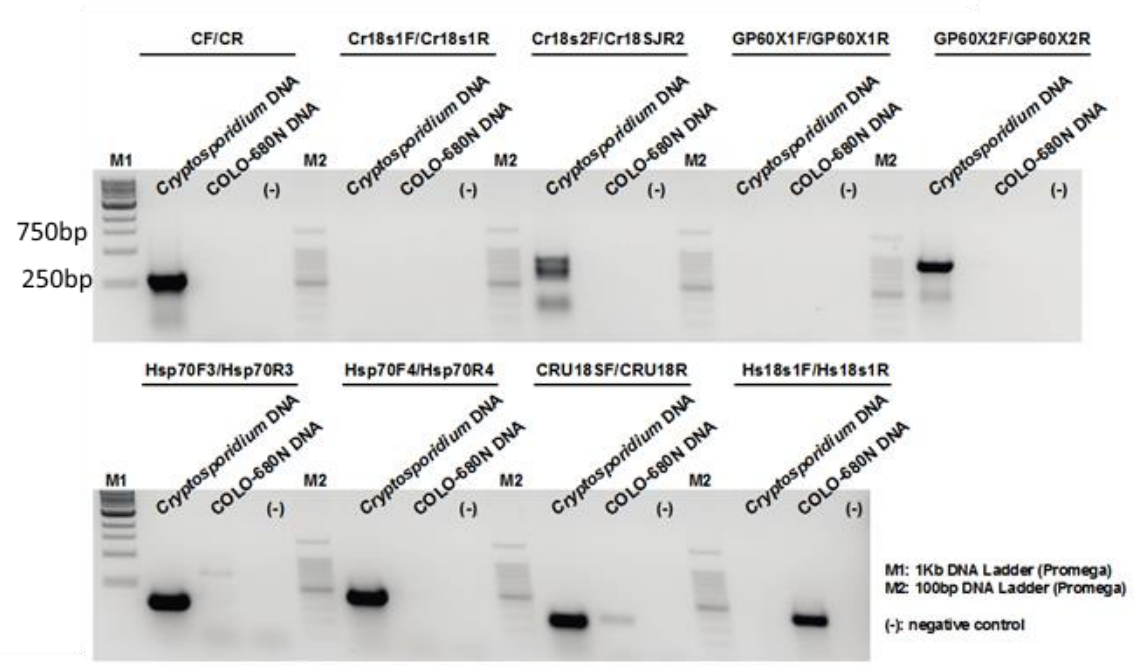

Figure 3-2: Optimisation of *C. parvum* detection via PCR. Custom primers, designed for specificity towards *C. parvum* gene segments (with the exemption of Hs18S which was used as a positive control to test for host DNA), were used in PCR performed on *C. parvum* DNA purified from whole oocyst

fractions and on COLO-680N DNA from 25cm^2 flasks to select for the greatest sensitivity and specificity to *C. parvum* DNA and not host DNA. Primers HSP70F4/R4 and Cr18s2F/JR2 were selected for further experiments.

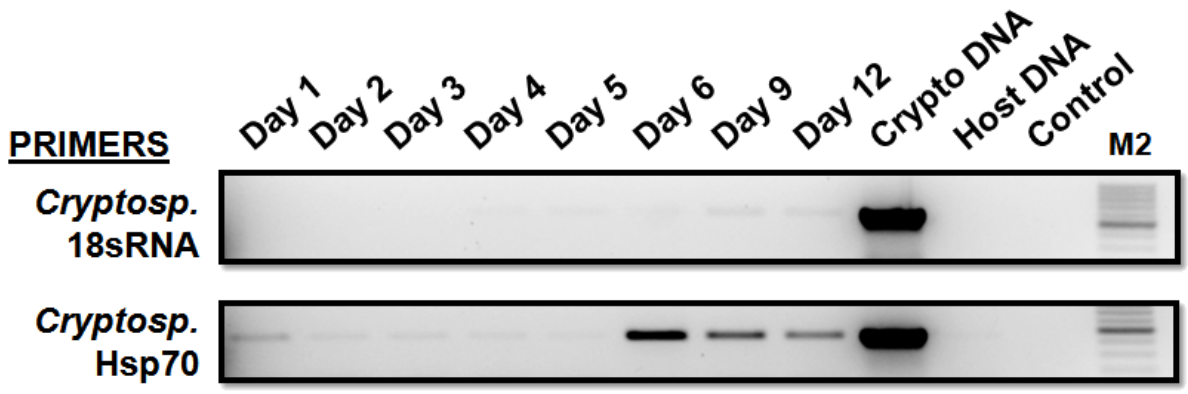

Figure 3-3: Detection of *C. parvum* in culture via PCR. Successful detection of *C. parvum* DNA after a period of six days was achieved by the HSP70 primers. Although slight, successful detection of *C. parvum* was also achieved by 18sRNA primers at nine days post-infection.

3.3.2.2 by Indirect Fluorescence Antibody assay

The identity of the COLO-680N-produced *C. parvum* oocysts was further confirmed using different specific staining methods. Crypt-a-glo (Waterborne^{TM}); an antibody that recognises the oocyst cell wall), Vicia Villosa lectin (VVL, Vector labs; binds to specific O-glycan mucin repeats on *C. parvum* sporozoites), a mucin-like glycoprotein that contains a C-type lectin domain (CpClec; binds to surface of the apical region and to dense granules of sporozoites and merozoites) and direct sporozoite staining using propidium iodide and SporoGlo (Waterborne^{TM}) resulted in near identical staining patterns in *C. parvum*-infected COLO-680N cells indicating the presence of oocysts and other non-extracellular life stages of *Cryptosporidium* (Figure 3-4).

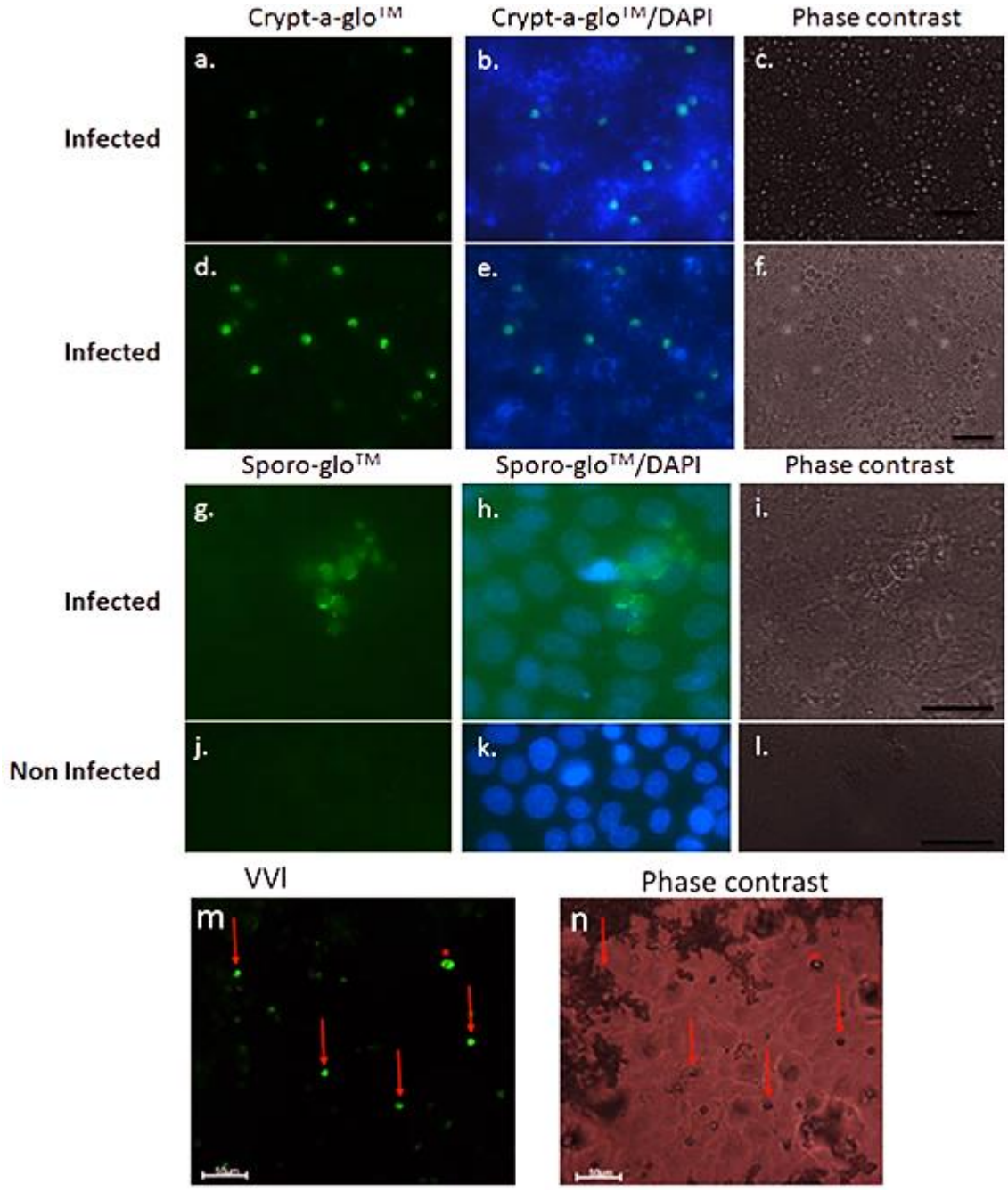

Figure 3-4: Infection detection via Indirect Immunofluorescence Assay (IFA). COLO-680N infections as visualised by a variety of commercially available IFA techniques including: (a-f) a FITC conjugated anti-oocyst wall protein COWP-1 antibody, Crypt-a-glo, (g-l) a FITC conjugated anti-apicomplexan sporozoite antibody, SporoGlo, and (m and n) TRITC conjugated lectin VVL. Scale bars: c and f: 20 µm, i and l: 15 µm, m and n: 50 µm. Each method produced corroborating imagery of cultures containing roughly spherical bodies, approximating 5-6µm in diameter, matching the description of a typical *C. parvum* oocyst. The oocysts were also visible via conventional light microscopy, but typically were considerably hard to spot without guidance from the IFA.

To confirm the production of fresh oocysts and eliminate the possibility of recounting the initial infection (though steps were taken to prevent this, as described in Chapter 2, section

2.3), Crypt-a-glo stained oocysts were excysted and used for the infection of COLO-680N cultures. Then, cell cultures were washed to remove remaining Crypt-a-glo stained oocysts. Upon harvesting neither the infected cultures nor the newly produced oocysts displayed Crypt-a-glo staining (Figure 3-5b i and iv). Imaging of stained oocysts that had been kept in a cell-free media suspension, did, however, display fluorescence confirming its viability as an experimental parameter (Figure 3-5a). However, oocysts were detected using DAPI and the corresponding phase contrast imaging, supporting the conclusion that only the new oocysts were being detected (Figure 3-5b ii, iii, v, vi). Subsequent experimentation with Iowa II and Weru strains also produced similar, successful infections of COLO-680N.

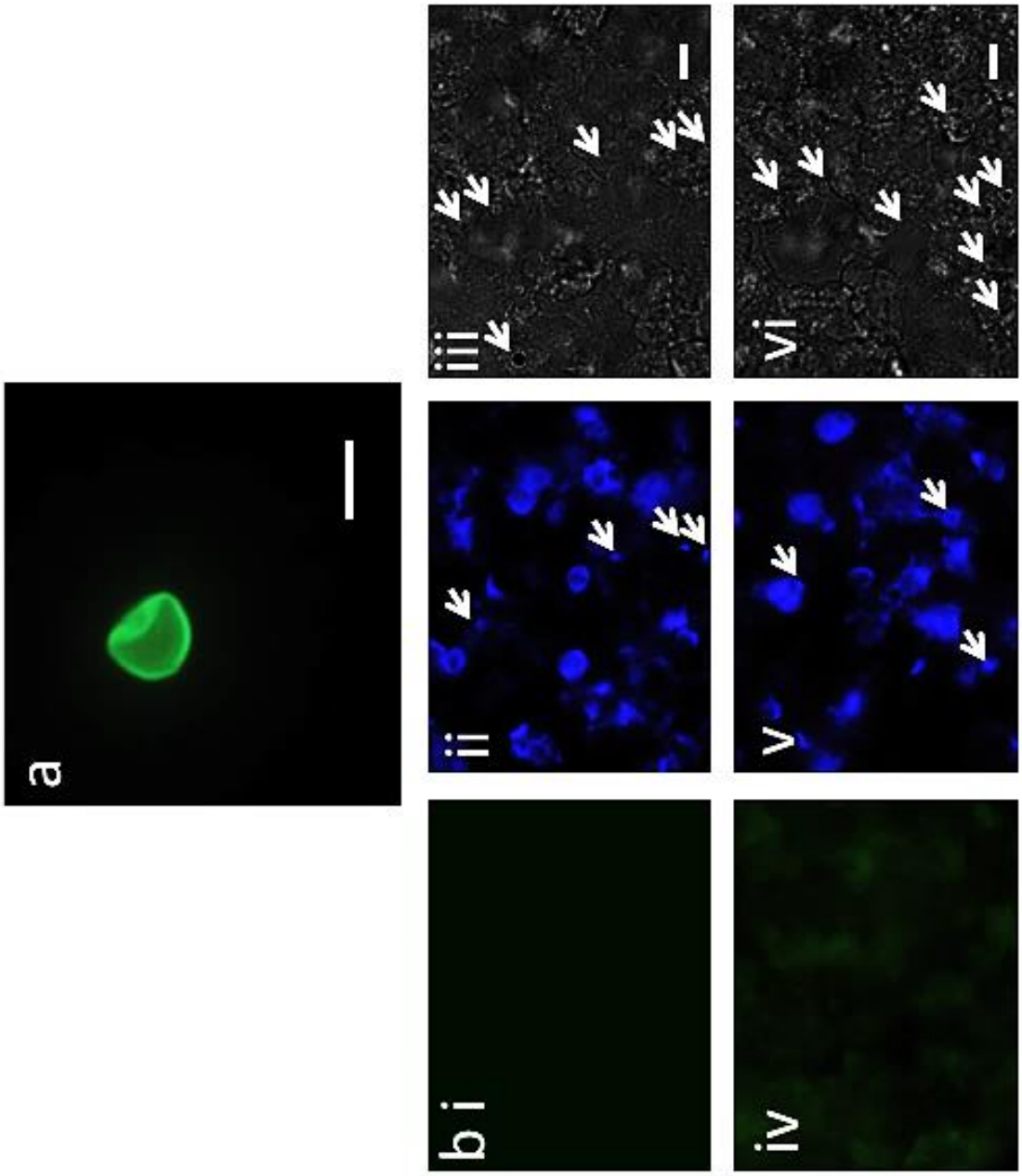

Figure 3-5: Confirmation of novel *C. parvum* production, via DAPI nuclear staining. (a) *C. parvum* oocyst stained with Crypt-a-glo retained its fluorescence after ten days in RPMI-1640, providing evidence that any original oocysts from the infection could be detected by fluorescence. (b i and iv) IFA of the ten-day cultures could not detect any green fluorescence, indicating that none of the original oocsysts from the infection remained in culture, being successfully removed during the post-infection wash step. (ii and V), nuclear DNA staining by DAPI revealed multiple circular structures that suggested the presence of *C. parvum* oocysts. (iii and vi) Phase contrast imaging of the same areas produced corroborating imagery of oocyst like structures that aligned with the structures from ii and v, strongly suggesting that there was a successful infection and the oocysts observed where not simply the remnants of the original infection. All scale bars represent 5 µm.

Conventional Crypt-a-glo and SporoGlo IFA studies also showed a clearly intracellular population of *C. parvum*. Moreover, it can be clearly seen that the larger stages of the parasite (most likely zygotes/developing oocysts) exert significant pressure on host nuclei, appearing to impact into the typically ovoid host nuclei. I consider this to be a sufficient body of evidence that *C. parvum* is an intracellular and not epicellular parasite.

3.3.2.3 by Scanning Electron Microscopy

Final verification of the presence of oocysts within the culture was performed via Scanning Electron Microscopy (SEM) as described in *2.13.* The resulting images detailed the presence of roughly spherical bodies, approximately 5 μm in diameter Figure 3-6. Combined with the IFA and PCR results, this data is conclusive evidence that COLO-680N can maintain a *C. parvum* infection and furthermore, at a rate that exceeds previous cultures such as HCT-8 and MDCK.

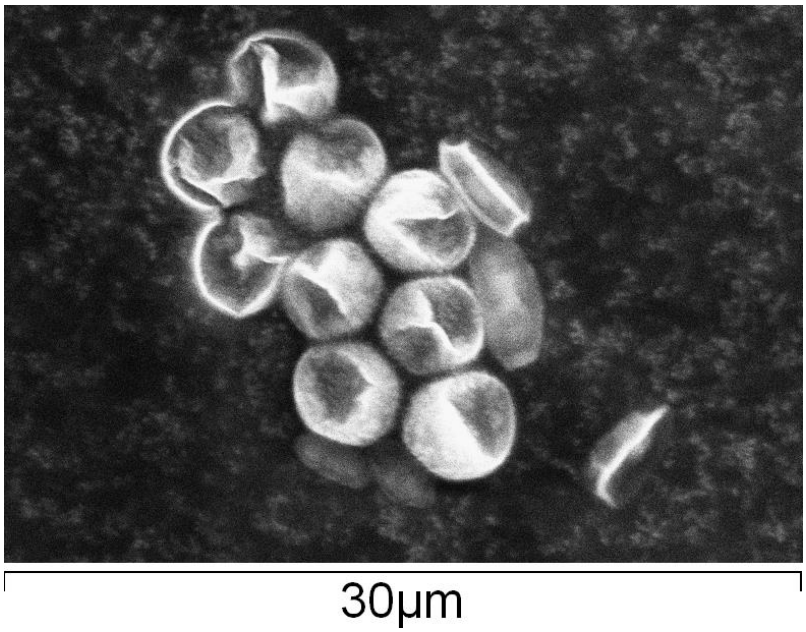

Figure 3-6 Scanning Electron Microscopy of purified oocysts recovered from a COLO-680N culture. The spherical bodies, approximately 5μm in diameter match the profile of a typical *C. parvum* oocyst and further confirmed the successful propagation of the parasite within the culture.

3.3.3 Infectivity of COLO680N derived *C. parvum* oocysts

Early exploration of the possible benefits of a COLO-680N culture focussed on the infectivity of *C. parvum* oocysts produced by the culture. Oocysts derived from the supernatants of COLO-680N cell cultures, but not from the supernatants of HCT-8 cell cultures, were able to initiate infection of novel cell cultures. Infection of COLO-680N cells with cattle-derived *C. parvum* oocysts resulted in similar amounts of infectious oocysts in 25 independent experiments. In addition, three rounds of infection using COLO-680N culture-derived oocysts were performed with no noticeable changes in oocyst production efficacy showing that COLO-680N cells are suited for the continuous long-term cultivation of *C. parvum* oocysts. These preliminary findings show that a COLO-680N platform for *C. parvum* propagation already provides many advantages over the previous platforms. This warranted further exploration, to establish the abilities and limits of this novel *C. parvum* culture and potential monoculture model of infection.

3.3.4 Cryopreservation of *C. parvum*-infected COLO-680N cultures

Among the other limitations of *C. parvum* culture that COLO-680N may address, is the nature of long term storage. Currently, cryopreservation of any *Cryptosporidium* results in parasite death and is therefore not a suitable method of storage. However, preservation of infected cell cultures was hypothesised to provide a solution to this. During the early experiments, the extended nature of COLO-680N parasite cultures suggested that the cell line may be suitably hardy to be used in this manner. Two-week-old *C. parvum* Moredun strain-infected COLO-680N cells were cryopreserved, as per *2.5*, stored for two weeks at -80°C, and resuscitated. Three days after resuscitation, the presence of new *C. parvum* stages was detected Figure 3-7. This demonstrates that *C. parvum*-infected COLO-680N can be cryoconserved, providing the first long-term storage system for any *Cryptosporidium.*

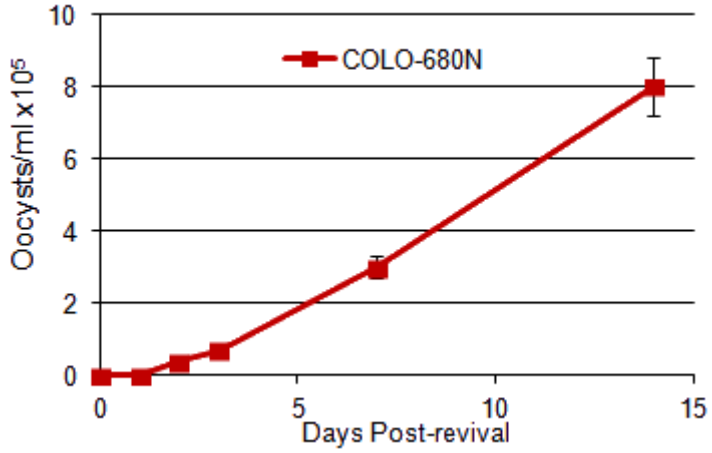

Figure 3-7: Detection of oocysts within COLO-680N cultures after resuscitation from cryoconservation. An upward trend in oocysts recovered from the culture, confirmed via IFA, suggests that oocysts survived the initial freezing process and can undergo the typical life cycle, producing oocysts, after resuscitation via typical mammalian cell cryoconservation methodology.

3.3.5 Comparing HCT-8 and COLO-680N cultures

3.3.5.1 Long term culture viability

To continue detailing the properties of *C. parvum* infected COLO-680N, the viability of infected and non-infected cultures was compared by electrical impedance monitoring using an xCELLigence system. Initial results were promising, with no evidence of significant culture death during infection in COLO-680N. However, longer studies revealed an unexpected effect wherein *C. parvum* infection appeared to increase the life-span of COLO-680N cultures. While the number of viable cells in non-infected COLO-680N cultures dropped after two weeks, *C. parvum*-infected cultures remained viable during the whole observation period of 50 days (Figure 3-8a, data only shown for first 10 days). HCT-8 cell cultures infected with 50 oocysts displayed a continuous proliferation rate of host cells until day five, after which cell cultures displayed data consistent with no change in cell numbers (Figure 3-8b). To test if the different growth patterns observed were of statistical significance I applied a one-way ANOVA analysis to the data. The results revealed infections of 500-1,000 oocysts (a multiplicity of infection of 0.01-0.05 at inoculation) resulted in significantly different data compared to the other infection

doses. Infected HCT-8 cultures did not display any noticeable differences. Following these results, I decided to examine the comparisons between the novel COLO-680N and established HCT-8 cultures further.

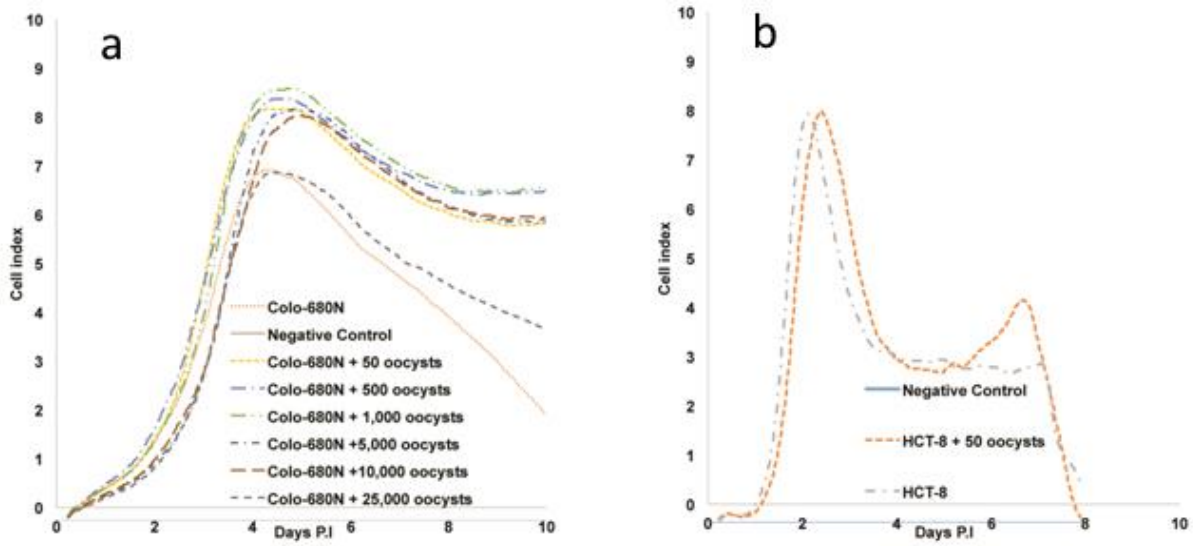

Figure 3-8: Infected culture growth patterns. Graphical representations of culture viability as detected by the xCELLigence cell viability detection system. The xCELLigence experiment monitored the changes in cell growth rates, utilising electroconductivity as an indirect measure of total cells in population. COLO680N cultures (a) displayed some degree of reactivity to infection, with certain ratios of parasite to host cell appearing to increase host longevity. HCT-8 cells (b) displayed no significant interaction, both the negative and infected samples confirmed the long observed notion that HCT-8 has a markedly short life-span in culture and undergoes rapid senescence at the end of a 7-8 culture cycle.

3.3.5.2 Mass Spectrometry fingerprinting of cultures

By comparing the changes of the proteomes of each culture, I theorised it may be possible to determine if signatures of successful infections could be detected, granting insight into the array of potential similarities or differences between COLO-680N and HCT-8 cultures during an infection. To achieve this, a MALDI-TOF mass spectrometry-based fingerprinting approach was used on infected and uninfected cultures (Figure 3-9b-f). PCA analysis of the resulting data produced separate groupings of the COLO-680N but not the HCT-8 sample conditions, suggesting either a greater amount of *C. parvum* proteins or a more profound change in the proteome of COLO-680N compared to HCT-8 (Figure 3-9a).

The principle component 1 value of over 95% indicates that the separations/groupings shown on the 2-dimensional graphs are an accurate representation of how different/similar the samples were (Figure 3-9a).

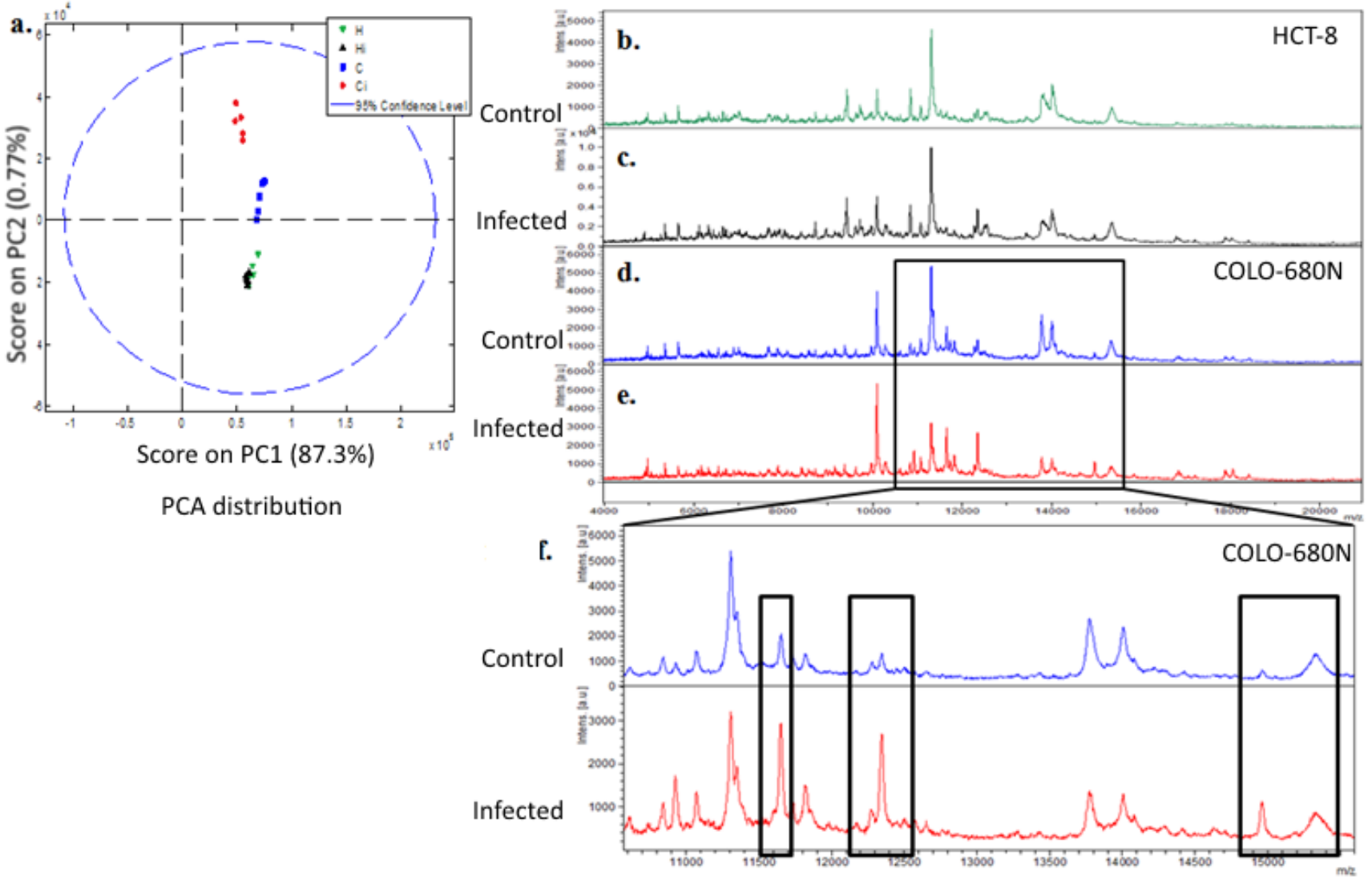

Figure 3-9: : MALDI-TOFF Protein fingerprinting of *C. parvum* infections. (a) PCA analysis of the raw data showed substantial separation between COLO-680N control and infected cultures. However, little to no separation could be established between HCT-8 cultures, suggesting a greater shift in protein content in the COLO-680N scenario, likely due to an increase in parasite. Manual analysis of the graphical data produced (b-e) identified 4 protein peaks in the infected culture (e) which differed from the relative pattern displayed in the uninfected control (d). Closer examination (f) revealed these peaks to approximate proteins of 12kDa, 12.4kDa and 15kDa. The y-axis was adjusted to display the patterns in their most comparable state, y-axis units (intensity, were arbitrary and not directly comparable, instead the relative sizes of the peaks are used to gauge differences between samples.

3.3.6 Comparing culture produced oocysts with commercial product

3.3.6.1 COLO-680N culture viability

COLO-680N cultures that were infected with either Cattle-produced oocysts or Lab produced (COLO-680N) oocysts showed similar growth patterns (Figure 3-10), a strong correlation co-efficient and insignificant ANOVA result from the numerical data strongly indicate that there was no statistically significant variation.

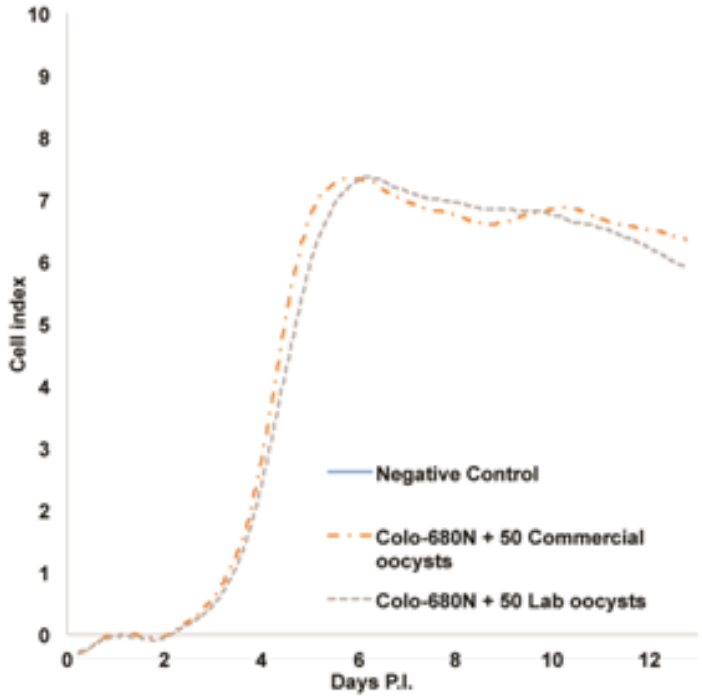

Figure 3-10: COLO-680N growth patterns. COLO-680N cultures were infected with either standard, commercially available oocysts (purple) or oocysts purified from COLO-680N cultures (orange). ANOVA and correlation statistical tests were used to determine the results reliability/significance. Uninfected cultures were used as the negative control. No differences in cell growth patterns could be determined from comparing the two populations infected with the different oocysts, confirming that the effect on growth rate was independat of extraneous factors such as potential protein/supplement from the source material the commercial oocysts were initially purified from.

3.3.6.2 Mass Spectrometry fingerprinting of oocyst lipidomics

COLO-680N and cattle-produced *C. parvum* oocysts were compared via a lipidomics approach. The lipidomics characterisation was performed using MALDI-TOF mass spectrometry for the analysis of lipids within the range of 600 to 2,000 Daltons (Figure 3-11 a-d). Principal Component Analysis at a 95% confidence level showed a pattern consistent with samples having a large degree of similarity between one another. The algorithm did not separate the sample groups, although some subtle differences seemed to be detectable. This can be seen in the 2D graphical representation of the results, with high X and Y axis scores (PC1 and PC2) indicating that the majority of the differences/similarities observed by the data analysis can be accurately represented in a 2 dimensional format for interpretation (Figure 3-11e and f).

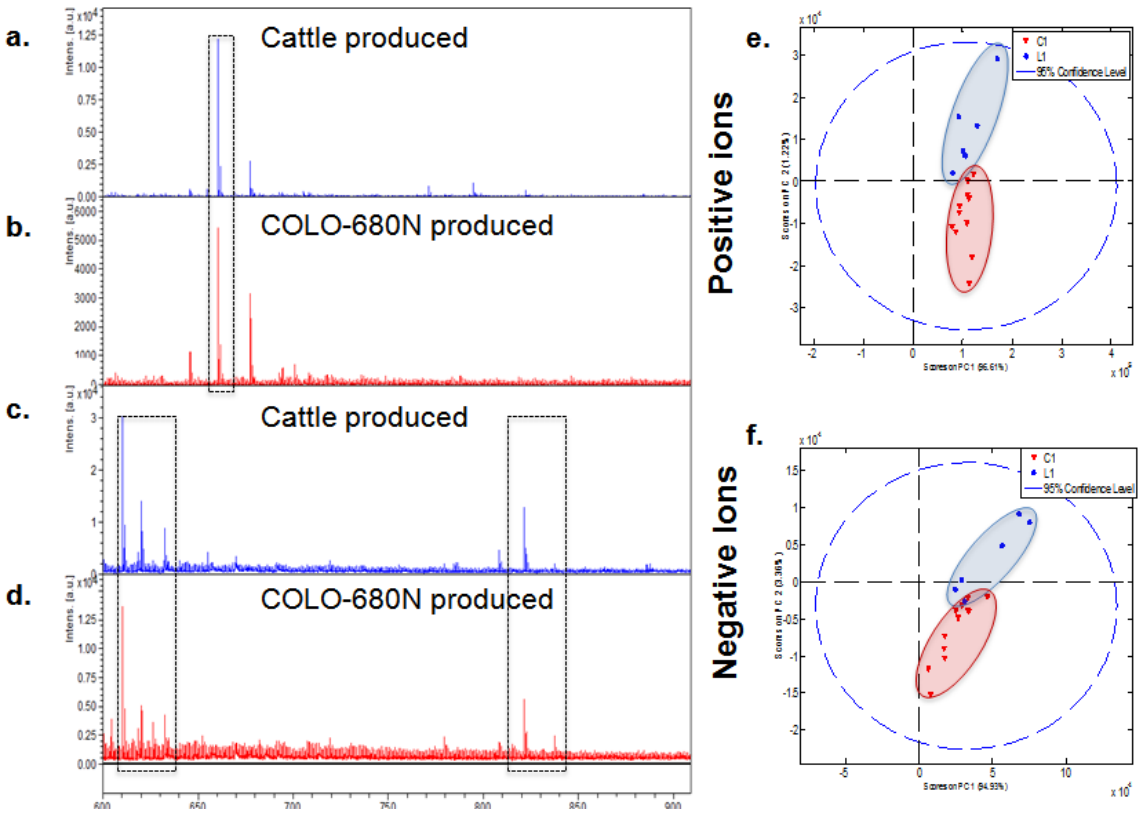

Figure 3-11: Lipidomic fingerprinting of the lipid contents of lab produced and commercially sourced oocysts. The spectra produced by both the positive (a-b) and negative (c-d) sampling sets appeared to be similar. PCA (e and f) analysis revealed that some differences could be detected between the Commercial and lab grown populations of oocyst. Y-axis units are arbitrary and not useful in direct comparison, instead graphs are compared via relative peak heights. However, the analysis was

unable to resolve the two sets completely, suggesting that whilst differences existed, they were not substantial enough to rule out the use of lab oocysts as an alternative to commercially sourced oocyst.

3.3.7 Life cycle stage identification

After establishing the initial validity of the parasite culture as a method of producing oocysts, it was important to explore the progression of the characteristic life cycle of *C. parvum* within COLO-680N.

The current understanding of the major stages of the *Cryptosporidium* life cycle, including sporozoite, trophozoite, meront, macrogamont, microgamont, zygote, immature oocyst, and matured oocyst have been defined based on the investigation of infected tissue from patient biopsies and animal dissections. However, mono-culture models of infection, such as HCT-8, have repeatedly fallen short of displaying full life cycle progression.

3.3.7.1 Identification of life cycle stages via Electron Microscopy

Examination of infected COLO-680N cells via conventional Transition Electron Microscopy (TEM) successfully identified the entire life cycle of the parasite could be demonstrated within a single COLO-680N culture (Figure 3-12a-h). Among those observed, the most frequently occurring were the larger extracellular stages, including type II merozoites and sporozoites (Figure 3-12 a and c). In each case a mitosome, nucleus, crystalloid body and typically the rhoptry could be observed. This is in keeping with previous findings in the *in-vivo* models of infection, whereas previous *in-vitro* models commonly failed to demonstrate comprehensive examples of typical life-cycle stages. Interestingly, again in keeping with previous findings, mitosomes could only regularly be observed in the extracellular stages, with exceptions occurring in very young intra-cellular stages (Figure 3-12b). This suggests that the mitosome is maintained throughout host-cell invasion and is instead lost during the maturation of the intracellular stage. This adds a point on the life cycle timeline that was previously vaguer.

Additionally, due to the high-resolution nature of EM, detailed parasite organelle and previously unreported structures were observed within the infected cells that do not constitute normal host-cell morphology. Among those features present was the feeder organelle that connects the host cell to the parasitophorous vacuole. Feeder organelles have been postulated to be involved in facilitating nutrient transport to the parasite; however, their exact roles during infection are largely not understood. The *C. parvum* mitosome and the crystalloid body were also identified. Notably, these cryptic organelles were described in life-stages other than the sporozoites which had not been previously, including trophozoites, merozoites and microgamonts. Previously, both organelles had only been detected in *C. parvum* oocysts or the excysted sporozoites. In addition, we observed the presence of dense arrangements of the host cytoskeleton around the periphery of the parasitophorous vacuole of *C. parvum*, suggesting a parasite-induced intracellular/epicellular rearrangement of host cells as supported by previous work. These observations also lend significant weight to the argument that *C. parvum* is indeed and intracellular and not epicellular parasite. A further and more novel observation was the peculiar arrangement of host cell cytoskeleton and host-mitochondrion. Whilst networks of host cytoskeleton interacting with the parasite is not un-described, this is the first time that evidence has been presented that this interaction includes the host mitochondria and may warrant further study.

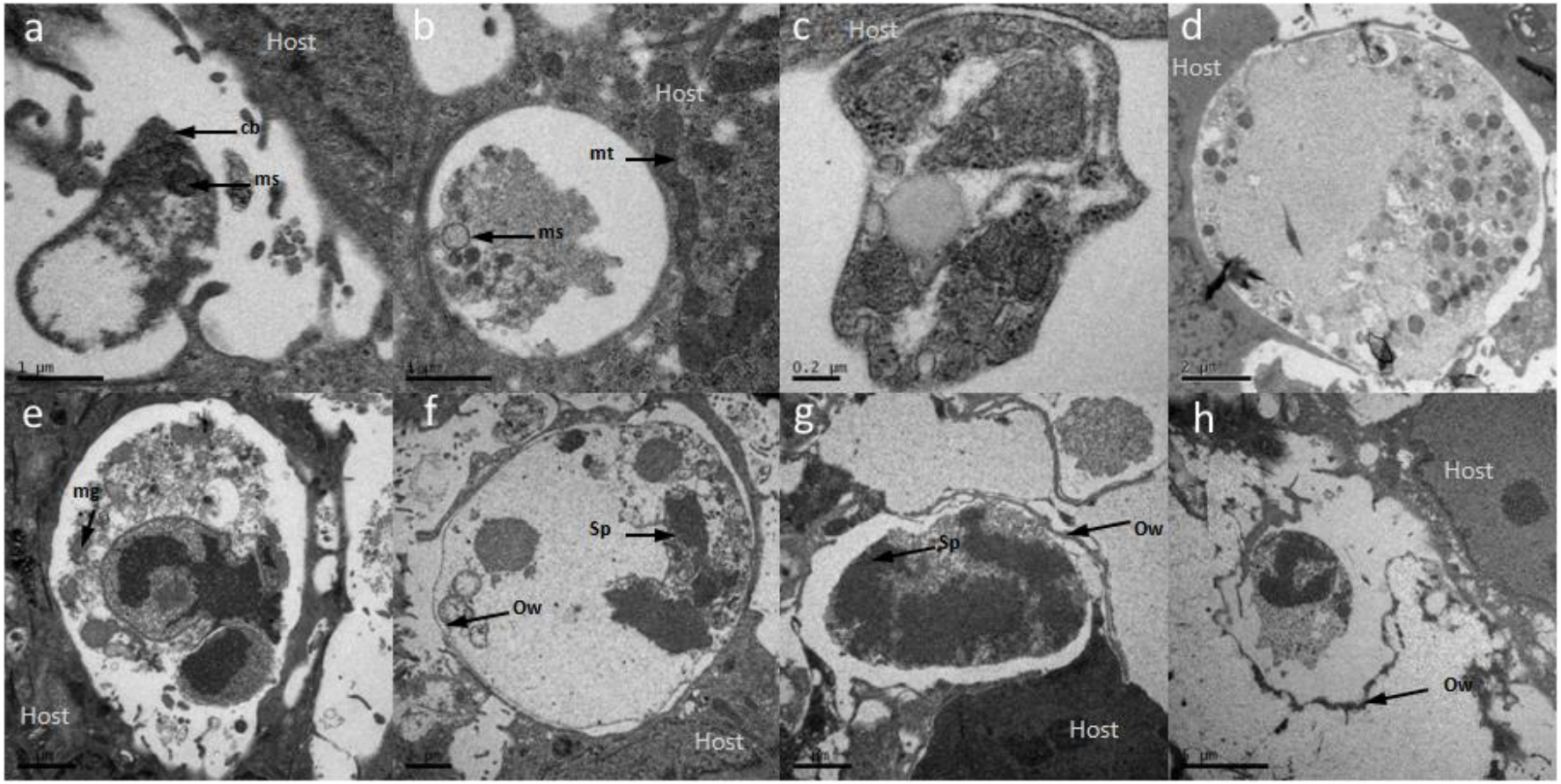

Figure 3-12: EM images of a *C. parvum* infection. the main stages of *C. parvum* during an infection. Starting from top left and going row by row the stages are: Sporozoite (a), trophozoite (b), meront, macrogamont (c), microgamont (d), zygote (e), immature oocyst (f) and matured oocyst (g and h). During these stages many structures become apparent including the mitosome (ms), crystalloid body (cb), micro gametes (mg), the oocyst wall (ow), formation of sporozoites (sp) as well as host organelles such as the mitochondrion (mt). Scale bars: a: 1 µm,, b, d-f: 2 µm, c: 0.2 µm h: 5 µm,

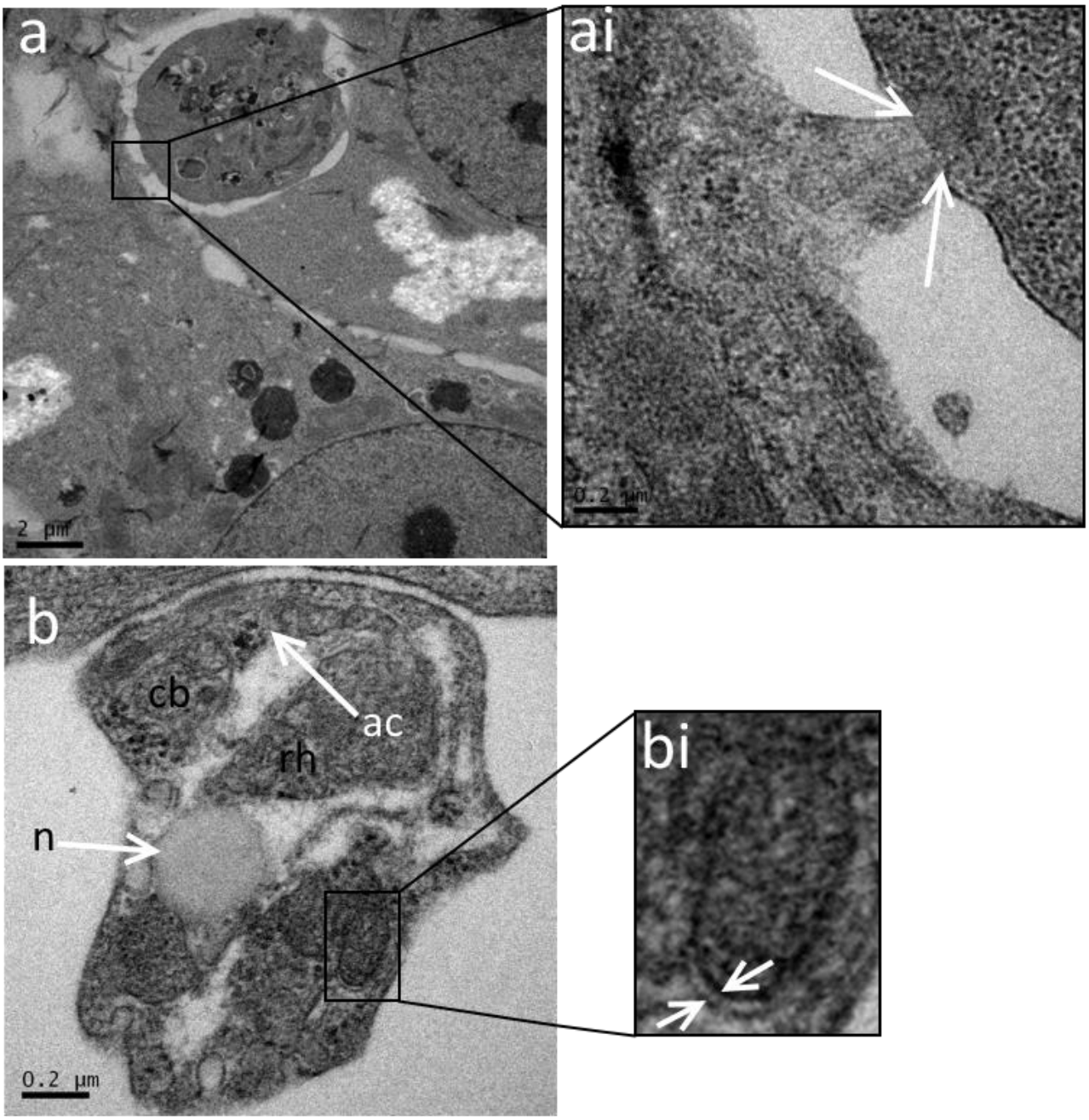

Figure 3-13: EM images of *C. parvum* structures of interest. (a) Clearly visible is the feeder organelle of an intracellular stage of *C. parvum*, most likely a meront. An enhanced image of the region (ai) reveals interesting topology of the organelle, suggesting that it may derive from the host machinery as invagination is clearly shown to occur on the parasite (arrows). (b) A merozoite, the same as imaged in Figure 3-12, reveals a number of interesting organelles including the nucleus (n), crystalloid body (cb), *C. parvum*'s single rhoptry (r) and the apical complex (ac). Also visible is the remnant mitochondrion that *C. parvum* possess, the mitosome (bi). The individual layers of the characteristic double membrane are clearly visible in the close-up (arrows).

3.3.7.2 Atomic force microscopy of isolated oocysts

AFM was employed to investigate the nature of the oocysts in a high magnification topological approach. AFM has been previously used to elucidate unique surface details at a level of resolution not visible using any other imaging modalities in other parasites (e.g. *Giardia* and of *Trypanosoma spp.*). Two distinct types of oocysts were observed in the force-distance curve-based imaging from *C. parvum*-infected COLO-680N cultures. Most oocysts imaged were of a larger type that was indistinguishable from the images obtained from the cattle-produced oocysts (Figure 3-14). The identity of these oocysts was determined to be the 'thick-walled' variety, owing to the nature of thin walled oocysts rarely passing into the environment and therefore unlikely to be present in the commercial sample. However, a smaller type was also observed that most likely represents thin-walled oocysts and may contribute to the continuous *C. parvum* infection pattern that we observed in cell culture, since thin-walled oocysts are thought to be responsible for infection dissemination within organisms and tissues.

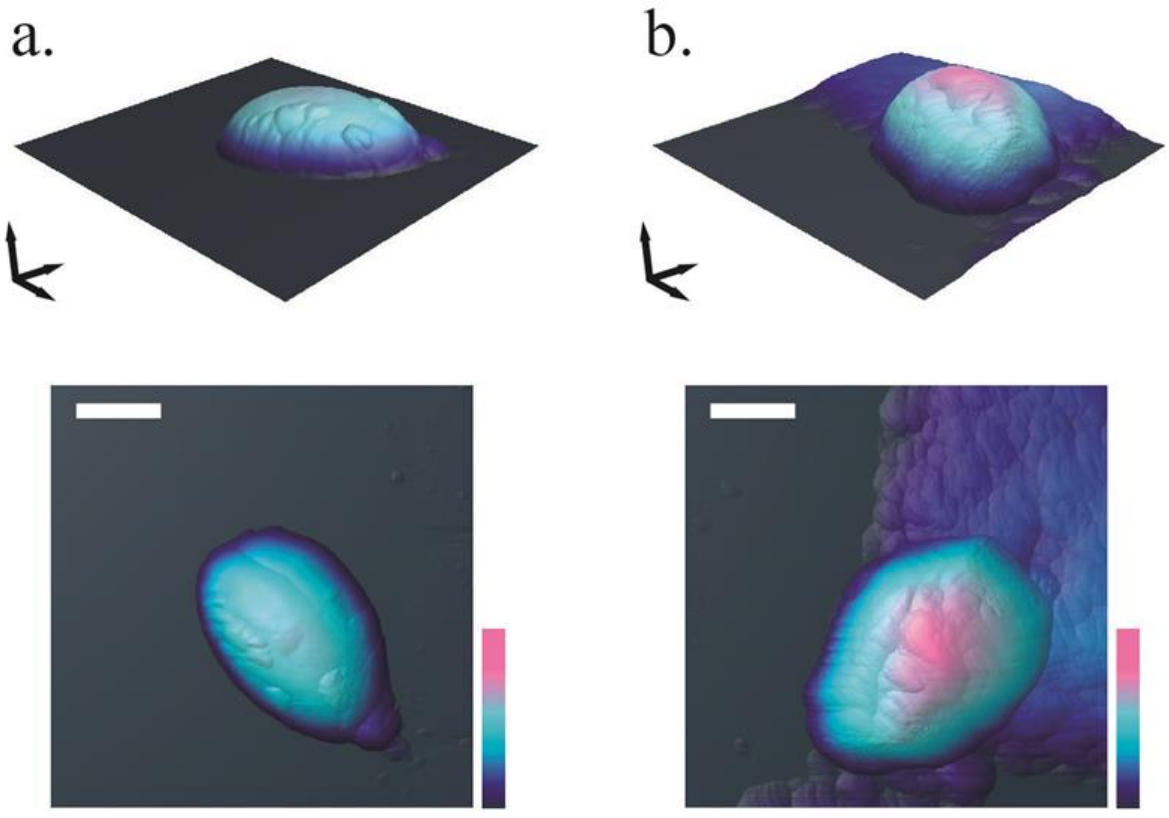

Figure 3-14: Atomic force microscopy (AFM) imaging of purified oocysts from COLO-680N cultures revealed two distinct populations. Population (a) is believed to be representative of the thin walled

variant of an oocyst, indicated by its slumped posture and comparatively less rigid structure when compared to oocysts from population (b), which are believed to be thick walled oocysts. Current understanding of *C. parvum* life cycle biology places the thick-walled oocyst (b) as essential for completing the life cycle and passing from the host into the environment whereas thin walled oocysts (a) are believed to be responsible for maintaining *C. parvum* autoinfection in healthy individuals where the asexual life cycle does not continue indefinitely (unlike in immunocompromised patients)

Similar observations of commercially supplied oocysts failed to produce evidence of thin-walled oocyst populations but did show comparable thick-walled oocysts, similar to those purified from the COLO-680N cultures Figure 3-15. No observations could be made that markedly distinguished commercial and COLO-680N produced oocysts except for the tendency for commercial oocysts to 'clump' together. However, this could be explained due to the expected hydrophobic nature of the lipid rich oocyst wall, which could be lessened in the COLO-680N oocyst sample due to the remaining cellular detritus after the simple purification method employed.

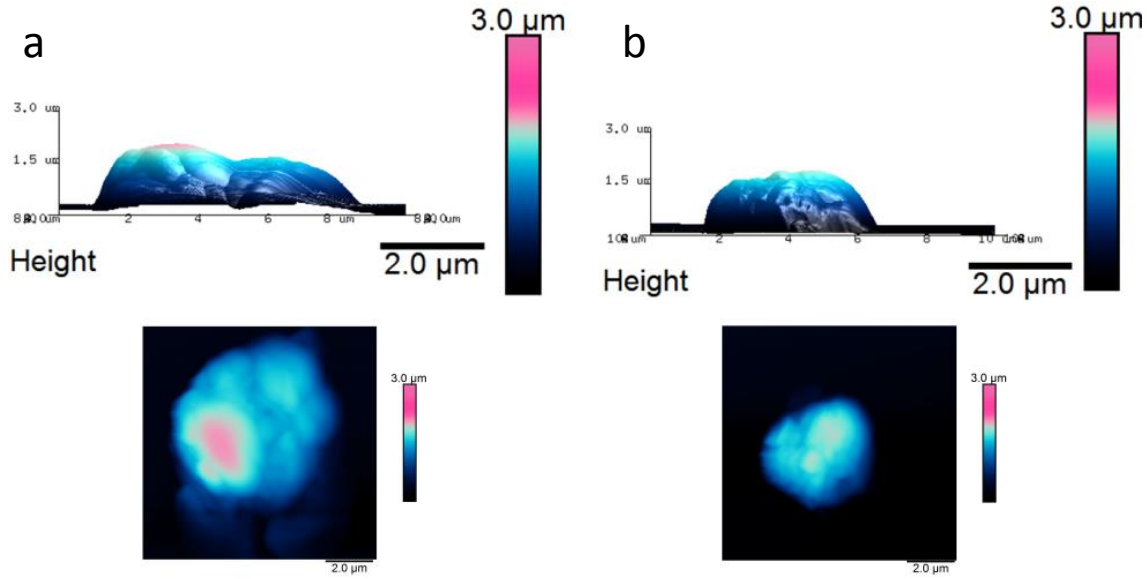

Figure 3-15: AFM captured images of commercial (a) and COLO-680N produced (b) oocysts. Whilst both commercial and COLO-680N produced oocysts displayed similar structures, typical of those described in the literature, commercially supplied oocysts showed a greatly enhanced likelihood of grouping together. This resulted in all AFM image captures of commercial oocysts capturing at least 2 and never a lone oocyst.

3.3.8 Observation of host, HUMAN-FASN activity during infection

Western blots of infected and control group cultures revealed an interesting difference in the response of COLO-680N cultures when infected, compared to the previous gold-standard HCT-8 and non-*C. parvum* permissible DLD-1 (Figure 3-16). Although COLO-680N has been shown to maintain higher than expected levels of fatty acids/lipids in previous literature, these results show that FASN activity is wholly insufficient in determining potentially effective host cell cultures for *C. parvum,* as DLD-1 clearly expresses a much higher level of FASN compared to either COLO-680N or HCT-8 and yet cannot be observed to maintain *C. parvum* cultures to any degree. However, unique to COLO-680N was a marked increase in FASN activity once infected, unlike HCT-8 or DLD-1. Perhaps as interestingly, HCT-8 FASN expression levels decreased in response to infection, highlighting further the potential importance of FASN responsiveness to infection as opposed to simply the typical expression levels.

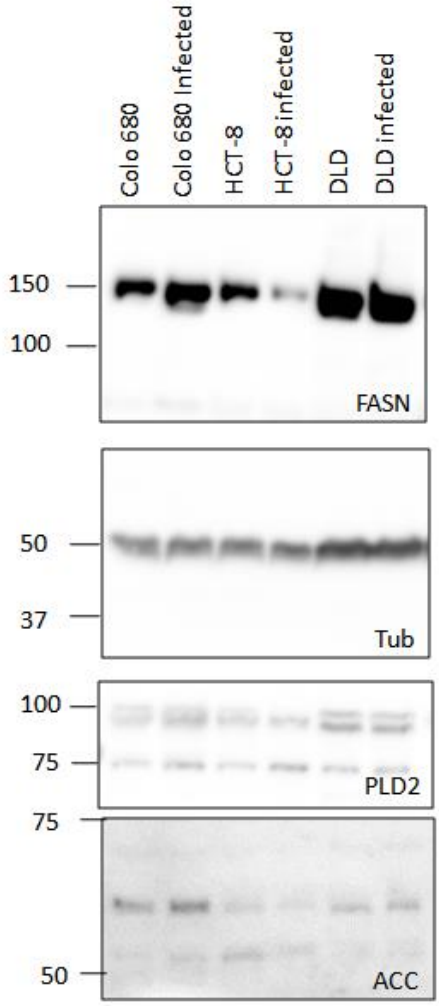

Figure 3-16: Anti-FASN western blot of various cancer cell lines and their subsequent response to *C. parvum* infection. Each sample was obtained from identically aged, 5 days post-infection, 2D, 75cm^2, 30ml cultures and adjusted via dilution with ddH_2O to obtain identical cell numbers. DLD-1 displayed the highest natural expression of FASN, whereas only COLO-680N and HCT-8 levels responded to infection.

3.4 Discussion

Here I have presented a novel cell culture that enables the sustainable, continuous propagation of infectious *C. parvum* oocysts and the systematic investigation of the *Cryptosporidium* life cycle. Previously attempts to cultivate *Cryptosporidium* in cell culture were affected by a lack of oocyst production or required sophisticated, expensive equipment and methodologies to support 3D cultures that are not commonly available to

research laboratories (Striepen, 2013, Hijjawi, 2010, Yin et al., 2010, Karanis and Aldeyarbi, 2011, Muller and Hemphill, 2013, Morada et al., 2016). The COLO-680N platform does not share these flaws. The COLO-680N platform enables *C. parvum* propagation, the sustainable production of *C. parvum* oocysts, and the investigation of the *C. parvum* biology at a laboratory scale in standard, easy to use 2D tissue cultures with commonly available equipment and know-how.

In addition, this data demonstrates a long-term maintenance of the cell-line and subsequently a prolonged production of oocysts as well, in addition to a first of its kind ability to cryoconserve the parasite for greater long term storage or transportation, systems both urgently needed by the field (Striepen, 2013, Checkley et al., 2014).

All *C. parvum* life cycle stages could be detected in infected COLO-680N cells, moreover, the presence of additional previously unrecognised and 'absent' structures indicate that the systematic analysis of *C. parvum* replication in COLO-680N cells will provide novel insights resulting in a substantially improved understanding of *C. parvum* biology. COLO-680N-produced oocysts were indistinguishable from cattle-produced oocysts by staining with antibodies that specifically bind to the *C. parvum* oocyst cell wall and though some variation could be seen utilising lipidomics, and atomic force microscopy techniques, it was often to the same degree as the variation seen within the groups. Thus, I present for the first time, a new collection of tools (lipidomics and AFM) for investigating the cell biology and the composition of *Cryptosporidium*, which can be incorporated in further studies to provide a better understanding of the infection and life-cycle of the parasite.

It remains unclear why COLO-680N cells, in contrast to other cell lines that have been investigated so far, support *C. parvum* propagation. Nevertheless, the whole cell MALDI-ToF fingerprinting studies suggested that *C. parvum* infection of COLO-680N cells results in a substantial change in the features of the cultures, while *C. parvum* infection of HCT-8 cells, a model commonly used for the studying of *C. parvum*, does not. This may indicate a specific susceptibility of COLO-680N cells towards *C. parvum* infection. There also exists a mounting body of evidence that suggests a link between squamous cell carcinomas and cryptosporidiosis which, given the nature of these results, I believe warrants closer examination (Shebl et al., 2012, Benamrouz et al., 2012b, Benamrouz et al., 2012a). In addition, the presence of two different populations of

oocysts (suggestive of the presence of thin oocysts) was detected in COLO-680N cultures by Crypt-a-glo/ DAPI double staining and atomic force microscopy. The presence of thin-walled oocysts may also contribute to the successful *C. parvum* propagation, since thin-walled oocysts are thought to be responsible for the maintenance and dissemination of infection within tissues and organisms it stands to reason that they would perform a crucial role in maintaining the 'autoinfection' cycle within an un-interfered with *in-vitro* culture (Current Wl Fau - Reese and Reese, 1986, Current et al., 1986, Mitschler et al., 1994, Hijjawi et al., 2001).

Additionally, previous studies of COLO-680N had suggested that the expression of high-levels of fatty acid synthase (FASN) might promote cell viability, and could also be beneficial to the parasite, since it is unable to synthesize fatty acids *de novo* (Orita et al., 2010, Abrahamsen et al., 2004). Rather, *C. parvum* has been shown to maintain a peculiar Fatty Acid Synthase, dubbed CpFAS-1, whilst no *de-novo* synthesis activity could be not observed, it was found that CpFAS-1 can act as an elongase, limited to expanding fatty acids at least 16 carbons long (Zhu et al., 2000). This is a potentially crucial insight into the parasite's metabolic reliance on the host cell as a significant portion of the oocyst wall *C. parvum* maintains in comprised of long chain fatty acids. Preliminary experiments exploring the potential links between this host fatty-acid dependence and COLO-680N's FASN activity displayed interesting results. Whereas high levels, such as those found in DLD-1, proved insignificant in determining permissibility, COLO-680N displayed a FASN expression level response to infection with the parasite. With the emerging, published, evidence that *C. parvum* RNA is exported into the host cell, the question is raised as to whether a) host FASN expression is a potential target of this RNA secretion and b) if COLO-680N is more susceptible, somehow, to the *C. parvum* RNA, which could explain the results I observed (Wang et al., 2017). This could represent a revolutionary step forward in not only predicting potentially suitable *in-vitro* cell cultures but in understanding host-and even specific host-cell specificity and warrants further examination by future investigations.

In conclusion, the discovery of COLO-680N as a cell culture platform to produce *C. parvum* will provide a step-change regarding research on *Cryptosporidium*: 1) It is the first easy-to-handle system that enables the long-term sustainable production of infectious oocysts at a laboratory scale and removes the constant dependence on immunosuppressed animals for production of *Cryptosporidium* oocysts along with all its ethical implications.

2) *C. parvum*-infected cell cultures can be frozen and stored. Prior to the establishment of the COLO-680N cultivation system for *C. parvum*, oocysts had to be freshly acquired from animals and could not be stored over longer periods. 3) This study paves the way for establishment of compound-screening platforms for the identification of anti-*C. parvum* drugs and the systematic elucidation of *C. parvum* biology, including the utilisation of a CRISPR transfection system (Vinayak et al., 2015).

The establishment of a robust culturing system also allows a more in-depth examination of the host-parasite relationship than previously possible as well as a life-cycle wide examination of parasite metabolic processes. As such it is the purpose of Chapter 4 to investigate the broader metabolic nature of the host-parasite interaction and Chapter 5 will investigate the potential role of the mitosome in iron-sulphur cluster biosynthesis, a highly evolutionary conserved and essential metabolic pathway.

Chapter 4 Host-pathogen interaction of a *Cryptosporidium* infection in a metabolic context

4.1 An introduction to metabolomics in parasitology

Among the collection of experiments now made available by the existence of long term culturing is the concept of metabolomics. As a parasite, *C. parvum* interacts directly with host tissue and therefore it is likely to have an array of complex relationships with the host metabolic processes. Previous studies utilised a Gas Chromatography Mass Spectrometry (GC-MS) approach to explore this concept, though only two papers have been published on the subject one on mouse and the other on human faecal samples, both showing a clear relation between infection and a change in metabolite levels (Ng Hublin et al., 2012, Ng Hublin et al., 2013). Whilst working on different sample sources, each identified hexadecanoic acid as a significant contributor to the change in the metabolome during infection. Hexadecanoic, or 'Palmitic', acid is a common fatty acid, found throughout the tree of life; its appearance is not surprising when considering that *C. parvum* appears to rely heavily on the host for fatty acid synthesis. Among the other shared observations was the large change in relative abundance of various amino acids and components of their pathways. However, while most of these metabolites appeared to decrease in infected mice faeces, an increase was seen in humans. This is not unusual, previous explorations of other metabolomes have highlighted a tendency for otherwise similar organisms to have almost contradictory changes in their metabolomes occur under the same environmental pressures (such as a change in diet or infection) (Lindon and Nicholson, 2008, Bezabeh et al., 2009, Jansson et al., 2009, Le Gall et al., 2011). Their closing marks included the call for further studies and the development of new methods of study to broaden the knowledgebase of metabolomics to shed light on its often-paradoxical qualities.

In response to the growing need for an alternative method of exploring metabolomes, the scientific community has begun exploring the usage of ^{1}H Nuclear Magnetic Resonance (NMR) (Sengupta et al., 2016, Jacobs et al., 2008, Saric et al., 2008, Bezabeh et al., 2009, Hong et al., 2010). ^{1}H NMR based metabolomics has been shown to be a powerful

alternative to GC-MS for metabolic screening. The methodology is simpler and with fewer steps between sample recovery and analysis, resulting in reduced loss of sample during preparation. This translates to a more reliable result in terms of quantification and reproducibility, although GC-MS still provides a higher level of resolution and NMR should not be considered a wholesale replacement of the technique.

Initially established in 2002 as a tool for toxicology, ^{1}H NMR has seen a significant uptake in the last five years, becoming an established technique in a variety of disciplines including immunology, drug design and increasingly within the medical field as an early warning diagnostic. However, adoption of ^{1}H NMR based metabolomics within the field of parasitology is still in its infancy, with less than 20 published papers, mostly concerning malaria (Sengupta et al., 2016, Teng et al., 2009, Wu et al., 2010, Balog et al., 2011, Li et al., 2011, Sengupta et al., 2011, Ghosh et al., 2012, Lamour et al., 2012, Sonawat and Sharma, 2012, Sengupta et al., 2013, Teng et al., 2014, Cheng et al., 2015, Arjmand et al., 2016). Although still early in its adoption, the results produced by these experiments have shown great promise in exploring host-parasite interactions and as such warrant further exploration.

As a potential model species for the evolutionary move from gregarines to other Apicomplexa, the development of a ^{1}H NMR protocol for the exploration of *C. parvum* infections could provide the necessary tools to bring ^{1}H NMR to the rest of the phylum in addition to furthering our understanding of the host-parasite interaction in cryptosporidiosis.

4.2 Goals

I decided to take a novel approach to exploring the metabolome of a *C. parvum* infection. Whilst I will examine the metabolic shift within mouse models of the infection, I will also examine for the first time the effects an infection has on the metabolome of a cell culture, an unprecedented observation in both the Apicomplexa and parasitology. One potential drawback of the methods used so far, especially in the previous GC-MS studies of cryptosporidiosis, is centred on the use of faecal samples as a sample source. Whilst a change in faecal metabolites is an important indicator of altered processes within the host,

it is impossible to comment on the cause of an observed change in a metabolite's abundance. An increased amount of a metabolite within a faecal sample could equally be the result of decreased absorption or increased production of the metabolite. By exploring the effects on the metabolome of the *in-vitro* culture I have developed, we can comfortably eliminate the effects of a decreased absorption by removing external contributors to the metabolome and, by comparing to the observations from the mouse faecal samples, further elucidate the host-pathogen relationship in the context of metabolism.

4.3 Results

4.3.1 Mice faecal sample extractions

Mouse models of infection, infected with *C. parvum* strains Weru or Iowa II, were monitored for several days for successful infection before culling and intra-intestinal faecal extraction as detailed in *2.16.1* before processing the samples for metabolite extraction and ^{1}H NMR analysis as detailed in *2.16*.3.

Casual observations of the spectra produced by the ^{1}H NMR already revealed clear distinctions between the infected and uninfected mice, as well as between the different strains of infections (Figure 4-1a). Several metabolites were readily distinguishable, including the peaks of metabolites indicating mitochondrial ADP-ATP synthesis; creatine and creatine phosphate (Figure 4-1b), taurine (Figure 4-1c) and lactate (Figure 4-1d) (Wallimann et al., 2011, Hansen and Grunnet, 2013, Schaffer et al., 2014).

These preliminary indicators of mitochondrial activity suggested that whatever effects the infection was having on the host gut metabolome, it included a substantial impact on host energy metabolism.

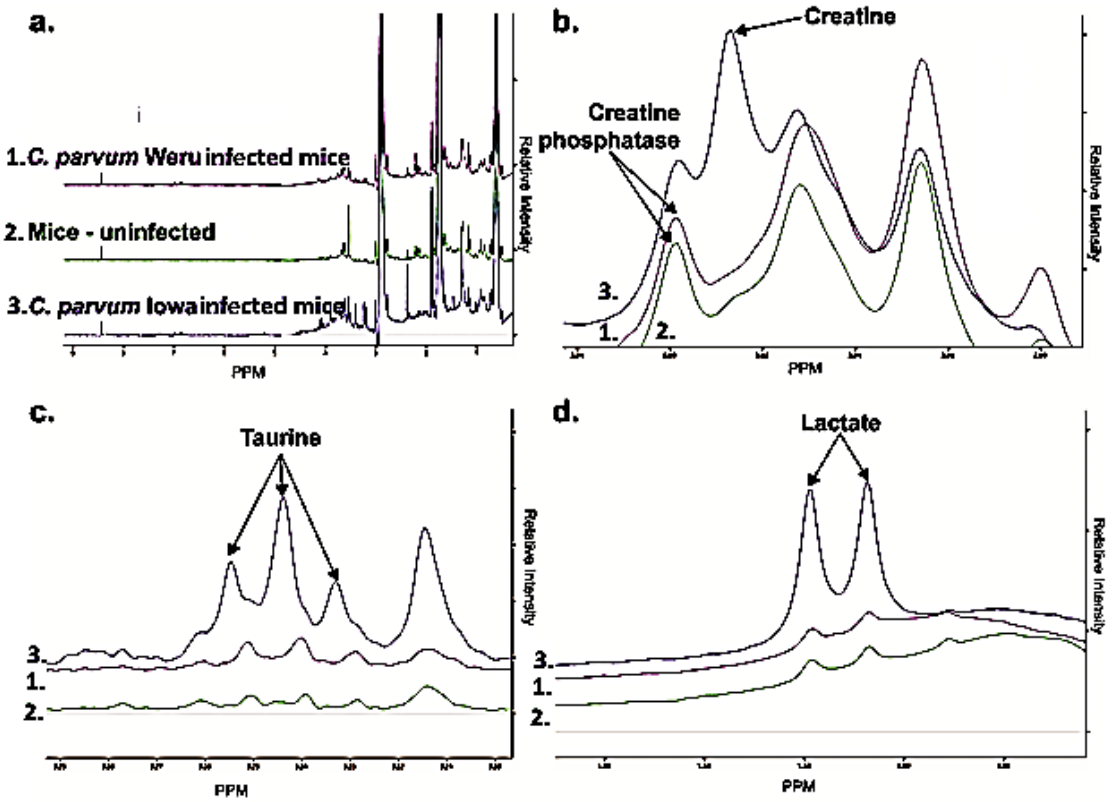

Figure 4-1: NMR spectra of infected mice intestinal samples. a) Stacked Spectra produced from infected mice samples after processing via the Chenomx software package, representing the average spectra obtained from each infection condition (from triplicate), including the negative control and Weru and Iowa II infections. Amongst other noticeable differences were the changes in peak intensities and shapes, displayed overlaid are the peaks for creatine and creatine phosphate (b), taurine (c) and Lactate (d). In each case higher peaks can be observed for the Iowa II infections, indicating more abundant amounts of these metabolites were present in Iowa II infected cultures. Further experimentation would be required to determine definitively if this was a result of over production or under-utilisation.

To explore the spectra in detail, the data from the mice guts (n=9) was processed through the Chenomx NMR Suite, version 8.2. The result was a list of 151 compounds that were detected within the spectra (Table 4-1).

Statistical analysis of the data, with freely available Microsoft Excel Add-in "multi-base 2015", by Partial Least Squares Discriminant Analysis (PLS-DA) determined significant separation of the three conditions, (Uninfected control, *C. parvum* Iowa II and *C. parvum* Weru infections), whilst maintaining group cohesion (Figure 4-2a). The loading values of the variable compound contributions (Figure 4-2b), suggest certain metabolites were more

considerable to the separation of the groups than others. To further illustrate the impact each sample had on the separation, the data from the PLS-DA loading values was extracted and used to create a heat map of the metabolites shown in Table 4-1. The presence of L-alanine and valine, two common amino acids, as large impact contributors agree with the previous literature and 2-oxoisocaproate is a component of the valine/leucine/isoleucine biosynthetic pathways (Ng Hublin et al., 2013, Ng Hublin et al., 2012). Whilst this data alone provides an intriguing insight into the effects on the host metabolome, importing the results into a metabolic pathway tree could produce a more detailed view of what aspects of the host's metabolism are most affected by the infection.

Table 4-1: A heatmap of compounds detected via chenomx. Their relative contributions towards the differences observed between the mice experimental groups as calcualted by a Partial Least Squares Analysis. Negative values (tending towards red) indicate the samples showed a greater degree of variation within sample groups and are therefore indicators of compounds that naturally vary in their levels, without external stimuli. Positive values (tending towards green) indicate the samples contributred more towards differences between sample groups. Compounds that did not show any difference between conditions were excluded

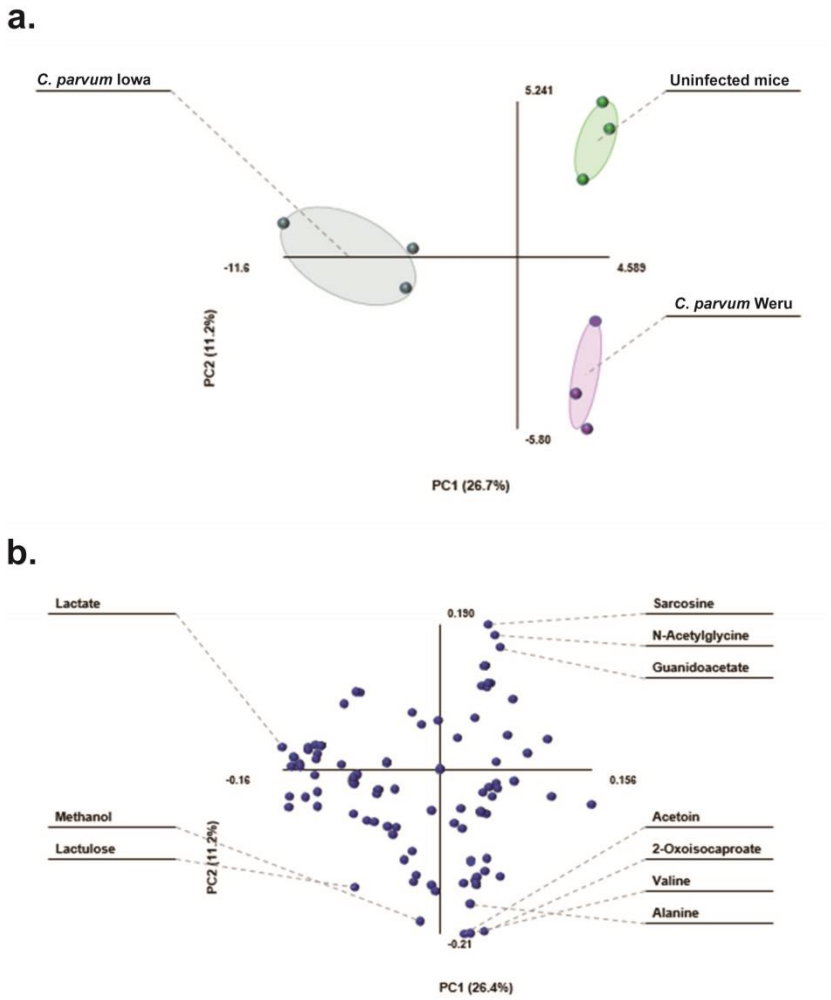

Figure 4-2: a) 2D graphical representation of a PLSDA Partial Least Squares Discriminant Analysis of the Chenomx data. Successful separation of the three experimental groups can be observed by the lack of overlap observed between different experimental groups. The lack of overlap between Iowa II (blue) and Weru (purple) groups suggest that the different strains assert consistently different effects on the metabolome. b) The loading plot, used in formulation of the PLS-DA. Those samples furthest to the extreme edges of the axis represent the samples contributing most notably to the differences observed, including Lactate and Alanine.

Upon exporting the results to MetaboAnalyst 3.0, an online "comprehensive tool suite for metabolomic data analysis", several metabolic pathways became immediately highlighted as being heavily involved in the changes observed during infection (Xia et al., 2015). As indicated in the preliminary observations, several amino acid biosynthesis pathways were among the first noted, including glycine, valine and taurine pathways. The

metabolic pathways discovered through MetaboAnalyst were presented graphically (Figure 4-3a) and those pathways of greatest note determined as those furthest from the x, y axis intercept, representing both the overall completeness of the pathways and number of contributing detected metabolites detected within the data. To better understand to what extent these pathways were involved, the MetaboAnalyst suite can also render the individual pathways, highlighting the metabolites seen within the data in red as shown in Figure 4-3 b-d and Figure 4-4a-c. Converting the KEGG compound codes within the pathways reveals the metabolites that contributed towards the predictions made by MetaboAnalyst (Table 4-2), this allows a more critical observation of the validity of the predicted pathways. When comparing the compounds listed in Table 4-2 to the heat map in Table 4-1, it becomes clear that every compound contributed positively to the characterisation/differentiation of one or more conditions, even if other conditions showed variable levels. From this observation it can be stated that the pathways predicted to be affected by infection are a reliable interpretation of the data.

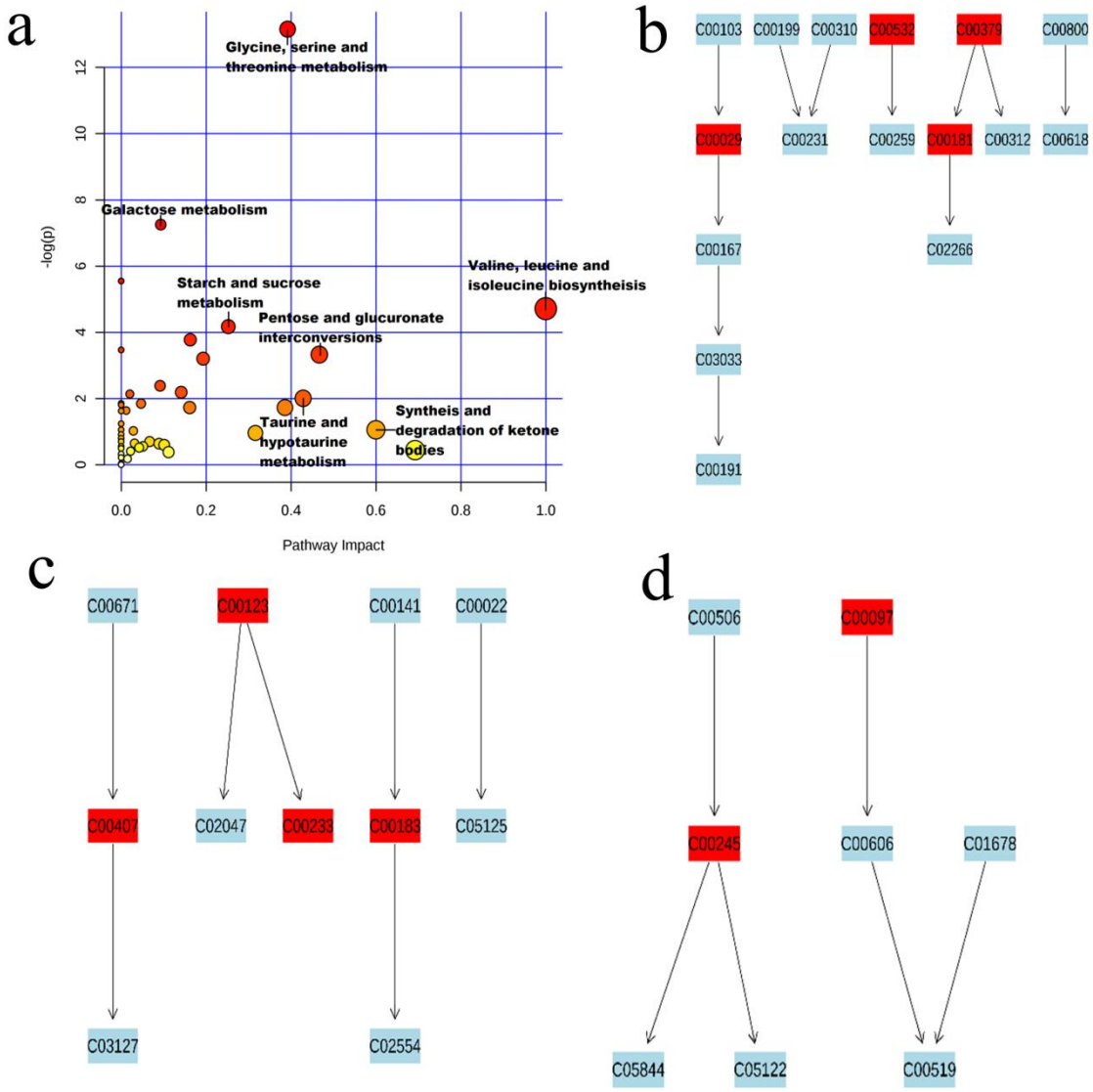

Figure 4-3: a) A graph representing the pathways detected by MetaboAnalyst 3.0 from the Chenomx data. The x-axis represents the relative completeness of a pathway based on the metabolite detected. The y-axis represents the relative size of the entire pathway and the size of the points represents the combined significance of both data points. Full maps of the pathways were rendered and metabolites present in the data highlighted in red for the following: (b) glucoronate interconversions, (c) Valine, leucine and isoleucine biosynthesis and (d) Taurine and hypotaurine metabolism.

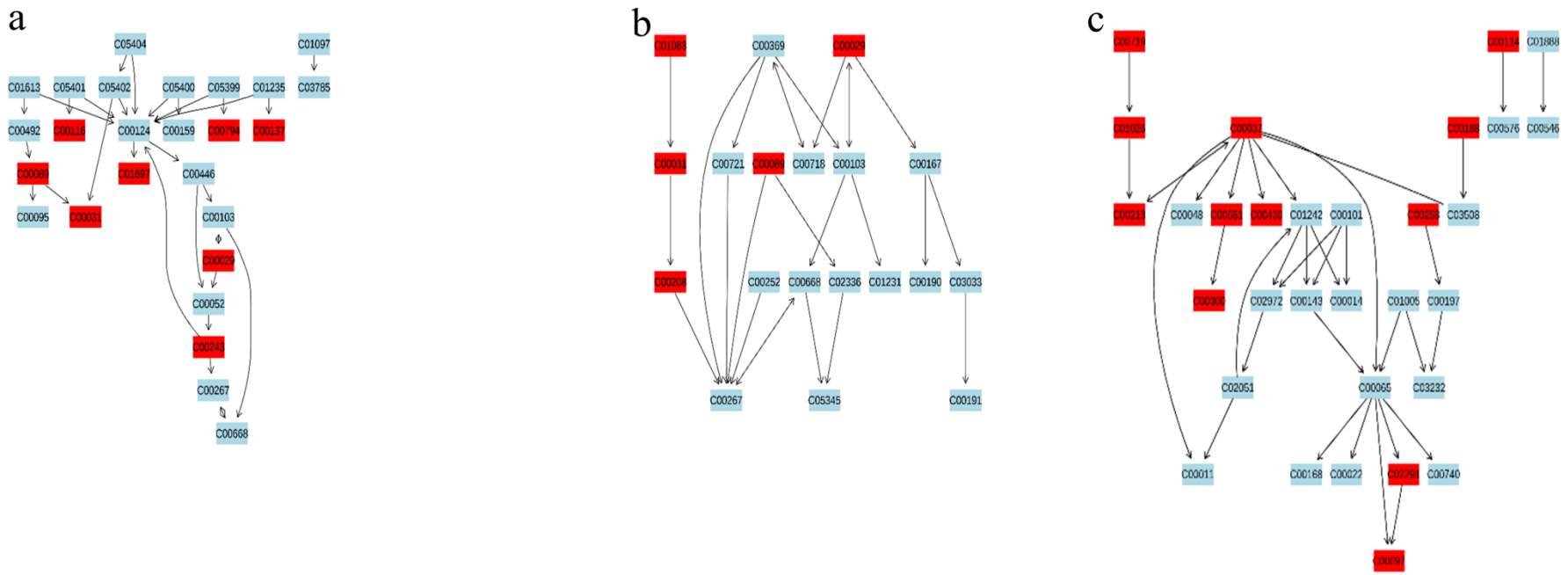

Figure 4-4: Full maps of the pathways were rendered and metabolites present in the data highlighted in red for the following: (a) glycine serine and threonine metabolism, (b) Galactose metabolism and (c) starch and sucrose metabolism.

Table 4-2: KEGG ID key. Extracting the KEGG ID tags from the produced pathway maps gives the following compounds, arranged by order of appearance throughout Figure 4-3 and Figure 4-4.

KEGG ID	Compound Name
C00029	Uridine diphosphate (UDP) glucose
C00532	Arabinitol
C00379	Xylitol
C00181	Xylose
C00407	Isoleucine
C00123	Leucine
C00183	Valine
C00245	Taurine
C00097	Cysteine
C00089	Sucrose
C00031	Glucose
C00116	Glycerol
C01697	Galactitol
C00243	Lactose
C00794	Sorbitol
C00137	Myoinositol
C01083	Trehalose
C00208	Maltose
C03719	Phenylacetate
C01026	N,N-Dimethylglycine
C00213	Sarcosine
C00037	Glycine
C00581	Guanidoacetate
C00300	Creatine
C00430	5-Aminolevulinate
C02291	Cystathionine
C00897	Maltodextrin
C00258	Glycerate
C00188	Threonine
C00114	Choline

One pathway of note from Figure 4-3 is that of Taurine/Hypotaurine synthesis (d). Existing medical reports from *C. parvum* infections have noted increased levels of taurine within the stool samples of patients. This would appear to agree with the observations from the experiments. Exploring the original spectra (Figure 4-1) also reveals that the difference observed is a relative increase in Taurine abundance.

However, as highlighted previously, whilst this data is useful in determining markers of infection, alone it cannot be used to imply with certainty the exact relationships between the infection and affected pathways. Taking taurine as an example, the current theory is that a decreased absorbance of host intestinal tissue, via destruction of villi surfaces by *C. parvum* infection, results in a relative increase in taurine passing out of the host. However, this assumption is fundamentally flawed. Taurine is an important amino-acid that is involved in a wide variety of biological processes, among which many are directly involved in osmo-regulation. Given that observations of damaged villi surfaces within the gut of patients is an established pathology of *C. parvum* and following that this damage is assumed to be the cause behind the watery diarrhoea that characterises cryptosporidiosis, it would be a reasonable assumption that osmo-regulation within the host gut would be heavily up-regulated. Therefore, without further evidence to support either theory it would seem premature to assume heightened taurine levels are a result of unabsorbed taurine and not possibly the result of up-regulated taurine biosynthesis. Thus, the experiments were repeated on cell culture models of infections as well.

4.3.2 Cell culture sample extractions

COLO-680N models of *C. parvum* infection were maintained for 10 days before extracting metabolites as described in *2.15.2* and *2.15.3*. The NMR spectra demonstrated clear differences between each strain and species of *Cryptosporidium* used (Figure 4-5). As with the mice samples, differences between creatine, creatine phosphate, taurine and lactate (Figures 6b-d) were readily visible in the raw spectra. As before, numerical data of the compound concentrations, as calculated by the Chenomx software, was exported into an excel graph and listing 161 total compounds of varying concentrations across samples when eliminating samples with no observable changes. The PLS-DA generated

by the same statistical analysis as before, produced ample separation of the different experimental conditions, (Figure 4-6a). Furthermore, the separation of the individual infection groups suggests that differences between both *Cryptosporidium* species and within individual strains of *C. parvum*, may illicit different metabolic responses in cell cultures, as supported by the previous *in-vivo* data from *4.2*. The loading scores plot of the PLS-DA showed many amino acids contributed heavily to the separations, as well lactate, several fatty acid derivatives and taurine (Figure 4-6b). This data was also used to inform the heat map of Table 4-3 and Table 4-4.

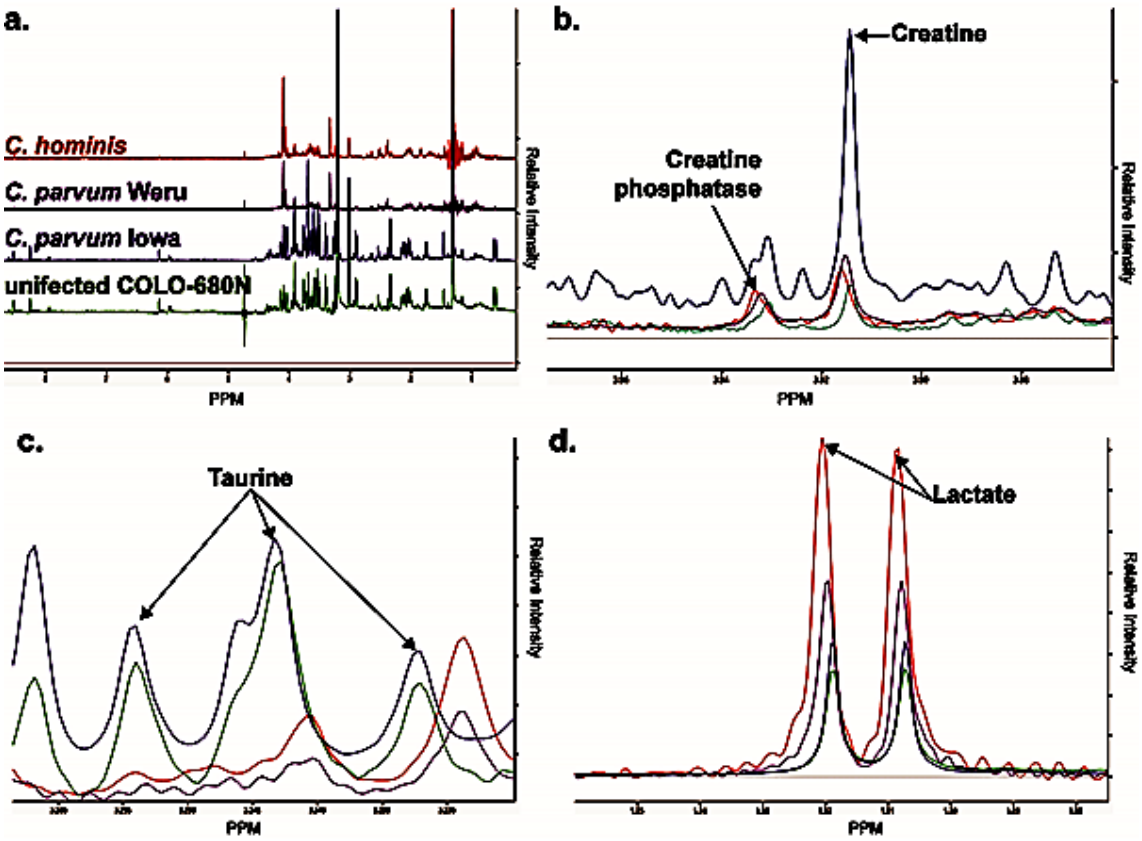

Figure 4-5: NMR spectra of infected cultures. Stacked Spectra produced from infected cell cultures after processing via the Chenomx software package, representing the average spectra obtained from each infection condition, including the negative control, *C. hominis C. parvum* Weru and Iowa II strain infections. Amongst other noticeable differences were the changes in peak intensities and shapes, displayed overlaid are the peaks for creatine and creatine phosphate (b), taurine (c) and Lactate (d).

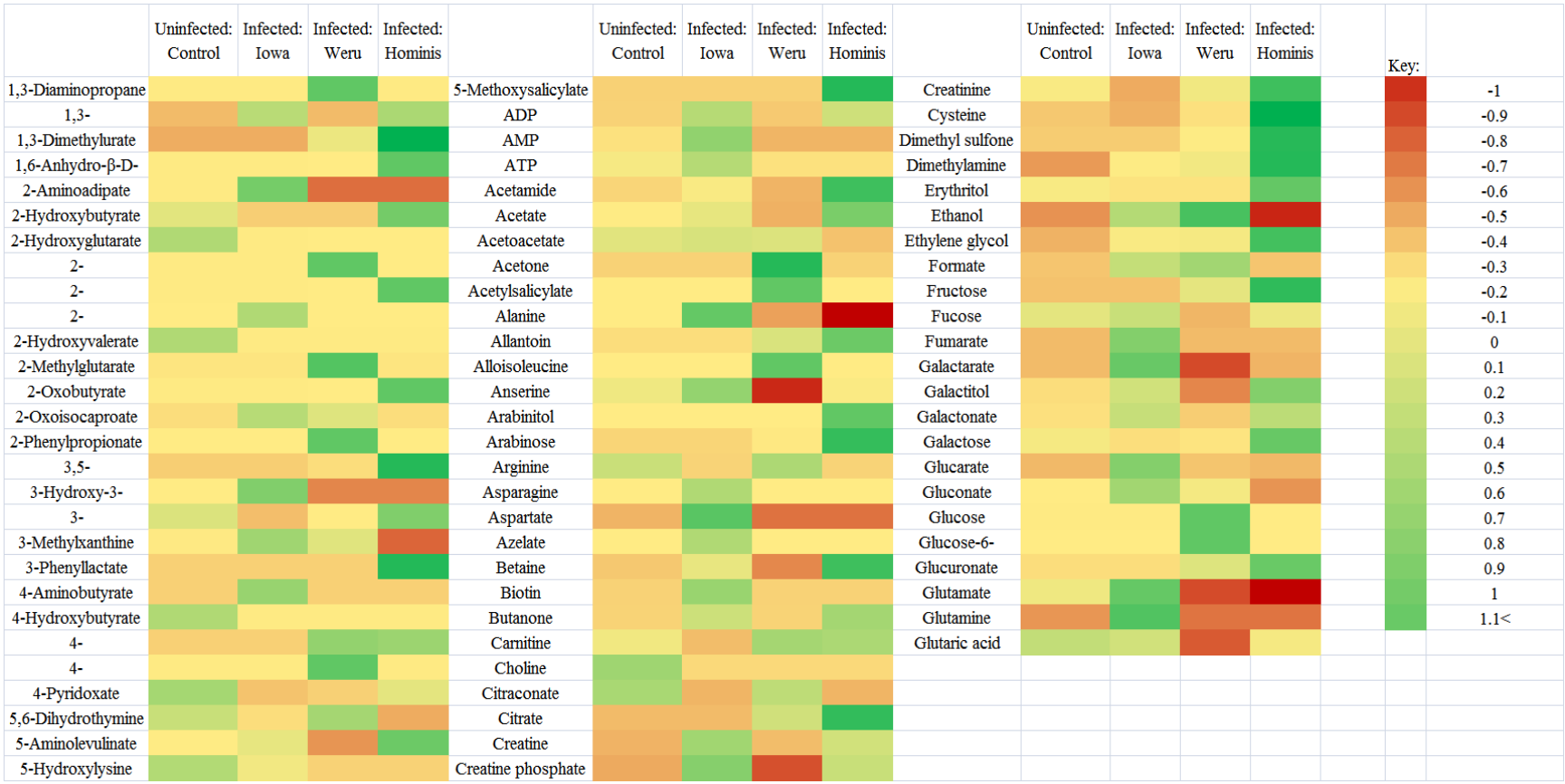

Table 4-3: The first half of a heatmap of compounds detected via chenomx. Their relative contributions towards the differences observed between the infected cultures samples as calcualted by a Partial Least Squares Analysis. Negative values (tending towards red) indicate the samples showed a greater degree of variation within sample groups. Positive values (tending towards green) indicate the samples contributred more towards differences between sample groups.

Table 4-4: The second half of the heatmap.

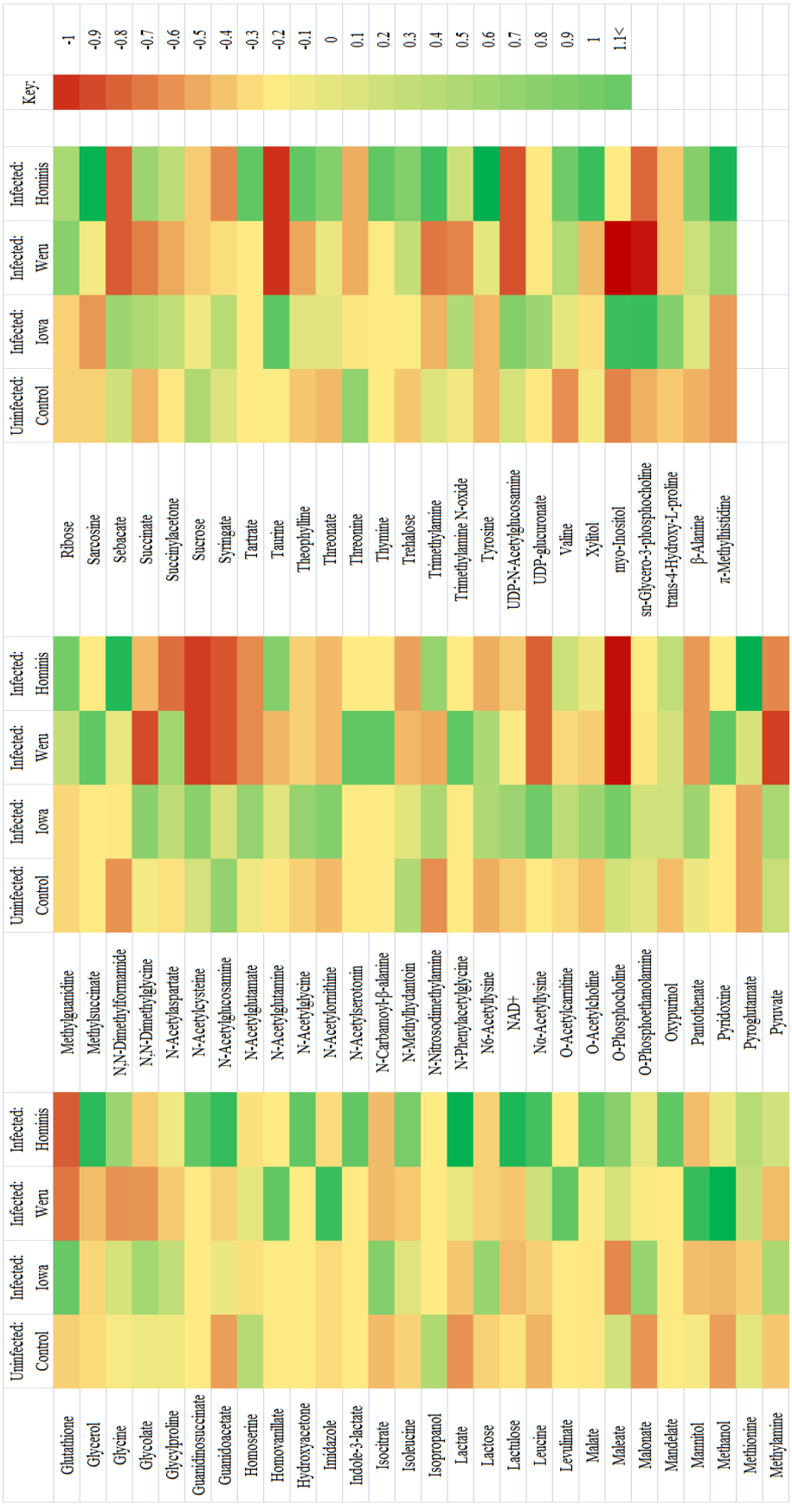

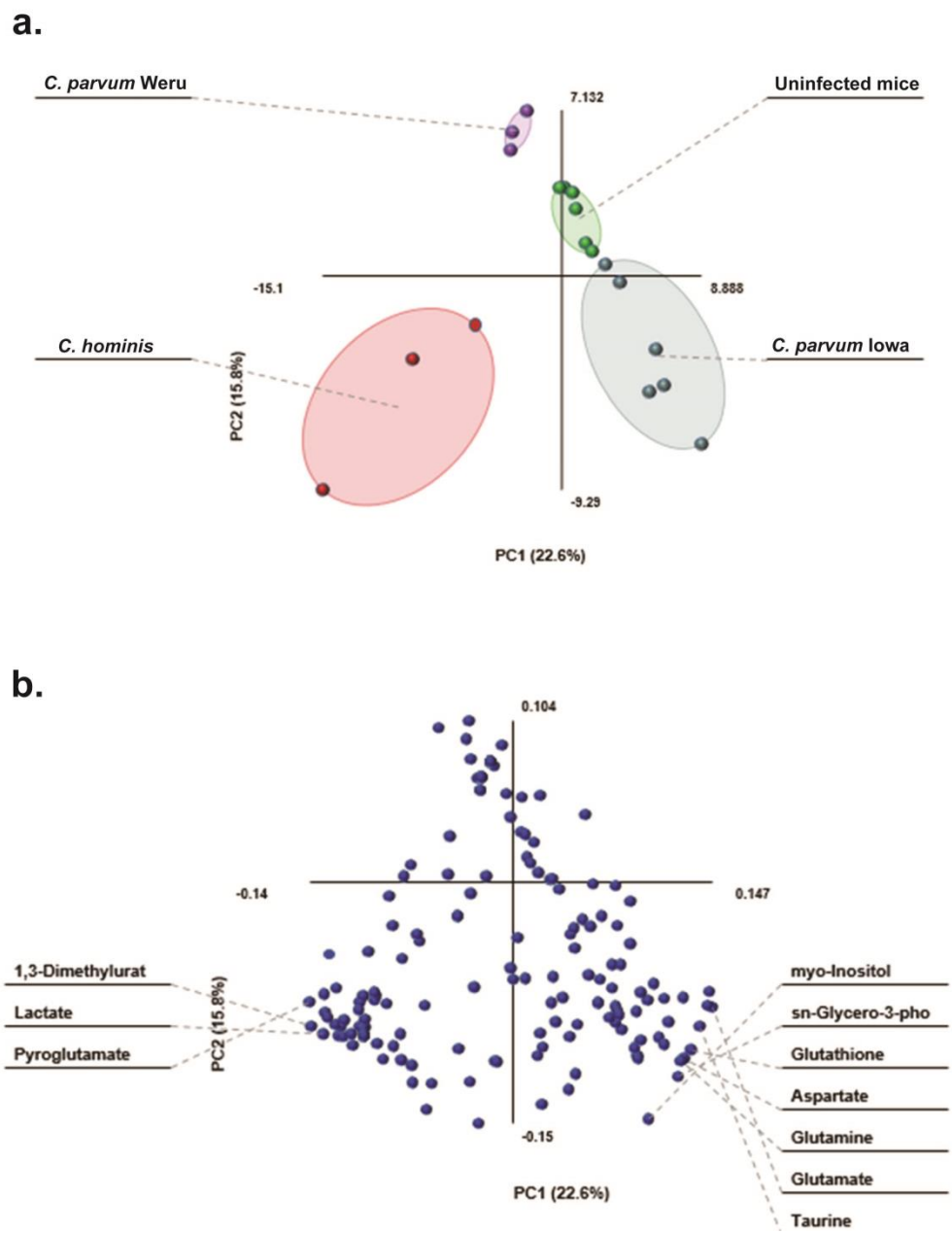

Figure 4-6: PLS-DA statistical analysis of the information provided by the Chenomx screening. Produced clear groupings, separating the controls (green), C. parvum Iowa infections (blue), C. parvum Weru infections (purple) and C. hominis infections (red). As the grouping areas do no overlap the separation between the infection conditions again indicates that metabolome differences can be at least in part explained by different *Cryptosporidium* strains/species. b. The loading biplot of the PLS-DA analysis shows lactate as a significant contributor to variation, as seen before in figure 2b, in addition to taurine and myo-inositol among others.

Metabolic pathway fitting via MetaboAnalyst 3.0 revealed that amino-acid biosynthesis pathways for glycine, alanine and arginine were influenced by infection. These were in addition to taurine, pantothenate and CoA biosynthetic pathways as shown in Figure 4-7a. As with Figures 5a-g, the graph shows a combination of how much of a pathway is

completed by data from the NMR, as well as simply how many metabolites were detected. Among other pathways, perhaps the most significant detections were glycine (Figure 4-7b), taurine (Figure 4-7c) alanine (Figure 4-7d) and arginine (Figure 4-7g) amino acid pathways as well as, potentially the synthesis and degradation of ketones (Figure 4-7e) and pantothenate and CoA biosynthesis (Figure 4-7f). Performing the same decoding as previously produced a table of compounds involved in the most likely affected metabolic pathways.

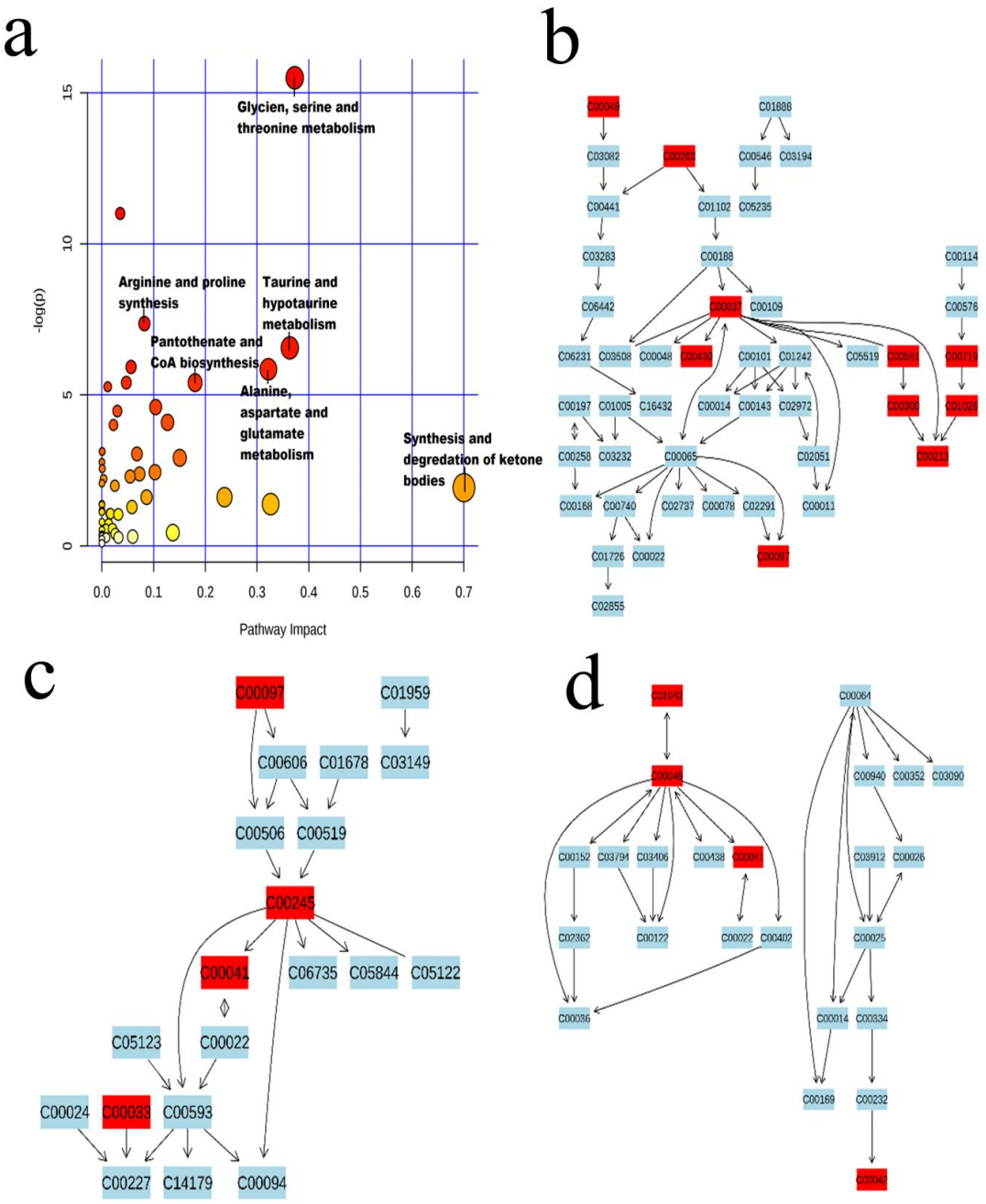

Figure 4-7: Metabolic pathways detected from NMR data of infected cells. (a) Data analysed by MetaboAnalyst 3.0, utilising all compounds which displayed some degree of change because of infection, produced a graph of pathways most heavily impacted (x axis) and pathways containing the most amount of the given compounds (pathway impact: y-axis), with statistical significance of the predicted pathways increasing as the colour ranges from yellow (low) to red (high). Six pathways were chosen to be of interest by their position on the graph, with metabolites present in the experimental samples highlighted in red, including: (b) glycine, serine and threonine metabolism, (c) taurine and hypotaurine metabolism, (d) Alanine, aspartate and glutamate metabolism. The remaining 3 are represented in Figure 4-8.

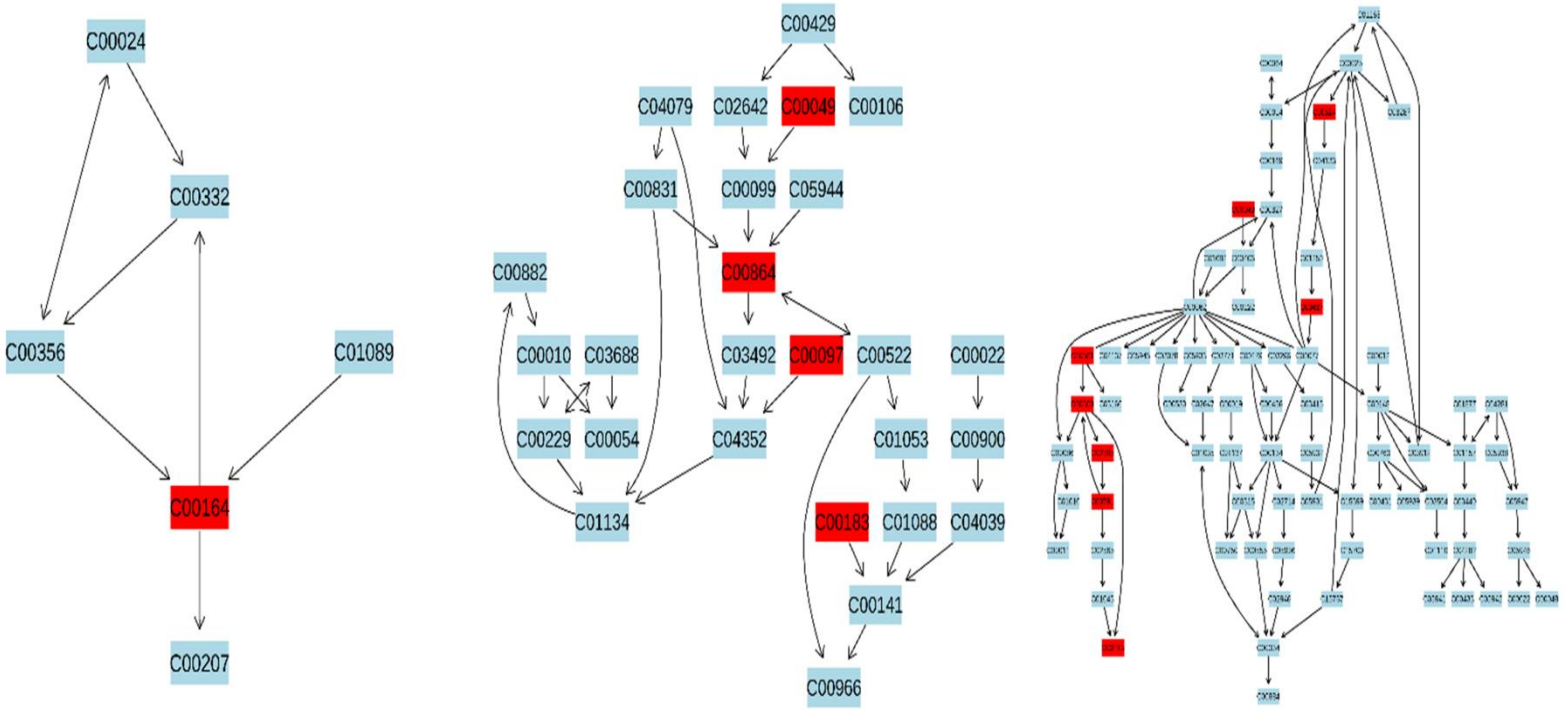

Figure 4-8: The remaining 3 major metabolic trees as derived from the MetaboAnalyst data, showing (a) synthesis and degradation of ketones, (b) pantothenate and CoA biosynthesis and (c) arginine and proline metabolism.

Table 4-5: KEGG ID key. Extracting the KEGG ID tags from the produced pathway maps gives the following compounds, arranged by order of appearance throughout Figure 4-7 and Figure 4-8.

KEGG ID	Compound Name
C00049	Aspartate
C00263	Homoserine
C00037	Glycine
C00430	5-Aminolevulinic acid
C00097	Cysteine
C00581	Guanidoacetate
C00300	Creatine
C00213	Sarcosine
C00719	Betaine
C01026	N,N-Dimethylgycine
C00213	Sarcosine
C00245	Taurine
C00041	Alanine
C00033	Acetate
C01042	N-Acetylaspartate
C00041	Alanine
C00042	Succinate
C00164	Acetoacetate
C00864	Pantothenate
C00183	Valine
C00062	Arginine
C00148	Proline
C02305	Phosphocreatine
C00791	Creatinine
C00624	N-Acetylglutamate

As was the case previously, the metabolites featured in

Table 4-5 represent defining characteristics of at least one experimental condition, indicated by their green filling in the heat map. Interestingly, several of the metabolites appear to be substantially red for *C. hominis* infections, suggesting that changes seen in these metabolite levels (for example glutamate) should not be considered reliable indicators of a *C. hominis* infection. Alanine, Ethanol and O-Phosphocholine also appear to represent variable changes within the host metabolome during *C. hominis* infection. On the other hand, changes in fructose, lactate and xylitol levels appear to be uniquely regular in *C. hominis* infections compared to *C. parvum*.

4.4.3 Comparison of mice faecal and COLO-680N metabolome changes

MetaboAnalyst data from and *4.2* and *4.3*, demonstrates that many altered pathways are shared between the mice and tissue culture metabolites, particularly taurine and amino acid metabolic pathways. To properly explore to what extent the two experiments may corroborate each other, compounds and their relative effects on the PLS-DA data were compared. Tabulation of only those compounds which showed positive loading values (reliable contribution towards separation of sample groups) generated a more succinct list of potential compounds of interest.

Table 4-6 displays the resulting compounds from *C. parvum* Iowa II infections, a total of 18 different compounds were revealed to share similar PLS-DA contributions across both the mouse and cell culture models of infection.

Table 4-6: Comparing the data for *C. parvum* Iowa II infections from *4.2* and *4.3*. Eliminating metabolites that do not show reliable contribution towards sample differences, results in a collection of 18 compounds. Further exploration of the compounds and their related biochemical properties revealed a large proportion of the compounds (13 of 18) to be involved with mitochondrial activity (red text), such as ATP synthesis or control of Reactive Oxygen Species (ROS).

Shared changes in *C. parvum* Iowa II infections				
	Mouse	Cells	Pathways	Function
1,3-Dihydroxyacetone			Glycolysis	Energy supply
3-Hydroxy-3-methylglutarate			Ketogenesis	Energy supply
Anserine			Carnosine synthesis	ROS scavenging
Asparagine			Numerous	Numerous
Aspartate			AA Synthesis	
Fucose			N-linked glycosylation	Cell surface signalling
Glycine			Purine synthesis	Numerous
Glycylproline			Collagen synthesis	Connective tissue
Isoleucine			Ketogenesis	Energy supply
N-Acetylaspartate			Numerous	Numerous
N-Acetylornithine			Waste	
N6-Acetyllysine			Epigenetics	Gene regulation
Pantothenate (Vitamin B5)			Numerous, CoA synthesis	Numerous, Energy Supply
Syringate			Krebs cycle	Energy supply
Taurine			Numerous	ROS, Osmoregulation
UDP-N-Acetylglucosamine			Sugar synthesis	Cytoskeleton and nuclear pore formation
UDP-glucose			Polysaccharide synthesis	Lipid formation
myo-Inositol			Numerous	Mitochondrial quality control

Among the individual compounds listed, several have already been noted in the literature as being characteristic of *C. parvum* infections; including taurine, aspartate and myo-inositol. These compounds have roles in osmo-regulation, protein biosynthesis and

cytoskeleton assembly among others. However, almost every metabolite shares one target in common: the mitochondrion. As highlighted in

Table 4-6 by the red text, mitochondrial pathways appear frequently in the list of pathways each metabolite is involved in.

Analysis of the metabolite level changes in *C. parvum* Weru strain infections resulted in a similar observation (Table 4-7). Among the compounds, those that have already been noted in the literature included pyroglutamate and valine.

Table 4-7: Comparing the data for *C. parvum* Weru infections from *4.2* and *4.3*. Eliminating metabolites that do not show reliable contribution towards sample differences, results in a collection of 10 compounds. Exploration of the compounds and their related biochemical properties revealed a large proportion of the compounds (8 of 10) to be involved with mitochondrial activity (red text), such as ATP synthesis or control of Reactive Oxygen Species (ROS).

Shared changes in *C. parvum* Weru infections				
	Mouse	Cells	Pathways	Function
2-Hydroxybutyrate			Cysteine synthesis	Oxidative stress response
Acetone			Ketosis	Energy supply
Citrate			TCA	Energy supply
Creatine			Creatine synthesis	Energy supply
Formate			Folate cycle	Metabolic regulation and methylation
Levulinate			Unknown	Potentially Ketosis based energy supply
Mannitol			Mannitol cycle (Non-mammalian)	Potential parasite energy source
Methylguanidine			Protein catabolism	Regulation of inflammation
Pyroglutamate			Glutathione cycle	Glutamate storage
Valine			CoA synthesis	Energy Supply

The potential implications are numerous are not necessarily radical, as an increase in mitochondrial activity would not be beyond expectation in the context of infection. However, current theories regarding the interactions between *C. parvum* and the host cell are limited to lipid scavenging and possible membrane hijacking, unlikely to illicit such a comprehensive mitochondrial response as seen in this data. A potential solution to this disparity could also explain the many morphological individualities of *C. parvum*. Considering that *C. parvum*, according to *in-silico* predictions, is only capable of producing ATP exclusively via a glycolytic pathway and lacks many other mitochondrial processes such as fatty acid synthesis, it may be possible that *C. parvum* is directly interacting with the host mitochondria/l processes in some manner. If this hypothesis could be proven correct, it would provide significant insight into how *C. parvum* managed to effectively remove so many apparently essential biochemical components whilst maintaining significant similarities to the other apicomplexans (such as the loss of porphyrin synthesis with the apicoplast).

4.3.4 The role of host mitochondria during *C. parvum* infection

To investigate the potential role of host mitochondria during infection, I employed an Indirect Fluorescence Assay (IFA) approach to determine if the mitochondria of the host cells were responding to *Cryptosporidium* infection. Our results demonstrate that on multiple occasions, the host mitochondria were shown to congregate in large densities near the *Cryptosporidium* infection (Figure 4-9). With confocal microscopy, a 3D imitation of the infection can be rendered from z stacks and displays an even more intricate association between host mitochondria and parasite (Figure 4-10). Transmission Electron Microscopy images of infected cells also show abnormal host's mitochondrial congregation around the parasitophorous vacuole, with evidence of cytoskeletal involvement (Figure 4-11a). A cartoon based upon the electron microscopy image was constructed to better illustrate how the observed morphology might be seen via IFA (Figure 4-11b).

With the combination of microscopy and metabolomic data, it can clearly be stated that an intricate relationship exists between the host mitochondria and *Cryptosporidium*

parvum, possibly guided via host cytoskeletal structures, although the exact mechanism and biochemical drivers are unknown.

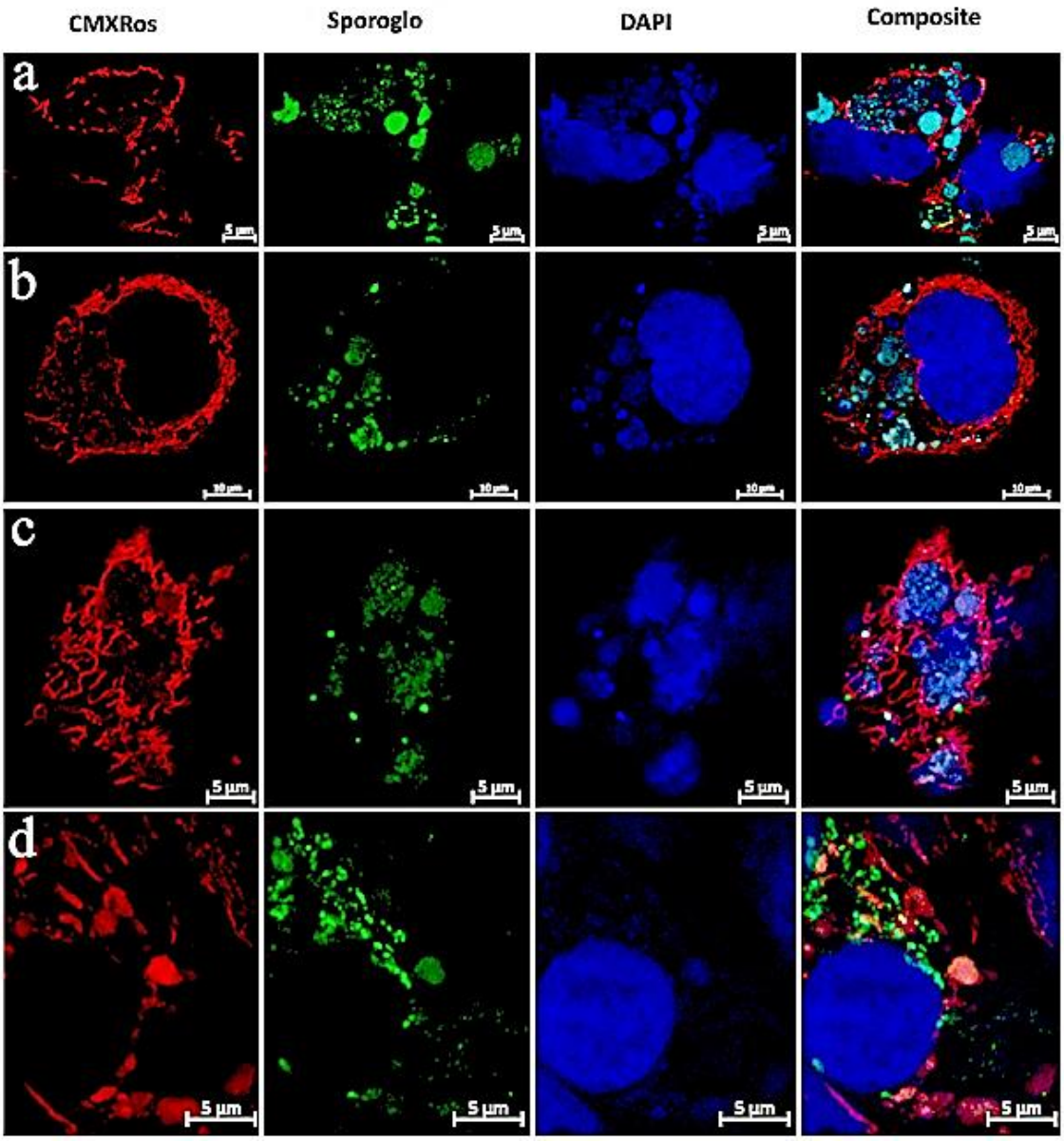

Figure 4-9: High resolution confocal scans, utilising the Zeiss Airyscan acquisition method, of infected COLO-680N monolayers. Scans revealed numerous examples of heavily infected host cells (largest nuclei, DAPI, blue) that displayed substantial mitochondrial networks (Mitotracker CMXRos, red) associated with the parasite (SporoGlo, green). A, b and d were all visualised through the median portion of the host cell, while c was acquired from the surface of the cell, indicated by the lack of a contiguous host nucleus. In each, it can be observed that mitochondrial arrangement within the host cell is highly associated with parasite presence. It can also be observed that the parasite is exerting a significant amount of physical force on the host nuclei, evidenced by the deformed nature of the typically oval nucleus.

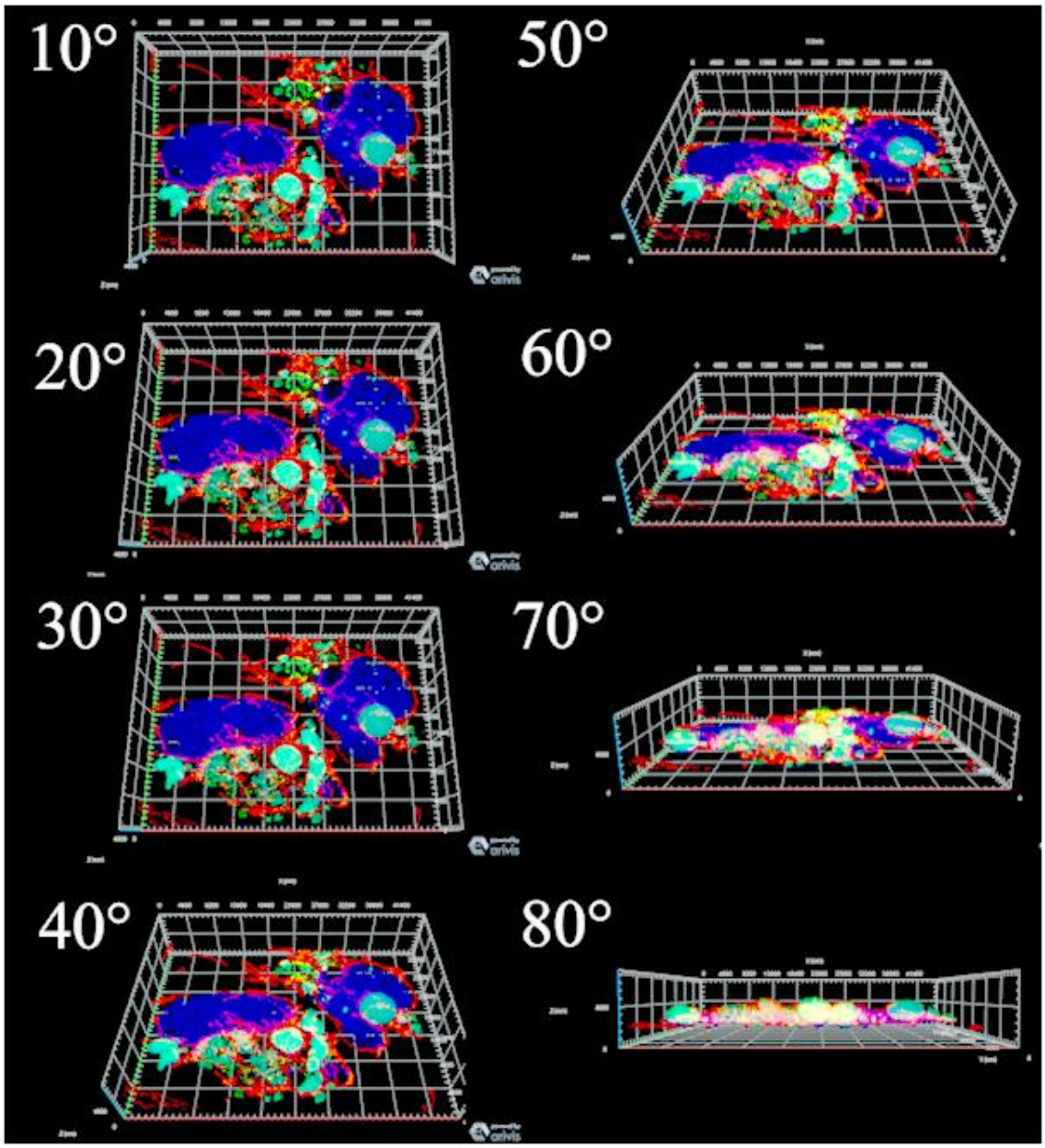

Figure 4-10: A 3D section of the same area as Figure 4-9a. Mitochondria (red) can be seen to 'climb' around the parasite (green). The close association and 'netting' effect seen in these images strongly indicates that the host mitochondria are drawn to the parasite after infection, allowing the established parasitophorous vacuole to become surrounded. The impacting effect of the parasite on the host nucleus (blue) can also be seen to greater effect.

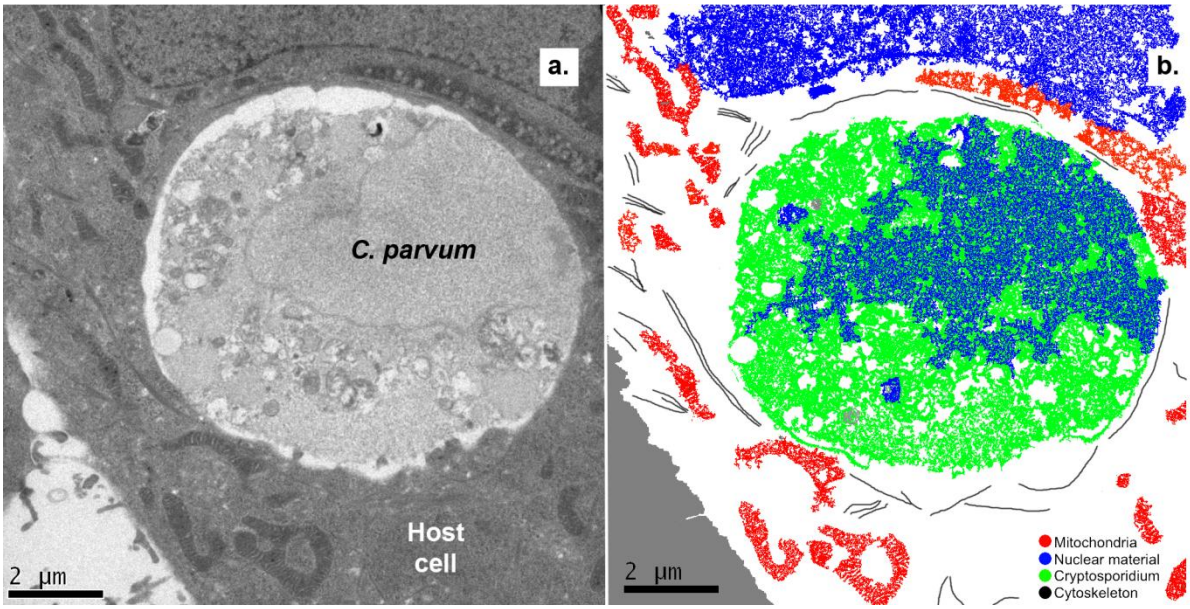

Figure 4-11: a. Infection of a host cell by C. parvum. Mitochondria of the host cell appear to closely associate with the parasitophorous vacuole surrounding the parasite, while cytoskeletal structures appear to be associated with the organelles. b. Cartoon of image a. demonstrating the presence of mitochondria, cytoskeleton, nuclear material and Cryptosporidium.

4.4 Discussion

Solution-state ^{1}H NMR offers a novel approach to metabolomics that is especially useful where sample volume sizes are particularly small. Although GC-MS holds an advantage for detecting low-levels of metabolites with unique mass signatures, to determining the change in metabolite quantities, NMR provides a viable alternative. Initial analysis of our data showed a clear distinction between the metabolic fingerprints of infected and uninfected samples, even between infections of different strains of the parasite (Figure 4-2).

Of importance is the degree to which these results, both from the in-vitro and in-vivo, agree with the previous literature. Our study also demonstrates that metabolic compounds L-alanine, isoleucine and succinate were detected as contributors to the variance between the sample conditions that indicated infection. Moreover, even though valine was not detected in the uninfected controls, it was visible in the infected samples and in agreement with previous reports.

The predictive fits of the metabolic pathways highlighted a remarkable selection of pathways including several involved in amino acid biosynthesis, sugar metabolism, CoA biosynthesis and taurine biosynthesis. Of the predicted metabolic pathways, which have been previously shown to be influenced by infection in *C. parvum* specifically as well as other apicomplexans, there are several whose presence should have been projected, such as the amino acid biosynthesis pathways for alanine and glycine as the previous reports had already highlighted their potential involvement (Ng Hublin et al., 2013, Ng Hublin et al., 2012, Sengupta et al., 2016).

As a parasite, *Cryptosporidium* is dependent on host derived biosynthetic pathways for survival, for example, *C. parvum* is incapable of producing the majority of amino acids de-novo, instead relying heavily on the import of host metabolites via active channelling (Abrahamsen et al., 2004, Rider and Zhu, 2010). One potential target of parasitism, as determined by my findings, was the biosynthetic pathway for glycine, threonine and serine which was upregulated in both cell culture and animal experimentations. *C. parvum* and *C. hominis* are incapable of manufacturing these amino acids de novo, instead relying on scavenging host serine and glycine, utilising serine and glycine hydroxy methyltransferases to convert one to the other when needed (Doyle et al., 1998). The reliance on host amino acids could provide a novel method for combating the infection, based upon previous studies that identified other amino acid metabolic chains as potential targets (Doyle et al., 1998, Zhu et al., 2010, Fritzler and Zhu, 2012, Sparks et al., 2015). For example, glycine reuptake inhibitors (GRIs) that are often used in treating schizophrenia, could be utilised to partially starve the parasite of the metabolite and offer an intriguing future direction of research that could incorporate statistical analysis of *C. parvum* occurrence in correlation with specific drug usage.

In addition to the amino acid biosynthesis pathways, it is also apparent that taurine synthesis is implicated in the metabolic profile of the disease. Primary links between taurine and *C. parvum* infections come from excystation techniques where taurine has frequently been used in the past as an agent for inducing excystation for in-vitro cultures as sodium taurocholate (Upton et al., 1994, Gold et al., 2001, Feng et al., 2006). Previous metabolomic studies of faecal samples from *Cryptosporidium*-infected patients also revealed a possible link between increased taurine concentrations and *C. parvum* infections, explained at the time as the result of characteristic decline in gut absorption via villi malformation caused by the parasite (Ng Hublin et al., 2012, Ng Hublin et al.,

2013). However, an even greater increase in taurine levels was observed in my experiments with the infected COLO-680N cell cultures, wherein malabsorption is not an applicable explanation as explained previously. Therefore, the malabsorption theory does appear to support these observations and a new hypothesis must be formed.

To form this new hypothesis, I will draw upon the collection of observations made during these experiments. In the host, taurine has several roles, those relevant to the cell types involved include: cell membrane integrity, osmoregulation and adipose tissue regulation. Combining this with the other pathways and relevant metabolites observed during the *in-vitro* and *in-vivo* infections (Figure 4-3, Figure 4-4, Figure 4-7 and Figure 4-8) presents a new possibility for a metabolomics based theory of host-parasite interaction, one that centres heavily on the host mitochondrial processes.

As may be expected in a theory wherein host-mitochondrial activity is affected, there is a substantial change in the abundance of adenosine derivatives (AMP, ADP and ATP); displaying increased abundance in *C. parvum* Iowa II infected models (cells and mice), with a similar increase in creatine levels in *C. parvum* Weru infections. This heavily implicates a role for the host mitochondria in the context of infection as each species and strain used lacks the creatine kinase needed to produce creatine phosphate therefore eliminating the parasite as a direct source of these compounds (Abrahamsen et al., 2004). Levels of pyruvate in *C. hominis* and pantothenate in *C. parvum* Iowa II infections highlight further a potential interaction with oxidative phosphorylation. Moreover, the further increase in lactate levels detected in *C. hominis* cell cultures and *C. parvum* Iowa II mouse infected samples, compared to the controls; indicate a strong contribution from anaerobic pathways most likely from the host (due to the relatively small biomass of the parasite and assumed corresponding contribution to metabolite levels). This suggests that more ATP is being produced than the oxidative capacity of the host mitochondria can maintain, producing a net increase in lactate as the oxygen debt increases.

These data suggest that *C. parvum* and *C. hominis* infections may be directly or indirectly inducing an increase in host mitochondrial activity. If factual, this would result in many oxygen free radicals being produced by the metabolic machinery. Consequently, cell(s) would respond with a matching increase in the synthesis of antioxidants such as taurine (Zhang et al., 2004, Giris et al., 2008).

Further support for this hypothesis, that host mitochondrial activity is deliberately interfered with by invading *C. parvum* can be seen in the way host mitochondria appear to congregate around the infection (i.e. parasitophorous vacuole) (Figure 4-9, Figure 4-10 and Figure 4-11).

Nevertheless, taurine also plays another role within cells, for example as a diuretic (Lin et al., 2016). Taurine is involved in the maintenance of the ionised forms of magnesium and potassium within the cell, producing a diuretic effect that may contribute towards the characteristic water-loss of a patient with cryptosporidiosis. Furthermore, it has been found that taurine levels influence production of short chained fatty acid, another aspect of host biology theorised to be scavenged by *C. parvum (Hansen and Grunnet, 2013, Yu et al., 2016)*. These observations and logical links place taurine at the centre of a metabolic web linking *C. parvum* parasitism, metabolism, host interactions and pathology.

These observations suggest that the increase in taurine typically detected in cryptosporidiosis patients' stool, is more than simply the result of the gut's decrease in absorptive qualities. It is likely that the intra-cellular role of taurine in this disease has been overlooked and that the pathophysiology of this disease is more complicated than currently understood, extending greatly beyond simple villi degradation.

These results provide a promising method of determining infections via a possible comparative ^{1}H NMR of patient and reference biopsies. This method offers an alternative approach in the medical field, where current methods of diagnosis are reliant on separate methods to achieve the same result as NMR, with infections detected by laborious and often inaccurate microscopy and strain typing dependant on successful PCR.

Lastly, it cannot be overstated the impact of observing the close relationship between the host mitochondria and the parasite, biochemically and physically, which has never been seen before at this level of detail or reproducibility. The comprehensive alteration of mitochondrial associated metabolites in association with the infections indicates strongly that *Cryptosporidium parvum* and therefore possibly other members of the *Cryptosporidia*, has significant interactions with the host biochemical machinery beyond that previously expected.

In conclusion, I have demonstrated for the first time that the use of ^{1}H NMR is indispensable in understanding host-pathogen interactions at a cellular level. With the application of a more user-friendly and reproducible approach of metabolomics, through the ^{1}H NMR methodology described, it will be easier for the *Cryptosporidium* and apicomplexan community to further explore the remaining aspects of the disease metabolome in patients' samples. Future experiments would be best approached by increasing the number of strains analysed both *in-vitro* and *in-vivo* to test the relevant proposed hypotheses, as well as applying the techniques to entirely new species such as the gregarines or coccidians. Additionally, elucidating the more pathogenic influences of taurine biosynthesis in the pathobiology of cryptosporidiosis is critical. With these data, a metabolomics-based method of diagnosing and treating the disease could become a reality.

Chapter 5 Experimental evidence for a functional Iron Sulphur Cluster biosynthesis pathway in the mitosome of *Cryptosporidium parvum*

5.1 An introduction to mitosomes and Iron Sulphur Clusters

The typical eukaryote maintains a standard complement of organelles that are recognisable to most with basic knowledge of eukaryotic biology: a nucleus, golgi apparatus, endoplasmic reticulum and mitochondria. Until as recently as the late 1990s, it was presumed that almost all eukaryotes possessed the standard 'canonical' mitochondrion. First described in the 19th century, the mitochondrion is a rod-shaped organelle, typically between one and five μm in diameter, encased in a double membrane and possessing characteristic cristae and matrix that provide a large surface area-to-volume ratio for efficient biochemical processes. Chief among these processes is oxidative phosphorylation, the main source of ATP and thus energy for the eukaryotic cell.

As mitochondria appear to be present throughout the eukaryotic tree of life, it has been postulated and widely accepted that during the development of the Last Eukaryotic Common Ancestor (LECA), an alpha-proteobacterium was engulfed, but not digested, instead being incorporated into the cell as a symbiotic intracellular organism, this is referred to as the Endosymbiotic event (Dunning Hotopp, 2011, Martin, 2017, Sagan, 1967). Over time, through horizontal genetic transfer events to the host nucleus and further adaptations to their new environment, the original mitochondrial-like prokaryote became fully integrated into its host, becoming the mitochondria, we know today. Evidence of this can be observed in the double membrane of the mitochondrion (a relic of the original engulfment), the prokaryotic genes within the mitochondrion (with sequence similarity to the alpha-proteobacterium) and their independent nature of replication (separate from host mitosis) among other biochemical clues such as pathways with homologues in the alpha-proteobacteria (Sagan, 1967, Martin, 2017, Picard et al., 2011, Kluge et al., 2013).

The dramatic increase in ATP availability, from the mitochondrion, within eukaryotic cells has been postulated to be essential to the development of the much more complex and eventually multi-cellular forms of eukaryotes, unseen in either of the other domains of life (Eubacteria or Archaea) (Huettenbrenner et al., 2003, Blackstone, 2013, Okie et al., 2016). This has, however, resulted in a strong dependence of the eukaryotic cell on the mitochondrion, with the volume of ATP produced and subsequently utilised preventing the loss of mitochondrial function from being anything but fatal. Further to this, until the late 1980's it was believed that any amitochondriate that was discovered could only be explained as the result of early evolutionary branching, occurring after LECA but before the endosymbiotic event (Tovar et al., 1999, Dyall and Johnson, 2000, Okie et al., 2016, Martin, 2017).

However, in 1999, an amitochondriate was described that appeared to maintain several mitochondrial genes within its nucleus, dismissing the notion that it evolved from a lineage that diverged prior to the endosymbiotic event. This organism, the entero-parasite *Entamoeba histolytica*, was shown instead to possess a drastically reduced form of mitochondria (Tovar et al., 1999). Initial identification of the organelle was achieved solely from the localisation of Chaperonin CPN60, one of the putative mitochondrial proteins detected within the genome of *E. histolytica*. This organelle lacked may key features of 'canonical' mitochondria, including genetic material, cristae and ATP generation. Localisation studies confirmed the mitochondrial nature of CPN60 and thus a new hypothesis was needed to explain the nature of this new organelle, now termed the 'mitosome'. It has therefore been postulated that the mitosome is the result of reductive evolution from an ancestral organism with a canonical mitochondria, where function loss and ultra-structural changes have produced highly specialised forms of the mitochondrion (Dyall and Johnson, 2000, Regoes et al., 2005, Makiuchi and Nozaki, 2014). An exact development timeline of this and other mitochondrial related organelles (MROs) has yet to reach consensus (van der Giezen, 2009, Makiuchi and Nozaki, 2014, Hjort et al., 2010).

Mitosomes can vary largely in size, from 90 nm to 2 μm, are oval shaped and possessing the characteristic double membrane of a mitochondrion (Tovar et al., 1999, Williams et al., 2002). Unlike the mitochondria, mitosomes do not possess any discernible cristae, membrane potential or, perhaps most notably, any form of ATP metabolism (Dyall and Johnson, 2000, Regoes et al., 2005, Makiuchi and Nozaki, 2014, van der Giezen, 2009, Tovar et al., 1999). Instead, mitosomes seem to have eschewed all but one major

biochemical pathway: that of Iron Sulphur Cluster biosynthesis via the ISC pathway (Ali and Nozaki, 2013, Makiuchi and Nozaki, 2014, van der Giezen, 2009).

Iron Sulphur (Fe/S) Clusters are, as the name implies, compounds consisting of Iron and Sulphur atoms arranged in a variety of possible geometric and ionic states. Fe/S clusters are utilised by many metalloproteins and are produced via one of few different pathways, depending on the organism in question. Currently, three pathways are known to be utilised throughout the Prokaryotes and Eukaryotes; the Iron Sulphur Cluster (ISC), Nitrogen Fixation (NIF) and Sulphur Assimilation (SUF) systems. Unusually, each of these pathways has been described in at least a bacterium and a eukaryote, with ISC typically residing in the mitochondrion of eukaryotes though it can also be found in the cytoplasm, where Fe/S clusters are then taken up by components of the Cytosolic Iron-sulphur protein Assembly (CIA) machinery (Xu and Moller, 2011, Ali and Nozaki, 2013, Lill et al., 2015). Perhaps most importantly, no organism has yet been described as lacking a form of Fe/S biosynthesis or usage, even among more atypical eukaryotes such as parasitic species (Figure 5-1) (Dellibovi-Ragheb et al., 2013). Indeed, the fact that mitosomes appear to have retained Fe/S cluster biosynthetic pathways and not the TCA cycle has led many to begin theorising, that perhaps the Fe/S pathways and not the increased production of ATP were the leading promoters of the endosymbiotic event (van der Giezen, 2009, Ali and Nozaki, 2013, Makiuchi and Nozaki, 2014).

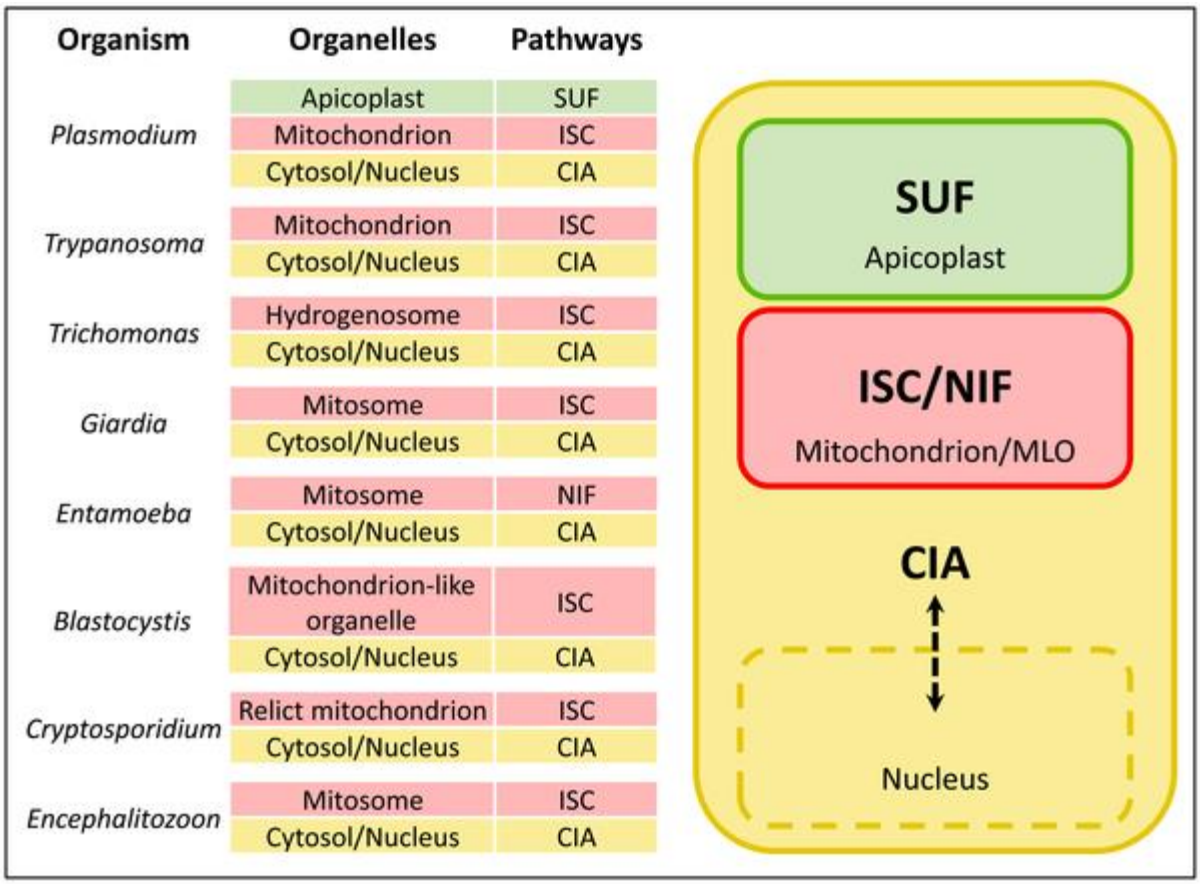

Figure 5-1: Distribution of the Fe/S cluster biosynthetic pathways throughout eukaryotic parasites. Whilst most parasitic organisms have maintained the ISC and CIA pathways, *E. histolytica* appears to have replaced the ISC pathway with the more commonly bacterial SUF mechanism. *P. falciparum* (in addition to other apicomplexans) has also acquired the SUF pathway which is found within the apicoplast. However, *C. parvum* appears to have lost the SUF pathway along with its apicoplast. (Adapted from Dellibovi-Ragheb *et al.*, 2013)

The mitosome of *Cryptosporidium parvum* appears to be no different in this regard. Ultra-structural analysis of *C. parvum* has shown the presence of a single, 300-500 nm long, double membrane bound, oval organelle, within the sporozoite of *C. parvum* which has been shown to typically associate with another cryptic organelle, the crystalloid body (Alcock et al., 2012, Keithly et al., 2005, Ctrnacta et al., 2006, Lemgruber and Lupetti, 2012). Like *E. histolytica*, *C. parvum* Cpn60 was found to target this organelle and no genetic material was present within (Riordan et al., 2003). The *in-silico* predictions have shown the absence of the citric acid cycle and the presence of potential ISC homologues, similar to the predicted contents of the rhizarian *Mikrocytos mackini* (Figure 5-2 and Figure 1-4)((Abrahamsen et al., 2004, Burki et al., 2013).

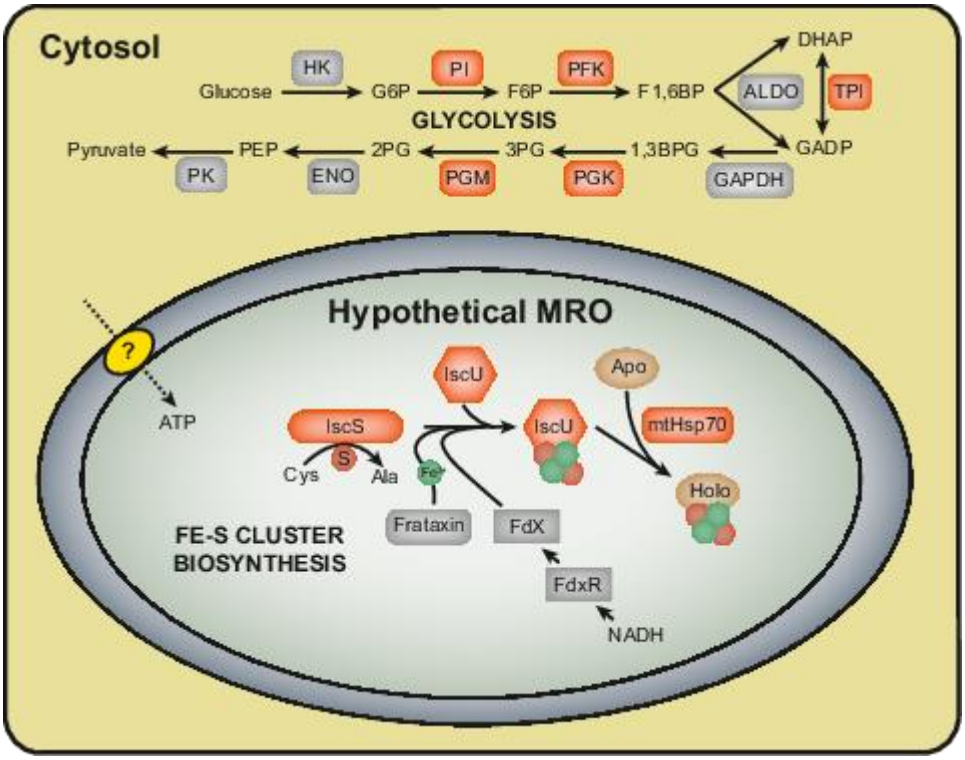

Figure 5-2 The hypothetical contents of *C. parvum*'s mitosome. It appears to be the same as *M. mackini*, maintaining only the ISC machinery, basic import/export machinery and a cytosolic glycolytic pathway. (Adapted from Burki *et al*., 2013)

Though the *in-silico* predictions regarding *C. parvum's* ISC pathway has been known for some time, it remains largely unexplored or verified. What little exploration there has been has focussed on phylogenetics and confirmation of putative mitochondrial targeting sequences in the sequences of CpIscS and CpIscU, with no actual proof of function or localisation to the mitosome (LaGier et al., 2003).

5.2 Goals

With the availability of a robust and easy to use cell culture, because of the efforts in Chapter 3, it is now possible to explore the hypothesis that *C. parvum* maintains an ISC pathway and that it is localised to within the mitosome. Secondly, it should be possible to use this to determine the location/nature of the mitosome in life cycle stages beyond the sporozoite, an unprecedented feat.

To achieve these goals, I propose to develop specific antibodies to several key components of the ISC pathway predicted to be within the genome of *C. parvum*; Frataxin, IscS and IscU (henceforth referred to CpFxn, CpIscS and CpIscU respectively). Doing so will add to the growing body of evidence behind the importance of Iron Sulphur clusters; in the evolution of the mitosome. Furthermore, the successful use of the new culturing system, will add credibility to its utility and scientific importance.

5.3 Results

5.3.1 Identification of ISC homologues in C. parvum

Potential ISC homologues were identified via a tblastn (protein to translated nucleotide) search of the *C. parvum* genomes listed in the NCBI. The search parameters were constructed using *S. cerevisiae* components of the ISC pathway; Nfs1p (IscS homologue), Isu1p (IscU homologue) and Yfh1p (Frataxin homologue). The closest matches to each within the genome of *C. parvum,* as determined via a blastn (protein sequence to translated nucleotide sequence) search, were chosen as the targets going forward (Table 2-2, Figure 5-3). Both putative Isu1p and Nfs1p homologues showed encouraging conservation of sequence whereas the putative Yfh1p sequence showed little amino acid conservation. However, the putative Yfh1p sequence did maintain a conserved secondary structure as predicted by two separate secondary structure prediction programs (PSIPRED and JPRED4) to contain mitochondrial frataxin like domains (McGuffin et al., 2000, Drozdetskiy et al., 2015)(Figure not shown, data available upon request).

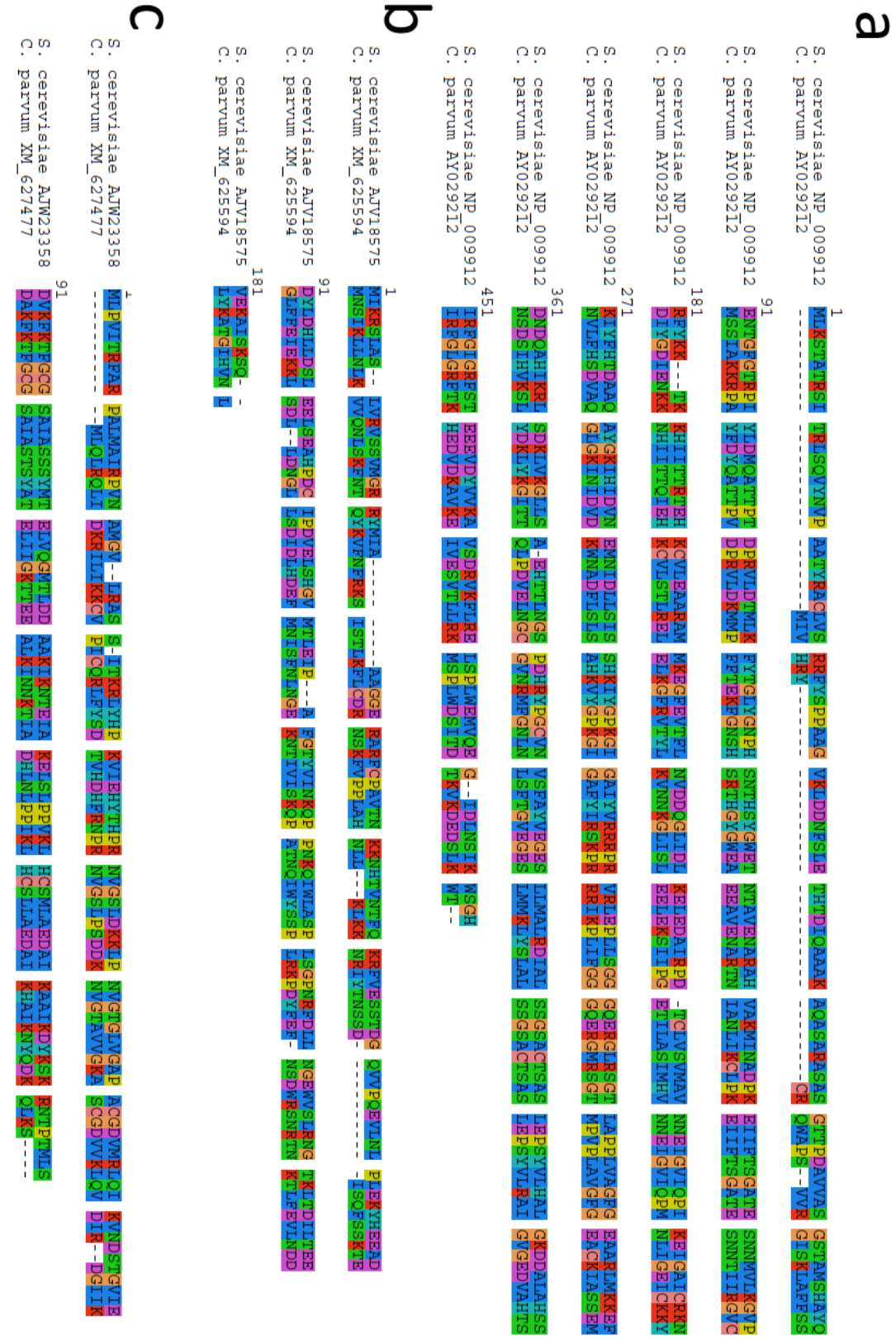

Figure 5-3: CLUSTALO alignments of *S. cerevisiae* and putative *C. parvum* ISC protein sequences. a. Nfs1p and IscS, Yfh1p and Frataxin, and finally Isu1p and IscU. Yfh1p and Frataxin similarities are more apparent in secondary structures than primary sequences.

The sequences were then parsed through a further search, using blastx (translated nucleotide to protein search) to identify and align the *C. parvum* sequences with similar proteins in other Apicomplexa (Figure 5-4 and Figure 5-5)(Altschul et al., 1990, States and Gish, 1994). Similar sequences for IscS and IscU were found throughout the Apicomplexa, but not frataxin, which was only present in a small selection, as had been previously demonstrated in past studies of apicomplexan Fe/S cluster pathways (Seeber et al., 2008). This remains true even when searching via predicted secondary structures using PredictProtein.com (Rost et al., 2004). Each gene was also processed through Mitoprot to determine the possibility of a mitochondrial targeting sequence, if any (Table 5-1)(Claros and Vincens, 1996). Genes of interest were then produced via PCR for recombinant integration into plasmids.

Table 5-1: Possibility of mitochondrial targeting sequence within the ISC peptides, as determined by Mitoprot.

Putative ISC protein	Accession number	Probability of mitochondrial targeting
C. parvum Iowa II frataxin like protein (CpFxn)	XM_625594	81.1%
C. parvum Iowa II IscU-like NifU protein (CpIscU)	XM_627477	96.1%
C. parvum NifS-like protein	AY029212	99.0%

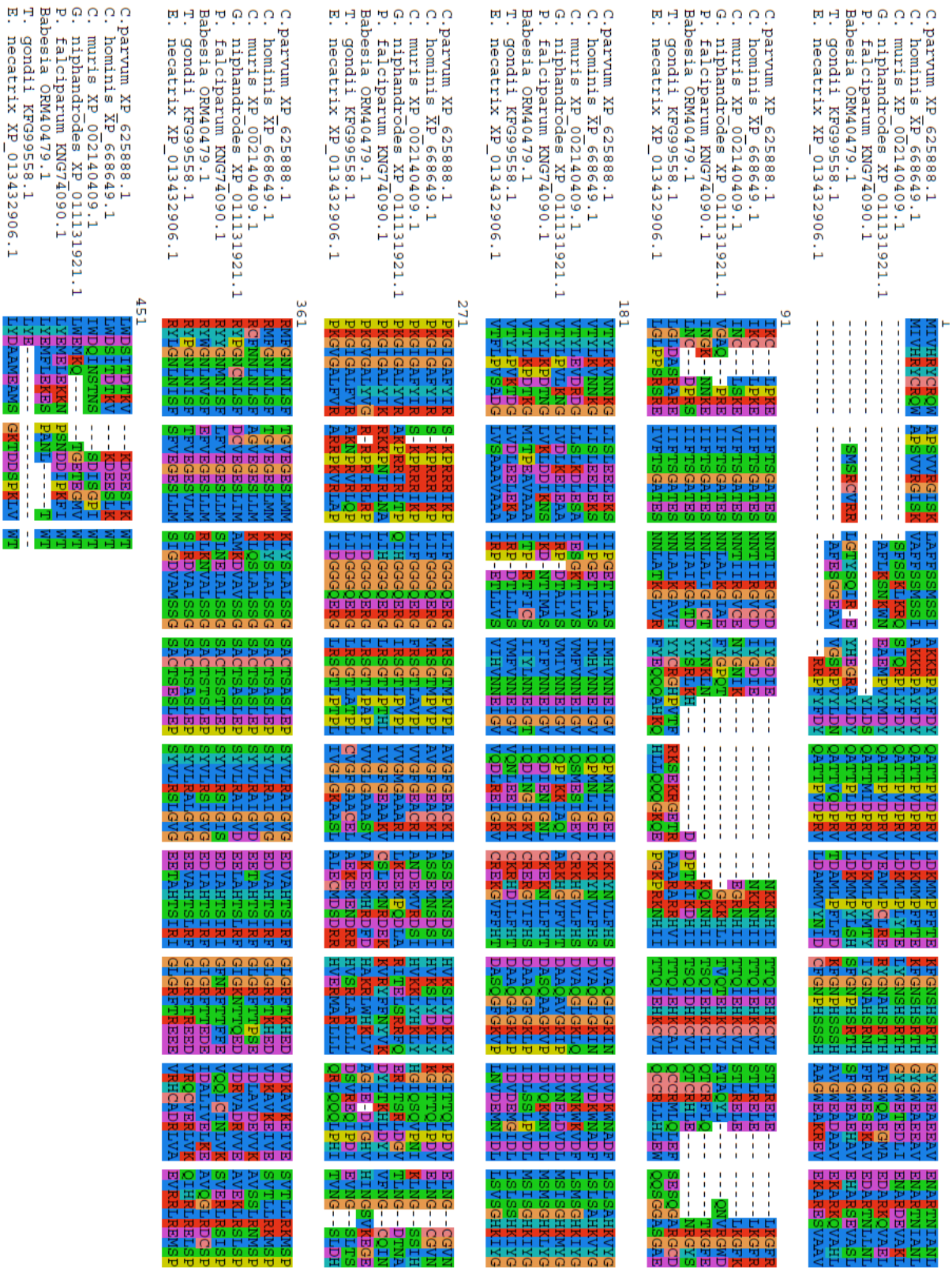

Figure 5-4: CLUSTALO alignment, via Seaview, of the putative *C. parvum* IscS protein and IscS proteins from other Apicomplexans, in descending order of similarity. The sequences were obtained via a blastx (translated nucleotide to protein) enquiry.

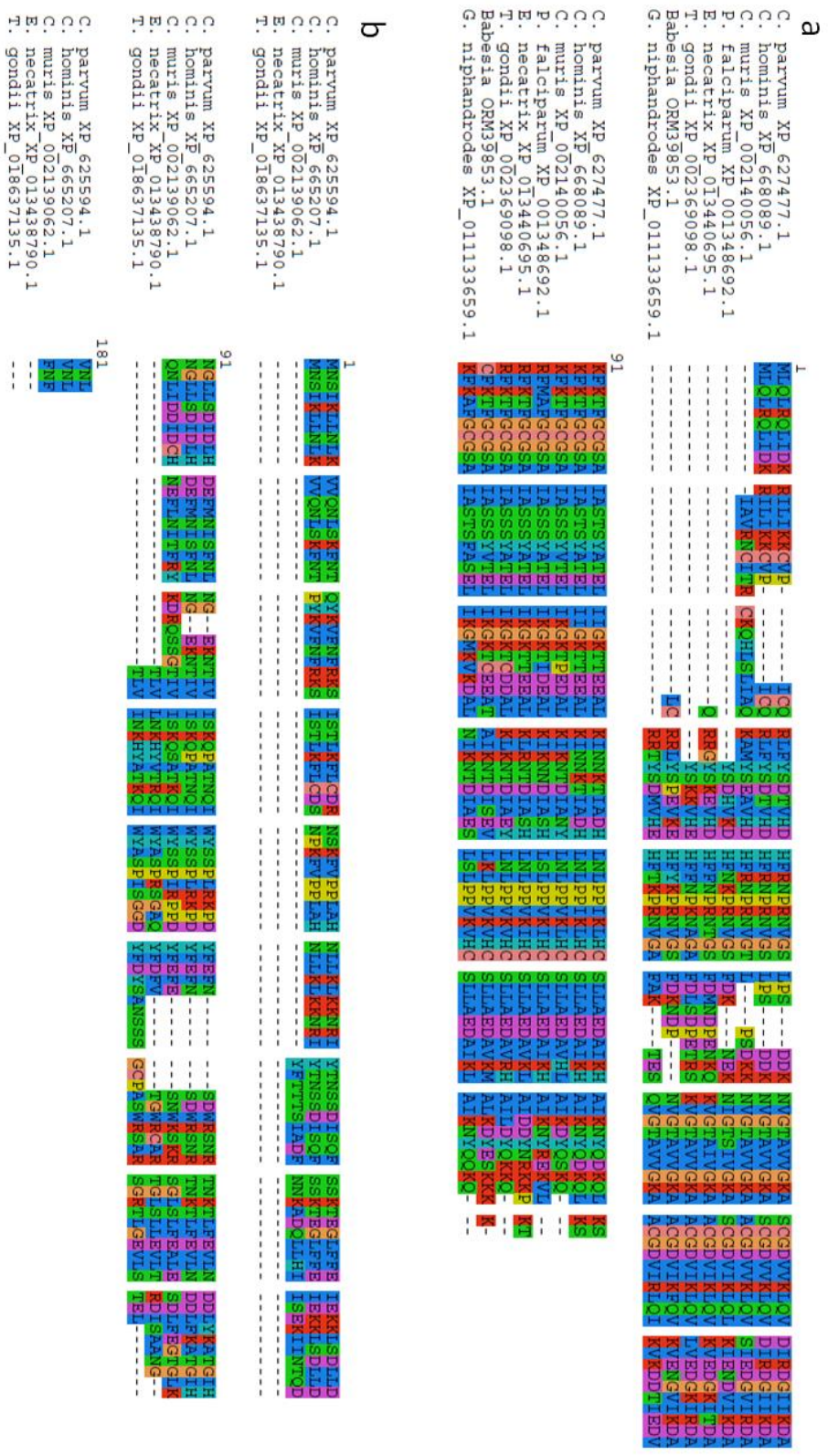

Figure 5-5: CLUSTALO alignments, of IscU (a) and Frataxin (b) sequences identified via blastx searches, using *C. parvum* Iowa II sequences as the query. Frataxin is not present in many apicomplexans.

5.3.2 Amplification and cloning ISC genes

Amplified ISC genes were produced via the PCR protocols described in chapter 2.7, (i.e. the gene of interest, plus complimentary restriction sites) and confirmed via an agarose gel separation (Figure 5-6). Integration of the construct into the pET14b vector was confirmed via select digestion and agarose gel separation, yielding the correct fragment sizes. Aliquots of the pET14b constructs, purified from the agarose gel, were sent for sanger sequencing at Eurogentec facilities, were mutations could be detected, allowing the selection of only those plasmids containing genes identical to the NCBI record. This was done to prevent the potential corruption of epitopes that would be detrimental to the final specificity/sensitivity of the produced antibodies. The recombinant plasmids identified as having identical insert sequences to those on the NCBI database were transformed into the expression *E. coli* strain, BL21(DE3)pLysS, and identified by the acquired Ampicillin resistance.

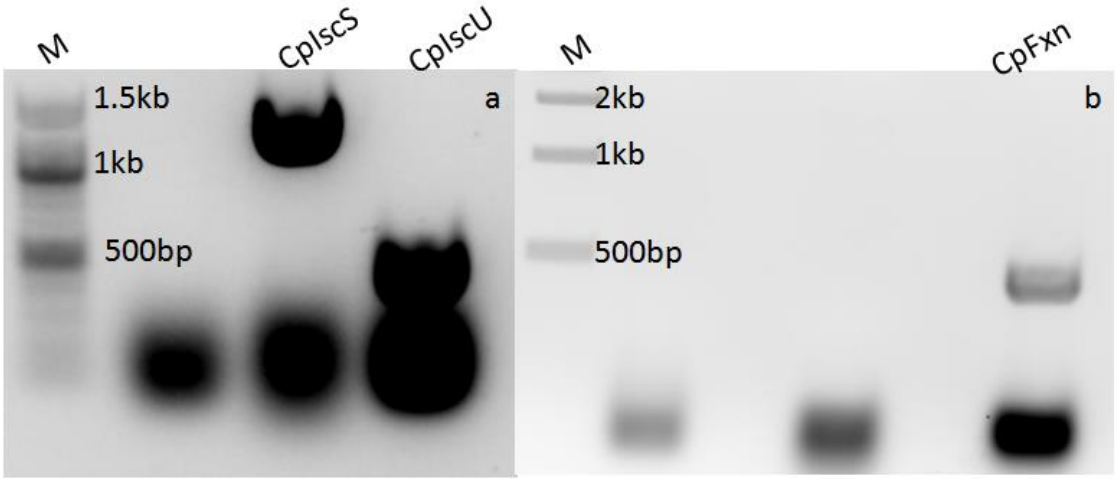

Figure 5-6: PCR product detection of target recombinant proteins. Black and white images of Ethidium bromide agarose gels, exposing DNA fragments via UV exposure. Initial attempts were successful in producing IscU and IscS sequences (a) whilst Frataxin proved more difficult, succeeding in a subsequent run (b).

5.3.1.3 Expression and purification of recombinant ISC components from E. coli

Optimum expression conditions for each recombinant were determined via multiple, tandem experiments utilising 50 ml cultures. Optimal conditions were defined as those that produced the most amount of protein within a six-hour period, detectable using an anti-poly-his tag antibody (Figure 5-7a). Optimal temperatures for all ISC recombinants was determined to be 37°C, CpFxn and CpIscU were best expressed utilising a final IPTG concentration of 0.5 mM and harvested at four hours post-induction. CpIscS, however, was most optimally expressed under 0.2mM IPTG induction and harvesting after six hours. NiCl affinity column-based purification of the large scale (2 L) cultures produced detectable and sufficient amounts of recombinant protein, as identified by western blot and comparable Coomassie brilliant blue staining. Excised acrylamide slices were then stored in 50ml screw-top tubes and received by Cambridge Research Biochemicals, who then produced the corresponding polyclonal antibodies. ELISAs, constructed from protein extracted from the gel slices, were used to estimate anti-body sensitivity (Figure 5-8). Anti-CpFxn gave a strong curve, indicating a high sensitivity. Anti-CpIscS and Anti-CpIscU provided poor curves; this was determined to be an issue with extracting the sample from the acrylamide slices, as subsequent western-blot analysis using recombinant protein extracts showed specific and sensitive binding of the antibodies (Figure 5-7b). None of the custom antibodies produced detectable signal in western blots of protein extracted from uninfected COLO-680N or non-expressing control strains of *E. coli* (data not shown).

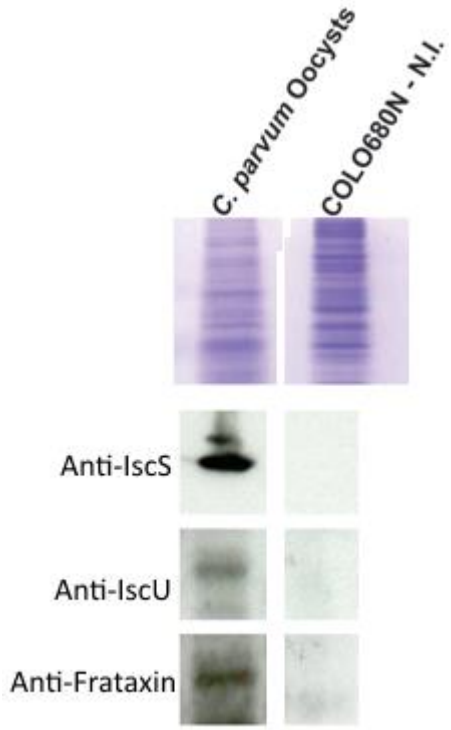

Figure 5-7: ISC Detection in *C. parvum* samples by Western Blot. Antibodies raised against the recombinant ISC proteins, in rabbits (anti-CpIscS) and rats (anti-CpIscU and anti-CpFrataxin), were used in a western blot assay of samples from *C. parvum* oocysts and control samples from uninfected COLO-680N cells. Development via Enhanced, luminol-based, Chemiluminesce (ECL) produced evidence that the antibodies used were able to detect the presence of their intended targets in the *C. parvum* samples but not in the negative, COLO-680N controls.

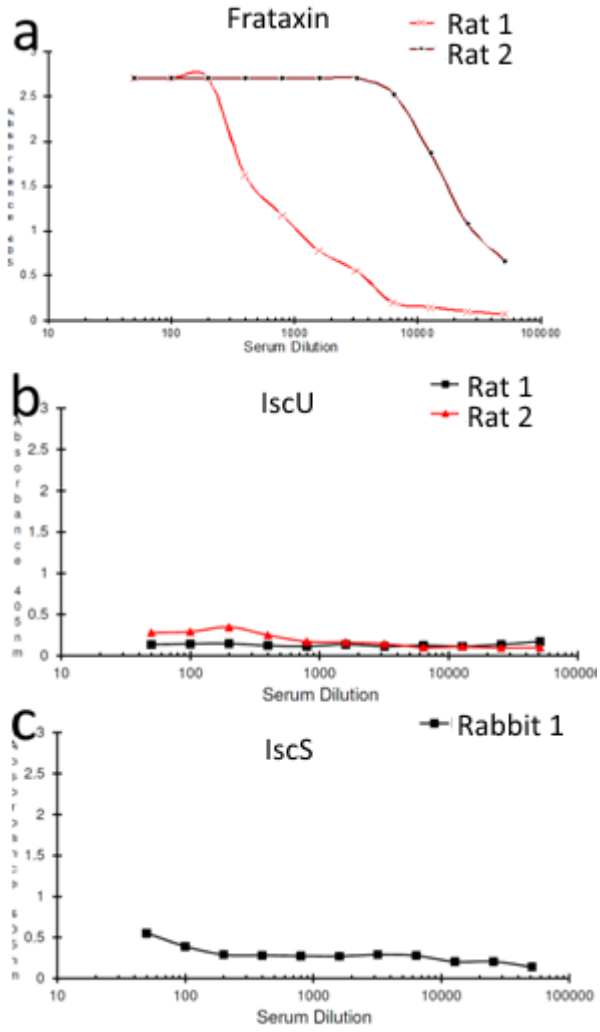

Figure 5-8: Determination of Recombinant ISC raised, Antibody Sensitivity to targets via ELISA. ELISA kits were prepared by Cambridge Research Biochemicals using protein extracted from the same acrylamide slices used to inoculate the animals. The antibodies produced were then tested for sensitivity via these ELISAs and the results recorded graphically a. anti-CpFxn from Rat 2 produced a very strong response curve, indicated by the high absorbance present across serum dilutions. b. and c. are poor absorbance curves, potentially because of acrylamide contamination in the preparation of the ELISA. Subsequent analysis via western blot confirmed a strong specific and sensitive response of both CpIscU and CpIscS.

5.3.3 Localisation of C. parvum ISC components in an infected culture

COLO-680N infection model systems were incubated for the standard 10 days, as established in chapter 3, in chamber slide cultures. The protocols demonstrated in Chapter 2.9.2 were then followed, utilising various combinations of cryptosporidial marker

antibodies, genetic material dyes and the custom made anti-CpFxn/IscU/IscS antibodies (visualised by the addition of TRITC conjugated anti-rat or anti-rabbit secondaries). Localisation of the various proteins within the oocyst of *C. parvum* was achieved by co-staining with Crypt-a-glo a, FITC conjugated, monoclonal antibody with high sensitivity and more importantly high specificity for a *Cryptosporidium* oocyst wall protein. Localisation within other stages of *C. parvum*, sporozoites and intracellular stages for example, was achieved by co-staining with SporoGlo, a sensitive, FITC conjugated polyclonal antibody raised against *C. parvum* sporozoites.

By using different combinations of the anti-*C. parvum* and anti-ISC antibodies, in addition to the DAPI nuclear stain, it was possible to determine the localisation of the ISC components during a variety of different *C. parvum* life cycle stages.

5.3.3.1 IscS

Treatment of infected cultures with the anti-CpIscS revealed a life cycle-dependant expression pattern of CpIscS (Figure 5-9). During the extracellular sporozoite and merozoites life cycle stages, IscS could be detected as punctate areas of signal (Figure 5-10). Often, the signal was restricted to regions typically between 500-800 nm in diameter. This agrees with the description of the mitosome as an approximately 500 nm oval shape.

DAPI stained oocysts of *C. parvum* showed successful permeation as the four nuclei of the contained sporozoites could reliably be observed. However, no convincing IscS signal could be observed within these sporozoites, with an absence of detectable fluorescence. It is entirely possible that this is due to the size difference between the DAPI molecule (~0.270kDa) and the antibody (~150kDa) and thus cannot be considered a signifier of any significance without further investigation.

IFA of the other life cycle stages revealed that whilst IscS remained expressed at detectable levels, its localisation did not remain consistent. In detectable extracellular life cycle stages, determined as any detectable SporoGlo not within/closely associated with a host cell and less than 4μm in diameter, IscS could be found concentrated in a region like that observed in the sporozoites. This indicates the presence of an organelle matching the

physical descriptions of the mitosome, corroborating the hypothesis that at least one aspect of the ISC pathway would localise to the mitosome of *C. parvum.* However, IFA of intracellular life cycle stages, determined by positive SporoGlo detection, proximity to host nucleus, amorphous/round shape and an approximate parasite size exceeding 4 μm, IscS appeared to be more diffuse. Indeed, it is hard to discern any regularly observable structural association with IscS expression in intracellular stages. Furthermore, in areas where many zygotes/maturing oocysts were present, IscS staining appeared to decrease inversely proportional to the diffusion of genetic material indicating that IscS expression declined in the final stages as the sporozoites were formed. This quality appears to offer a biochemical basis for determining when a zygote has become an oocyst, a state previously entirely dependent on visual analysis.

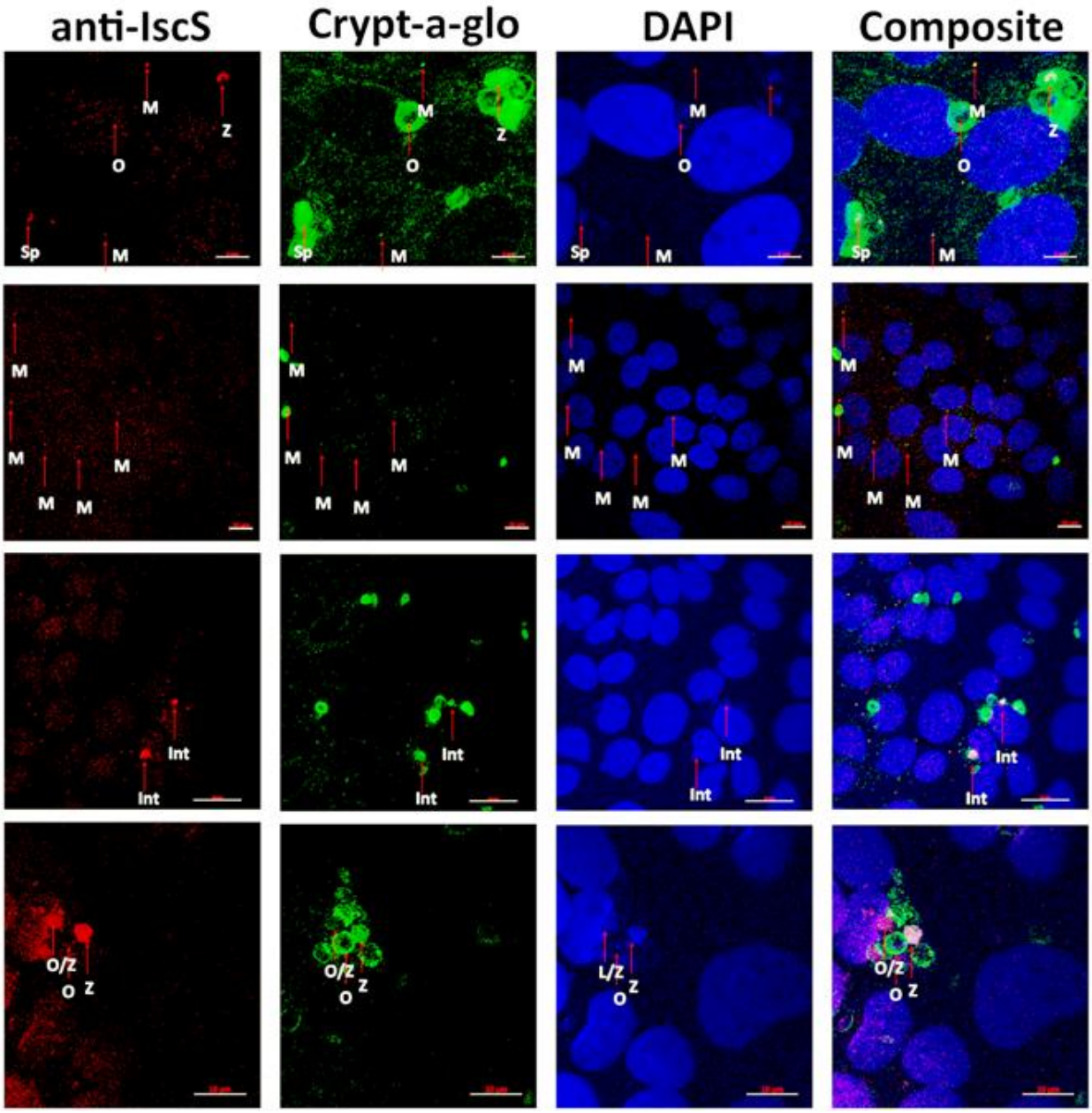

Figure 5-9: Confocal images of infected COLO-680N cultures, stained with anti-CpIscS. A variety of IscS localisation patterns were observed, although appearing to remain consistent based on parasite life cycle stage. *C. parvum* oocysts (O), determined by the circular Crypt-a-glo staining and 3-4 detectable punctate DAPI stains (denoting sporozoite nuclei), routinely showed no detectable levels of IscS. However, oocyst like structures, that lacked discernible sporozoite nuclei contained detectable levels of expressed IscS, this is most noticeable in panels d, where diffuse TRITC signal could be detected. These structures were determined to be Zygotes (Z) in various stages of maturity, with the hypothesis that lowered IscS signalling, corresponding to more concentrated DAPI stain, indicated the zygote was entering the final stage as an immature oocyst (O/Z). Multiple other sites of IscS expression were also detected, either as punctate extracellular signal (M) or as diffuse but high levels, lacking Crypt-a-glo staining (int). Scale bars: a. 5 µm b. 10 µm c. 20 µm d. 10 µm

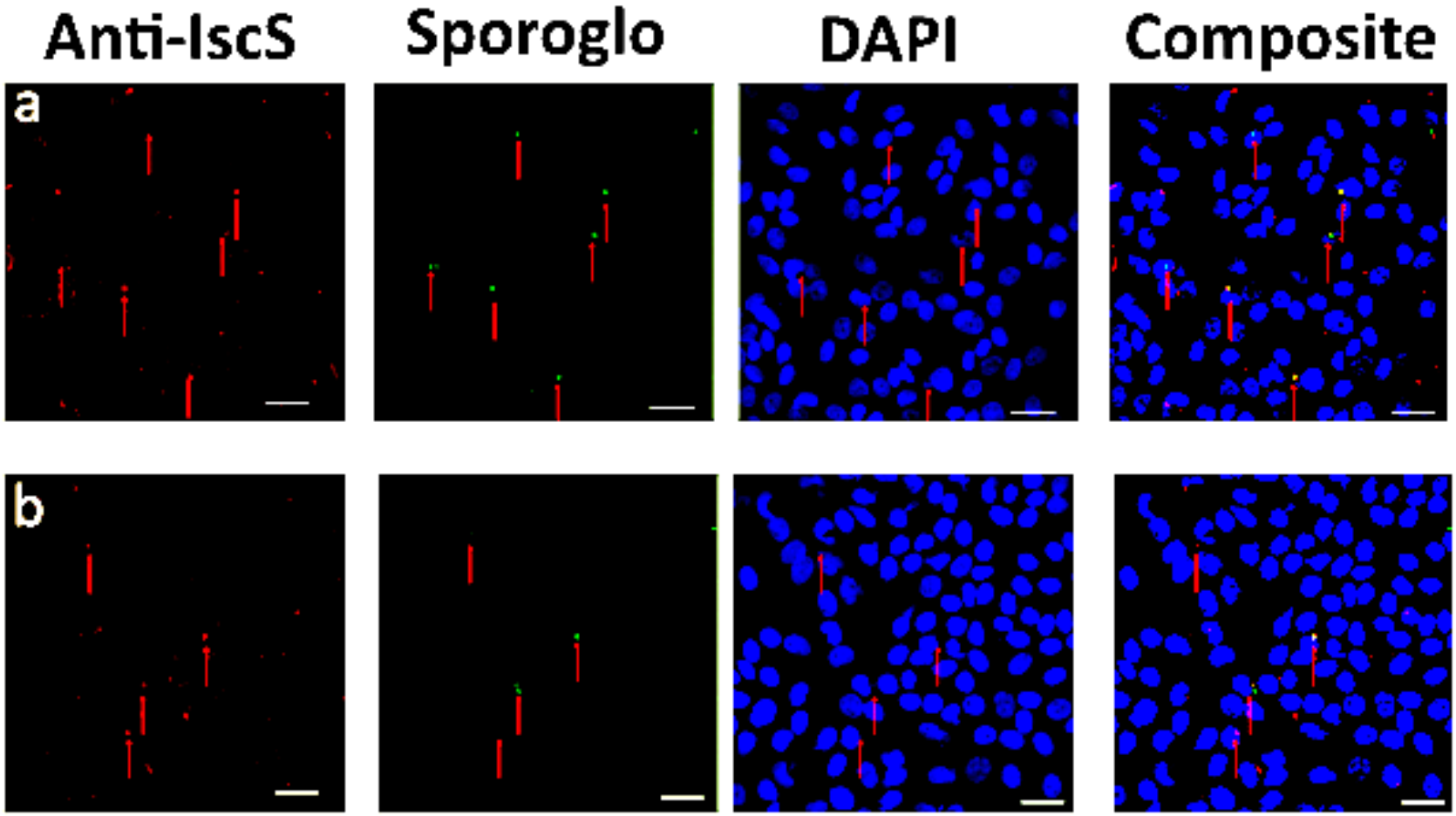

Figure 5-10: IFA of infected COLO-680N cultures with SporoGlo (green) and anti-CpIscS (red) with a DAPI nuclear stain (blue) revealed multiple incidences of co-localisation between punctate IscS signal and *C. parvum* sporozoites/extracellular stages. This agrees with the previous findings that the extracellular stages expressed detectable levels of IscS, which remained confined to an approximately 500 nm region within the parasite. It was not uncommon for IscS signal to be detected where there was no SporoGlo. Subsequent attempts to replicate this in uninfected controls did not produce similar stains, eliminating the possibility that this was background/cross-reactivity of the anti-body. Scale bars for a. and b. are 30 µm.

5.3.3.2 IscU

Anti CpIscU produced similar results to that of CpIscS when observed via IFA (Figure 5-11). Life cycle stage dependant expression continued to be present; with Crypt-a-glo stained oocysts presenting DAPI stained sporozoite nuclei but no detectable CpIscU signal. Conversely, several extracellular life cycle stages could be detected by residual Crypt-a-glo labelling or punctate DAPI stain which did display detectable levels of CpIscU. However, CpIscU signal appeared to be more diffuse than that of CpIscS throughout all life cycle stages (Figure 5-12). This would indicate that CpIscU may not be localised to the mitosome, or at least not exclusively.

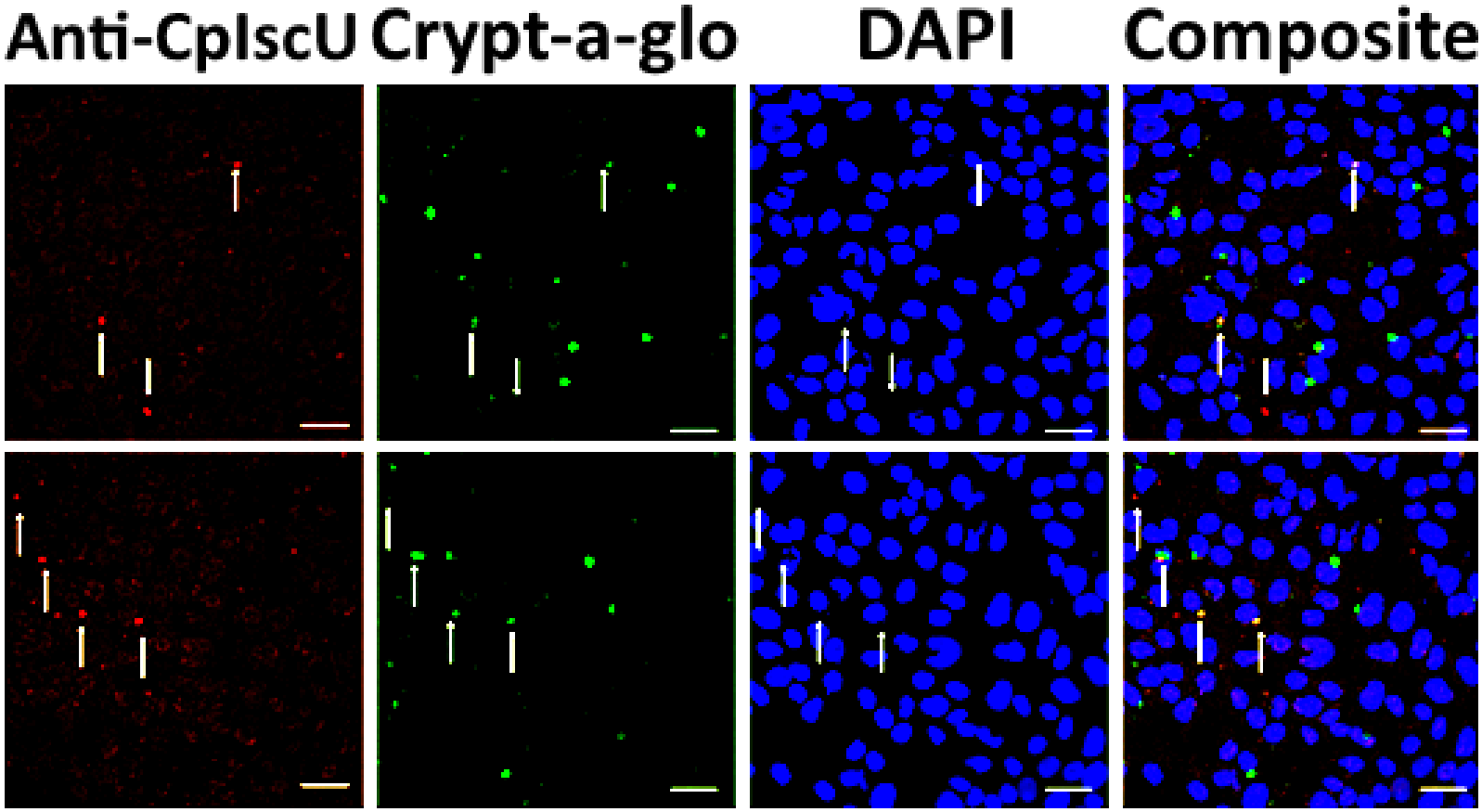

Figure 5-11: IFA of infected COLO-680N cultures, with Crypt-a-glo (green), anti-CpIscU (red) and DAPI nuclear stain (blue). Highly stained (by Crypt-a-glo) *C. parvum* oocysts did not display any detectable IscU signal. However, IscU expression could be detected throughout the culture, often correlating with regions of host nuclei that appeared 'indented' whilst lacking corresponding Crypt-a-glo signal. This indicated the presence of *C. parvum*, expressing IscU, that was not detectable by Crypt-a-glo, such as merozoites or gamont stages. Scale bars for a. and b. are 30 µm.

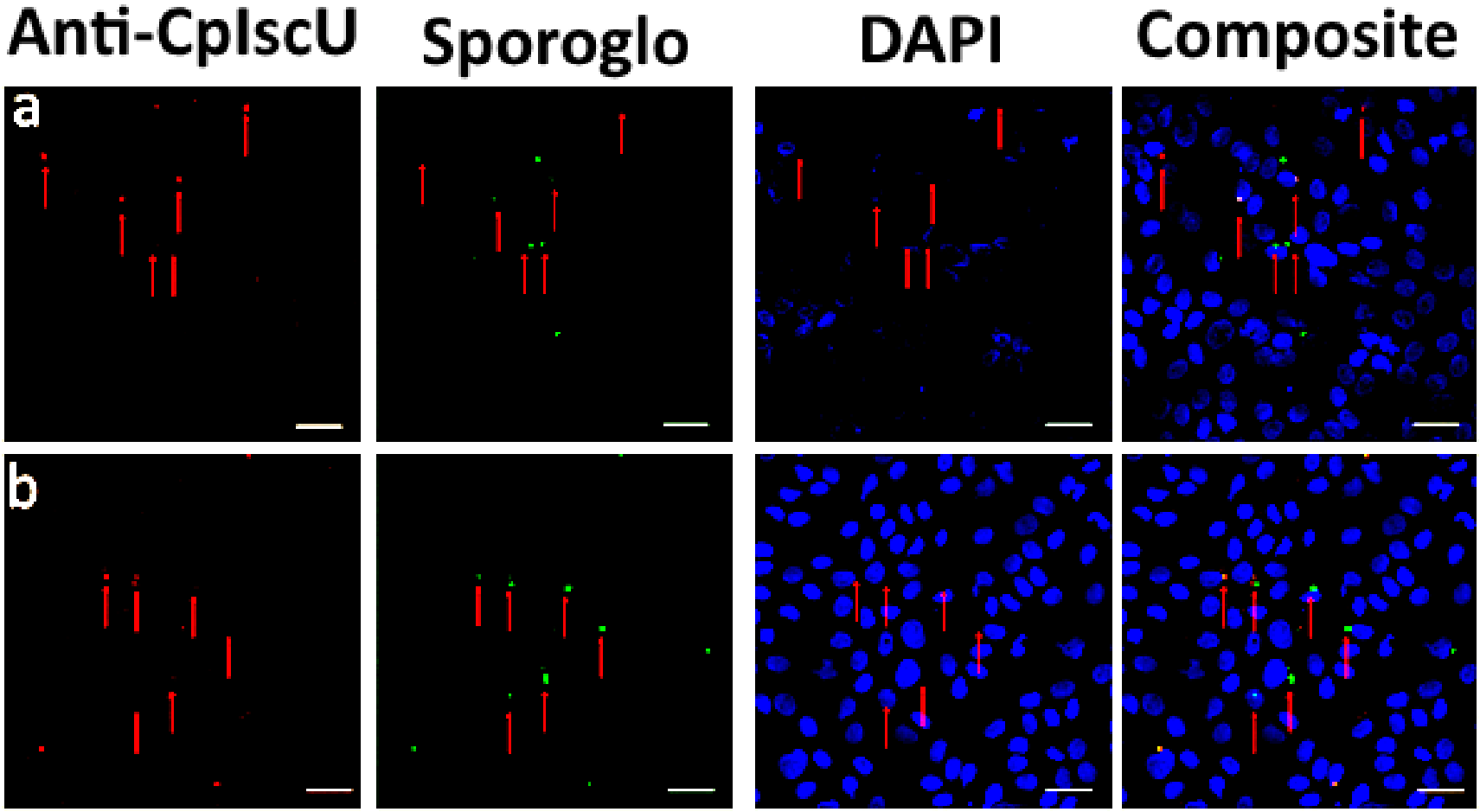

Figure 5-12: IFA of infected COLO-680N cultures, with SporoGlo (green), anti-CpIscU (red) and DAPI nuclear stain (blue). Detectable CpIscU was always detected in tandem with SporoGlo labelling and vice versa. Though IscU stain was relatively diffuse in extracellular stages compared to IscS, it becomes drastically more so in Intracellular stages, suggesting a lack of localisation of CpIscU at the intracellular portions of *C. parvum*'s life cycle. This suggests that IscU is localised, to some degree, in extracellular stages. Though there may be cytosolic expression also. Scale bars for a. and b. are 30 µm

5.3.3.3 Frataxin

Anti-CpFxn results were again similar to those of CpIscS and CpIscU. CpFxn antibody labelling of infected cultures showed, again, a lack of CpFxn in mature oocysts but abundance in other life cycle stages (Figure 5-13 and Figure 5-14). Most notably, CpFxn signal remained intense even in late stage zygotes, denoted by the intense Crypt-a-glo signal that lacked the characteristic 'ring' of a mature oocyst. This is in contrast to both CpIscS and CpIscU that showed decreasing levels of expression leading up to zygote maturation.

CpFxn signal also remained relatively diffuse throughout the life cycle, although dramatically more so in intracellular stages, like CpIscU. This is not entirely unexpected, as previous studies have revealed that cytoplasmic IscU can be found associated with Frataxin. However, CpFxn labelling in sporozoites appeared considerably more localised than any other life cycle stage, appearing to congregate in a defined, approximately 500 nm oval near the apical end of the parasite (Figure 5-14b).

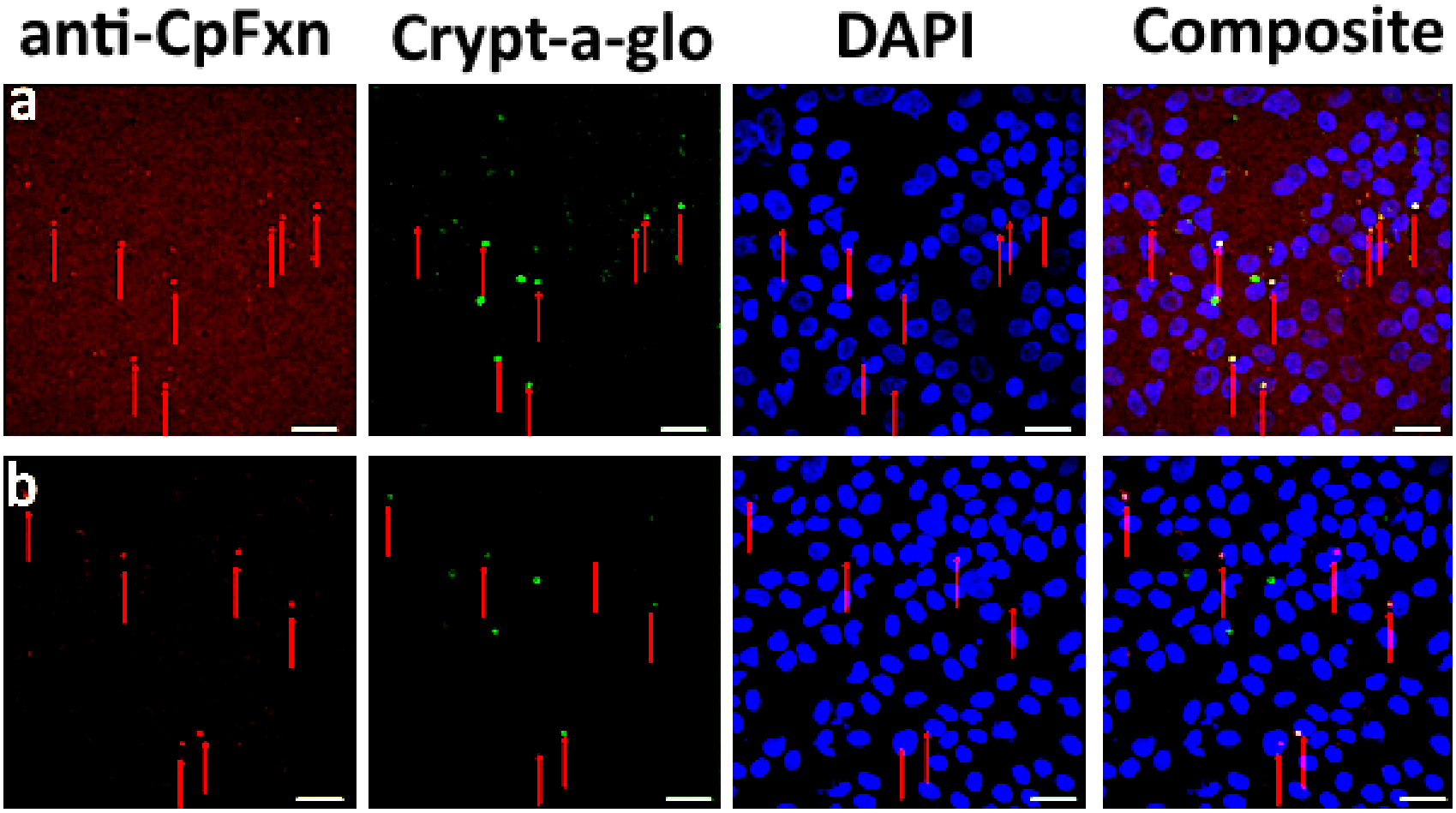

Figure 5-13: IFA of infected COLO-680N cultures treated with anti-CpFxn (red), Crypt-a-glo (green) and DAPI nuclear stain (blue). Whilst some co-localisation of *C. parvum* oocysts stained with Crypt-a-glo can be seen to occur with the CpFxn labelling, no CpFxn signal can be detected in circumstances where the Crypt-a-glo is not reacting with immature stages of oocyst development. CpFxn signal appears to be relatively diffuse within the parasite. Scale bars for a and b are 30µm

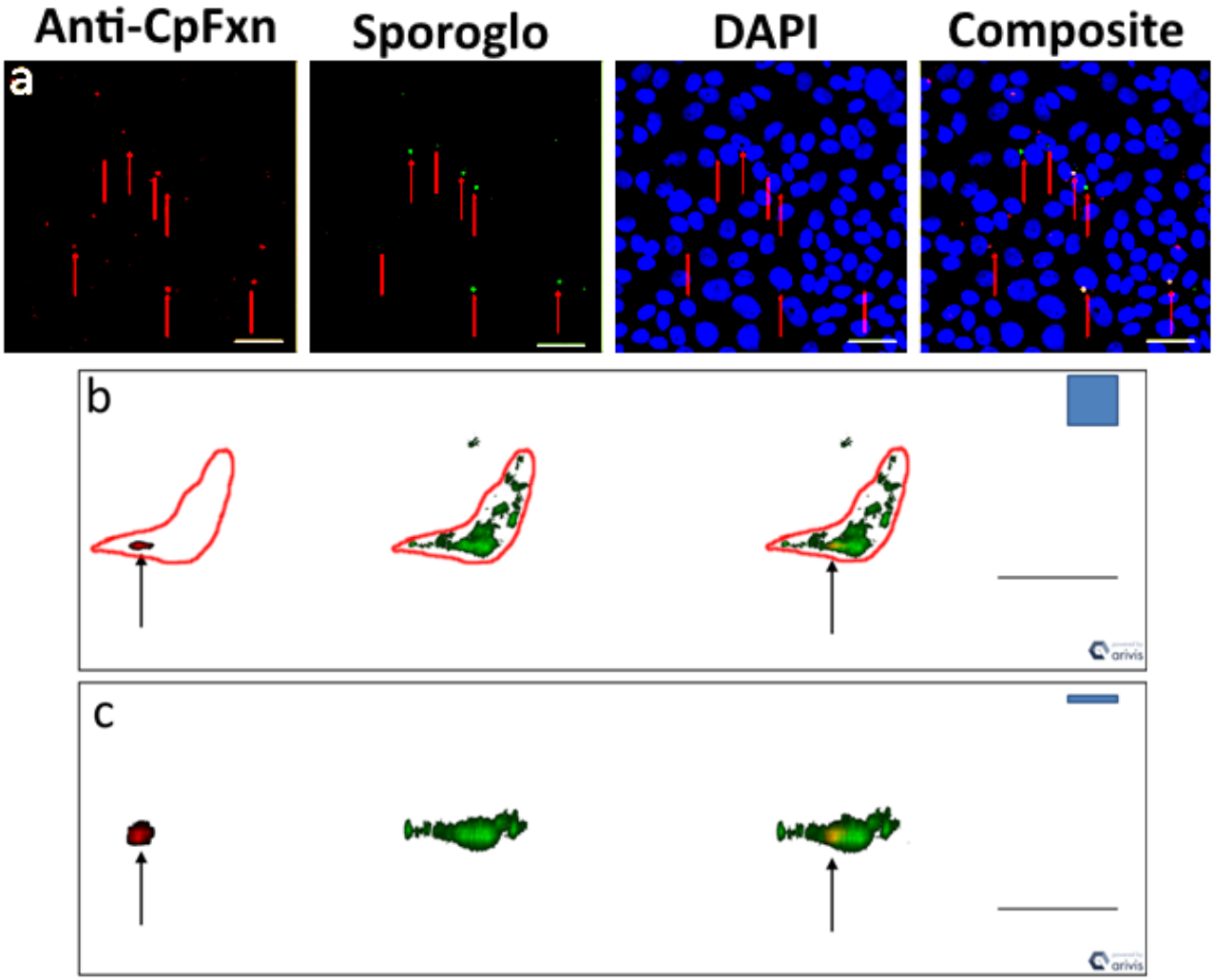

Figure 5-14: Frataxin detection in *C. parvum* in culture. a. IFA of an infected COLO-680N culture, labelled with anti-CpFxn (red), SporoGlo (green) and a DAPI nuclear stain (blue). CpFxn signal co-localises with SporoGlo, demonstrating that putative Frataxin homologue is expressed by the parasite. Scale bar: 30 µm. b. A 3D, high resolution confocal image of a *C. parvum* sporozoite in an infected COLO-680N culture. Clear labelling of CpFxn (red) highlights an approximately 700 nm wide oval (arrow) at the apical end of the parasite, a red outline has been drawn to illustrate the shape of the parasite and to highlight the location of the mitosome c. The same image rotated through 90° on the x-axis. Scale bars a-c: 5µm

5.3.4 Cloning of *C. parvum* ISC components into *Saccharomyces cerevisiae*

It was decided that to further validate the discovery of the ISC pathway in *C. parvum*, it would be necessary to demonstrate that at least one of the proteins was metabolically active as an ISC protein. To do this, a simple complementation experiment was designed,

to determine if the target protein could recover a lethal knockout of its homologue in the yeast *Saccharomyces cerevisiae*. IscS was selected to be the target of the yeast experiments, as previous studies have shown the protein to be non-toxic even when over-expressed, therefore already eliminating a potential difficulty (LaGier et al., 2003). Additionally, IscS is the only protein of the 3 examined here that is a lethal knockout in the model yeast *S. cerevisiae* and as such represents the experiment with the least ambiguous result and thus the best indicator of whether *C. parvum* ISC components perform the same function as their putative homologues (Muhlenhoff et al., 2004). The recombinant plasmid construct, on the pBEVY-L backbone (Figure 2-3), was assembled via selective restrictive digest as before. The PCR insert was derived using the plasmid DNA from the expression experiments as the template, to best minimise the possibility of non-specific binding and thus unwanted products. Again, successful constructs were identified via selective digestion and agarose gel analysis.

The IscS recombinant construct was transformed into a heterozygous Nfs1p (IscS) knockout, strain YCL017C, where a homozygous knockout is fatal. In the Knockout strain of YCL017C IscS is replaced by a G418 resistance marker, on chromosome III.

5.3.5 Confirmation of Sporolating and mating type

Colonies of transformants were grown on leucine knockout plates to select for *S. cerevisiae* containing the plasmid. Liquid cultures were then grown from selected colonies and sporolated. Examination of CpIscS transformed *S. cerevisiae* was performed via microscopic analysis of aliquots from the culture, to identify the characteristic formation of spores (Figure 5-15). Sporolated *S. cerevisiae* was detected in all three experimental replicates. Microscopic analysis was used again to confirm the successful production of spheroblasts by the lyticase exposure. Successfully sporolated and spheroblasted cultures were vortexed to induce separation and plated on non-selective YPD plates. Once sufficiently grown, colonies were picked and re-plated onto selective media and tested for mating type via colony PCR (Figure 5-16).

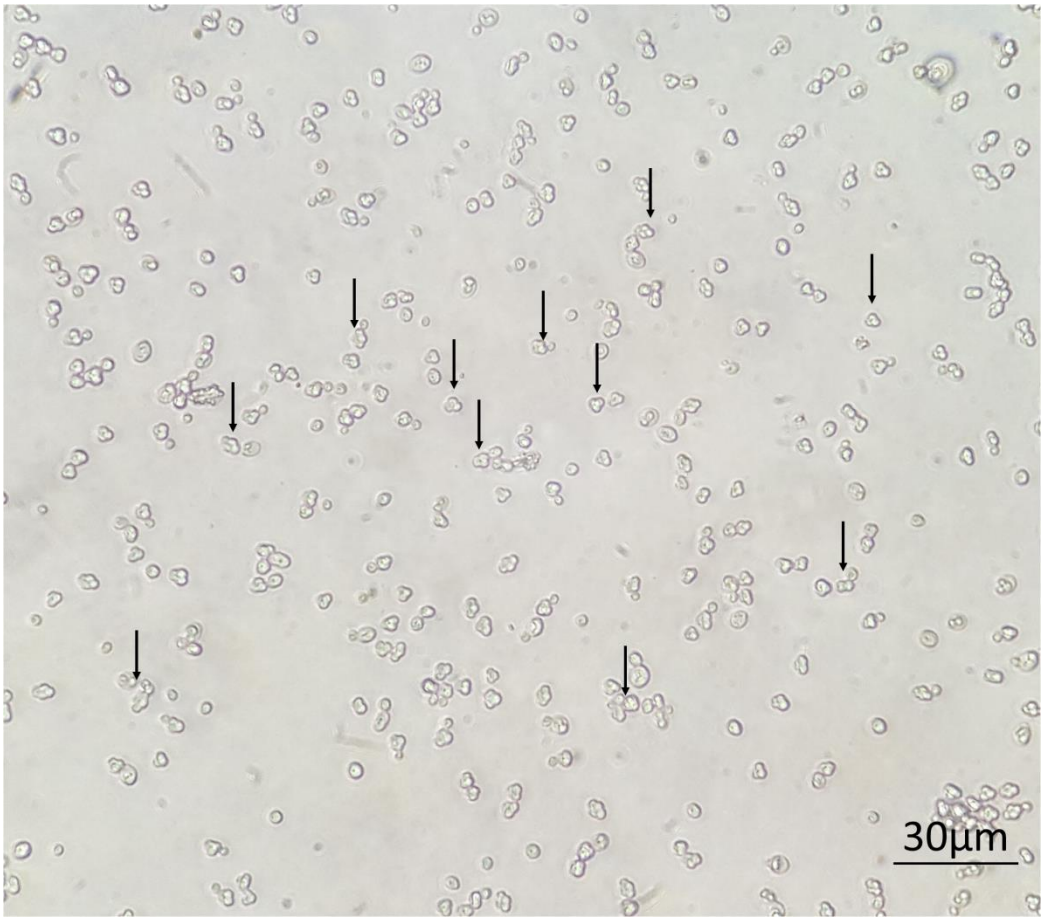

Figure 5-15: Sporulation of yeast. The sporulation of *S. cerevisiae* was confirmed by microscopy analysis of culture samples. Spores can be identified via distinct triplets or quadruplet collections of cells, approximately the same size of a single non-sporolated cell. Each spore would be homozygous for all genes and therefore either homozygous knockouts or wild type NFS1.

Figure 5-16: Colony PCR of colonies formed from sporolated culture. The lower weight bands are primer dimers and expected. The higher bands, approximately 400 bp, represent either α or a mating types. The lack of dual banding in these areas (ignoring the primer dimers) indicates each colony is homozygous for the mating type and therefore all other chromosomal genes. Primer dimers are not present in colonies 20-23 due to space restrictions on the gel.

5.3.6 Functional complementation of Nfs1p with CpIscS

Selected colonies which displayed only a single mating type were placed on the leucine knockout and G418 plates in matching sequence. Pattern observation and decoding can be done via reference to Figure 5-17. Sporulated, homozygous strains were capable of producing matching colonies on both selective media plates, indicating the presence of the G418 resistance marker and pBEVY-L as well as the absence of the lethal phenotype (Figure 5-18 a and b).

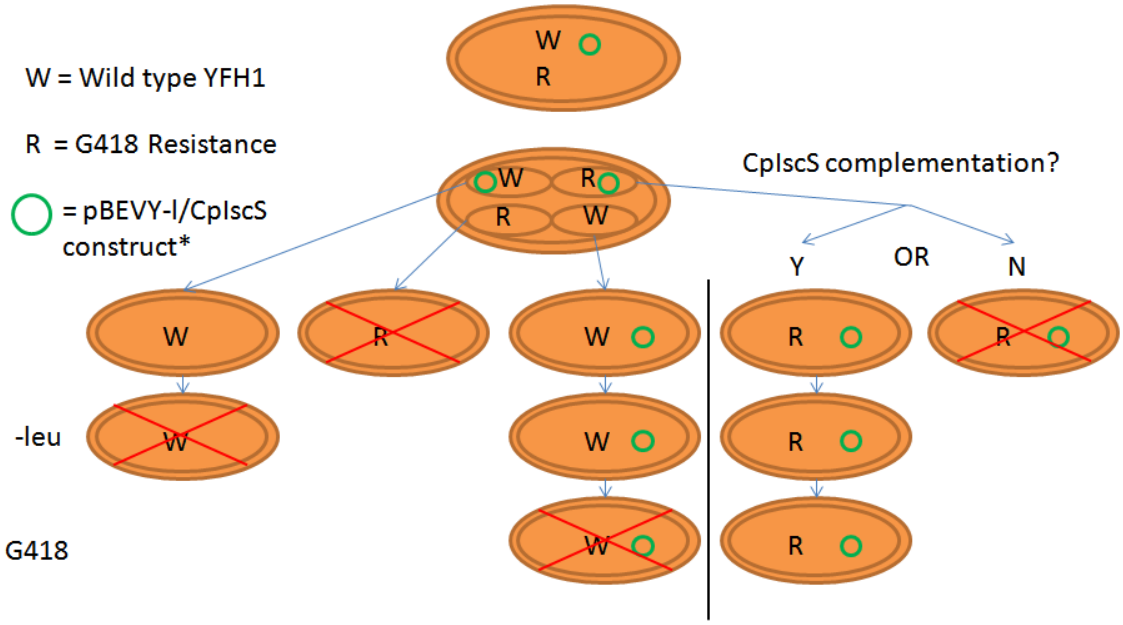

Figure 5-17: A cartoon flow chart of the possible outcomes after sporulation. In the case that CpIscS can successfully recover the fatal NFS1 knockout, colonies should be able to grow on both plate conditions. Only a successful complementation will produce matching colonies on both plates. Colonies that can only grow on leucine deficient plates do not contain the G418 resistance marker and therefore still maintain a wild-type gene. *Actual transformants would distribute copies of the plasmid to all spores, this discrepancy is deliberate and for illustrative purposes only.

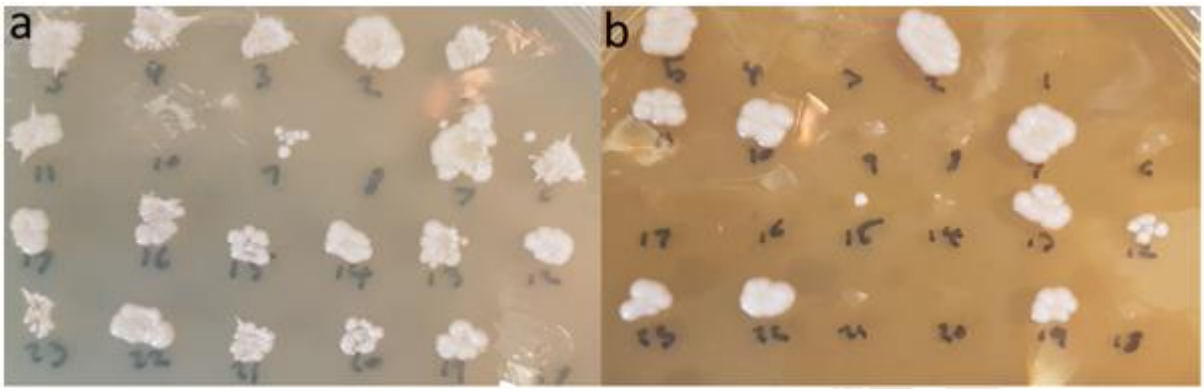

Figure 5-18: pBEVY-L/CpIscS selection plates. pBEVY-L/CpIscS plasmid transformed and sporolated *S. cerevisiae* colonies were grown on a non-selective YPD plate then picked and used to seed Leucine deficient minimal media (a) and G418 (b) antibiotic selective YPD plates. 19 out of the 23 (82.5%) colonies contained the pBEVY-l/CpIscS construct. Colony formation on a. was indicative of a successful transformation, with pBEVY-L conferring survival in the absence of environmental Leucine. Survival (48%) on b. was indicative of the G418 resistance marker that had replaced yeast NFS1 and therefore a lethal knockout. Therefore, any colony that survived plate b and was positive for only a single mating type must be a knockout; else it would not contain the resistance marker for G418 in place of NFS1 (IscS). As NFS1 knockouts are invariably lethal, the only method by which the colony could survive would be via functional complementation, utilising the recombinant CpIscS.

5.4 Discussion

In-silico analysis of the genome of *C. parvum* revealed a full complement of possible ISC pathway proteins. These included the sulphur donor IscS, the iron donor Frataxin and the scaffold protein IscU. Each showed a high similarity to their putative homologues in the model organism *S. cerevisiae*, NFS1, YFH1 and ISU1 respectively. Furthermore, the presence of potential mitochondrial targeting peptides, as predicted by further *in-silico* analysis, in organism lacking a canonical mitochondrion, appeared to suggest that the pathway proteins would localise to *C. parvum*'s mitosome. Considering the lengths to which *C. parvum* appears to have gone to streamline its genome, it would be unusual to have maintained a non-functional localisation sequence. In turn this would suggest that during the evolution of this organelle, the production of Fe/S clusters within a specialised organelle was more essential to *C. parvum* than the efficient production of ATP and thus the TCA cycle was lost and the ISC pathway conserved. To date, only recombinant *C. parvum* Frataxin has been expressed; localised to the mitochondrion of *S. cerevisiae*.

However, until now the nature of the ISC pathway, including its localisation and life cycle expression patterns remained entirely unexplored for all three proteins.

As shown above, I have successfully produced recombinant proteins of *C. parvum* IscS, IscU and Frataxin and subsequently utilised them to produce effective antibodies to the corresponding proteins. In doing so, I have shown that the proteins are indeed expressed during the life cycle of *C. parvum* and are not simply remnants of inherited pathways. Furthermore, the fluorescent microscopy analysis of infected cultures, made possible only by the new culturing system developed in Chapter 3, has shown that not only do the proteins localise to an approximately 500 nm, oval organelle, but that this is dependent on life cycle stage. Although the much more diffuse signalling of CpIscU during all life cycle stages suggests that CpIscU is also present in the parasite's cytoplasm, as is the case for many IscU homologues throughout eukaryotes. This would agree with the currently understood role of IscU, where the otherwise potentially toxic intermediates of ionised iron and sulphur are now assembled into a Fe/S cluster on the IscU scaffold, it would no longer be necessary to exclude the remaining process from the cytosol. To this end, IscU is frequently localised to both the mitochondria and cytoplasm of expressing organisms, theoretically supplying the CIA machinery directly with Fe/S clusters.

CpIscS, CpIscU and CpFxn appear to lose all localisation during intracellular life cycle stages. Given the extremely unlikely (and unprecedented) prospect that the mitosome has disappeared at any point during the life cycle, the simplest explanation is a shift in localisation from organelle to cytoplasm. This is of particular interest as it had been hypothesised that the ISC pathway was localised to mitochondria/mitosomes to protect cells from high levels (found naturally in the mitochondria) of the iron and sulphide ions produced during Fe/S cluster biosynthesis (Horowitz and Greenamyre, 2010, Dlouhy and Outten, 2013, Lill et al., 2012). It is, however, worth noting that whilst detailed knowledge of *C. parvum* life cycle stages beyond sporozoites remains limited, mitosomes have not been demonstrated in stages other than sporozoites and potentially merozoites. This poses another question, if the contents of canonical mitochondria were largely superfluous to *C. parvum*, such that they were readily lost, why has *C. parvum* maintained the mitosome at all if its seemingly only pathway appears not to require the organelle.

Furthermore CpIscS, IscU and Fxn were all absent from any detectable mature oocysts, although as discussed this may be due to a failing in the permeabilization method.

However, whilst Crypt-a-glo repeatedly generated high quality images of *C. parvum* oocysts, SporoGlo performance was continually sub-standard. Before the implication of the ISC anti-bodies it was already a foregone conclusion that SporoGlo was not detecting all parasites within a culture. Comparing SEM, TEM and basic microscopy imaging with SporoGlo imagery revealed that SporoGlo was underestimating parasite populations. Whilst this does not undermine the results of any experiments performed with SporoGlo as a means of localisation, it does call into question the reliability of SporoGlo in an epidemiological setting. Especially now that some papers are reporting the possibility that *C. parvum* and other *Cryptosporidium* are potentially not obligate parasites and therefore may exist in the wild in extra-cellular life stages, although this appears unlikely considering the number of essential amino acids and other metabolites the parasites would not have access to in such environments (Hijjawi et al., 2010, Clode et al., 2015, Ryan et al., 2016). Regrettably SporoGlo remains the only commercially available anti-sporozoite/non-oocyst antibody for *C. parvum*. Other antibodies, such as those that target proteins in the apical complex are available but only in limited amounts as they are made to order by non-dedicated laboratories. However, as the apical complex is only present in the extra-cellular stages, this still would not completely resolve the problem. Therefore, the production of three new effective antibodies that appear to be able to detect all but the oocyst stage of *C. parvum* is a significant result in of its self.

The final and perhaps most important result of these experiments is the confirmation of a functional IscS in *C. parvum's* genome. The Iron Sulphur Cluster assembly protein IscS is an essential part of the ISC pathway, serving as the primary donator of Sulphur, via cysteine residues, to the scaffold protein IscU. Due to the seemingly ubiquitous and predominant nature of Fe/S proteins in biology, it is therefore no surprise that silencing IscS expression can have a lethal effect on an organism. This can be seen in the non-viable knockout of IscS in *S. cerevisiae*, hence the reliance on heterozygous knockouts and sporulation for complementation studies. The introduction and expression of the recombinant putative IscS, found within the genome of *C. parvum*, appears to recover this lethal edit. With both selective criteria (-Leu and G418 survival) present and the PCR confirmation of haploid mating type, I have shown conclusively that the lethal double knockout phenotype of *S. cerevisiae* can be recovered with the expression of the recombinant IscS from the genome of *C. parvum*. This offers significant evidence that the ISC pathway present in the mitosome of *C. parvum* is a functionally conserved

homologue to the ISC pathway found in the mitochondrion of *S. cerevisiae*. This strongly supports the hypothesis that the mitosome of *C. parvum* shares a common ancestor with the mitochondrion of *S. cerevisiae*. Furthermore, the conserved presence of an Fe/S cluster biosynthetic pathway and not a form of the TCA cycle adds considerable weight to the emerging hypothesis that suggests Fe/S cluster pathways played a significant role in endosymbiotic event, perhaps even more so than ATP generation (Dellibovi-Ragheb et al., 2013).

These results also establish proof of a functional ISC pathway within the gregarines, where previously only *in-silico* predictions existed and even then, restricted to a single organism (Toso and Omoto, 2007, Templeton et al., 2010). That *C. parvum* has maintained this pathway, despite disregarding the apicoplast and much of the mitochondria, without appearing to have obtained many further unique adaptations, further adds weight to the concept of *C. parvum* as an essential model for the essential adaptations of gregarines and the Apicomplexa to a parasitic lifestyle.

Therefore, it can be said with some confidence that my hypothesis was correct; *C. parvum* maintains a functional ISC pathway which localises to the mitosome. Furthermore, it appears that the ISC pathway is not always localised to the mitosome. However, using the antibodies generated during these experiments, I have demonstrated a possible timeline for the degeneration of this localisation.

Chapter 6 Discussion

6.1 Purposes and findings of the study

The aims of this project were primarily twofold; to develop a novel model system for the observation and experimentation of *C. parvum* and to use this system to explore the adaptations present in *C. parvum* that enable it to successfully survive via parasitism. The latter goal was to be split into two separate areas of study; the broad analyses of the effects *Cryptosporidium* infections have on host metabolism and the metabolic role of *C. parvum*'s relict mitochondrion like organelle: the mitosome (Figure 6-1).

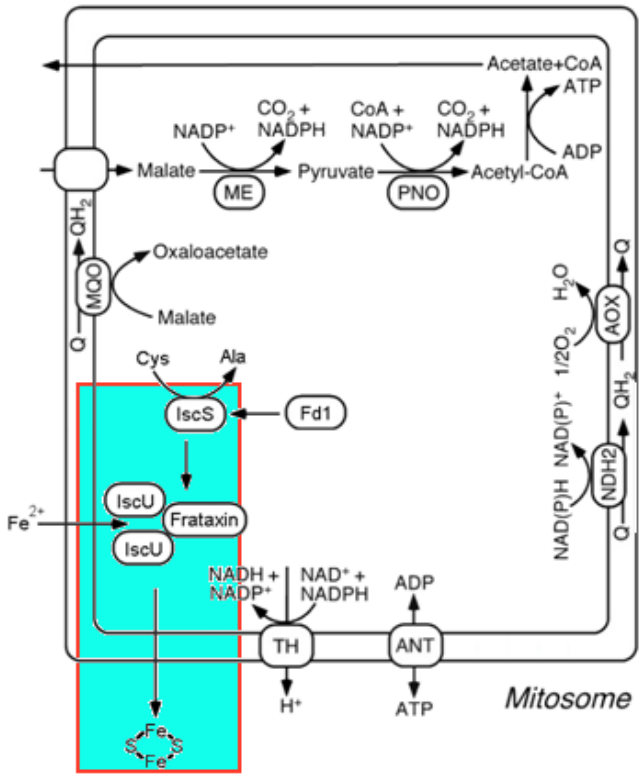

Figure 6-1: The proposed contents of the mitosome. The proteins/pathway of interest highlighted which have now been proven experimentally to be expressed within *C. parvum* and localised to the mitosome. (adapted from Mogi and Kita, 2010)

6.1.1 Maintenance of infection in a COLO-680N cell line

6.1.1.1 Development of an in-vitro C. parvum culture

In order to further the field of *Cryptosporidium* research it had become abundantly clear that a new *in-vitro* model of infection was required. Although previous work had identified such systems as HCT-8, MDCK and Caco-2 cell lines as potential solutions, they had were unsuccessful in their attempts to reliably produce: a repeatedly completing life cycle, long term sustained infections or economically/ergonomically viable options of studying an important pathogen (Upton et al., 1994, Hijjawi et al., 2001, Arrowood, 2002, Girouard et al., 2006, Alcantara Warren et al., 2008, Hijjawi, 2010, Yin et al., 2010, Muller and Hemphill, 2013, Morada et al., 2016, Striepen, 2013). Therefore, it was the goal of this thesis to produce not only a system capable of maintaining a repeated life cycle for extended periods of time, but one that could do so in as simple and cost-effective manner as possible. The latter aspect is increasingly important, as set-up costs are often prohibitive and few research labs already study *C. parvum* (Striepen, 2013).

Fortunately, this study was able to demonstrate such a culture; utilising the Oesophageal Squamous Cell Carcinoma COLO-680N cell line, discovered by a semi random investigation of a panel of potential cultures. In doing so, I was able to produce structural and topographic imagery of life cycle stages which until now remained woefully understudied outside of *in-vivo* investigations. However, the results are broadly consistent with the findings of the previous *in-vivo* research, identifying each life cycle stage previously reported (Current et al., 1986, Arrowood, 2002, Borowski et al., 2010, Leitch and He, 2012, Ryan et al., 2016). This serves to add credibility to the model as a viable model of infection. In addition to sporozoites and novel oocysts, the COLO-680N culture was identified as containing: merozoites, meronts, gamonts (both micro and macro) and zygotes. The latter stages are frequently reported as absent in other *in-vitro* models of *C. parvum* infection (Arrowood, 2002, Girouard et al., 2006, Hijjawi, 2010, Yin et al., 2010, Karanis and Aldeyarbi, 2011, King et al., 2011).

The successful development of this culture allowed me to investigate in greater depth the nature of *C. parvum* infections and the biology of the parasite itself, utilising tools that

had previously been unavailable to the community as a result of the short falls present within other culture solutions.

6.1.1.2 Development of novel protocols to examine C. parvum

Protocols for the examination of *C. parvum* oocysts by Mass spectrometry (MS) lipidomics and proteomics and Atomic Force Microscopy (AFM) were two such outcomes of this research, in addition to other methodologies that are further expanded upon in the other two results chapters. By utilising commercially sourced oocysts as controls, I was able to demonstrate the value of a MALDI-TOF lipidomics approach to identifying differences between commercial and culture produced *C. parvum* oocysts. Though differences were not absolute, which showed the validity of the *in-vitro* culture, there were nonetheless noticeable variations in the abundance of several key lipids (identified via their relative abundance). These techniques open wide the door to further study of the nature of *Cryptosporidium* oocysts; including potential identification of species specific markers and indicators of infection.

Likewise, AFM showed promising results. Primarily, AFM was capable of producing high fidelity topographic scans of oocyst surfaces. This allowed me to conclusively demonstrate that the surface of the cattle-produced and many *in-vitro C. parvum* oocysts were virtually indistinguishable. However, during this investigation, I also described a second set of oocysts, present only within the *in-vitro* population. These oocysts appeared less structurally rigid, more 'deflated' and more elongated than the population present in both *in-vitro* and *in-vivo* sources. It was determined that these oocysts may be representative of the 'thin-walled' oocyst, a less well described alternative end life cycle stage of *C. parvum*. Thin walled oocysts characteristically have a much thinner and less environmentally robust oocyst wall, theoretically due to this version being adapted to an autoinfection life cycle and are therefore not found in *in-vivo* sources of *C. parvum* oocysts. This was an encouraging observation, as it not only indicated a full life cycle present within the COLO-680N model, but also because previous studies had failed to report the presence of both oocyst subsets. It is, therefore, possible that the absence of a thin-walled variant in previous *in-vitro* systems prevented the autoinfection life cycle

from occurring, or at least can be seen as a reliable signal that a *C. parvum* culture is unhealthy/failing.

Now that an AFM protocol has been established, future experiments are able to take it further. Unlike conventional, emitter (photon/electron) based microscopic techniques, AFM can intuit mechanical properties. By analysing peak force and surface strength properties, it will be possible to greatly enhance our understanding of the physical properties of the oocyst in addition to their biochemical.

6.1.1.3 Possible importance of thin-walled oocyst populations

These findings are of particular interest as they would indicate that it is the nature of the final stage of the life cycle that could be hindering the progress of the previous culture systems. Combining the observations from the lipidomics and AFM, as well as previous studies, I propose that the limiting factor, present in most failed *in-vitro* systems, is the ability of the host cell to effectively produce thin-walled oocysts. It is possible that the changes seen in the lipidomics, between *in-vivo* and *in-vitro* produced *C. parvum*, are the result of the thin walled oocyst populations, which could be expected to have a different lipid fingerprint to that of thick walled oocysts. A host cell's inability to provide key lipid components could potentially prevent the successful maturation of thin-walled oocysts, if their lipid make-up is different from the thick-walled variant. This is in keeping with the understanding of *C. parvum* biology, as it is entirely reliant on the host cell for *de-novo* lipid synthesis. My hypothesis, therefore, was that COLO-680N lipid synthesis was substantially different from those cultures previously used and was instead sufficient for the production of either oocyst variant. This theory was supported further by the published observation that COLO-680N produces significantly high levels of lipids (Orita et al., 2010).

6.1.1.4 Observations of FASN activity in infection models

To further explore the implications that lipid synthesis by the host was a potential indicator of viable *in-vitro* cultures, I examined the nature of FASN expression levels in

a variety of known permissible and non-permissible infected cultures. Unsurprisingly and in agreement with publications, COLO-680N produced a strong signal of FASN expression. However, this signal was negligibly stronger than HCT-8 and substantially weaker than DLD-1. Conversely, DLD-1 did not show promise as an *in-vitro* model of infection in earlier experiments. PLD2 levels were also consistent across the tested cell types. However, unlike HCT-8 and DLD-1, COLO-680N displayed an increase in FASN expression upon infection. It is possible, therefore, that the native levels of lipid production are not the determining factors behind the suitability of a cell type as *C. parvum* hosts. Instead it would appear as if a yet unexplored susceptibility or compatibility between *C. parvum* and an aspect of COLO-680N biology allows the parasite to hijack the lipid biosynthesis of this cell type and not the others. The concept of *C. parvum* influencing host cell metabolism is also not unprecedented, as recent work has begun to show that *C. parvum* exports mRNA into the host cytoplasm and lipid synthesis could be a potential target of this export (Wang et al., 2017).

6.1.1.5 Issues with modern nomenclature

At this point, I would like to take issue with a worrisome trend that is emerging within the *C. parvum* community; the use of the term 'epicellular'. Previously, *C. parvum* has been referred to as an intracellular/extra-cytoplasmic parasite. This is in reference to the observable parasitophorous vacuole that forms as a result of host cell invasion by extracellular life cycle stages of *C. parvum*. The material for the vacuole is derived from host membranous extrusions, determined in at least one species of *Cryptosporidium* as a specific host response to *Cryptosporidium* infection. The end result is the encapsulation of the parasite in a host-membrane derived vacuole that does not fully enter the host cytoplasm, instead occupying an inter-membranous region of the phospholipid bi-layer. The work of this thesis also supports this version of events, as demonstrated by the unusual morphologies of infected host nuclei, which suggest strong mechanical forces being applied by the parasite without actually puncturing a membrane, ergo the parasite is within the boundaries of the host cell, not simply associating with it. However, recent publications have begun using the term 'epicellular' to describe *C. parvum* (Thompson et al., 2005, Valigurova et al., 2008, Clode et al., 2015) . This is a misleading use of the

term, as epicellular pathogens by definition associate with host membrane but remain outside of the boundaries of the host cell. Most likely this misunderstanding is a result of overinterpreting field emission scanning electron microscopy images. Whilst at first glance the images present clearly distinguishable host and parasite, many confocal and electron microscopy images show that the distinction is not so clear cut, as supported by the findings I present in the various figures of this thesis. The boundaries of a cell are defined by the outer most aspect of the phospholipid bilayer, anything within that boundary is intracellular and anything associating with, however closely, but remaining outside is epicellular. *Giardia lamblia* is one such epicellular parasite, utilising a concave surface architecture to 'suction cup' onto host cells. In contrast, *C. parvum* is enveloped by host membrane and therefore should not be described as epicellular. Doing so otherwise is encouraging a false description of the infection cycle and is counterproductive to understanding the organism.

As an addendum, I would also like to call in to question the observation that *C. parvum* oocysts maintain an active glycolytic pathway. The sole evidence for this is given in a paper wherein their method of extraction for the assay was essentially an excystation. Therefore, the glycolytic activity observed was more likely the result of activating sporozoites, following excystation, rather than an indicator of activity whilst encysted. I propose this study be repeated, with ^{1}H NMR and ^{13}C NMR studies, utilising the metabolite extraction processes detailed in this thesis to better determine whether the glycolytic pathway is active *inside* an oocyst.

6.1.2 A Host-pathogen metabolome hints at mitochondrial involvement

As a result of developing a novel, robust and easy to use culturing system of *C. parvum*, a number of new areas of research were made available. One such area was that of metabolomics. As a parasite, it is a foregone conclusion that *C. parvum* likely interacts/interferes with host processes of some description. The nature of these processes, however, was largely unknown and understudied due to the aforementioned lack of suitable models of infection. Metabolomics is a particularly underexplored aspect of *C. parvum*. Indeed, pre-existing literature covers only the faecal metabolome of human and mouse infections and via a single method of examination: Mass-spectrometry (MS).

Whilst there is nothing inherently wrong with the Mass-spectrometry technique, it is nonetheless a relatively complex protocol, with sample loss a significant issue during preparation. This would not be an issue in situations where sample is abundant, but is extremely prohibitive in hostile conditions, such as fieldwork. Furthermore, whilst gas chromatography mass-spectrometry (GC-MS) is a highly sensitive technique, it lacks the ability to quantify compound abundance. Therefore, it was the purpose of this study to use the novel COLO-680N *C. parvum* infection model to explore a viable alternative to MS: ^{1}H NMR metabolomics.

6.1.2.1 Development of a ^{1}H NMR protocol

^{1}H NMR has successfully been used to examine the metabolomes of many microorganisms, including the yeast *S. cerevisiae* and apicomplexan *P. falciparum* (Gonzalez et al., 1997, Balog et al., 2011, Li et al., 2011, Lamour et al., 2012, Teng et al., 2014, Sengupta et al., 2016). Whilst this study examined the metabolome of the infection model in its entirety, I decided to draw upon these existing protocols so as to best ensure that both host and parasite were effectively treated for metabolite extraction. Additionally, the use of high temperatures (80°C) to rapidly denature enzymes and prevent metabolite degradation, provided an advantage to field sample preparation where higher temperatures are easier to obtain than lower.

The results were promising and showed some immediately obvious differences between the spectra of infected and uninfected cultures. To expand upon and potentially add further depth to these observations, I introduced several other *Cryptosporidium* species to the dataset. While the COLO-680N culture system was developed with the *C. parvum* Iowa II strain, it had also proven permissive to the Weru strain. Additionally, *C. hominis* also displayed some ability to propagate within the culture. I therefore decided to collect metabolomics data from COLO-680N cultures of these parasites as well. The resultant spectra from these infections were immediately distinguishable from each other. Before whole-spectra analysis was performed, specific peak analysis of the revealed that creatine, taurine and lactate levels of the infected samples were both different from the controls and also from each other. These preliminary results were promising and particularly intriguing as each metabolite was directly related to host mitochondria.

6.1.2.2 Involvement of host mitochondria in infection

The observation that the most obvious differences in the spectra were related to host mitochondrial metabolism were not entirely surprising. Earlier Transmission Electron Microscopy images from the development of the COLO-680N culture, in addition to previous literature, suggested a close association at least physically between the host mitochondria and the parasite. This is also supported by the revelation that host fatty acid synthesis, which largely takes part associated with the mitochondrion, is potentially hijacked by *C. parvum*. To this end, infected COLO-680N cultures were observed utilising Zeiss's Super-resolution Airyscan. The resulting images agreed with the hypothesis, as they too showed co-localisation between high host mitochondrial concentration and *C. parvum*. This is a promising avenue of research, which may explain how or why *C. parvum* has survived after drastically reducing the functionality of its own mitochondrion.

6.1.2.3 The first recorded metabolome of a C. parvum in-vitro culture

After further analysis of the NMR spectra, utilising the Chenomx NMR suite, full lists of metabolites present in each experimental condition were produced and compared. The concentrations of the various compounds were used to construct PCA models, which showed clear differences in metabolic fingerprints between the various infections but more so between any infection and the uninfected control. This data represents the first time ^{1}H NMR had been used to examine the metabolome of any cryptosporidia but also the first time the metabolome of a *C. parvum* infected tissue culture has ever been explored.

6.1.2.4 A role for taurine

By using the values ascribed by the PCA from both *in-vitro* and *in-vivo* experiments, it was then possible to elucidate those compounds which most profoundly differed between the conditions. For both *C. parvum* strains, Iowa II and Weru, the lists predominantly contained metabolites involved in energy supply or other typically mitochondrial processes. This further supports the theory of close host-mitochondria and *C. parvum* interaction. Of those identified, Taurine was perhaps one of the most interesting. High levels of taurine are frequently observed in stool samples of *C. parvum* patients, however this had been theorised to be a result of reduced Taurine uptake, as a result of damaged microvilli by the infection. As there is not external source of Taurine in the *in-vitro* cultures, I offer an alternative explanation. In keeping with the observation that *C. parvum* infections appear to mostly affect the mitochondrial metabolism of the host, the observed increase in Taurine levels may in fact be a protective response by the host cell. Taurine is a multi-role metabolite and is involved in many pathways depending on cell type and localisation. One such role is as an antioxidant and barrier to oxidative stress. As is shown in the effects on other metabolic compounds, the infection appears to have a drastic effect on mitochondrial activity. Up-regulation in protective compounds, therefore, seems a logical response to this. This new interpretation of increased Taurine levels, among other similar responses seen throughout the results, promises a new interpretation of old observations and could be the key to understanding the host-parasite interaction in greater detail.

6.1.2.5 Future of ^{1}H NMR and MS approaches

As a result of these experiments, I have shown both the validity and utility of a ^{1}H NMR approach to *C. parvum* metabolomic studies. However, this does not mean to say that NMR should replace MS approaches to metabolomics, on the contrary it would serve best to develop future methodologies that combined the two approaches. The sensitivity of MS and quantification of NMR could further our understanding of the underlying metabolic exchanges between the host and parasite even further. Additionally, these techniques and the differences observed between the metabolic profiles of individual species suggest that NMR could become a very powerful yet easy to use tool for diagnosing and identifying *C. parvum* infections.

6.1.3 *C. parvum* maintains a functional ISC pathway, with life cycle stage dependant expression patterns

6.1.3.1 Successful identification of putative ISC components

The purpose of this study was to experimentally demonstrate the existence and function of the ISC components purported to be within the genome of *C. parvum* and potentially the only complete pathway within its mitosome (Figure 6-2)(Abrahamsen et al., 2004). Successful recombinant constructs, derived from the gene sequences identified via a blast search, were used to create antibodies that identified expression of their protein counterparts in parasite cultures. Analysis of the sequences via Mitoprot also revealed that each translated genes contained peptide chains that were likely to be mitochondrial targeting sequences. This has been explored previously for the ISC components CpIscS and CpIscU which localised to the mitochondria when expressed in *S. cerevisiae* and were the only experimental evidence of a functional ISC pathway within *C. parvum* until this work (LaGier et al., 2003). With direct experimental evidence of the expression of these ISC homologues, from the western blots of infected cultures, it was possible to explore further and examine in greater detail the nature of ISC expression in *C. parvum.*

6.1.3.2 The ISC components of C. parvum localise to an approximately 500 nm organelle

The original intent of this study was to confirm the hypothesis that the ISC components would localise to the mitosome of *C. parvum.* This was achieved via the observed localisation of CpFxn, CpIscU and CpIscS to a small, approximately 500 nm organelle. This suggests that the mitochondrial targeting signal, identified via Mitoprot prediction (ref), is likely still recognised by *C. parvum* export machinery and targets the mitosome.

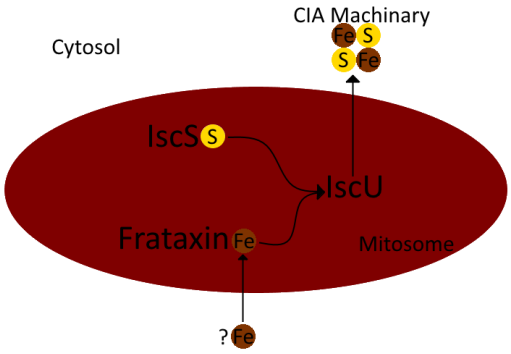

Figure 6-2: Cartoon of the mitosome of *C. parvum*. is purported to contain only 1 complete, active pathway: the ISC Fe/S biosynthetic pathway. The key components of this pathway are the sulphur donating IscS, the supposed iron storage protein Frataxin and the scaffold protein IscU. Once constructed, the Fe/S cluster, potentially still attached to IscU, is exported into the cell cytoplasm for use by the CIA pathway and other enzymes.

6.1.3.3 The expression and localisation of ISC components of C. parvum is life cycle stage dependant

However, what was not expected was the observation that the localisation and even expression of the components would be dependent on the life cycle stage. Though no mitosome has been observed within the intracellular life cycle stages of *C. parvum*, it was presumed that the ISC pathway would remain active and localised throughout even these stages. This is due to the conservation of an active Fe/S cluster biosynthetic pathway throughout all known cellular life. There is precedent for cytoplasmic localisation for each protein studied, though only in addition to organellar expression. Furthermore, the ISC components studied are not expressed at detectable levels within the oocysts. Although the functional parts of the oocyst are essentially sporozoites, they are metabolically different from the excysted forms. This could be explained as a form of metabolic 'hibernation', though the few studies that have explored the metabolism of oocysts appear to show an active glycolytic pathway.

6.1.3.4 The sulphur donor, CpIscS is a functional homologue of Nfs1p

Though the localisation of the proteins proves the hypothesis of their presence in the mitosome, it does not prove that they function as intended or at all. Therefore, it was important to demonstrate functional complementation by at least one of the identified proteins. CpIscS was chosen for this due to its status as an essential protein in the model organism, *S. cerevisiae* and therefore a suitable target for lethal knockout recovery. Expression of the recombinant CpIscS was shown to successfully recover the lethal phenotype and it can therefore be stated that CpIscS is indeed a functional homologue of *S. cerevisiae* Nfs1p and, more importantly, a strong indicator that the ISC pathway within the mitosome of *C. parvum* functions in a manner like the other documented examples of ISC.

This provides yet another example of an MRO, in this case a mitosome, where a complete Fe/S pathway has been conserved. Throughout the examples of MROs, pathways such as the TCA cycle are repeatedly absent and yet a Fe/S is always present, even in the rare cases where the typical mitochondrial ISC pathway has been replaced with the more bacterial SUF system (such as in *E. histolytica*) (Burki et al., 2013, Makiuchi and Nozaki, 2014, Tovar et al., 1999). The main implications of these findings are that Fe/S cluster biosynthesis and not ATP synthesis is the primary role of the mitochondrion, as the loss of ATP pathways from MROs has occurred multiple times independently, yet not one example of an MRO lacking an Fe/S cluster pathway has been found. Furthermore, due to the functional complementation of CpIscS of yeast Nfs1p and the respective positions of *C. parvum* and *S. cerevisiae* in the eukaryotic tree of life it can also be asserted with increasing confidence that LECA contained a mitochondrion and therefore all examples of organisms appearing to lack canonical mitochondria that may arise are more likely examples of further reductive evolution of the mitochondrion, as opposed to diverging before the endosymbiotic event. Together, these conclusions have potentially massive implications on the currently accepted timeline of mitochondrial evolution in relation to eukaryotes.

6.2 Avenues of future research

6.2.1 New directions in in-vitro culture design

Following the discovery of the thin-walled oocysts in *in-vitro* culture and their possible relation to host lipid content, future investigations into new culture design should prioritise cell cultures that display high levels of lipid synthesis. Additionally, further experimentation regarding the potential interaction between host and parasite, in regard to FASN and other fatty acid pathways could produce greater detailed information regarding this hypothesis.

Moreover, it may be worth using cell types with known high levels of mitochondrial activity, such as hepatic cell lines. Previous work had touched on this, with MDCK cells being amongst those cultures that preceded COLO-680N. Likewise, it would be interesting to observe the effects, if any, that attempting to infect cell lines with low levels of mitochondrial activity would have. To this end, detailed examination of mitochondrial activity in any infected culture could further shed light on this hypothesis, such as the colorimetric MTT (3-(4,5-dimethylthiazol-2-yl)-2,5-diphenyltetrazolium bromide) or Rezasurin mitochondrial respiration assays or oxygen consumption assays. The implied importance of host fatty acid machinery could also pose an interesting, potential drug target that could be explored through the COLO-680N system.

Now that the cultures have been established in earnest, it would also be possible to utilise the cultures in mass drug screens. By utilising the COLO-680N cultures of *C. parvum* it will be possible to determine with more confidence than previously possible whether a given drug will be effective. The robust nature of the infection model will also allow the exploration of longer term drug regimens and to develop drugs that can remain effective throughout the different life cycle stages of *C. parvum*. The latter provides a potential solution to the current lack of drugs for the immune-compromised as autoinfection stages are currently not available for proper drug studies utilising past culture systems (Striepen, 2013).

6.2.2 Expanding ^{1}H NMR applications

Whilst the ^{1}H NMR studies were expansive, and certainly novel, they were by no means exhaustive. As was observed in both the mice and cell cultures, individual strains of *C. parvum*, in addition to different *Cryptosporidium* species, all presented metabolic

fingerprints that were distinguishable by PCA analysis. Expanding future ^{1}H NMR research to include the metabolomes of other *in-vitro* cultures as well as other strain/species could serve only to increase our understanding of the infection metabolome. Most importantly it could enhance the theory that *Cryptosporidium* heavily influence host mitochondrial metabolism. Potentially, this could show whether the interaction is related to the mitosome of *C. parvum* and *C. hominis* or not dependant on the differences observed in cultures of the mitochondrion containing *C. muris*.

^{13}C NMR could also use this developed protocol and would offer a much higher resolution, opening up the possibility of tracking the flux of metabolites during an infection and confirming the hypothesis set out in the discussion and Chapter 4. This would allow the *Cryptosporidium* community the opportunity to finally observe what aspects of the host are actually parasitized by *C. parvum*. A natural partner in this investigation would be the use of transcriptomics, with the combination of the two approaches potentially providing insight into the host-parasite interface, another first for *Cryptosporidium* study as well as the gregarines.

Lastly, the proven effectiveness and field-work friendly preparation technique can be applied outside of *C. parvum* work and has already seen applications in other parasitological studies. If ^{1}H NMR were to be more broadly adopted as either an alternative or companion to MS based metabolomics, it could vastly increase our knowledge of host-pathogen interactions for parasites and other neglected tropical diseases.

The new model will also finally allow for a comprehensive study of the crystalloid body organelle, utilising a combination of the utility of the COLO-680N culture and effectiveness of the various novel methodologies presented throughout this thesis.

6.2.3 Future applications of fledgling genetic tools

The most unexpected feature of the ISC pathway, uncovered by my investigation, was undoubtedly its life cycle stage dependant expression levels. Further investigations into this, such as mRNA sequencing of oocysts or further MS/MS proteomics could elucidate how *C. parvum* has appeared to shun other heavily conserved biological pathways,

including most of the amino-acid biosynthetic pathways. It would also be prudent to investigate the nature of CIA expression in *C. parvum*, to determine whether the life cycle dependant aspects of ISC expression are mirrored in the cytosolic pathway.

Although it is currently not possible to genetically alter *C. parvum* in any efficient or effective manner, there have been promising advances with a CRISPR construct (Vinayak et al., 2015). One such barrier to an effective methodology had been the lack of an effective culturing method. With the advent of the COLO-680N model of infection, one roadblock has been lifted. Therefore, a future angle of research could be to remove the mitochondrial targeting sequence from the ISC compounds, via selective mutation, and observe if the cytoplasmic localisation is toxic or not. With the observation that the ISC pathway is not localised to a compartment during intracellular stages, this could add weight to the argument that mitochondrial localisation of Fe/S cluster biosynthetic pathways is either not one based on intermediate toxicity or that *C. parvum* maintains an as of yet undetected means of protecting against said toxic intermediates.

6.3 Major findings; a summary

(Pictorial summary viewable in Figure 6-3)

- COLO-680N is a suitable cell culture and viable alternative for the propagation and study of *C. parvum in-vitro*
    - This opens the field of *Cryptosporidium* for study to many labs that were previously incapable of affording the start-up costs (in either equipment or training)
- *C. parvum* appears to interact heavily with host mitochondrial processes and localises to areas of high host mitochondrial activity
    - This highlights new avenues of study and understanding of the host-parasite interaction of *Cryptosporidium* species and potentially the gregarines group as a whole
- NMR metabolomics can detect species specific changes in host-parasite metabolomes
    - This potentially offers new methods for diagnosing and tracking infections, an invaluable epidemiological tool
- *C. parvum* maintains expression of ISC homologues within the mitosome in extracellular stages and in the cytoplasm during intracellular stages but not in the oocyst
    - CpIscS is a functional homologue of yeast Nfs1p and therefore the ISC pathway, in addition to its localisation, adding evidence for the conservation of MRO functions across the eukaryotic tree of life.

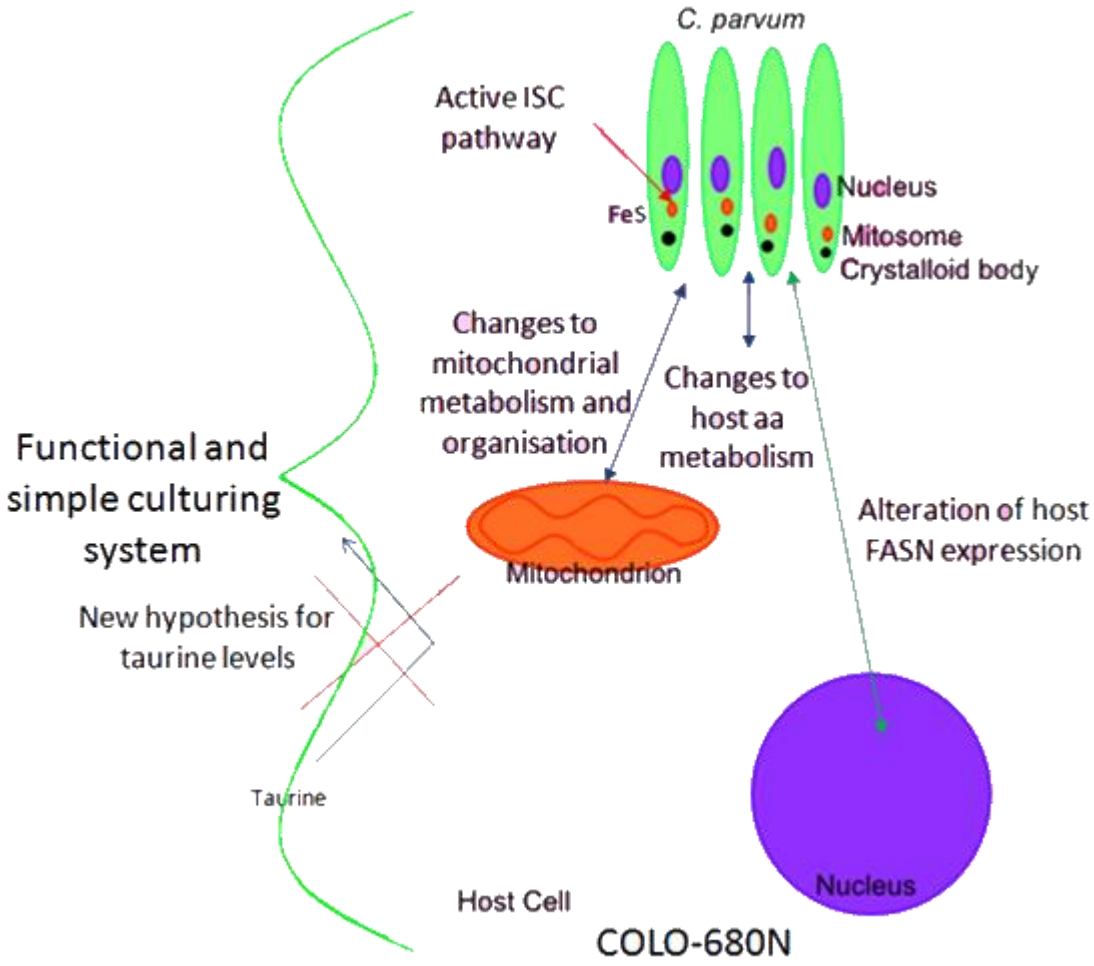

Figure 6-3: A cartoon summarisation of the major accomplishments and findings of this thesis. Each arrow has been colour coded corresponding to the relevant chapter: Chapter 3: Green, Chapter 4: Blue, Chapter 5: Red.

Chapter 7 Supplementary Tables

Comprehensive list of figures and tables

Table of abbreviations

AA	Amino Acid
ABC	ATP-Binding Cassette
ADP	Adenosine Diphosphate
AFM	Atomic Force Microscopy
AMP	Adenosine Monophosphate
ANOVA	Analysis of Variance
AOX	Alternative Oxidase
ATP	Adenosine Triphosphate
CB	Crystalloid Body
CIA	Cytosolic Iron sulphur cluster Assembly (pathway)
CoA	Coenzyme A
CpClec	*Cryptosporidium parvum* C-type lectin
CPN60	Chaperonin protein 60
CpX	Protein (X) of *Cryptosporidium parvum* origin
CRISPR	Clustered Regularly Interspaced Short Palindromic Repeats
CSL	*Cryptosporidium C*ircumsporozoite-Like glycoprotein
DAPI	4',6-diamidino-2-phenylindole
DNA	Deoxyribonucleic Acid
DSS	3-(Trimethylsilyl)-1-propanesulfonic acid
EM	Electron Microscopy
ETC	Electron Transport Chain
EU	European Union
FASN	Fatty Acid Synthase

G418	Geneticin
GC-MS	Gas Chromatography Mass Spectrometry
GRI	Glycine Reuptake Inhibitor
HCT-8	Human Colo-Rectal Carcinoma
HetDip	Heterozygous and Diploid
HIV	Human Immunodeficiency Virus
HSP-70	Heat Shock Protein 70
IFA	Indirect Fluorescent Assay
ISC	Iron Sulphur Cluster (pathway)
IscS	Iron Sulphur Cluster pathway component S
IscU	Iron Sulphur Cluster pathway component U
KEGG	Kyoto Encyclopedia of Genes and Genomes
LACA	Last apicomplexan Common Ancestor
LB	Lysogeny Broth
LECA	Last Eukaryotic Common Ancestor
LEU	Leucine
MALDI-ToF	Matrix-Assisted Laser Desorption/Ionization Time of Flight
MDCK	Madin Darby Canine Kidney
MRO	Mitochondrial Related Organelle
MS	Mass Spectrometry
MTP	MALDI Target Plate
MTT	3-(4,5-dimethylthiazol-2-yl)-2,5-diphenyltetrazolium bromide)
NADP	Nicotinamide adenine dinucleotide phosphate
NCBI	National Center for Biotechnology Information
NFS1	Yeast Cysteine Disulphurase Gene
Nfs1p	Yeast Cysteine Disulphurase Gene product/protein
NHS	National Health Service
NIF	Nitrogen Fixation
NMR	Nuclear Magnetic Resonance
PBS	Phosphate Buffered Saline
PCA	Principal Componenet Analysis
PCR	Polymerase Chain Reaction
PLS-DA	Partial Least Squares Discriminant Analysis
PNO	Pyruvate-NADP+ Oxidoreductase
PV	Parasitophorous Vacuole
rDNA	Ribosomal Deoxynuceleic Acid
SCID	Severe Combined Immunodeficiency
SDS PAGE	Sodium Dodecyl Sulphate Poly-Acrylamide Gel Electrophoresis
SEM	Scanning Electron Microscopy
SUF	Sulphur Formation (pathway)
TCA	Tricarboxylic Acid
TEM	Transmission Electron Microscopy
UV	Ultra Violet
VVL	Vicia Villosa Lectin

YFH1	Yeast Frataxin Homologue gene
Yfh1p	Yeast frataxin homologue protein
YPD	Yeast extract Peptone Dextrose

Chapter 8 References

Abrahamsen, M. S., Templeton, T. J., Enomoto, S., Abrahante, J. E., Zhu, G., Lancto, C. A., Deng, M., Liu, C., Widmer, G., Tzipori, S., Buck, G. A., Xu, P., Bankier, A. T., Dear, P. H., Konfortov, B. A., Spriggs, H. F., Iyer, L., Anantharaman, V., Aravind, L. and Kapur, V. (2004) 'Complete genome sequence of the apicomplexan, *Cryptosporidium parvum*', *Science,* 304(5669), pp. 441-5.

Alcantara Warren, C., Destura Rv Fau - Sevilleja, J. E. A. D., Sevilleja Je Fau - Barroso, L. F., Barroso Lf Fau - Carvalho, H., Carvalho H Fau - Barrett, L. J., Barrett Lj Fau - O'Brien, A. D., O'Brien Ad Fau - Guerrant, R. L. and Guerrant, R. L. (2008) 'Detection of epithelial-cell injury, and quantification of infection, in the HCT-8 organoid model of cryptosporidiosis', (0022-1899 (Print)).

Alcock, F., Webb, C. T., Dolezal, P., Hewitt, V., Shingu-Vasquez, M., Likic, V. A., Traven, A. and Lithgow, T. (2012) 'A small Tim homohexamer in the relict mitochondrion of Cryptosporidium', *Mol Biol Evol,* 29(1), pp. 113-22.

Ali, V. and Nozaki, T. (2013) 'Iron-sulphur clusters, their biosynthesis, and biological functions in protozoan parasites', *Adv Parasitol,* 83, pp. 1-92.

Altschul, S. F., Gish, W., Miller, W., Myers, E. W. and Lipman, D. J. (1990) 'Basic local alignment search tool', *J Mol Biol,* 215(3), pp. 403-10.

Arjmand, M., Madrakian, A., Khalili, G., Najafi Dastnaee, A., Zamani, Z. and Akbari, Z. (2016) 'Metabolomics-Based Study of Logarithmic and Stationary Phases of Promastigotes in Leishmania major by 1H NMR Spectroscopy', *Iran Biomed J,* 20(2), pp. 77-83.

Arrowood, M. J. (2002) 'In vitro cultivation of *Cryptosporidium* species', *Clin Microbiol Rev,* 15(3), pp. 390-400.

Balog, C. I., Meissner, A., Goraler, S., Bladergroen, M. R., Vennervald, B. J., Mayboroda, O. A. and Deelder, A. M. (2011) 'Metabonomic investigation of human Schistosoma mansoni infection', *Mol Biosyst,* 7(5), pp. 1473-80.

Barnes, D. A., Bonnin, A., Huang, J. X., Gousset, L., Wu, J., Gut, J., Doyle, P., Dubremetz, J. F., Ward, H. and Petersen, C. (1998) 'A novel multi-domain mucin-like glycoprotein of Cryptosporidium parvum mediates invasion', *Mol Biochem Parasitol,* 96(1-2), pp. 93-110.

Benamrouz, S., Conseil, V., Creusy, C., Calderon, E., Dei-Cas, E. and Certad, G. (2012a) 'Parasites and malignancies, a review, with emphasis on digestive cancer induced by Cryptosporidium parvum (Alveolata: Apicomplexa)', *Parasite : journal de la Société Française de Parasitologie,* 19(2), pp. 101-115.

Benamrouz, S., Guyot, K., Gazzola, S., Mouray, A., Chassat, T., Delaire, B., Chabé, M., Gosset, P., Viscogliosi, E., Dei-Cas, E., Creusy, C., Conseil, V. and Certad, G. (2012b) 'Cryptosporidium parvum Infection in SCID Mice Infected with Only One Oocyst: qPCR Assessment of Parasite Replication in Tissues and Development of Digestive Cancer', *PLOS ONE,* 7(12), pp. e51232.

Bezabeh, T., Somorjai, R. L. and Smith, I. C. P. (2009) 'MR metabolomics of fecal extracts: applications in the study of bowel diseases', *Magnetic Resonance in Chemistry,* 47(S1), pp. S54-S61.

Bhat, N., Joe, A., PereiraPerrin, M. and Ward, H. D. (2007) 'Cryptosporidium p30, a galactose/N-acetylgalactosamine-specific lectin, mediates infection in vitro', *J Biol Chem,* 282(48), pp. 34877-87.

Blackstone, N. W. (2013) 'Why did eukaryotes evolve only once? Genetic and energetic aspects of conflict and conflict mediation', *Philos Trans R Soc Lond B Biol Sci,* 368(1622), pp. 20120266.

Bonnin, A., Ojcius, D. M., Souque, P., Barnes, D. A., Doyle, P. S., Gut, J., Nelson, R. G., Petersen, C. and Dubremetz, J. F. (2001) 'Characterization of a monoclonal antibody reacting with

antigen-4 domain of gp900 in Cryptosporidium parvum invasive stages', *Parasitol Res,* 87(8), pp. 589-92.

Borowski, H., Thomson, R. C. A., Armstrong, T. and Clode, P. L. (2010) 'Morphological characterization of Cryptosporidium parvum life-cycle stages in an in vitro model system', *Parasitology,* 137(01), pp. 13-26.

Bouzid, M., Hunter, P. R., Chalmers, R. M. and Tyler, K. M. (2013) 'Cryptosporidium pathogenicity and virulence', *Clin Microbiol Rev,* 26(1), pp. 115-34.

Briggs, A. D., Boxall, N. S., Van Santen, D., Chalmers, R. M. and McCarthy, N. D. (2014) 'Approaches to the detection of very small, common, and easily missed outbreaks that together contribute substantially to human Cryptosporidium infection', *Epidemiol Infect,* 142(9), pp. 1869-76.

Brunkard, J. M., Ailes, E., Roberts, V. A., Hill, V., Hilborn, E. D., Craun, G. F., Rajasingham, A., Kahler, A., Garrison, L., Hicks, L., Carpenter, J., Wade, T. J., Beach, M. J., Yoder Msw, J. S. and CDC (2011) 'Surveillance for waterborne disease outbreaks associated with drinking water---United States, 2007--2008', *MMWR Surveill Summ,* 60(12), pp. 38-68.

Burki, F., Corradi, N., Sierra, R., Pawlowski, J., Meyer, Gary R., Abbott, Cathryn L. and Keeling, Patrick J. (2013) 'Phylogenomics of the Intracellular Parasite Mikrocytos mackini Reveals Evidence for a Mitosome in Rhizaria', *Current Biology,* 23(16), pp. 1541-1547.

Caccio, S. M. (2005) 'Molecular epidemiology of human cryptosporidiosis', *Parassitologia,* 47(2), pp. 185-92.

Cantey, P. T., Kurian, A. K., Jefferson, D., Moerbe, M. M., Marshall, K., Blankenship, W. R., Rothbarth, G. R., Hwang, J., Hall, R., Yoder, J., Brunkard, J., Johnston, S., Xiao, L., Hill, V. R., Sarisky, J., Zarate-Bermudez, M. A., Otto, C. and Hlavsa, M. C. (2012) 'Outbreak of cryptosporidiosis associated with a man-made chlorinated lake--Tarrant County, Texas, 2008', *J Environ Health,* 75(4), pp. 14-9.

Carreno, R. A., Martin, D. S. and Barta, J. R. (1999) '*Cryptosporidium* is more closely related to the gregarines than to coccidia as shown by phylogenetic analysis of apicomplexan parasites inferred using small-subunit ribosomal RNA gene sequences', *Parasitol Res,* 85(11), pp. 899-904.

Cavalier-Smith, T. (2014) 'Gregarine site-heterogeneous 18S rDNA trees, revision of gregarine higher classification, and the evolutionary diversification of Sporozoa', *European Journal of Protistology,* 50(5), pp. 472-495.

Chatterjee, A., Banerjee, S., Steffen, M., O'Connor, R. M., Ward, H. D., Robbins, P. W. and Samuelson, J. (2010) 'Evidence for mucin-like glycoproteins that tether sporozoites of Cryptosporidium parvum to the inner surface of the oocyst wall', *Eukaryot Cell,* 9(1), pp. 84-96.

Chauret, C., Nolan, K., Chen, P., Springthorpe, S. and Sattar, S. (1998) 'Aging of Cryptosporidium parvum oocysts in river water and their susceptibility to disinfection by chlorine and monochloramine', *Can J Microbiol,* 44(12), pp. 1154-60.

Checkley, W., White, A. C., Jr., Jaganath, D., Arrowood, M. J., Chalmers, R. M., Chen, X. M., Fayer, R., Griffiths, J. K., Guerrant, R. L., Hedstrom, L., Huston, C. D., Kotloff, K. L., Kang, G., Mead, J. R., Miller, M., Petri, W. A., Jr., Priest, J. W., Roos, D. S., Striepen, B., Thompson, R. C., Ward, H. D., Van Voorhis, W. A., Xiao, L., Zhu, G. and Houpt, E. R. (2014) 'A review of the global burden, novel diagnostics, therapeutics, and vaccine targets for cryptosporidium', *Lancet Infect Dis*.

Chen, X. M., Huang, B. Q., Splinter, P. L., Cao, H., Zhu, G., McNiven, M. A. and LaRusso, N. F. (2003) 'Cryptosporidium parvum invasion of biliary epithelia requires host cell tyrosine phosphorylation of cortactin via c-Src', *Gastroenterology,* 125(1), pp. 216-28.

Chen, X. M., Huang, B. Q., Splinter, P. L., Orth, J. D., Billadeau, D. D., McNiven, M. A. and LaRusso, N. F. (2004a) 'Cdc42 and the actin-related protein/neural Wiskott-Aldrich syndrome

protein network mediate cellular invasion by Cryptosporidium parvum', *Infect Immun,* 72(5), pp. 3011-21.

Chen, X. M., Splinter, P. L., Tietz, P. S., Huang, B. Q., Billadeau, D. D. and LaRusso, N. F. (2004b) 'Phosphatidylinositol 3-kinase and frabin mediate Cryptosporidium parvum cellular invasion via activation of Cdc42', *J Biol Chem,* 279(30), pp. 31671-8.

Cheng, C., MacIntyre, L., Abdelmohsen, U. R., Horn, H., Polymenakou, P. N., Edrada-Ebel, R. and Hentschel, U. (2015) 'Biodiversity, Anti-Trypanosomal Activity Screening, and Metabolomic Profiling of Actinomycetes Isolated from Mediterranean Sponges', *PLoS One,* 10(9), pp. e0138528.

Claros, M. G. and Vincens, P. (1996) 'Computational method to predict mitochondrially imported proteins and their targeting sequences', *Eur J Biochem,* 241(3), pp. 779-86.

Clode, P. L., Koh, W. H. and Thompson, R. C. (2015) 'Life without a Host Cell: What is Cryptosporidium?', *Trends Parasitol,* 31(12), pp. 614-24.

Cook, W. J., Senkovich, O., Aleem, K. and Chattopadhyay, D. (2012) 'Crystal structure of *Cryptosporidium parvum* pyruvate kinase', *PLoS One,* 7(10), pp. e46875.

Cope, J. R., Prosser, A., Nowicki, S., Roberts, M. W., Roberts, J. M., Scheer, D., Anderson, C., Longsworth, A., Parsons, C., Goldschmidt, D., Johnston, S., Bishop, H., Xiao, L., Hill, V., Beach, M. and Hlavsa, M. C. (2015) 'Preventing community-wide transmission of Cryptosporidium: a proactive public health response to a swimming pool-associated outbreak--Auglaize County, Ohio, USA', *Epidemiol Infect,* 143(16), pp. 3459-67.

Ctrnacta, V., Ault, J. G., Stejskal, F. and Keithly, J. S. (2006) 'Localization of pyruvate:NADP+ oxidoreductase in sporozoites of *Cryptosporidium parvum*', *J Eukaryot Microbiol,* 53(4), pp. 225-31.

Current Wl Fau - Reese, N. C. and Reese, N. C. (1986) 'A comparison of endogenous development of three isolates of Cryptosporidium in suckling mice', *Journal of Protozoology,* 33(1), pp. 98-108.

Current, W. L., Upton, S. J. and Haynes, T. B. (1986) 'The Life Cycle of Cryptosporidium baileyi n. sp. (Apicomplexa, Cryptosporidiidae) Infecting Chickens', *The Journal of Protozoology,* 33(2), pp. 289-296.

Dahal, K. and Vanlerberghe, G. C. (2017) 'Alternative oxidase respiration maintains both mitochondrial and chloroplast function during drought', *New Phytol,* 213(2), pp. 560-571.

Dellibovi-Ragheb, T. A., Gisselberg, J. E. and Prigge, S. T. (2013) 'Parasites FeS Up: Iron-Sulfur Cluster Biogenesis in Eukaryotic Pathogens', *PLOS Pathogens,* 9(4), pp. e1003227.

Deshpande, A. P., Jones, B. L., Connelly, L., Pollock, K. G., Brownlie, S. and Alexander, C. L. (2014) 'Molecular characterization of Cryptosporidium parvum isolates from human cryptosporidiosis cases in Scotland', *Parasitology*, pp. 1-8.

Dlouhy, A. C. and Outten, C. E. (2013) 'The Iron Metallome in Eukaryotic Organisms', *Metal ions in life sciences,* 12, pp. 241-278.

Domjahn, B. T., Hlavsa, M. C., Anderson, B., Schulkin, J., Leon, J. and Jones, J. L. (2014) 'A survey of U.S. obstetrician-gynecologists' clinical and epidemiological knowledge of cryptosporidiosis in pregnancy', *Zoonoses Public Health,* 61(5), pp. 356-63.

Doyle, P. S., Kanaani, J. and Wang, C. C. (1998) 'Hypoxanthine, guanine, xanthine phosphoribosyltransferase activity in Cryptosporidium parvum', *Exp Parasitol,* 89(1), pp. 9-15.

Dreelin, E. A., Ives, R. L., Molloy, S., Rose, J. B., Deshpande, A. P., Jones, B. L., Connelly, L., Pollock, K. G., Brownlie, S., Alexander, C. L., Briggs, A. D., Boxall, N. S., Van Santen, D., Chalmers, R. M., McCarthy, N. D., Domjahn, B. T., Hlavsa Mc Fau - Anderson, B., Anderson B Fau - Schulkin, J., Schulkin J Fau - Leon, J., Leon J Fau - Jones, J. L., Jones, J. L., Cantey, P. T., Kurian Ak Fau - Jefferson, D., Jefferson D Fau - Moerbe, M. M., Moerbe Mm Fau - Marshall, K., Marshall K Fau - Blankenship, W. R., Blankenship Wr Fau - Rothbarth, G. R.,

Rothbarth Gr Fau - Hwang, J., Hwang J Fau - Hall, R., Hall R Fau - Yoder, J., Yoder J Fau - Brunkard, J., Brunkard J Fau - Johnston, S., Johnston S Fau - Xiao, L., Xiao L Fau - Hill, V. R., Hill Vr Fau - Sarisky, J., Sarisky J Fau - Zarate-Bermudez, M. A., Zarate-Bermudez Ma Fau - Otto, C., Otto C Fau - Hlavsa, M. C., Hlavsa, M. C., Shirley, D. A., Moonah Sn Fau - Kotloff, K. L. and Kotloff, K. L. 'Cryptosporidium and Giardia in surface water: a case study from michigan, USA to inform management of rural water systems

Molecular characterization of Cryptosporidium parvum isolates from human cryptosporidiosis cases in Scotland

Approaches to the detection of very small, common, and easily missed outbreaks that together contribute substantially to human Cryptosporidium infection

A survey of U.S. obstetrician-gynecologists' clinical and epidemiological knowledge of cryptosporidiosis in pregnancy

Outbreak of cryptosporidiosis associated with a man-made chlorinated lake--Tarrant County, Texas, 2008

Burden of disease from cryptosporidiosis', (1660-4601 (Electronic)).

Drozdetskiy, A., Cole, C., Procter, J. and Barton, G. J. (2015) 'JPred4: a protein secondary structure prediction server', *Nucleic Acids Research,* 43(Web Server issue), pp. W389-W394.

Dubey, J. P. (1998) 'Advances in the life cycle of Toxoplasma gondii', *International Journal for Parasitology,* 28(7), pp. 1019-1024.

Dunning Hotopp, J. C. (2011) 'Horizontal gene transfer between bacteria and animals', *Trends Genet,* 27(4), pp. 157-63.

DuPont, H. L., Chappell, C. L., Sterling, C. R., Okhuysen, P. C., Rose, J. B. and Jakubowski, W. (1995) 'The infectivity of Cryptosporidium parvum in healthy volunteers', *N Engl J Med,* 332(13), pp. 855-9.

Dyall, S. D. and Johnson, P. J. (2000) 'Origins of hydrogenosomes and mitochondria: evolution and organelle biogenesis', *Curr Opin Microbiol,* 3(4), pp. 404-11.

Edwinson, A., Widmer, G. and McEvoy, J. (2016) 'Glycoproteins and Gal-GalNAc cause Cryptosporidium to switch from an invasive sporozoite to a replicative trophozoite', *Int J Parasitol,* 46(1), pp. 67-74.

Egger, M., Mausezahl, D., Odermatt, P., Marti, H. P. and Tanner, M. (1990) 'Symptoms and transmission of intestinal cryptosporidiosis', *Arch Dis Child,* 65(4), pp. 445-7.

Elliott, D. A. and Clark, D. P. (2000) 'Cryptosporidium parvum induces host cell actin accumulation at the host-parasite interface', *Infect Immun,* 68(4), pp. 2315-22.

Entrala, E. and Mascaro, C. (1997) 'Glycolytic enzyme activities in *Cryptosporidium parvum* oocysts', *FEMS Microbiol Lett,* 151(1), pp. 51-7.

Fayer, R. and Ungar, B. L. (1986) 'Cryptosporidium spp. and cryptosporidiosis', *Microbiological Reviews,* 50(4), pp. 458-483.

Feng, H., Nie, W., Sheoran, A., Zhang, Q. and Tzipori, S. (2006) 'Bile acids enhance invasiveness of Cryptosporidium spp. into cultured cells', *Infect Immun,* 74(6), pp. 3342-6.

Fichera, M. E. and Roos, D. S. (1997) 'A plastid organelle as a drug target in apicomplexan parasites', *Nature,* 390(6658), pp. 407-9.

Flanigan, T. P. and Graham, R. (1990) 'Extended spectrum of symptoms in cryptosporidiosis', *Am J Med: Vol. 2*. United States, pp. 252.

Flegr, J., Prandota, J., Sovičková, M. and Israili, Z. H. (2014) 'Toxoplasmosis – A Global Threat. Correlation of Latent Toxoplasmosis with Specific Disease Burden in a Set of 88 Countries', *PLOS ONE,* 9(3), pp. e90203.

Florens, L., Washburn, M. P., Raine, J. D., Anthony, R. M., Grainger, M., Haynes, J. D., Moch, J. K., Muster, N., Sacci, J. B., Tabb, D. L., Witney, A. A., Wolters, D., Wu, Y., Gardner, M. J., Holder, A. A., Sinden, R. E., Yates, J. R. and Carucci, D. J. (2002) 'A proteomic view of the Plasmodium falciparum life cycle', *Nature,* 419(6906), pp. 520-526.

Fritzler, J. M. and Zhu, G. (2012) 'Novel anti-Cryptosporidium activity of known drugs identified by high-throughput screening against parasite fatty acyl-CoA binding protein (ACBP)', *J Antimicrob Chemother,* 67(3), pp. 609-17.

Gardner, M. J., Hall, N., Fung, E., White, O., Berriman, M., Hyman, R. W., Carlton, J. M., Pain, A., Nelson, K. E., Bowman, S., Paulsen, I. T., James, K., Eisen, J. A., Rutherford, K., Salzberg, S. L., Craig, A., Kyes, S., Chan, M.-S., Nene, V., Shallom, S. J., Suh, B., Peterson, J., Angiuoli, S., Pertea, M., Allen, J., Selengut, J., Haft, D., Mather, M. W., Vaidya, A. B., Martin, D. M. A., Fairlamb, A. H., Fraunholz, M. J., Roos, D. S., Ralph, S. A., McFadden, G. I., Cummings, L. M., Subramanian, G. M., Mungall, C., Venter, J. C., Carucci, D. J., Hoffman, S. L., Newbold, C., Davis, R. W., Fraser, C. M. and Barrell, B. (2002) 'Genome sequence of the human malaria parasite Plasmodium falciparum', *Nature,* 419(6906), pp. 10.1038/nature01097.

Gatei, W., Wamae, C. N., Mbae, C., Waruru, A., Mulinge, E., Waithera, T., Gatika, S. M., Kamwati, S. K., Revathi, G., Hart, C. A., Flanigan, T. P., Graham, R., Egger, M., Mausezahl, D., Odermatt, P., Marti, H. P. and Tanner, M. (2006) 'Cryptosporidiosis: prevalence, genotype analysis, and symptoms associated with infections in children in Kenya

Extended spectrum of symptoms in cryptosporidiosis

Symptoms and transmission of intestinal cryptosporidiosis', *Am J Trop Med Hyg: Vol. 1*. United States

England, pp. 78-82.

Gertler, M., Durr, M., Renner, P., Poppert, S., Askar, M., Breidenbach, J., Frank, C., Preussel, K., Schielke, A., Werber, D., Chalmers, R., Robinson, G., Feuerpfeil, I., Tannich, E., Groger, C., Stark, K. and Wilking, H. (2015) 'Outbreak of Cryptosporidium hominis following river flooding in the city of Halle (Saale), Germany, August 2013', *BMC Infect Dis,* 15, pp. 88.

Ghosh, S., Sengupta, A., Sharma, S. and Sonawat, H. M. (2012) 'Metabolic fingerprints of serum, brain, and liver are distinct for mice with cerebral and noncerebral malaria: a (1)H NMR spectroscopy-based metabonomic study', *J Proteome Res,* 11(10), pp. 4992-5004.

Giris, M., Depboylu, B., Dogru-Abbasoglu, S., Erbil, Y., Olgac, V., Alis, H., Aykac-Toker, G. and Uysal, M. (2008) 'Effect of taurine on oxidative stress and apoptosis-related protein expression in trinitrobenzene sulphonic acid-induced colitis', *Clin. Exp. Immunol.,* 152(1), pp. 102.

Girouard, D., Gallant, J., Akiyoshi, D. E., Nunnari, J. and Tzipori, S. (2006) 'Failure to propagate Cryptosporidium spp. in cell-free culture', *J Parasitol,* 92(2), pp. 399-400.

Gold, D., Stein, B. and Tzipori, S. (2001) 'The utilization of sodium taurocholate in excystation of Cryptosporidium parvum and infection of tissue culture', *J Parasitol,* 87(5), pp. 997-1000.

Gonzalez, B., Francois, J. and Renaud, M. (1997) 'A rapid and reliable method for metabolite extraction in yeast using boiling buffered ethanol', *Yeast,* 13(14), pp. 1347-55.

Goodgame, R. W., Kimball, K., Ou, C.-N., White, A. C., Genta, R. M., Lifschitz, C. H. and Chappell, C. L. (1995) 'Intestinal function and injury in acquired immunodeficiency syndrome—related cryptosporidiosis', *Gastroenterology,* 108(4), pp. 1075-1082.

Guo, F., Zhang, H., Payne, H. R. and Zhu, G. (2016) 'Differential Gene Expression and Protein Localization of Cryptosporidium parvum Fatty Acyl-CoA Synthetase Isoforms', *J Eukaryot Microbiol,* 63(2), pp. 233-46.

Hansen, S. H. and Grunnet, N. (2013) 'Taurine, glutathione and bioenergetics', *Adv Exp Med Biol,* 776, pp. 3-12.

Hayes, J., Kirf, D., Garvey, M. and Rowan, N. (2013) 'Disinfection and toxicological assessments of pulsed UV and pulsed-plasma gas-discharge treated-water containing the waterborne protozoan enteroparasite Cryptosporidium parvum', *J Microbiol Methods,* 94(3), pp. 325-37.

Hijjawi, N. (2010) '*Cryptosporidium*: new developments in cell culture', *Exp Parasitol,* 124(1), pp. 54-60.

Hijjawi, N., Estcourt, A., Yang, R., Monis, P. and Ryan, U. (2010) 'Complete development and multiplication of *Cryptosporidium hominis* in cell-free culture', *Vet Parasitol,* 169(1-2), pp. 29-36.

Hijjawi, N. S., Meloni Bp Fau - Morgan, U. M., Morgan Um Fau - Thompson, R. C. and Thompson, R. C. (2001) 'Complete development and long-term maintenance of Cryptosporidium parvum human and cattle genotypes in cell culture', *International Journal of Parasitology,* 31(10), pp. 1048-1055.

Hjort, K., Goldberg, A. V., Tsaousis, A. D., Hirt, R. P. and Embley, T. M. (2010) 'Diversity and reductive evolution of mitochondria among microbial eukaryotes', *Philos Trans R Soc Lond B Biol Sci,* 365(1541), pp. 713-27.

Hlavsa, M. C., Roberts, V. A., Anderson, A. R., Hill, V. R., Kahler, A. M., Orr, M., Garrison, L. E., Hicks, L. A., Newton, A., Hilborn, E. D., Wade, T. J., Beach, M. J., Yoder, J. S. and CDC (2011) 'Surveillance for waterborne disease outbreaks and other health events associated with recreational water --- United States, 2007--2008', *MMWR Surveill Summ,* 60(12), pp. 1-32.

Hlavsa, M. C., Roberts, V. A., Kahler, A. M., Hilborn, E. D., Mecher, T. R., Beach, M. J., Wade, T. J., Yoder, J. S. and (CDC), C. f. D. C. a. P. (2015) 'Outbreaks of Illness Associated with Recreational Water--United States, 2011-2012', *MMWR Morb Mortal Wkly Rep,* 64(24), pp. 668-72.

Hlavsa, M. C., Roberts, V. A., Kahler, A. M., Hilborn, E. D., Wade, T. J., Backer, L. C., Yoder, J. S. and (CDC), C. f. D. C. a. P. (2014) 'Recreational water-associated disease outbreaks--United States, 2009-2010', *MMWR Morb Mortal Wkly Rep,* 63(1), pp. 6-10.

Hong, Y. S., Ahn, Y. T., Park, J. C., Lee, J. H., Lee, H., Huh, C. S., Kim, D. H., Ryu, D. H. and Hwang, G. S. (2010) '1H NMR-based metabonomic assessment of probiotic effects in a colitis mouse model', *Arch. Pharmacal Res.,* 33(7), pp. 1091.

Horowitz, M. P. and Greenamyre, J. T. (2010) 'Mitochondrial Iron Metabolism and Its Role in Neurodegeneration', *Journal of Alzheimer's disease : JAD,* 20(Suppl 2), pp. S551-S568.

Huang, M. Z., Li, J., Guan, L., Li, D. Q., Nie, X. M., Gui, R. and Chen, X. (2015) 'Therapeutic effects of acetylspiramycin and garlicin on cryptosporidiosis among drug users', *Int J Parasitol Drugs Drug Resist,* 5(3), pp. 185-90.

Huettenbrenner, S., Maier, S., Leisser, C., Polgar, D., Strasser, S., Grusch, M. and Krupitza, G. (2003) 'The evolution of cell death programs as prerequisites of multicellularity', *Mutat Res,* 543(3), pp. 235-49.

Hussien, S. M., Abdella, O. H., Abu-Hashim, A. H., Aboshiesha, G. A., Taha, M. A., El-Shemy, A. S. and El-Bader, M. M. (2013) 'Comparative study between the effect of nitazoxanide and paromomycine in treatment of cryptosporidiosis in hospitalized children', *J Egypt Soc Parasitol,* 43(2), pp. 463-70.

Jacobs, D. M., Deltimple, N., van Velzen, E., van Dorsten, F. A., Bingham, M., Vaughan, E. E. and van Duynhoven, J. (2008) '(1)H NMR metabolite profiling of feces as a tool to assess the impact of nutrition on the human microbiome', *NMR Biomed,* 21(6), pp. 615.

Jansson, J., Willing, B., Lucio, M., Fekete, A., Dicksved, J., Halfvarson, J., Tysk, C. and Schmitt-Kopplin, P. (2009) 'Metabolomics Reveals Metabolic Biomarkers of Crohn's Disease', *PLoS ONE,* 4(7), pp. e6386.

Jenkins, M. B., Eaglesham, B. S., Anthony, L. C., Kachlany, S. C., Bowman, D. D. and Ghiorse, W. C. (2010) 'Significance of wall structure, macromolecular composition, and surface polymers to the survival and transport of Cryptosporidium parvum oocysts', *Appl Environ Microbiol,* 76(6), pp. 1926-34.

Joe, A., Hamer, D. H., Kelley, M. A., Pereira, M. E., Keusch, G. T., Tzipori, S. and Ward, H. D. (1994) 'Role of a Gal/GalNAc-specific sporozoite surface lectin in Cryptosporidium parvum-host cell interaction', *J Eukaryot Microbiol,* 41(5), pp. 44s.

Kar, S., Daugschies, A., Cakmak, A., Yilmazer, N., Dittmar, K. and Bangoura, B. (2011) 'Cryptosporidium parvum oocyst viability and behaviour of the residual body during the excystation process', *Parasitol Res,* 109(6), pp. 1719-23.

Karanis, P. and Aldeyarbi, H. M. (2011) 'Evolution of *Cryptosporidium* in vitro culture', *Int J Parasitol,* 41(12), pp. 1231-42.

Karnkowska, A., Vacek, V., Zubáčová, Z., Treitli, S. C., Petrželková, R., Eme, L., Novák, L., Žárský, V., Barlow, L. D., Herman, E. K., Soukal, P., Hroudová, M., Doležal, P., Stairs, C. W., Roger, A. J., Eliáš, M., Dacks, J. B., Vlček, Č. and Hampl, V. (2016) 'A Eukaryote without a Mitochondrial Organelle', *Current Biology,* 26(10), pp. 1274-1284.

Keithly, J. S., Langreth, S. G., Buttle, K. F. and Mannella, C. A. (2005) 'Electron Tomographic and Ultrastructural Analysis of the Cryptosporidium parvum Relict Mitochondrion, its Associated Membranes, and Organelles', *Journal of Eukaryotic Microbiology,* 52(2), pp. 132-140.

King, B. J., Keegan, A. R., Robinson, B. S. and Monis, P. T. (2011) '*Cryptosporidium* cell culture infectivity assay design', *Parasitology*, pp. 1-11.

Kluge, M. A., Fetterman, J. L. and Vita, J. A. (2013) 'Mitochondria and endothelial function', *Circ Res,* 112(8), pp. 1171-88.

Kumar, B., Chaubey, S., Shah, P., Tanveer, A., Charan, M., Siddiqi, M. I. and Habib, S. (2011) 'Interaction between sulphur mobilisation proteins SufB and SufC: evidence for an iron-sulphur cluster biogenesis pathway in the apicoplast of *Plasmodium falciparum*', *Int J Parasitol,* 41(9), pp. 991-9.

Kuo, C. H., Wares, J. P. and Kissinger, J. C. (2008) 'The Apicomplexan whole-genome phylogeny: an analysis of incongruence among gene trees', *Mol Biol Evol,* 25(12), pp. 2689-98.

LaGier, M. J., Tachezy, J., Stejskal, F., Kutisova, K. and Keithly, J. S. (2003) 'Mitochondrial-type iron-sulfur cluster biosynthesis genes (IscS and IscU) in the apicomplexan Cryptosporidium parvum', *Microbiology,* 149(Pt 12), pp. 3519-30.

Lamour, S. D., Choi, B. S., Keun, H. C., Muller, I. and Saric, J. (2012) 'Metabolic characterization of Leishmania major infection in activated and nonactivated macrophages', *J Proteome Res,* 11(8), pp. 4211-22.

Langer, R. C. and Riggs, M. W. (1999) 'Cryptosporidium parvum apical complex glycoprotein CSL contains a sporozoite ligand for intestinal epithelial cells', (0019-9567 (Print)).

Le Gall, G., Noor, S. O., Ridgway, K., Scovell, L., Jamieson, C., Johnson, I. T., Colquhoun, I. J., Kemsley, E. K. and Narbad, A. (2011) 'Metabolomics of Fecal Extracts Detects Altered Metabolic Activity of Gut Microbiota in Ulcerative Colitis and Irritable Bowel Syndrome', *Journal of Proteome Research,* 10(9), pp. 4208-4218.

Leitch, G. J. and He, Q. (2012) 'Cryptosporidiosis-an overview', *J Biomed Res,* 25(1), pp. 1-16.

Lemgruber, L. and Lupetti, P. (2012) 'Crystalloid body, refractile body and virus-like particles in Apicomplexa: what is in there?', *Parasitology,* 139(3), pp. 285-93.

Li, J. V., Saric, J., Wang, Y., Utzinger, J., Holmes, E. and Balmer, O. (2011) 'Metabonomic investigation of single and multiple strain Trypanosoma brucei brucei infections', *Am J Trop Med Hyg,* 84(1), pp. 91-8.

Lill, R., Dutkiewicz, R., Freibert, S. A., Heidenreich, T., Mascarenhas, J., Netz, D. J., Paul, V. D., Pierik, A. J., Richter, N., Stumpfig, M., Srinivasan, V., Stehling, O. and Muhlenhoff, U.

(2015) 'The role of mitochondria and the CIA machinery in the maturation of cytosolic and nuclear iron-sulfur proteins', *Eur J Cell Biol,* 94(7-9), pp. 280-91.

Lill, R., Hoffmann, B., Molik, S., Pierik, A. J., Rietzschel, N., Stehling, O., Uzarska, M. A., Webert, H., Wilbrecht, C. and Muhlenhoff, U. (2012) 'The role of mitochondria in cellular iron-sulfur protein biogenesis and iron metabolism', *Biochim Biophys Acta,* 1823(9), pp. 1491-508.

Lim, L. and McFadden, G. I. (2010) 'The evolution, metabolism and functions of the apicoplast', *Philos Trans R Soc Lond B Biol Sci,* 365(1541), pp. 749-63.

Lin, S., Sanders, D. S., Gleeson, J. T., Osborne, C., Messham, L. and Kurien, M. (2016) 'Long-term outcomes in patients diagnosed with bile-acid diarrhoea', *Eur J Gastroenterol Hepatol,* 28(2), pp. 240-5.

Lindon, J. C. and Nicholson, J. K. (2008) 'Analytical technologies for metabonomics and metabolomics, and multi-omic information recovery', *TrAC, Trends Anal. Chem.,* 27(3), pp. 194.

Lingelbach, K. and Joiner, K. A. (1998) 'The parasitophorous vacuole membrane surrounding Plasmodium and Toxoplasma: an unusual compartment in infected cells', *Journal of Cell Science,* 111(11), pp. 1467.

Liu, L., Johnson, H. L., Cousens, S., Perin, J., Scott, S., Lawn, J. E., Rudan, I., Campbell, H., Cibulskis, R., Li, M., Mathers, C. and Black, R. E. (2012) 'Global, regional, and national causes of child mortality: an updated systematic analysis for 2010 with time trends since 2000', *Lancet,* 379(9832), pp. 2151-61.

Mac Kenzie, W. R., Hoxie, N. J., Proctor, M. E., Gradus, M. S., Blair, K. A., Peterson, D. E., Kazmierczak, J. J., Addiss, D. G., Fox, K. R., Rose, J. B. and Davis, J. P. (1994) 'A Massive Outbreak in Milwaukee of Cryptosporidium Infection Transmitted through the Public Water Supply', *New England Journal of Medicine,* 331(3), pp. 161-167.

Makiuchi, T. and Nozaki, T. (2014) 'Highly divergent mitochondrion-related organelles in anaerobic parasitic protozoa', *Biochimie,* 100, pp. 3-17.

Manjunatha, U. H., Chao, A. T., Leong, F. J. and Diagana, T. T. (2016) 'Cryptosporidiosis Drug Discovery: Opportunities and Challenges', *ACS Infect Dis,* 2(8), pp. 530-7.

Martin, W. F. (2017) 'Physiology, anaerobes, and the origin of mitosing cells 50 years on', *J Theor Biol*.

Matsubayashi, M., Teramoto-Kimata I Fau - Uni, S., Uni S Fau - Lillehoj, H. S., Lillehoj Hs Fau - Matsuda, H., Matsuda H Fau - Furuya, M., Furuya M Fau - Tani, H., Tani H Fau - Sasai, K. and Sasai, K. (2013) 'Elongation factor-1alpha is a novel protein associated with host cell invasion and a potential protective antigen of Cryptosporidium parvum', (1083-351X (Electronic)).

Mazumdar, J. and Striepen, B. (2007) 'Make it or take it: fatty acid metabolism of apicomplexan parasites', *Eukaryot Cell,* 6.

McGuffin, L. J., Bryson, K. and Jones, D. T. (2000) 'The PSIPRED protein structure prediction server', *Bioinformatics,* 16(4), pp. 404-5.

McKerr, C., Adak, G. K., Nichols, G., Gorton, R., Chalmers, R. M., Kafatos, G., Cosford, P., Charlett, A., Reacher, M., Pollock, K. G., Alexander, C. L. and Morton, S. (2015) 'An Outbreak of Cryptosporidium parvum across England & Scotland Associated with Consumption of Fresh Pre-Cut Salad Leaves, May 2012', *PLoS One,* 10(5), pp. e0125955.

Mead, J. R. (2014) 'Prospects for immunotherapy and vaccines against', *Hum Vaccin Immunother: Vol. 6*, pp. 1505-1513.

Meisel, J. L., Perera, D. R., Meligro, C. and Rubin, C. E. (1976) 'Overwhelming watery diarrhea associated with a cryptosporidium in an immunosuppressed patient', *Gastroenterology,* 70(6), pp. 1156-60.

Meloni, B. P. and Thompson, R. C. (1996) 'Simplified methods for obtaining purified oocysts from mice and for growing Cryptosporidium parvum in vitro', *J Parasitol,* 82(5), pp. 757-62.

Miller, C. N., Jossé, L., Brown, I., Blakeman, B., Povey, J., Yiangou, L., Price, M., Cinatl jr, J., Xue, W.-F., Michaelis, M. and Tsaousis , A. D. (2017) 'A cell culture platform for C*ryptosporidium* that enables long-term cultivation and the systematic investigation of its biologyA cell culture platform for Cryptosporidium that enables long-term cultivation and the systematic investigation of its biology'.

Mitschler, R. R., Welti, R. and Upton, S. J. (1994) 'A Comparative Study of Lipid Compositions of Cryptosporidium parvum (Apicomplexa) and Madin-Darby Bovine Kidney Cells', *Journal of Eukaryotic Microbiology,* 41(1), pp. 8-12.

Mogi, T. and Kita, K. (2010) 'Diversity in mitochondrial metabolic pathways in parasitic protists *Plasmodium* and *Cryptosporidium*', *Parasitol Int,* 59(3), pp. 305-12.

Morada, M., Lee, S., Gunther-Cummins, L., Weiss, L. M., Widmer, G., Tzipori, S. and Yarlett, N. (2016) 'Continuous culture of Cryptosporidium parvum using hollow fiber technology', *Int J Parasitol,* 46(1), pp. 21-9.

Moredun strains of Cryptosporidium parvum (2015). http://www.creative-science-company.com/moredun-strain-of-cryptosporidium-parvum/. Available at: http://www.creative-science-company.com/moredun-strain-of-cryptosporidium-parvum/ (Accessed: 8th of September 2015).

Morrison, D. A. (2009) 'Evolution of the Apicomplexa: where are we now?', *Trends Parasitol,* 25(8), pp. 375-82.

Muhlenhoff, U., Balk, J., Richhardt, N., Kaiser, J. T., Sipos, K., Kispal, G. and Lill, R. (2004) 'Functional characterization of the eukaryotic cysteine desulfurase Nfs1p from Saccharomyces cerevisiae', *J Biol Chem,* 279(35), pp. 36906-15.

Muller, J. and Hemphill, A. (2013) 'In vitro culture systems for the study of apicomplexan parasites in farm animals', *Int J Parasitol,* 43(2), pp. 115-24.

Nair, P., Mohamed, J. A., DuPont, H. L., Figueroa, J. F., Carlin, L. G., Jiang, Z.-D., Belkind-Gerson, J., Martinez-Sandoval, F. G. and Okhuysen, P. C. (2008) 'Epidemiology of Cryptosporidiosis in North American Travelers to Mexico', *American Journal of Tropical Medicine and Hygiene,* 79(2), pp. 210-214.

Nanduri, J., Williams, S., Aji, T. and Flanigan, T. P. (1999) 'Characterization of an immunogenic glycocalyx on the surfaces of Cryptosporidium parvum oocysts and sporozoites', *Infect Immun,* 67(4), pp. 2022-4.

Ng Hublin, J. S., Ryan, U., Trengove, R. and Maker, G. (2013) 'Metabolomic profiling of faecal extracts from Cryptosporidium parvum infection in experimental mouse models', *PLoS One,* 8(10), pp. e77803.

Ng Hublin, J. S. Y., Ryan, U., Trengove, R. D. and Maker, G. L. (2012) 'Development of an untargeted metabolomics method for the analysis of human faecal samples using Cryptosporidium-infected samples', *Molecular and Biochemical Parasitology,* 185(2), pp. 145-150.

Okie, J. G., Smith, V. H. and Martin-Cereceda, M. (2016) 'Major evolutionary transitions of life, metabolic scaling and the number and size of mitochondria and chloroplasts', *Proc Biol Sci,* 283(1831).

Omoto, C. K., Toso, M., Tang, K. and Sibley, L. D. (2004) 'Expressed sequence tag (EST) analysis of Gregarine gametocyst development', *Int J Parasitol,* 34(11), pp. 1265-71.

Orita, H., Coulter, J., Tully, E., Abe, M., Montgomery, E., Alvarez, H., Sato, K., Hino, O., Kajiyama, Y., Tsurumaru, M. and Gabrielson, E. (2010) 'High levels of fatty acid synthase expression in esophageal cancers represent a potential target for therapy', *Cancer Biol Ther,* 10(6), pp. 549-54.

Perkins, M. E., Riojas, Y. A., Wu, T. W. and Le Blancq, S. M. (1999) 'CpABC, a Cryptosporidium parvum ATP-binding cassette protein at the host-parasite boundary in intracellular stages', *Proc Natl Acad Sci U S A,* 96(10), pp. 5734-9.

Petersen, C., Barnes, D. A. and Gousset, L. (1997) 'Cryptosporidium parvum GP900, a unique invasion protein', *J Eukaryot Microbiol,* 44(6), pp. 89s-90s.

Picard, M., Taivassalo, T., Gouspillou, G. and Hepple, R. T. (2011) 'Mitochondria: isolation, structure and function', *J Physiol,* 589(Pt 18), pp. 4413-21.

Putignani, L., Tait, A., Smith, H. V., Horner, D., Tovar, J., Tetley, L. and Wastling, J. M. (2004) 'Characterization of a mitochondrion-like organelle in *Cryptosporidium parvum*', *Parasitology,* 129, pp. 1-18.

Reduker, D. W., Speer, C. A. and Blixt, J. A. (1985) 'Ultrastructure of Cryptosporidium parvum Oocysts and Excysting Sporozoites as Revealed by High Resolution Scanning Electron Microscopy1', *The Journal of Protozoology,* 32(4), pp. 708-711.

Regoes, A., Zourmpanou, D., Leon-Avila, G., van der Giezen, M., Tovar, J. and Hehl, A. B. (2005) 'Protein import, replication, and inheritance of a vestigial mitochondrion', *J Biol Chem: Vol. 34*. United States, pp. 30557-63.

Rider, S. D., Jr. and Zhu, G. (2010) '*Cryptosporidium*: genomic and biochemical features', *Exp Parasitol,* 124(1), pp. 2-9.

Riordan, C. E., Ault, J. G., Langreth, S. G. and Keithly, J. S. (2003) '*Cryptosporidium parvum* Cpn60 targets a relict organelle', *Current Genetics,* 44(3), pp. 138-147.

Roberts, C. W., Roberts, F., Henriquez, F. L., Akiyoshi, D., Samuel, B. U., Richards, T. A., Milhous, W., Kyle, D., McIntosh, L., Hill, G. C., Chaudhuri, M., Tzipori, S. and McLeod, R. (2004) 'Evidence for mitochondrial-derived alternative oxidase in the apicomplexan parasite Cryptosporidium parvum: a potential anti-microbial agent target', *Int J Parasitol: Vol. 3*. England, pp. 297-308.

Rossignol, J.-F. (1994) *Composition and galenic formulation suitable for combatting affections of the lower abdomen*. Google Patents. [Online].

Rossignol, J.-F. (1999) *Method for treatment of opportunistic infections with pharmaceutical compositions of tizoxanide and nitazoxanide*. Google Patents. [Online].

Rossignol, J. F., Hidalgo, H., Feregrino, M., Higuera, F., Gomez, W. H., Romero, J. L., Padierna, J., Geyne, A. and Ayers, M. S. (1998) 'A double-'blind' placebo-controlled study of nitazoxanide in the treatment of cryptosporidial diarrhoea in AIDS patients in Mexico', *Trans R Soc Trop Med Hyg,* 92(6), pp. 663-6.

Rost, B., Yachdav, G. and Liu, J. (2004) 'The PredictProtein server', *Nucleic Acids Research,* 32(Web Server issue), pp. W321-W326.

Rotte, C., Stejskal, F., Zhu, G., Keithly, J. S. and Martin, W. (2001) 'Pyruvate : NADP+ oxidoreductase from the mitochondrion of Euglena gracilis and from the apicomplexan Cryptosporidium parvum: a biochemical relic linking pyruvate metabolism in mitochondriate and amitochondriate protists', *Mol Biol Evol,* 18(5), pp. 710-20.

Ryan, U., Paparini, A., Monis, P. and Hijjawi, N. (2016) 'It's official – Cryptosporidium is a gregarine: What are the implications for the water industry?', *Water Research,* 105, pp. 305-313.

Sagan, L. (1967) 'On the origin of mitosing cells', *J Theor Biol,* 14(3), pp. 255-74.

Saha, B., Borovskii, G. and Panda, S. K. (2016) 'Alternative oxidase and plant stress tolerance', *Plant Signal Behav,* 11(12), pp. e1256530.

Saric, J., Wang, Y., Li, J., Coen, M., Utzinger, J., Marchesi, J. R., Keiser, J., Veselkov, K., Lindon, J. C., Nicholson, J. K. and Holmes, E. (2008) 'Species variation in the fecal metabolome gives insight into differential gastrointestinal function', *J Proteome Res,* 7(1), pp. 352-60.

Sauvage, V., Aubert, D., Escotte-Binet, S. and Villena, I. (2009) 'The role of ATP-binding cassette (ABC) proteins in protozoan parasites', *Mol Biochem Parasitol,* 167(2), pp. 81-94.

Schaffer, S. W., Jong, C. J., Ito, T. and Azuma, J. (2014) 'Role of taurine in the pathologies of MELAS and MERRF', *Amino Acids,* 46(1), pp. 47-56.

Seeber, F., Limenitakis, J. and Soldati-Favre, D. (2008) 'Apicomplexan mitochondrial metabolism: a story of gains, losses and retentions', *Trends Parasitol,* 24(10), pp. 468-78.

Seeber, F. and Soldati-Favre, D. (2010) 'Metabolic pathways in the apicoplast of apicomplexa', *Int Rev Cell Mol Biol,* 281, pp. 161-228.

Sengupta, A., Ghosh, S., Basant, A., Malusare, S., Johri, P., Pathak, S., Sharma, S. and Sonawat, H. M. (2011) 'Global host metabolic response to Plasmodium vivax infection: a 1H NMR based urinary metabonomic study', *Malar J,* 10, pp. 384.

Sengupta, A., Ghosh, S., Das, B. K., Panda, A., Tripathy, R., Pied, S., Ravindran, B., Pathak, S., Sharma, S. and Sonawat, H. M. (2016) 'Host metabolic responses to Plasmodium falciparum infections evaluated by 1H NMR metabolomics', *Mol Biosyst*.

Sengupta, A., Ghosh, S., Sharma, S. and Sonawat, H. M. (2013) '1H NMR metabonomics indicates continued metabolic changes and sexual dimorphism post-parasite clearance in self-limiting murine malaria model', *PLoS One,* 8(6), pp. e66954.

Shebl, F. M., Engels, E. A. and Goedert, J. J. (2012) 'Opportunistic Intestinal Infections and Risk of Colorectal Cancer Among People with AIDS', *AIDS Research and Human Retroviruses,* 28(9), pp. 794-799.

Shirley, D. A., Moonah, S. N. and Kotloff, K. L. (2012) 'Burden of disease from cryptosporidiosis', *Curr Opin Infect Dis,* 25(5), pp. 555-63.

Slapeta, J. (2017) 'Cryptosporidium: Identification and Genetic Typing', *Curr Protoc Microbiol,* 44, pp. 20b.1.1-20b.1.17.

Sonawat, H. M. and Sharma, S. (2012) 'Host responses in malaria disease evaluated through nuclear magnetic resonance-based metabonomics', *Clin Lab Med,* 32(2), pp. 129-42.

Sparks, H., Nair, G., Castellanos-Gonzalez, A. and White, A. C., Jr. (2015) 'Treatment of Cryptosporidium: What We Know, Gaps, and the Way Forward', *Curr Trop Med Rep,* 2(3), pp. 181-187.

Sponseller, J. K., Griffiths, J. K. and Tzipori, S. (2014) 'The evolution of respiratory Cryptosporidiosis: evidence for transmission by inhalation', *Clin Microbiol Rev,* 27(3), pp. 575-86.

States, D. J. and Gish, W. (1994) 'Combined use of sequence similarity and codon bias for coding region identification', *J Comput Biol,* 1(1), pp. 39-50.

Stockis, A., De Bruyn, S., Gengler, C. and Rosillon, D. (2002) 'Nitazoxanide pharmacokinetics and tolerability in man during 7 days dosing with 0.5 g and 1 g b.i.d', *Int J Clin Pharmacol Ther,* 40(5), pp. 221-7.

Striepen, B. (2013) 'Parasitic infections: Time to tackle cryptosporidiosis', *Nature,* 503(7475), pp. 189-91.

Sturbaum, G. D., Schaefer, D. A., Jost, B. H., Sterling, C. R. and Riggs, M. W. (2008) 'Antigenic differences within the Cryptosporidium hominis and Cryptosporidium parvum surface proteins P23 and GP900 defined by monoclonal antibody reactivity', *Mol Biochem Parasitol,* 159(2), pp. 138-41.

Suzuki, T., Hashimoto, T., Yabu, Y., Kido, Y., Sakamoto, K., Nihei, C., Hato, M., Suzuki, S., Amano, Y., Nagai, K., Hosokawa, T., Minagawa, N., Ohta, N. and Kita, K. (2004) 'Direct evidence for cyanide-insensitive quinol oxidase (alternative oxidase) in apicomplexan parasite Cryptosporidium parvum: phylogenetic and therapeutic implications', *Biochem Biophys Res Commun: Vol. 4*. United States, pp. 1044-52.

Templeton, T. J., Enomoto, S., Chen, W. J., Huang, C. G., Lancto, C. A., Abrahamsen, M. S. and Zhu, G. (2010) 'A genome-sequence survey for *Ascogregarina taiwanensis* supports evolutionary affiliation but metabolic diversity between a Gregarine and *Cryptosporidium*', *Mol Biol Evol,* 27(2), pp. 235-48.

Teng, R., Junankar, P. R., Bubb, W. A., Rae, C., Mercier, P. and Kirk, K. (2009) 'Metabolite profiling of the intraerythrocytic malaria parasite Plasmodium falciparum by (1)H NMR spectroscopy', *NMR Biomed,* 22(3), pp. 292-302.

Teng, R., Lehane, A. M., Winterberg, M., Shafik, S. H., Summers, R. L., Martin, R. E., van Schalkwyk, D. A., Junankar, P. R. and Kirk, K. (2014) '1H-NMR metabolite profiles of different strains of Plasmodium falciparum', *Biosci Rep,* 34(6), pp. e00150.

Thivierge, K., Iqbal, A., Dixon, B., Dion, R., Levesque, B., Cantin, P., Cedilotte, L., Ndao, M., Proulx, J. F. and Yansouni, C. P. (2016) 'Cryptosporidium hominis Is a Newly Recognized Pathogen in the Arctic Region of Nunavik, Canada: Molecular Characterization of an Outbreak', *PLoS Negl Trop Dis,* 10(4), pp. e0004534.

Thompson, R. C., Olson, M. E., Zhu, G., Enomoto, S., Abrahamsen, M. S. and Hijjawi, N. S. (2005) 'Cryptosporidium and cryptosporidiosis', *Adv Parasitol,* 59.

Torgerson, P. R., de Silva, N. R., Fevre, E. M., Kasuga, F., Rokni, M. B., Zhou, X. N., Sripa, B., Gargouri, N., Willingham, A. L. and Stein, C. (2014) 'The global burden of foodborne parasitic diseases: an update', *Trends Parasitol,* 30(1), pp. 20-6.

Torgerson, P. R. and Macpherson, C. N. (2011) 'The socioeconomic burden of parasitic zoonoses: global trends', *Vet Parasitol,* 182(1), pp. 79-95.

Toso, M. A. and Omoto, C. K. (2007) 'Gregarina niphandrodes may lack both a plastid genome and organelle', *J Eukaryot Microbiol,* 54(1), pp. 66-72.

Tovar, J., Fischer, A. and Clark, C. G. (1999) 'The mitosome, a novel organelle related to mitochondria in the amitochondrial parasite Entamoeba histolytica', *Mol Microbiol,* 32(5), pp. 1013-21.

Tsaousis, A. D., Ollagnier de Choudens, S., Gentekaki, E., Long, S., Gaston, D., Stechmann, A., Vinella, D., Py, B., Fontecave, M., Barras, F., Lukes, J. and Roger, A. J. (2012) 'Evolution of Fe/S cluster biogenesis in the anaerobic parasite *Blastocystis*', *Proc Natl Acad Sci U S A,* 109(26), pp. 10426-31.

Tyzzer, E. E. (1910) 'An extracellular Coccidium, Cryptosporidium Muris (Gen. Et Sp. Nov.), of the gastric Glands of the Common Mouse', *J Med Res,* 23(3), pp. 487-510 3.

Ungar, B. L., Mulligan, M. and Nutman, T. B. (1989) 'Serologic evidence of Cryptosporidium infection in US volunteers before and during Peace Corps service in Africa', *Arch Intern Med,* 149(4), pp. 894-7.

Upton, S. J., Tilley, M., Nesterenko, M. V. and Brillhart, D. B. (1994) 'A simple and reliable method of producing in vitro infections of cryptosporidium parvum (apicomplexa)', *FEMS Microbiology Letters,* 118(1-2), pp. 45-49.

Utsi, L., Smith, S. J., Chalmers, R. M. and Padfield, S. (2016) 'Cryptosporidiosis outbreak in visitors of a UK industry-compliant petting farm caused by a rare Cryptosporidium parvum subtype: a case-control study', *Epidemiol Infect: Vol. 5*. England, pp. 1000-9.

Valigurova, A., Jirku, M., Koudela, B., Gelnar, M., Modry, D. and Slapeta, J. (2008) 'Cryptosporidia: epicellular parasites embraced by the host cell membrane', *Int J Parasitol,* 38(8-9), pp. 913-22.

van der Giezen, M. (2009) 'Hydrogenosomes and mitosomes: conservation and evolution of functions', *J Eukaryot Microbiol,* 56(3), pp. 221-31.

van der Giezen, M. and Tovar, J. (2005) 'Degernerate mitochondria', *Embo reports,* 6(6), pp.525-30.

van Dooren, G. G. and Striepen, B. (2013) 'The algal past and parasite present of the apicoplast', *Annu Rev Microbiol,* 67, pp. 271-89.

Vinayak, S., Pawlowic, M. C., Sateriale, A., Brooks, C. F., Studstill, C. J., Bar-Peled, Y., Cipriano, M. J. and Striepen, B. (2015) 'Genetic modification of the diarrhoeal pathogen Cryptosporidium parvum', *Nature,* 523(7561), pp. 477-80.

Wallimann, T., Tokarska-Schlattner, M. and Schlattner, U. (2011) 'The creatine kinase system and pleiotropic effects of creatine', *Amino Acids,* 40(5), pp. 1271-96.

Wang, D. and Zhang, Y. Y. (2013) '[Therapeutic efficacy of allitridin and azithromycin on Cryptosporidium infection in mice]', *Zhongguo Ji Sheng Chong Xue Yu Ji Sheng Chong Bing Za Zhi,* 31(6), pp. 477-9.

Wang, Y., Gong, A. Y., Ma, S., Chen, X., Li, Y., Su, C. J., Norall, D., Chen, J., Strauss-Soukup, J. K. and Chen, X. M. (2017) 'Delivery of Parasite RNA Transcripts Into Infected Epithelial Cells During Cryptosporidium Infection and Its Potential Impact on Host Gene Transcription', *J Infect Dis,* 215(4), pp. 636-643.

Wanyiri, J. W., Kanyi, H., Maina, S., Wang, D. E., Steen, A., Ngugi, P., Kamau, T., Waithera, T., O'Connor, R., Gachuhi, K., Wamae, C. N., Mwamburi, M. and Ward, H. D. (2014) 'Cryptosporidiosis in HIV/AIDS patients in Kenya: clinical features, epidemiology, molecular characterization and antibody responses', *Am J Trop Med Hyg,* 91(2), pp. 319-28.

Widmer, G., Klein, P. and Bonilla, R. (2007) 'Adaptation of Cryptosporidium oocysts to different excystation conditions', *Parasitology,* 134(Pt 11), pp. 1583-8.

Widmer, G. and Sullivan, S. (2012) 'Genomics and population biology of *Cryptosporidium* species', *Parasite Immunol,* 34(2-3), pp. 61-71.

Wilhelm, C. L. and Yarovinsky, F. (2014) 'Apicomplexan infections in the gut', *Parasite Immunol,* 36(9), pp. 409-20.

Williams, B. A., Elliot, C., Burri, L., Kido, Y., Kita, K., Moore, A. L. and Keeling, P. J. (2010) 'A broad distribution of the alternative oxidase in microsporidian parasites', *PLoS Pathog,* 6(2), pp. e1000761.

Williams, B. A., Hirt, R. P., Lucocq, J. M. and Embley, T. M. (2002) 'A mitochondrial remnant in the microsporidian Trachipleistophora hominis', *Nature,* 418(6900), pp. 865-9.

Wu, J. F., Holmes, E., Xue, J., Xiao, S. H., Singer, B. H., Tang, H. R., Utzinger, J. and Wang, Y. L. (2010) 'Metabolic alterations in the hamster co-infected with Schistosoma japonicum and Necator americanus', *Int J Parasitol,* 40(6), pp. 695-703.

Xia, J., Sinelnikov, I. V., Han, B. and Wishart, D. S. (2015) 'MetaboAnalyst 3.0--making metabolomics more meaningful', *Nucleic Acids Res,* 43(W1), pp. W251-7.

Xiao, L. (2010) 'Molecular epidemiology of cryptosporidiosis: an update', *Exp Parasitol,* 124.

Xu, X. M. and Moller, S. G. (2011) 'Iron-sulfur clusters: biogenesis, molecular mechanisms, and their functional significance', *Antioxid Redox Signal,* 15(1), pp. 271-307.

Yin, J. H., Shen, Y. J. and Cao, J. P. (2010) '[Progress on the application of *Cryptosporidium* infected animal models and in vitro cultivation]', *Zhongguo Ji Sheng Chong Xue Yu Ji Sheng Chong Bing Za Zhi,* 28(5), pp. 387-92.

Yoder, J., Roberts, V., Craun, G. F., Hill, V., Hicks, L. A., Alexander, N. T., Radke, V., Calderon, R. L., Hlavsa, M. C., Beach, M. J., Roy, S. L. and (CDC), C. f. D. C. a. P. (2008) 'Surveillance for waterborne disease and outbreaks associated with drinking water and water not intended for drinking--United States, 2005-2006', *MMWR Surveill Summ,* 57(9), pp. 39-62.

Yoder, J. S., Harral, C., Beach, M. J. and (CDC), C. f. D. C. a. P. (2010) 'Cryptosporidiosis surveillance - United States, 2006-2008', *MMWR Surveill Summ,* 59(6), pp. 1-14.

Yu, H., Guo, Z., Shen, S. and Shan, W. (2016) 'Effects of taurine on gut microbiota and metabolism in mice', *Amino Acids,* 48(7), pp. 1601-17.

Zapata, F., Perkins, M. E., Riojas, Y. A., Wu, T. W. and Le Blancq, S. M. (2002) 'The Cryptosporidium parvum ABC protein family', *Mol Biochem Parasitol,* 120(1), pp. 157-61.

Zhang, M., Izumi, I., Kagamimori, S., Sokejima, S., Yamagami, T., Liu, Z. and Qi, B. (2004) 'Role of taurine supplementation to prevent exercise-induced oxidative stress in healthy young men', *Amino Acids,* 26(2), pp. 203-7.

Zhu, G. (2004) 'Current progress in the fatty acid metabolism in Cryptosporidium parvum', *J Eukaryot Microbiol,* 51.

Zhu G., Guo F. (2014) 'Cryptosporidium Metabolism' Cacciò S., Widmer G. (eds) Cryptosporidium: parasite and disease. Springer, Vienna

Zhu, G., Li, Y., Cai, X., Millership, J. J., Marchewka, M. J. and Keithly, J. S. (2004) 'Expression and functional characterization of a giant Type I fatty acid synthase (CpFAS1) gene from Cryptosporidium parvum', *Mol Biochem Parasitol,* 134.

Zhu, G., Marchewka, M. J., Woods, K. M., Upton, S. J. and Keithly, J. S. (2000) 'Molecular analysis of a Type I fatty acid synthase in Cryptosporidium parvum', *Molecular and Biochemical Parasitology,* 105(2), pp. 253-260.

Zhu, G., Shi, X. and Cai, X. (2010) 'The reductase domain in a Type I fatty acid synthase from the apicomplexan Cryptosporidium parvum: Restricted substrate preference towards very long chain fatty acyl thioesters', *BMC Biochemistry,* 11(1), pp. 46.